FAST Facility for Accelerated Service Testing

HAL Heavy Axle Load

TECHNICAL NOTE

FRA/ORD/95-07

TRIAL LOW TRACK MODULUS TESTS AT FAST

W. Ebersöhn, E. T. Selig, and M.C. Trevizo

NOTICE

This document reflects events relating to testing at the Facility for Accelerated Service Testing (FAST) at the Transportation Technology Center, which may have resulted from conditions, procedures, or the test environment particular to that facility. This document is disseminated for the FAST Program under the sponsorship of the Federal Railroad Administration, the Association of American Railroads, and the Railway Progress Institute in the interest of information exchange. The sponsors assume no liability for its contents or use thereof.

The FAST Program does not endorse products or manufacturers. Trade or manufacturers' names appear herein solely because they are considered essential to the object of this report.

(Because there are an extensive number of plots included in this report, they will appear at the end of the document.)

ACKNOWLEDGMENTS

Carmen Trevizo supervised the Trial LTM tests. Members of the TTC staff in Pueblo conducted the field work and collected the data. Prof. Alan J. Lutenegger, with the help of UMass and TTC personnel, conducted the CPT tests and the CPT equipment was provided by UMass. The test section was based on designs and specifications prepared by Prof. E.T. Selig. Data processing and plotting were done by W. Ebersöhn. CTC staff member Steven M. Chrismer contributed to this report. The research was sponsored by the Association of American Railroads.

1. Report Number	2. Government Accession No.	3. Recipient's Catalog No.
FRA/ORD/95-07		

4. Title and Subtitle	5. Report Date
Trial Low Track Modulus Tests at FAST	June 1995
	6. Performing Organization Code
7. Author(s)	
W. Ebersöhn, E.T. Selig and M.C. Trevizo	8. Performing Organization Report No.
9. Performing Organization Name and Address	10. Work Unit No. (TRAIS)
Association of American Railroads Transportation Technology Center P.O.Box 11130 Pueblo, CO 81001	11. Contract or Grant No. DTFR54-93-C-00001
12. Sponsoring Agency Name and Address	13. Type of Report or Period Covered
U.S. Department of Transportation Federal Railroad Administration Office of Research and Development 400 7th St. SW Washington, D.C. 20590	Research 14. Sponsoring Agency Code

15. Supplementary Notes

16. Abstract

A study to investigate the influence of low track modulus on track performance under traffic was conducted by the Association of American Railroads, Transportation Test Center, Pueblo, Colorado.

A 100-foot trial section of track was constructed to control track modulus. The existing stiff natural silty sand subgrade was excavated, and a 5-foot layer of low stiffness clay was installed providing the low modulus. For a comparison, a control section was established nearby over the natural subgrade, which provided a much greater track modulus. Both sections were monitored to determine the track performance with tonnage accumulation and with maintenance.

Of primary interest were the track deflection, stiffness and modulus measurements and how these changed with tonnage accumulation and maintenance. It was determined that as variance in track stiffness along the track increases, differential settlement or track roughness also increases. The factor causing rough track was not the low modulus itself; rather, it was due to the increased variability of track stiffness in the low track modulus section.

Although this report is intended to describe the test procedures and present the results in a general manner, a number of very promising leads are suggested by the research. For example, the test illustrated the maintenance forecasting potential which could result from measuring track deflection or stiffness on a moving basis. Also indicated by the test results is the manner in which such data should be measured and analyzed to provide meaningful information to the track maintenance engineer.

17. Key Words	18. Distribution Statement
Low track modulus, track performance	This document is available through the National Technical Information Service Springfield, VA 22161

19. Security Classification (of the report)	20. Security Classification (of this page)	21. No. of Pages	22. Price

Form DOT F 1700.7 (8-72)

Table of Contents

List of Tables

List of Figures

List of Figures -- (Continued)

List of Figures -- (Continued)

List of Figures -- (Continued)

1.0 INTRODUCTION

The natural silty sand at the Association of American Railroads (AAR), Transportation Test Center (TTC), Pueblo, Colorado, is an excellent subgrade soil for track support. As a consequence, the substructure conditions at the Facility for Accelerated Service Testing (FAST) track does not represent the variability of subgrade conditions that are encountered in normal revenue track. Thus tests conducted with track supported on the natural subgrade at FAST do not give an indication of the effects of low quality subgrade on track performance.

The principal objective of the Heavy Axle Load (HAL) program on the High Tonnage Loop (HTL) is to determine the change in track deterioration rate and the costs which accompany a 20 percent increase in static axle loads. A plan was adopted by AAR to create a test site with a low stiffness subgrade to provide a single variation in the subgrade conditions for the HAL program. To evaluate the feasibility of this plan, a Trial Low Track Modulus (TLTM) test site 30 meters (100 ft) long was constructed. A stiffness simulating the lower end of acceptable mainline track (not a worst case situation) was targeted for this project.

The track performance with the TLTM and an equivalent length of track on the natural subgrade was monitored. Although the purpose of the TLTM was to determine the feasibility of constructing a longer (180 m or 600 ft) Low Track Modulus (LTM) test site, valuable results became available from the TLTM providing an indication of the influence of substructure conditions on track maintenance requirements.

2.0 OBJECTIVES

The objectives of this report are to describe the procedures followed in the TLTM investigation, and to document the results so that they may be used by interested persons.

3.0 PROCEDURES

3.1 LOW TRACK MODULUS DESIGN

The basic concept adopted for the LTM test section was to excavate a trench in the natural subgrade under a length of track and fill it with a low stiffness clay. The clay subgrade was covered by a layer of subballast to support the superstructure and ballast. The clay stiffness and layer depth was selected in combination with the properties of the superstructure and remaining substructure to provide a track modulus of substantially lower value than represented by the existing FAST track.

Because the existing track modulus was typically 20.7 to 41.4 MPa (3,000 to 6,000 psi) with wood ties, the design track modulus for the LTM was targeted at 13.8 MPa (2,000 psi) maximum.

Other specified design criteria were as follows:

1. Locate the test site in Section 29 of the FAST loop. This section provides tangent track with a parallel bypass track (Figure 1).

2. Use 65.5 to 67.6 kg/m (132 to 136 lb/yd) rail.

3. Use 175 mm (7 in.) high x 225 mm (9 in.) wide x 2.6 m (8 ft 6 in.) long wood ties with 350 mm (14 in.) tie plates and cut spikes. Box anchor every other tie.

4. Use durable crushed rock ballast placed 300 mm (12 in.) depth below bottom of the tie with a 150 mm (6 in.) shoulder width, and a shoulder slope of two horizontal to one vertical (2H:1V).

5. Use a broadly graded gravelly sand material for the subballast (particle size ranging approximately between 30 mm and 0.075 mm) previously used at FAST. A subballast thickness of 150 mm (6 in.) is proposed.

6. The low stiffness clay should have a minimum plasticity index (PI) of 15-20 and a liquid limit (LL) below about 60-70. Such a soil will give a low resilient modulus while being relatively insensitive to changes in moisture content. The selected moisture content for the installed clay layer should be high enough to give a low modulus, but not so high that excessive track settlement will occur under traffic.

7. The trench depth should be in the range of 1.2 to 2.4 m (4 to 8 ft). The depth should be the smallest possible to minimize cost, while still providing a substantial track modulus reduction. The existing subgrade generally has enough cohesion to permit excavating a trench with vertical walls to a depth of 1.2 to 1.5 m (4 to 5 ft) on a temporary basis if surcharge is avoided on the ground surface. Greater depths will require trench side support to meet safety standards.

8. The maximum desired width at top of trench is 4.6 m (15 ft).

9. The wall of the trench should be no closer to the adjacent bypass track than the toe of the ballast slope or about 2.4 m (8 ft) from the center of the adjacent track. This is to prevent the low stiffness zone from significantly influencing the settlement of the bypass track.

10. A means must be provided to maintain reasonably constant moisture conditions in the clay for a period of 5 to 10 years.

A GEOTRACK analysis was carried out to evaluate the effect of the clay layer on the track modulus. A resilient modulus of 103.4 to 206.7 MPa (15,000 to 30,000 psi) was assumed for the natural subgrade, and 20.7 MPa (3,000 psi) was assumed for the clay. The track modulus value

calculated for wood tie track with the existing subgrade was about 42.0 MPa (6,100 psi). The values with clay layers varying from 1.2 to 2.4 m (4 to 8 ft) are given in Table 1.

Table 1: Track Modulus Estimates

Clay thickness m (ft)	Track modulus MPa (psi)
1.2 (4)	22.1 (3,200)
1.5 (5)	20.0 (2,900)
1.8 (6)	18.6 (2,700)
2.4 (8)	17.2 (2,500)

The track modulus only diminishes gradually with depth. Thus considering the trench depth constraints, and assuming that the clay layer surface is at the existing subgrade surface, a trench depth of 1.5 m (5 ft) appears to be the best compromise. This should reduce the track modulus to less than 50 percent of that with the existing subgrade.

Figure 2 shows the cross section of the TLTM substructure. The trench is lined on the sides and bottom with an impermeable plastic sheet to isolate the clay from the existing subgrade. The liner was omitted from the top of the clay, however, to avoid creating an unnatural interface with low friction and potential reinforcement. As a result, water can be expected to enter and leave the clay through the top boundary. The trench sides were to be inclined on a slope of one horizontal to two vertical (1H:2V), but this proved difficult to construct with available equipment. Thus the sides were stepped instead as shown in Figure 2. The main purpose of the slope was to simplify placing and compacting the clay without disturbing the liner.

An internal drain system for adding water in case of moisture loss was planned. This was not included in the TLTM because of the short duration of the trial.

3.2 CONSTRUCTION

3.2.1 Site Layout

The TLTM test section was constructed in Section 29 of the HTL (see Figure 1).

The TLTM test section started at tie 405 and ended at tie 484, as indicated in Figure 3. The ramp into the trench extended from tie 484 to tie 464. A comparison test section on the natural subgrade extended from tie 309 to 385.

Figure 4 shows a cross section of the TLTM and the natural subgrade test sections, indicating the main line and the bypass line. The survey extended far enough on both sides to include the surface drainage conditions. Note that the natural subgrade section had no subballast. Instead the ballast was placed directly on the subgrade.

3.2.2 Track Components

3.2.2.1 Superstructure

The rail weights changed along the length of the test sites (Figure 5). Starting at tie 484, the rails consisted of a 65.9 kg/m (133 lb/yd) on the outer leg and a 67.6 kg/m (136 lb/yd) rail on the inner leg. At tie 357, the outer rail was jointed and for the rest of the natural subgrade site both legs consisted of 67.6 kg/m rails. An insulated joint was installed at tie 377 in the inner rail.

At 39.15 MGT (May 28, 1991), a track panel was removed from tie 426 to tie 405 to construct a cross drain in the clay test section. The track panel was replaced with only 67.6 kg/m (136 lb/yd) rails. Figure 5 shows the rail weights and joint positions for each test section as well as the change in superstructure after the drain construction.

Softwood ties with dimensions 175 mm (7 in.) high x 225 mm (9 in.) wide x 2.6 m (8 ft 6 in.) long were used. The ties were creosote treated and alternate ties were fully box-anchored spaced at 495 mm (19.5 in.) The fastener system was the AREA 355 mm (14 in.) tie plate (Plan No 12) used on rails with 150 mm (6 in.) base width. The rails were tied down with 2 cut track spikes -- one on either side of the rail base. The tie plate was tied down with 2 cut track spikes, also one on either side of the rail.

3.2.2.2 Ballast

Dolomite crushed rock ballast was placed over the subballast with approximately 300 mm (12 in.) depth below the tie and a 150 mm (6 in.) ballast shoulder sloping 2H:1V. The dolomite ballast gradation was not determined before testing began. However, an indication of the expected gradation was obtained from previous FAST ballast tests done on Section 03 by Trevizo.[1]

A ballast sample was taken from underneath the ties at the end of the experiment (July 1991) from both test sites. The gradations for these three samples are given in Table 2 and are shown in Figure 6. The gradation from the previous tests does not appear to be representative of the initial gradation.

Table 2: Ballast Gradations				
Sieve Size		Percent Passing		
(mm)	(in.)	Previous Tests	Clay Test Site	Natural Subgrade Test Site
63.5	2.5	100	100	100
50.8	2.0	84.8	93.4	94.8
38.1	1.5	67.4	62.8	63.0
25.4	1.0	33.9	26.8	23.1
19.1	.75	17.3	12.5	8.1
12.7	.50	9.0	*	*
9.50	.375	6.3	4.9	1.0
6.40	.250	*	4.3	0.8
4.75	#4	3.9	4.0	0.7
2.00	#10	*	3.2	0.7
.180	#80	*	1.5	0.5
.075	#200	1.2	0.7	0.4

* Sieve sizes not used.

The dolomite ballast particle characteristics, as determined during the FAST ballast tests, are given in Table 3.[1] Test procedures to determine these material properties are described by Roner and Selig.[2] The following definitions are used in these tests:

-- An elongated particle is one where the length/width is more than 1.8. The Elongation Index is the percentage by weight of elongated particles in a sample.

-- A flaky particle is one in which the thickness/width is less than 0.6. The Flakiness Index is the percentage by weight of flaky particles in a sample.

-- The shape factor is the ratio of the sum of the longest dimensions to the sum of the least widths.

Table 3: Ballast Material Properties		
Properties	**Units**	**Values**
Elongation Index	Dimensionless	46.09
Flakiness Index	Dimensionless	15.18
Shape Factor	Dimensionless	2.09
Mill Abrasion	% loss	8.60
Los Angeles Abrasion	% loss	34.1
Soundness of aggregate - Magnesium Sulfate	% loss	0.23
- Sodium Sulfate	% loss	0.26
Clay Lump and Friable Particles	% loss	3.37
Scratch Hardness of Coarse Aggregate	% soft particles	no loss
Unit Weight	kg/m^3 (lb/cuft)	1666 (104)

Based on hand sample examination, the ballast is composed mainly of cryptocrystalline, massive nonporous siliceous dolomite.[1] The dolomite is generally very clean and variable colored pink, gray, red, and pure white, with a small amount of gray quartzite as thin lenses in the dolomite. The rock may be of low metamorphic grade. A small amount of dark green, well foliated quartz-chlorite schist, and dark green to black massive basalt is also present in the ballast sample. In general, ballast particles are angular with minor rounding of edges and corners.

The ballast thickness beneath the ties was measured at various locations along the length of each test section at the end of the TLTM experiment. Figure 7 shows a plot of the thickness measurements. The positions of the joints are also shown. The average ballast thickness was 285 mm (11 in.) for the clay section and 300 mm (12 in.) for the natural subgrade section.

3.2.2.3 Subballast

Beneath the ballast was a 150 mm (6 in.) thick subballast layer of well graded sand with silt and gravel. This subballast was constructed only on the clay test site.

An indication of the subballast gradations was obtained from a sample taken in Section 20 and tested by Adegoke and Selig[3] and from tests conducted by Thompson.[4] At the end of the TLTM experiment, a subballast sample was taken from the clay test site and analyzed by the TTC. The results are shown in Figure 8 and listed in Table 4.

Other available subballast material properties as obtained by Adegote and Selig[3] and by Thompson[4] are given in Table 5.

Table 4: Subballast Gradations

Sieve Size		Percent passing		
(mm)	(in.)	Adegoke and Selig[3]	Thompson[4]	TTC Sample
25.4	1.0	93	100	92.6
19.1	0.75	86	82	85.0
12.7	0.50	81	*	*
9.50	0.375	*	77	77.3
6.40	0.250	*	*	72.7
4.75	#4	72	59	62.9
2.36	#8	61	*	53.0
2.00	#10	58	44	51.4
0.60	#30	33	*	34.8
0.420	#40	25	27	*
0.180	#80	*	*	27.7
0.150	#100	7	8	*
0.075	#200	4	2	11.0

*Sieve sizes not used.

Table 5: Subballast Material Properties		
Property	**Adegoke and Selig[3]**	**Thompson[4]**
ASTM Identification	Well graded gravelly sand	
Unified Classification	SW	Non plastic
PI of <0.42 mm size		
LL of <0.42 mm size		
Moisture Content	3% to 5%	
Resilient Modulus		Equation 1

The subballast resilient modulus is estimated by cyclic triaxial tests to be:[4]

$$E_r = 941 P_a \left(\frac{\Theta}{P_a} \right)^{0.687}, \quad (1)$$

where P_a = atmospheric pressure = 14.7 psi, and

Θ = bulk stress = $\sigma_1 + 2\ \sigma_3$

3.2.2.4 Subgrade

The natural subgrade gradations in the vicinity of the test section are shown in Figure 9 and listed in Table 6, as obtained by Adegoke and Selig,[3] Thompson,[4] and Stewart.[5] The range in clay subgrade gradations is shown in Figure 10, as obtained by Coleman.[6] Between 95 percent and 98 percent passed the 0.075 mm (#200) sieve.

Table 6: Natural Subgrade Gradations					
Sieve Size		Percent Passing			
(mm)	(in.)	Adegoke and Selig[3]		Thompson[4]	Stewart[5]
		Range of Borings	Composite Sample		
4.75	#4	*	*	100	96
2.36	#8	*	*	*	*
2.00	#10	98 - 100	97	99	92
1.18	#16	*	*	94	86
0.85	#20	91 - 97	*	*	*
0.60	#30	*	83	*	*
0.425	#40	74 - 92	77	29	58
0.250	#60	56 - 87	51	*	*
0.180	#80	*	*	*	*
0.150	#100	33 - 80	34	*	17
0.075	#200	17 - 61	13	0	6

* Sieve sizes not used.

The available natural subgrade material properties, as obtained by Adegoke and Selig,[3] Thompson,[4] and Stewart[5] are given in Table 7. The available clay properties as obtained by Coleman[6] and Thompson[7] are given in Table 8.

Table 7: Natural Subgrade Material Properties			
Property	Adegoke and Selig[3]	Thompson[4]	Stewart[5]
ASTM Identification	Sandy Silt or Silty Sand		Sandy Silt or Silty Sand
Unified Classification	ML or SM		ML or SM
PI			5.9
LL			18.5
Moisture Content 0.3 to 1.2 m depth (%)	6 to 12		
Moisture Content 1.2 to 3.0 m depth (%)	1 to 5		
Specific Gravity			2.61
Resilient Modulus		Equation 2	Equation 3
Optimum Moisture Content (%)			9.5 - 10.7
Maximum Dry Density, kg/m^3 (pcf)			1,970 (123)

The natural subgrade resilient is estimated from cyclic triaxial tests, as follows, by Thompson[4]

$$E_r = 654\, P_a \left(\frac{\Theta}{P_a} \right)^{1.083}, \tag{2}$$

or by Stewart[5]

$$E_r = 774\, P_a \left(\frac{\Theta}{P_a} \right)^{1.206}. \tag{3}$$

Table 8: Clay Subgrade Material Properties		
Property	**Coleman[6]**	**Thompson[7]**
ASTM Identification	Very plastic clay	
Unified Classification	CH	
PI	45	
LL	67	
Natural Moisture Content (%)	35	
Specific Gravity	2.7	
Resilient Modulus		Refer to Figure 11
Optimum Moisture Content (%)	22.8	
Maximum Dry Density, kg/m^3 (pcf)	1,472 (91.9)	

Figure 11 presents the resilient modulus test results obtained by Thompson[7] on the subgrade clay. The shape of the curves changes with the moisture content, compaction and loading condition, as described by Selig.[8]

The unconfined compression strengths for the natural subgrade and for the clay layer are given as a function of moisture content in Figure 12. The tests were conducted by Stewart[5] and Thompson[4] for the natural subgrade, and by Thompson[7] for the clay.

Two borings, B1 and B2, were made in Section 20 at ties 285 and 917, respectively. Each hole was located midway between the rails. The holes were advanced by means of a 40 mm (4 in.) auger. Penetration tests were performed at close intervals. The sampler consisted of a "California" spoon with outer diameter of 63.5 mm (2.5 in.) and inner diameter of 50.8 (2 in.). The sampler was driven for 305 mm (1 ft) at each sampling interval by dropping a 65 kg (140 lb) hammer 457 mm (18 in.). The blow counts were recorded for each 150 mm (6 in.) penetration. Plots of blow count (N_c), as a function of depth, are shown on the boring logs in Figures 13(a) and (b). Figure 13 also includes the water content and the visual identifications of each sample. Adegoke and Selig[3] found that the natural subgrade is relatively uniform with indications that the silt content increases with depth and that the moisture content decreases with depth.

Moisture samples taken in the natural subgrade by a hand auger, after the completion of the TLTM experiment (July 1991), indicated that the average moisture content in the first 1.5 m (5 ft) was 9.7 percent and that the moisture content decreases with depth.

The moisture content in the clay layer was taken during layer placement with a nuclear gage. Table 9 lists the tie positions for the measurements and the associated compaction as a percent of the standard maximum dry density. The depths varied as layers were added. The order listed in Table 9 corresponded to the order measured. Thus the depths decreased toward the bottom of the table.

The measurements of percent compaction were used only to confirm that the compacting effort was adequate. Because most measurements were in the desired range of 90 to 95 percent, the compaction level is thought to be sufficient. Although the occasional reading is below or above this level, this is due to the statistical distribution of compaction itself and the variability of the measuring device. Two consecutive measurements of compaction with the nuclear gage at the same location may yield very different values.

Table 9: "At Construction" Clay Moisture Content		
Tie No.	**Moisture (%)**	**Compaction (%)**
455	29.3	98.7
435	30.5	100.2
404	30.8	86.9
411	32.8	94.6
430	31.6	86.8
453	30.7	96.6
407	31.8	91.0
423	30.0	96.6
451	27.7	103.7
404	31.7	84.5
430	32.2	94.4
448	30.8	94.6
414	32.7	97.9
426	34.2	92.2
456	30.1	97.6
403	31.2	95.1
426	31.3	96.2
408	34.3	91.0
437	31.7	98.0
459	27.0	98.4

The moisture contents, after TLTM experiment, were measured by taking 25 mm (1 in.) hand auger samples at selected tie locations every 150 mm (6 in.) in depth. Table 10 lists the average and range of moisture readings for each tie location. Figure 14 gives an indication of the moisture content distributions along the length of the sections based on Tables 9 and 10.

Table 10: "After Construction" Moisture Content		
Tie No.	**Moisture (%)**	**Moisture Content Range (%)**
464 Clay Subgrade	28.4	24.8 - 30.9
458 Clay Subgrade	28.0	25.2 - 30.2
452 Clay Subgrade	28.6	26.9 - 30.0
444 Clay Subgrade	28.9	25.3 - 31.1
436 Clay Subgrade	28.9	27.1 - 31.3
430 Clay Subgrade	29.9	28.0 - 31.5
413 Clay Subgrade	29.6	28.1 - 33.2
405 Clay Subgrade	29.8	25.5 - 33.3
381 Natural Subgrade	9.8	7.3 - 12.5

3.2.3 Construction Procedure

The clay layer was constructed by removing the existing track and excavating to the trench dimensions as indicated in Figure 14. The trench bottom was graded and compacted to provide a firm base. To prevent the clay from losing moisture, the trench was lined with 0.5 mm (0.02 in.) thick plastic liner on the sides and bottom of the trench.

Prior to construction, the clay was pulverized and brought to a specified moisture content of 30-33 percent. The clay was compacted in layer thicknesses of approximately 200 mm (8 in.) to an average dry density equal to or exceeding 90 percent ASTM D698 maximum dry density.

With the trench filled with clay, the liner was not folded over the top of the clay layer to avoid creation of an unnatural interface with low friction. The subballast layer was placed directly on the clay section and compacted.

The ballast and superstructure were then placed onto the subballast in the clay section and directly onto the existing subgrade in the control section.

At the beginning of May 1991 (approximately 35 MGT), water was noticed to be collecting on top of the clay layer, saturating the subballast from tie 425 to tie 400. The drainage problem was corrected by installing a sheet of Hydroway edge drain, 300 mm (12 in.) wide and 25 mm (1 in.) thick, vertically at the top edge of the clay on the field side of the track. The sheet extended from tie 430 to tie 400 underneath the ballast shoulder. The water was drained out of the Hydroway by a 50 mm (2 in.) pipe installed at tie 400.

The procedure to install the Hydroway sheet was as follows:

1. The ballast shoulder was removed.
2. A narrow trench was cut at the edge of the clay layer to fit the Hydroway sheet vertically against the side of the clay and the subballast.
3. A drain pipe was installed.
4. The ballast shoulder was replaced.
5. The track was tamped.

4.0 VERTICAL TRACK STIFFNESS

The vertical track stiffness measurements were done using the equipment as shown in Figure 15. The load was applied to each rail in four 44.5 kN (10 kips) load increments. The first set of measurements was taken December 14, 1990, at 22.3 kN (5 kips) load intervals. Each rail was loaded using two independently controlled hydraulic actuators. The maximum wheel load applied was 178 kN (40 kips). At each load increment, the track deflection was measured using a digital level. The level was set up well outside the load influence base of the equipment to ensure accurate readings.

The vertical track stiffness measurements were taken after construction and prior to traffic, and at regular intervals during traffic. Table 11 gives the date of each set of measurements, and the cumulative traffic up to each measurement.

Table 11: Vertical Track Stiffness Schedule	
Date	**Cumulative Traffic (MGT)**
December 14, 1990	0.0
December 18, 1990	1.255
January 22, 1991	2.253
February 6, 1991	5.109
February 19, 1991	9.832
April 1, 1991	20.427
April 29, 1991	31.660
May 28, 1991	34.153
June 5, 1991	41.442
June 12, 1191	45.078
June 12, 1991 after tamp	45.078
June 17, 1991	47.678
June 23, 1991	50.869

Figures 16 to 26 present the load-deflection relationships for each load test on both rails for the clay test site and Figures 27 to 37 for the natural subgrade test site.

The slope of the line between 0 and 44.5 kN gives an indication of the voids or slacks between the ties and the ballast in the influence length of the wheel. The 44.5 kN (10 kips) load is referred to as the seating load, and the modulus or stiffness calculated for this interval will be referred to as the seating modulus or seating stiffness.

In most of the tests, the load deflection relationship between 44.5 kN and 178 kN was found to be approximately linear, although in some cases stiffening was found at the maximum load range applied. Track stiffness in the influence length of the wheel load is then based on the deflection between 44.5 kN and 178 kN (10 to 40 kips) loads. The modulus or stiffness where the tie is in contact with the ballast will be referred to as the contact stiffness or contact modulus.

The deflections for each test on each rail, under the seating and maximum loads, are given in Figures 38 to 49 for the clay section and Figures 50 to 59 for the natural subgrade section. The vertical lines show the position of the joints in the natural subgrade section. These plots are direct indications of the change in support conditions with increasing traffic.

Based on Figures 38 to 59, the two sections were divided into three subsections which have inherently the same performance characteristics. These subsections contain the data that are most suitable for analysis. The presentation of the stiffness measurements will present first all measurements taken in the field and second only the measurements applicable to the subsections.

The clay subsection extends from tie 464 to 434. This subsection was monitored from the beginning of the investigation. Some measurements also were taken from tie 415 to 405, but at irregular intervals. As a result of drainage problems, this section was reconstructed; hence, these data could not be used for the performance investigation.

The natural subgrade section was divided into two subsections, a jointed subsection and an unjointed subsection well away from the influence of the joints. The jointed subsection extended from tie 385 to 355 and the unjointed subsection extended from tie 339 to 325. Unfortunately the track stiffness was not measured at 0 MGT for the natural subgrade section, and the joints in the natural subgrade section reduced the length of track that could be used for performance comparison with the unjointed clay section.

In summary the subsections suitable for stiffness analysis are as follows:

Clay subsection - Tie 464 to 434

Natural subgrade jointed subsection - Tie 385 to 355

Natural subgrade unjointed subsection - Tie 339 to 325

The clay section had to be maintained at frequent intervals (see Section 10.0, Maintenance for details). Table 12 shows the dates and traffic when each section was fully maintained.

Table 12: Maintenance Summary

Date	Traffic (MGT)	Maintenance on:		
		Clay Site	Natural Jointed Site	Natural Unjointed Site
April 15, 1991	25.699	Surfaced, lined & tamped	Surfaced, lined & tamped	Surfaced, lined & tamped
May 10, 1991	37.287	Raised & tamped	-	-
May 23, 1991	38.775	Surfaced & tamped	-	-

Spot maintenance was done June 12, 1990, (45.078 MGT). Localized stiffness and unloaded measurements were taken at these locations.

Due to the maintenance, the data will be presented over two periods: December 14, 1990, to April 1, 1991, and April 29, 1991, to June 17, 1991.

Figure 60 and 61 indicate the change in contact deflection along the length of the subsection during the first period, which corresponds to the first tamping cycle. The inner and outer rails are shown separately. Figures 62 and 63 show the change in contact deflection for the second period. The vertical lines in Figures 61 and 63 indicate the position of the joints in the natural subgrade subsection.

To calculate the track stiffness and track modulus, the following procedure was used. The track stiffness S for a selected load increment is given by

$$S = \frac{P_f - P_o}{y_f - y_o}, \qquad (4)$$

where P_f = final vertical rail force,

P_o = initial vertical rail force,

y_f = final rail elevation,

y_o = initial rail elevation.

The track modulus, *u*, was determined using the beam-on-elastic-foundation model as given by Zarembski and Choros[9] as follows:

$$u = \frac{(S)^{4/3}}{(64EI)^{1/3}}, \tag{5}$$

where E = Young's modulus of rail steel,

I = rail moment of inertia.

The average seating and contact modulus for the three subsections are shown in Figures 64, 65 and 66 for the total experiment. The corresponding variability is shown in Figures 67 to 69. The vertical lines show when tamping took place. The plots during the second period are not connected because full sets of load tests were not taken before and after tamping during this period.

Notice that the contact modulus increases and then decreases with cumulative tamping. The initial increase may be due to the weather conditions and the compaction of the newly constructed substructure. The subsequent decrease may be due to redistribution of the tie bearing support.

In all three subsections the seating modulus coefficient of variation (Figure 67 to 69) is more than the contact modulus variation during the first period. In all the subsections, it seems as if the modulus variation increases sharply, then decreases and thereafter either stabilizes or gradually increases with traffic. This trend might be a result of the changes in the tie support conditions or changes in layer properties.

In the unjointed natural subgrade section, the trends are less clear as the variation in support in this section is small. The unnecessary tamping of this subsection during the second period actually caused an increase in the modulus variation over that for the first period.

5.0 DEFLECTION BASIN

The shape of the deflected track under a single wheel load (Deflection Basin) was measured using the same loading equipment as discussed in Section 4, Vertical Track Stiffness. Deflections were measured at the point of applied load and at the next five ties to one side of the applied load. The deflection basin measurements were taken at the end of the experiment (50.689 MGT). The seating basin is obtained from the deflections measured at each tie between 0 and 44.5 kN (10 kips). The contact basin is obtained from the deflection difference at each tie between 44.5 kN and 178 kN (40 kips). Figure 70 and 71 show the seating and total deflection basins for the clay and natural subgrade sections, respectively. Both the inner and outer rail basins are shown.

The average seating and total deflection basins for all three subsections for both the inner and outer rail are indicated in Figure 72. Figure 73 shows the average contact basins for the subsections. The inner and outer rail results are shown separately.

The track modulus, u, can also be calculated using the deflection basin measurements. Based on the fact that for vertical equilibrium of forces, with the beam-on-elastic foundation model, the integral of the supporting line force must be equal to the applied force.[8]

Hence.

$$P = \int_{-\infty}^{\infty} u\, y\, dx \ . \tag{6}$$

If u is considered constant along the rail then Eq. (6) becomes

$$P = uA_y \text{ ,} \tag{7}$$

where A_y is the area of the deflection basin caused by the vertical force P.

Table 13 compares the modulus calculated with Eq. 5 and Eq. 7.

Table 13: Modulus Calculation Comparison

Tie No.	Clay subgrade							
	Modulus According to Eq. 5				Modulus According to Eq. 7			
	Seating		Contact		Seating		Contact	
	Out	In	Out	In	Out	In	Out	In
	(MPa)	(MPa)	(MPa)	(MPa)	(MPa)	(MPa)	(MPa)	(MPa)
464	6.7	19.8	14.7	29.1	6.2	15.6	12.2	21.1
458	5.2	3.7	16.2	19.8	5.3	4.3	13.2	18.5
452	5.2	5.8	12.5	22.3	5.1	9.2	10.1	18.1
444	4.1	5.2	12.5	22.3	5.6	6.0	12.1	15.8
436	6.7	2.3	13.5	11.6	5.2	2.5	11.5	9.8
430	3.4	14.7	13.5	25.3	3.8	21.8	12.6	22.0
Average:	5.2	8.6	13.8	21.7	5.2	9.9	11.9	17.5
	Natural Subgrade							
381	11.6	14.7	34.1	40.7	11.0	11.6	35.6	34.1
375	4.6	5.8	25.3	22.3	5.2	7.2	23.7	27.7
367	5.2	11.6	29.1	25.3	5.7	7.3	23.9	23.7
335	9.4	9.4	40.7	50.0	9.9	9.6	31.7	30.4
327	3.7	14.7	22.3	34.1	3.7	17.4	15.2	24.1
Average:	6.9	11.3	30.3	34.5	7.1	10.6	26.0	28.0

The two sets of modulus values compare reasonably well. The average seating modulus values are about the same for the two methods. However, the average contact modulus is greater using the single point method compared to the basin method.

By using Eq. 5, the assumption is made that the support conditions under each tie in the influence length of the load applied are constant; using Eq. 7 this assumption is not made and so the modulus depends on the deflected shape.

6.0 INSITU TESTS

The thickness and relative strengths of the substructure layers for each section were determined using the Cone Penetrometer Test (CPT) setup, as shown in Figure 74. Figures 75(a) and (b) and Figures 76(a) and (b) show each individual CPT profile in the clay subgrade section and the natural subgrade section, respectively. The depth is measured from the top of the rail and the ballast was removed before probing. The tip resistance measurements started in the bottom of the subballast and in some instances in the top of the clay layer, depending on the depth of the access hole.

Figure 77 gives the combined profiles for each subsection for both the outer and inner rails. The CPT profiles in the middle of each tie were used to represent these profiles at depths greater than 3 m (10 ft), because only the middle CPT profile went below 3 m (10 ft).

The clay layer can be distinguished clearly by its low tip resistance. The outer rail has a distinctly harder zone in the natural subgrade underneath the clay layer. Both the natural subgrade subsections have the same profiles with a distinctly harder layer from 0.75 m (2.5 ft) to 1.6 m (5.3 ft) below the top of rail with a softer layer starting at 1.6 m (5.3 ft) and gradually becoming harder with further depth.

7.0 UNLOADED TRACK PROFILE

The unloaded track profiles were measured using a digital level taking elevation readings on the tip of both rails at every 1.5 m (5 ft) along the track. The starting point of each set of measurements was at tie 464, and the measurements continued for 30.5 m (100 ft) over the clay section up to tie 402. The survey started again at tie 372 in the natural subgrade section at 45.75 m (50 ft) and continued for 30.5 m (100 ft) up to tie 308. The profiles were measured before and during traffic. Table 14 gives the date of each set of measurements and the cumulative traffic up to each set. The profiles were tied into an elevation reference system to determine the absolute settlement.

Table 14: Unloaded Profile Schedule	
Date	**Cumulative Traffic (MGT)**
December 14, 1990	0
December 18, 1990	1.255
January 7, 1991	2.207
February 6, 1991	5.109
February 20, 1991	9.832
June 7, 1991	42.34
June 12, 1991	45.07
June 12, 1991 after tamping (partial survey)	45.07 only on clay
June 17, 1991	47.678
June 17, 1991 after tamping (partial survey)	47.678
July 23, 1991	50.869

The elevation changes over both sections for all the sets of unloaded profile measurements are indicted in Figures 78 and 79 for the clay and natural subgrades, respectively. The elevation change is referenced to the initial elevation. The figures are plotted against both distance and tie numbers.

Based on Figures 78 and 79, as well as Figures 38 to 59, the two sections were divided into three similar subsections as used for the stiffness tests. The natural subgrade profile subsections extend beyond the natural subgrade stiffness subsections. These subsections contain the data most suitable for analysis. The presentation of the profile measurements will present first all measurements taken in the field and second only the measurement applicable to the subsections.

The subsections for the unloaded profile measurements are as follows:

- Tie 464 to 430 for the clay subgrade subsection
- Tie 372 to 347 for the natural subgrade jointed subsection
- Tie 347 to 313 for the natural subgrade unjointed subsection

The clay subsection is the same as the full clay section except for elimination of the disturbed area where the drain was installed. The natural subgrade sections separate the total section surveyed into jointed and unjointed zones.

7.1 SETTLEMENT

The track settlement was calculated relative to the initial profile measured at 0 MGT taken on December 14, 1990. The average settlement in each total section was plotted against cumulative traffic as shown in Figures 80 and 81 for the clay and natural subgrade, respectively. The inner and outer rail settlements are shown separately. Figure 82 shows the settlement of each subsection separately.

To mathematically describe the settlement rate of each section, a power function was fitted through the average settlement determined from each set of unloaded profiles. The power function starts at 0 settlement and 0 MGT, and rises at a rate described by *a* and *b* as follows:

$$y = ax^b, \tag{8}$$

where y = settlement,

x = traffic MGT,

a = scale factor,

b = shape factor.

This equation, determined from a non-linear regression (Marquardt-Levenberg algorithm) to fit the data in Figures 80 to 82, is plotted for each set of data on the figures, and the values of the parameters *a* and *b* are also shown on the figures.

7.2 ROUGHNESS

Track roughness is determined by the unevenness that occurs over a designated length of track. The designated length may be the response length of a vehicle. A response length of a vehicle is a wavelength that occurs in track that is long enough so that even greater wavelengths that are present in the track can be ignored because they do not influence the vehicle response.

To remove the long wavelength components from the measured elevations a "boxcar filter" can be used.[8] A boxcar filter calculates the mean of all the elevations in the response length under consideration. The deviation of the point in the center of the response length is calculated by subtracting the mean elevation from the elevation of the center point.

For the TLTM, the response length was taken as 12.2 m (40 ft) and the measurement spacings were 1.5 m (5 ft). The unevenness of a section of track was determined as follows:

$$R = \sqrt{\frac{\sum_{i=1}^{n} d_i^2}{n}} \quad , \tag{9}$$

where R = roughness,

n = number of observations in subsection, and

d_i= deviations as calculated above.

Figures 83 and 84 show the relationship of roughness to traffic for both sections, and Figure 85 shows the relationship for each subsection.

To mathematically describe the increase in track roughness with traffic for each section, the following modification of Eq. 8 may be used:

$$y = r + ax^b , \tag{10}$$

where r = initial roughness (0 MGT)

8.0 TRACK RECORDING CAR

The track geometry at FAST was measured using a Plasser EM80 recording car. The mid-chord ordinate readings were taken over 9.5 m (31 ft) chord length every 300 mm (12 in.) along the rail. Mid-chord ordinate measurements over 9.5 m (31 ft) will be referred to as "top." Versine and cant measurements also were obtained.[8] The top mid-chord values were corrected to an 18.9 m (62 ft) base length. These measurements will be referred to as "profile" measurements. Figure 86 shows the geometry car axle configuration.

Table 15 gives the date of each measuring run and the cumulative traffic up to the date of each measuring run.

Figures 87 to 96 show the top measurements (31 ft chord) for both sections extending from tie 298 to 481. Figures 97 to 106 show the profile measurements (62 ft chord) for both sections over the same tie positions.

Table 15: Geometry Measuring Schedule	
Date	**Cumulative Traffic (MGT)**
December 14, 1990	0.0
December 18, 1990	1.255
January 4, 1991	2.207
February 6, 1991	5.109
February 14, 1991	8.543
March 4, 1991	13.330
April 2, 1991	20.427
April 10, 1991*	23.721
May 7, 1991*	35.880
May 24, 1991	38.989
June 7, 1991*	42.340
June 12, 1991	45.078
June 18, 1991	48.653

* Data not yet received

Track roughness, as measured by the recording car, was calculated from Eq. 9, using for the deviation, d_i, the mid-chord top measurements; i.e., no filter is applied to the data. Figures 107 and 108 show the change in roughness calculated from the top measurements for the clay and natural subgrade sections. Figure 109 shows the change in roughness for each subsection.

This technique for calculating roughness filters out waves with lengths equal to half the chord length and measures double the amplitude for waves with lengths equal to the recording car chord length.

9.0 TRACK LOADING

To measure the distribution of the wheel loads exerted onto a track, a set of axles loaded at 347 kN (78 kips) per axle or 173.5 kN (39 kips) per wheel was instrumented to measure the load when moving at 64 km/h (40 mph). At each wheel, the vertical and lateral loads were measured to 50 MGT. Figures 110 to 113 show the vertical and lateral wheel load distribution for each instrumented wheel. The average vertical wheel load and the static wheel load are indicated with horizontal lines in each figure.

At the time of testing, the HAL train normally consisted of 60 to 70 four-axle cars weighing 143 ton (315,000 lb) being pulled by four or five 4-axle 120-ton (264,000 lb) locomotives. The cumulative traffic over the sections, against days since the start of the experiment, December 14, 1990, is shown in Figure 114.

10.0 MAINTENANCE

Hand maintenance was performed as required at localized spots, but when the track geometry exceeded the FRA Class 4 standards, the section was lined and surfaced using a Canron Electromatic tamper. The various maintenance inputs during the experiment are given in Tables 16 and 17. Figure 115 shows the difference in the maintenance input required between the clay and the natural subgrade sections.

11.0 SUMMARY AND CONCLUSIONS

A trial test section was constructed to determine the feasibility of achieving a low track modulus using a soft clay layer. The low track modulus test section at FAST was desired as a contrast to the high track modulus on the natural FAST subgrade to provide information on the effect of track modulus on track performance.

Table 16: Clay Subgrade Maintenance Input						
Date	**Traffic**	**Work Performed**	**Ties**		**Maintenance**	
			Inner	**Outer**	**Spot**	**Mechanized**
	(MGT)				**(Number of ties)**	
Feb. 20, 1991	9.832	Lined track	430-418	430-418	12	
April 10, 1991	23.721	Raise and tamp	440		1	
April 15, 1991	25.699	Surface & tamp	464-404	464-404		60
May 5, 1991	34.981	Raise and tamp	430-400	430-400	30	
May 9, 1991	37.278	Raise and tamp	429		1	
May 10, 1991	37.638	Raise and tamp		460-410	50	
May 23, 1991	38.775	Raise and tamp (after drain installation)	464-404	464-404		60
May 24, 1991	38.989	Raise and tamp	425-400	425-400	25	
June 12, 1991	45.078	Raise and tamp	406-401 432-420	413-408	11	
June 17, 1991	47.678	Lined track	432-408	432-408	24	
				Total:	154	120

Table 17: Natural Subgrade Maintenance Input						
Date	**Traffic**	**Work Performed**	**Ties**		**Maintenance**	
			Inner	**Outer**	**Spot**	**Mechanized**
	(MGT)				**(Number of ties)**	
Feb. 13, 1991	7.812	Raise and tamp	380		1	
Feb. 25, 1991	11.178	Raise and tamp		355	1	
March 28, 1991	20.022	Raise and tamp	380		1	
April 4, 1991	22.358	Raise and tamp		357	1	
April 10, 1991	24.131	Raise and tamp		355	1	
April 15, 1991	25.699	Surface & tamp	385-325	385-325		60
May 6, 1991	34.981	Raise and tamp		355	1	
May 23, 1991	38.775	Raise and tamp		356	1	
June 7, 1991	42.340	Raise and tamp		355	1	
June 17, 1991	47.678	Raise and tamp		355	1	
				Total:	9	60

The low track modulus condition was obtained by excavating a 1.52 m (5 ft) deep trench 30.5 m (100 ft) long in the natural subgrade, and then filling the trench with soft clay. Details of the design and construction are given in the report along with information on the properties of the track components.

Vertical track stiffness was determined at various intervals of traffic by measuring the rail deflections corresponding to a range of applied loads. The load-deflection relationship was nearly linear initially but became progressively curved with increasing traffic. The portion of the curve below a load of 44.5 kN (10 kips) is believed to represent the extent of voids or slack between the tie and ballast. The track modulus or stiffness corresponding to this load range is termed the seating modulus or stiffness. The portion of the curve from a load of 44.5 kN (10 kips) to a load of 178 kN (40 kips) was approximately linear and represents the track stiffness with the slack removed. This track modulus or stiffness is termed the contact modulus or stiffness.

The contact track modulus of the clay stiffness clay section was about 50 percent of that for the adjacent section with the natural stiff subgrade. Because the only significant difference between the two sections is the upper 1.52 m (5 ft) of subgrade, the difference in modulus was caused by the difference in the upper subgrade.

Rail deflection basins were measured under the seating and maximum verical loads. The basin was observed to extend 2.5 m (8.2 ft) each side of the load point.

CPT's were conducted to obtain profiles of subgrade strength and stiffness. The profiles in the low track modulus section showed the soft clay layer. The CPT appeared to be a useful method for representing the subgrade effect on track modulus.

Unloaded vertical track profiles were measured by top of rail level surveys. These were obtained initially and at periodic traffic intervals. From these profiles, the average track settlement with traffic was calculated. Within a tamping cycle for both the clay and the natural subgrade sections, settlement increased at a decreasing rate with increasing traffic. After the first 20 MGT of

traffic, the average settlement in the clay section was about 60 percent higher than in the natural subgrade section.

Track roughness was calculated from both filtered survey data and track geometry car data. Within a tamping cycle, roughness increased almost linearly with increasing traffic in the clay subgrade section, but at a diminishing rate in the natural subgrade section. After the first 20 MGT of traffic, the roughness in the clay section was 60 percent to 90 percent greater than that in the natural subgrade section.

Considerably more tamping was required for the clay section than for the natural subgrade section. However, the clay subgrade did not fail during 50 MGT of traffic.

Ballast samples were taken after 50 MGT of traffic. More ballast breakdown appeared to occur in the clay section than in the natural subgrade section. However, because the initial gradations were not obtained, this observation is uncertain.

This study showed that the test section constructed using an imported clay layer was successful in achieving the desired low track modulus. The study further showed that the low track modulus section performance was very different from that of the higher modulus natural subgrade section.

REFERENCES

1. Trevizo, M. C. "FAST/HAL Ballast and Subgrade Experiments." AAR, Transportation Test Center, Pueblo, Colorado, AAR Report R-788, FRA/ORD-91/10, August, 1991.

2. Roner, C. J. and Selig, E. T. "Ballast Shape Test Methods." Report No. AAR84/316I, Department of Civil Engineering, University of Massachusetts, Amherst, Massachusetts, June, 1985.

3. Adegoke, C. W. and Selig, E. T. "Observed Subbased and Subgrade Conditions at the FAST Track." Project Report, Ballast Compaction Study, Department of Civil Engineering, State University of New York, Buffalo, February, 1977.

4. Thompson, M. R. "Ballast and Subgrade Materials Evaluation." Report No. FRA/ORD-77/32, Department of Civil Engineering, University of Illinois, Urbana-Champaign, Illinois, December, 1977.

5. Stewart, H. E. "Index and Property Testing of FAST Subgrade." Report No. OUR-80-240I, Department of Civil Engineering, University of Massachusetts, Amherst, Massachusetts, March, 1980.

6. Coleman, D. M. "Results of Laboratory Testing on Vicksburg "Buckshot" Clay." Testing performed by Soils Testing Facility, Soil and Rock Mechanics Division, Geotechnical Laboratory, U.S. Army Engineer Waterways Experiment Station, October, 1990.

7. Thompson, M. R. Unpublished test results, December, 1990.

8. Selig, E. T. et al, Lectures on Track geotechnology and substructure management. Lecture Notes. Department of Civil Engineering, University of Pretoria, 1992.

9. Zarembski, A. M., and Choros, J. "On the Measurement and Calculation of Vertical Track Modulus," *AREA Bulletin 675*, November-December 1979, pp. 156-173.

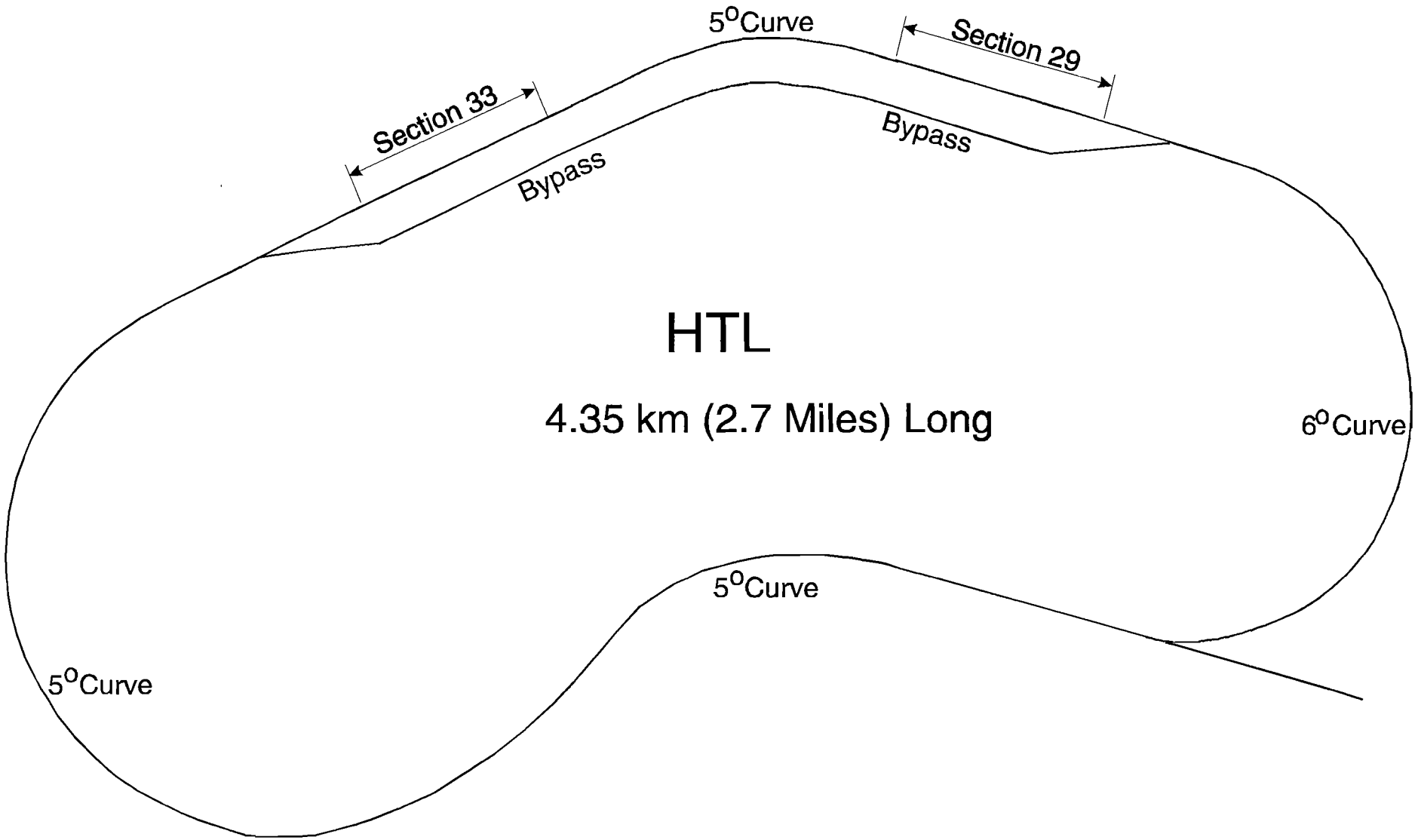

Figure 1: Layout of High Tonnage Loop at FAST

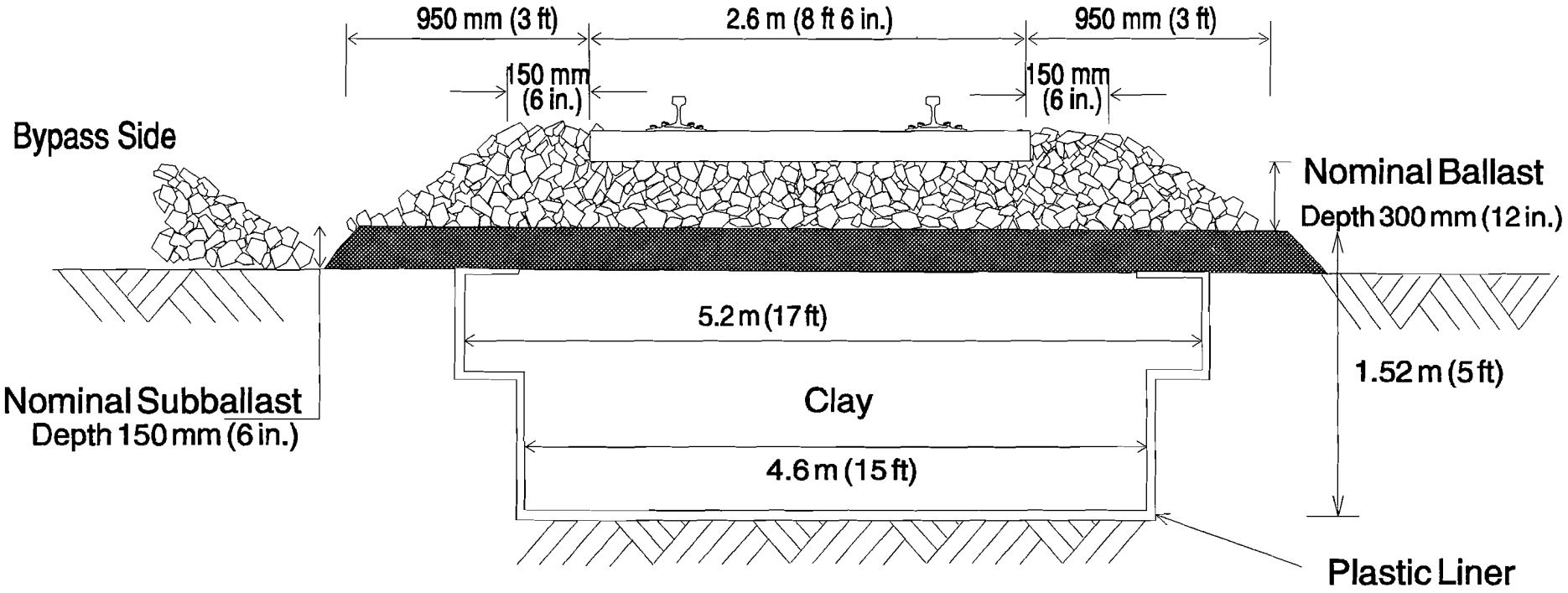

Figure 2: Cross Section of Clay Test Section

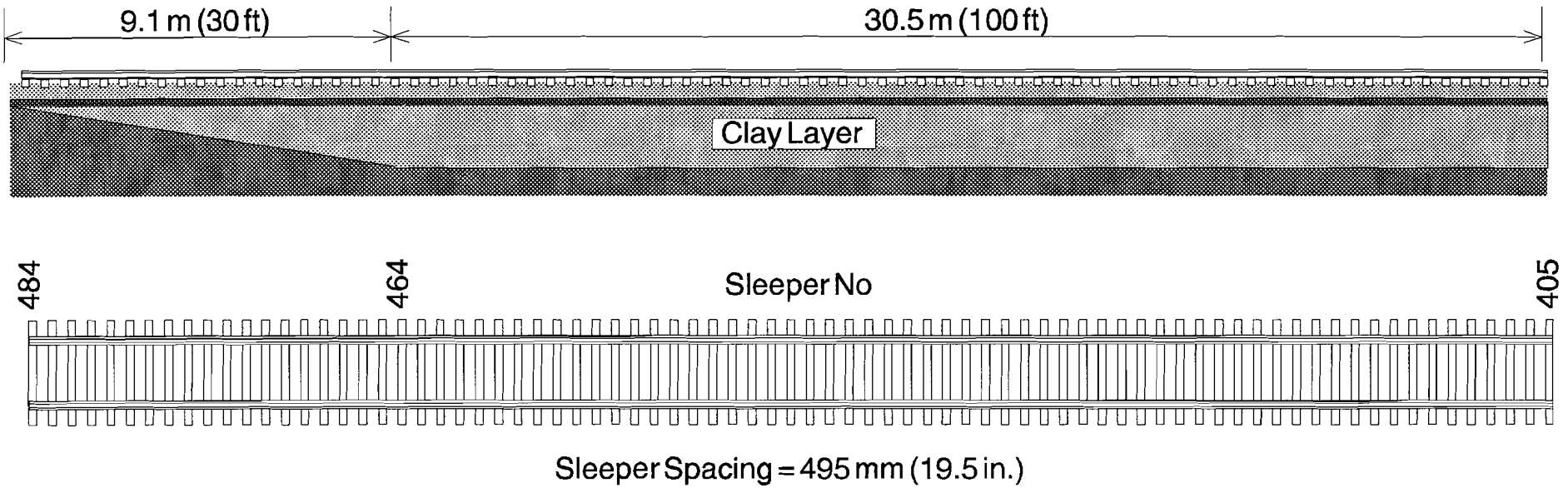

Figure 3: Longitudinal Section of Clay Section

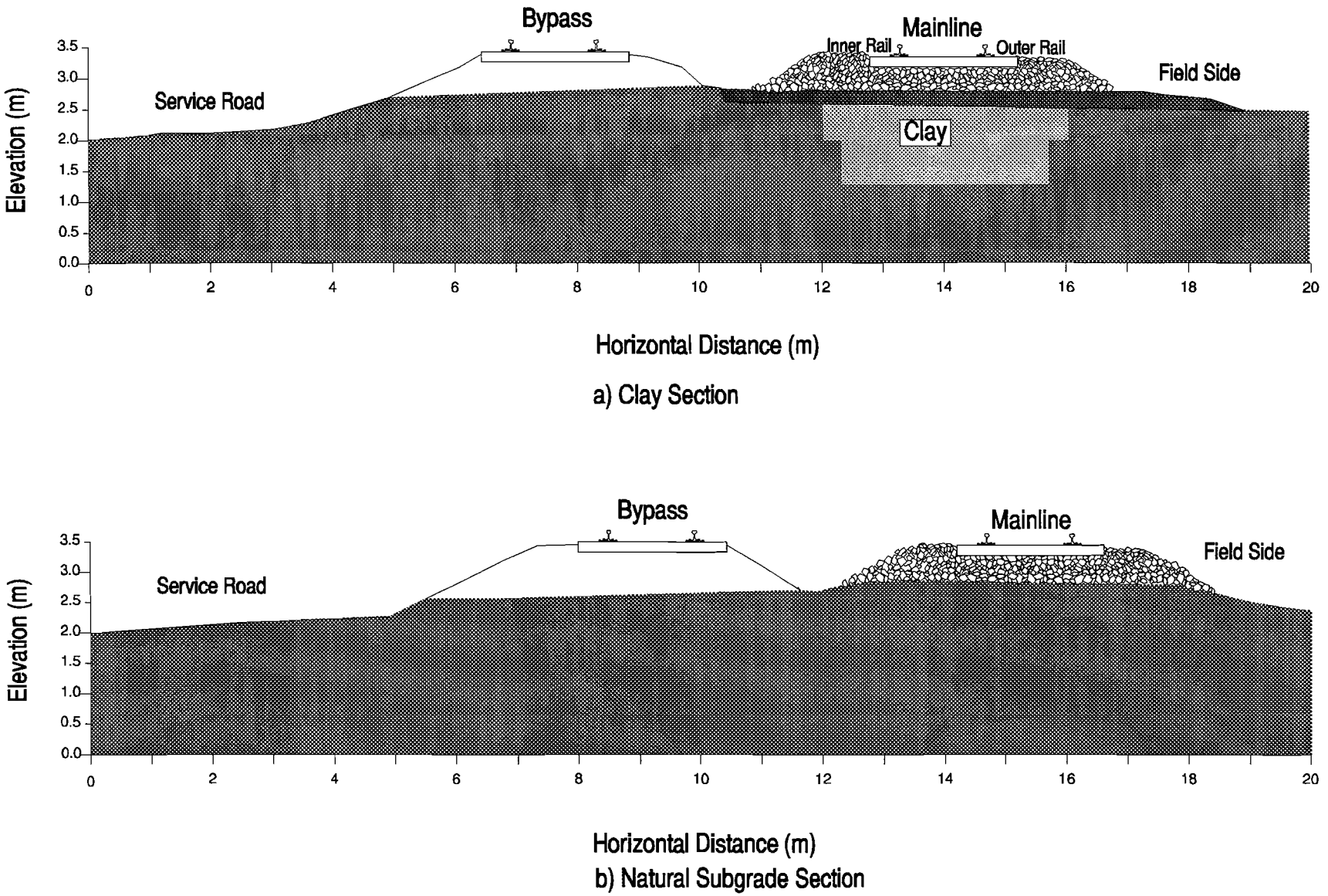

Figure 4: Cross Section of Both Sections Including Bypass

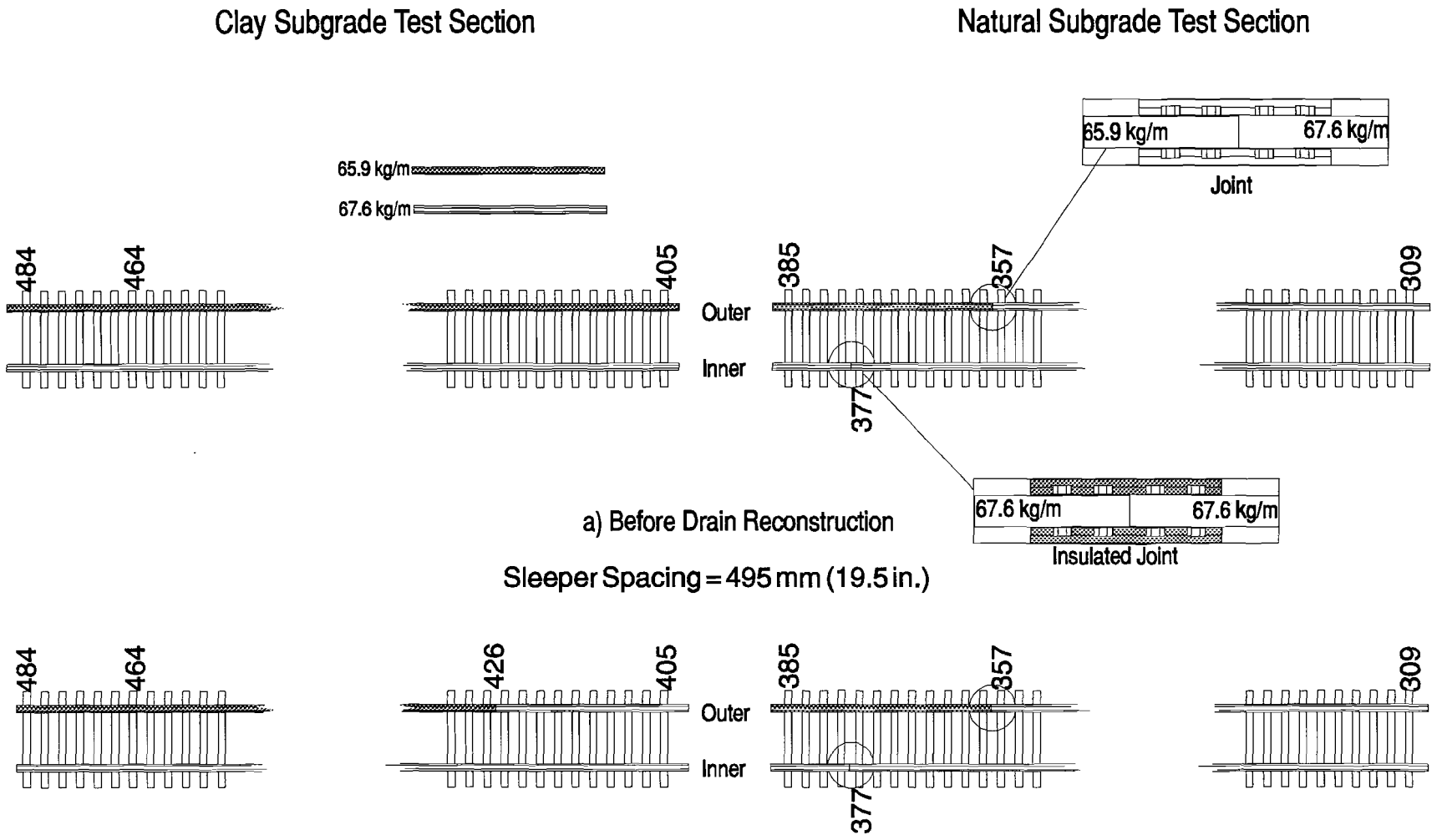

Figure 5: Tie Numbering and Joint Positions

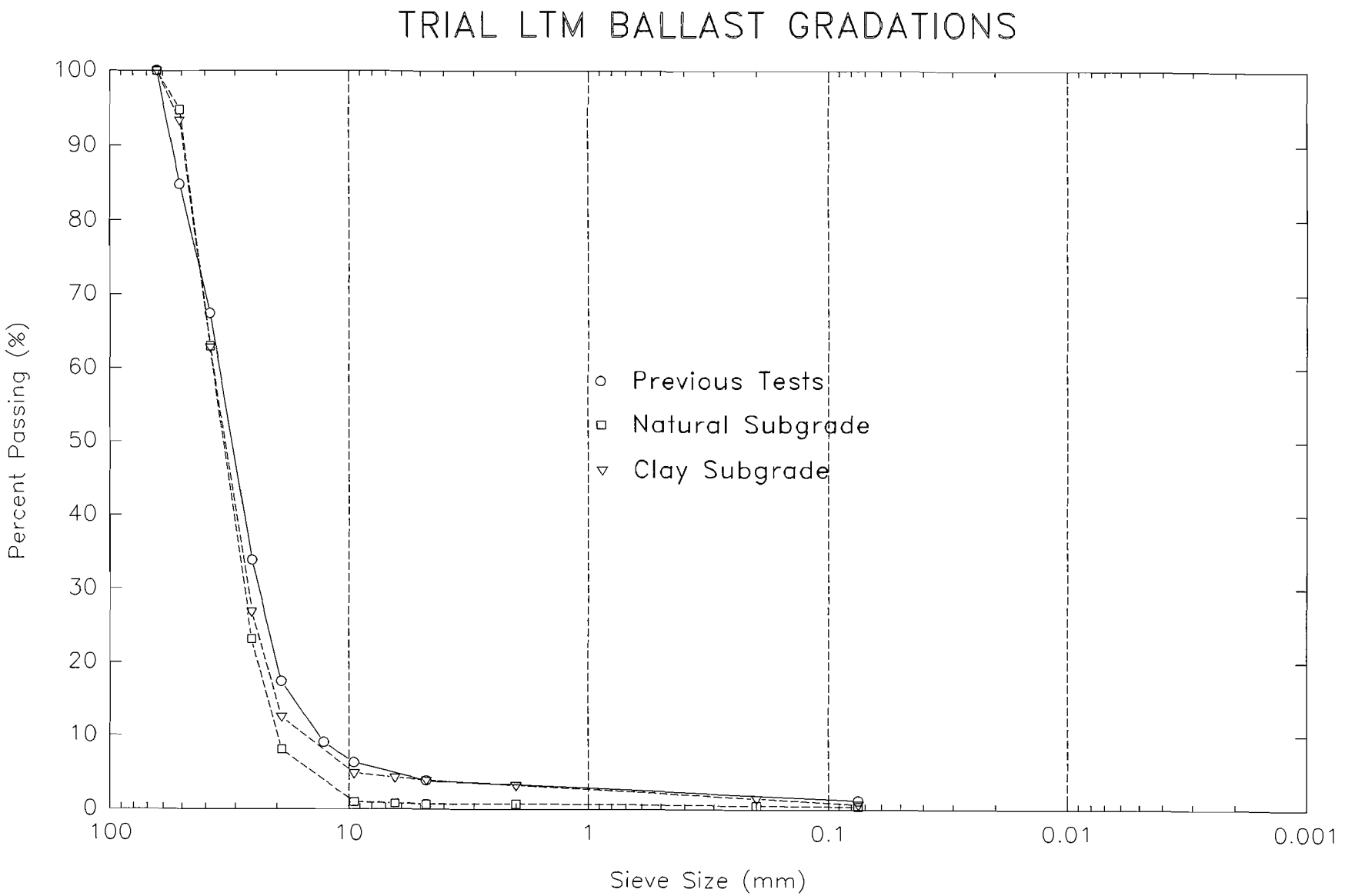

Figure 6: Ballast Gradations

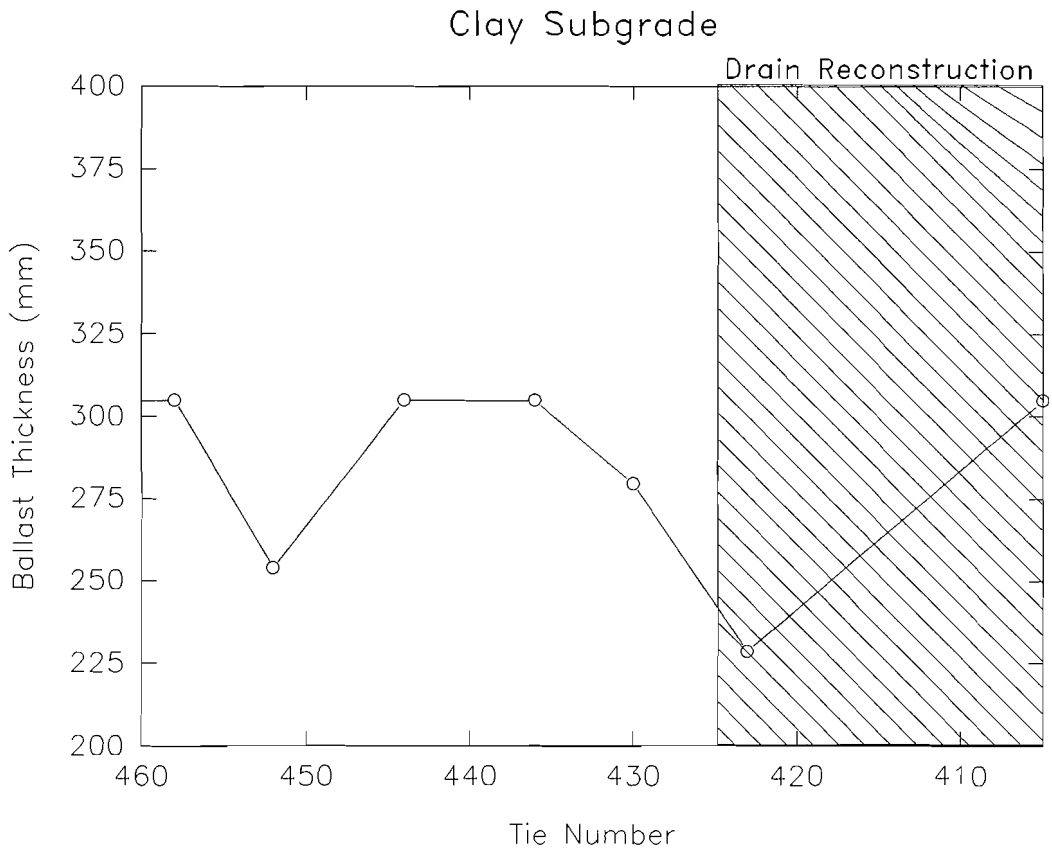

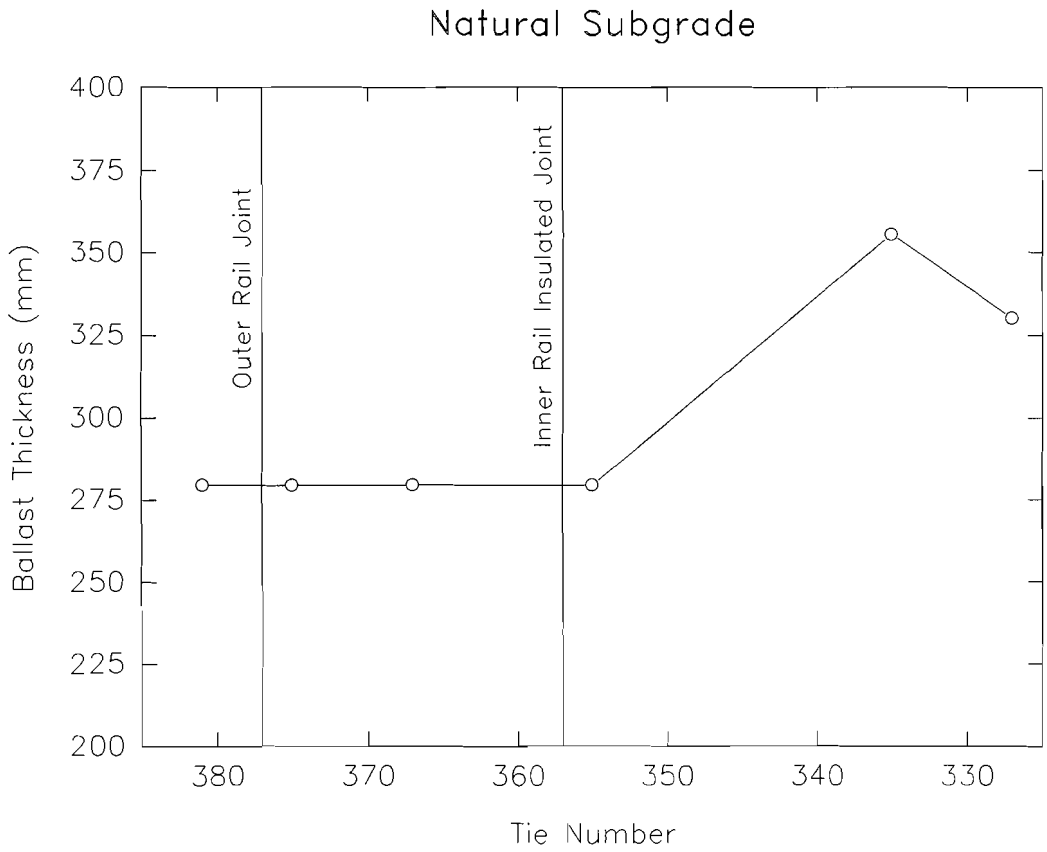

Figure 7: Ballast Thickness Variation

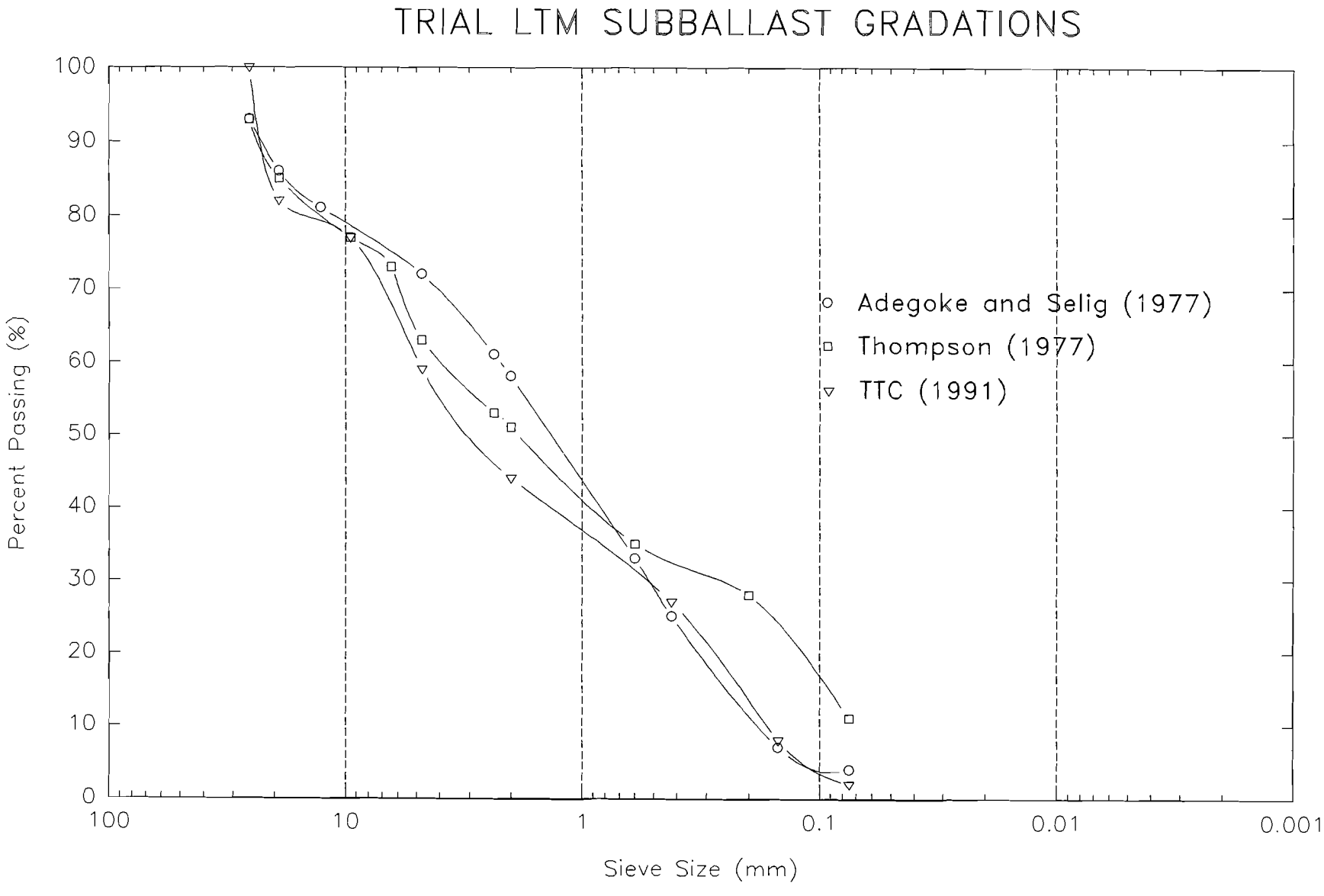

Figure 8: Subballast Gradations

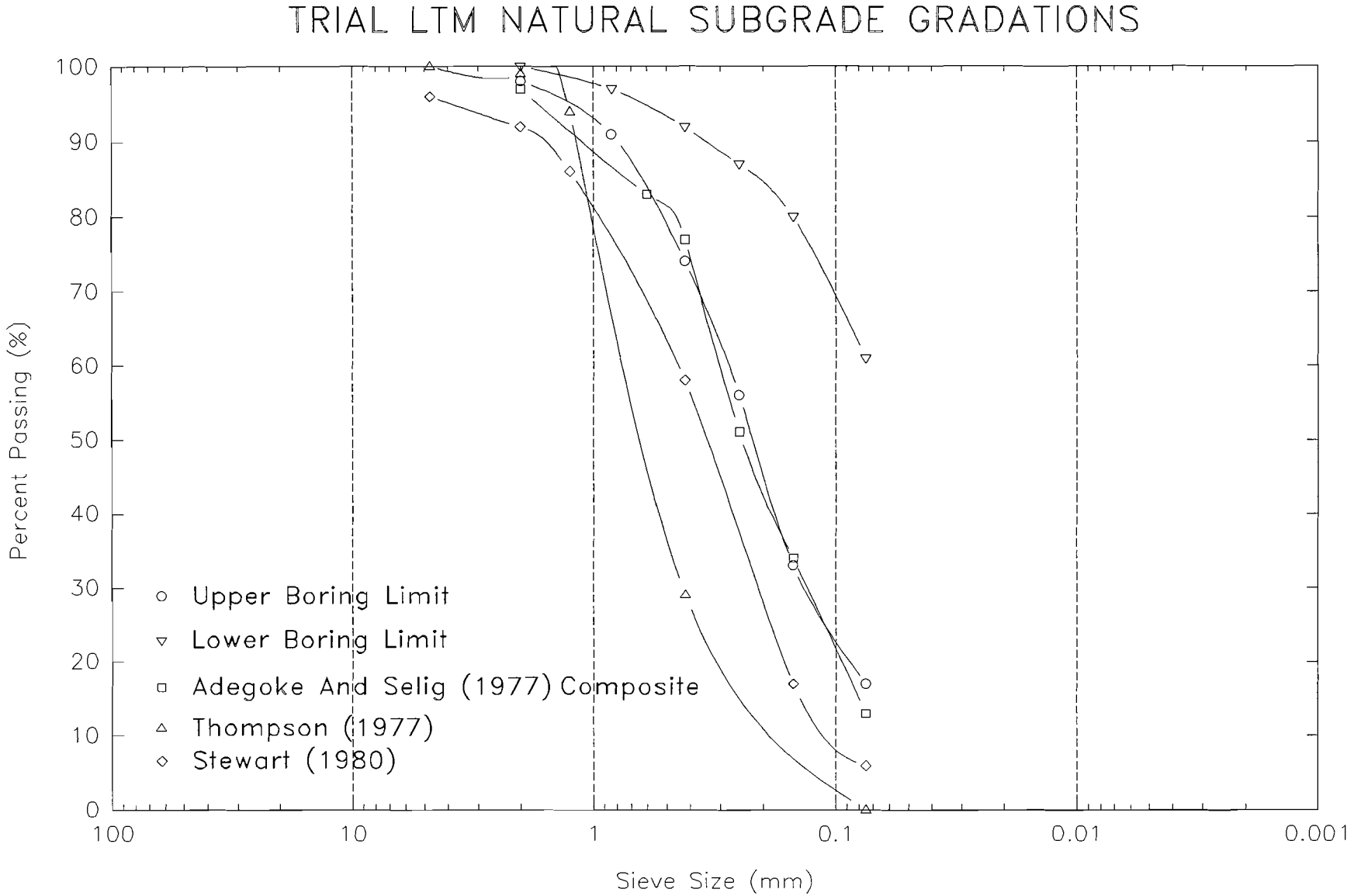

Figure 9: Natural Subgrade Gradations

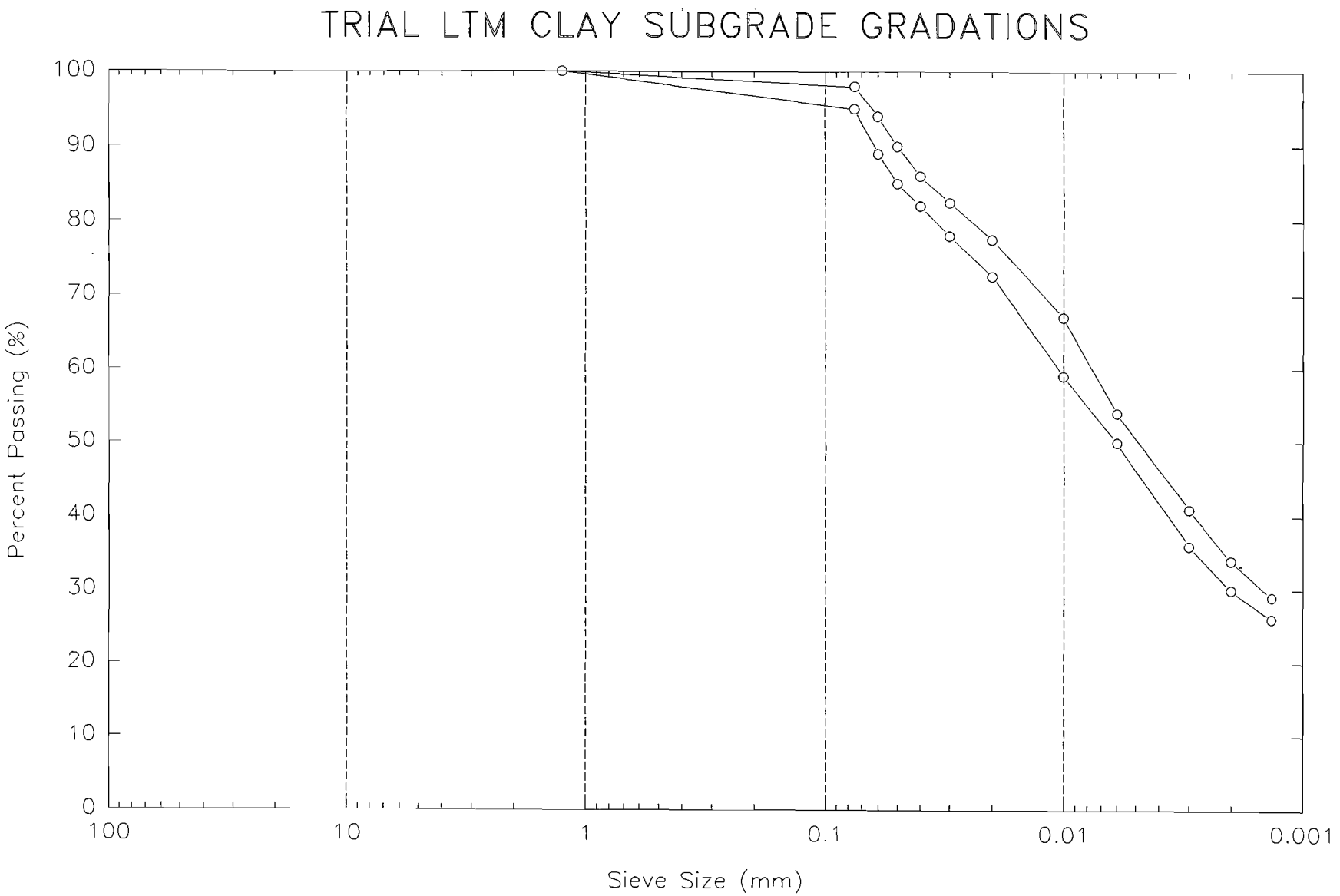

Figure 10: Range in Clay Gradations

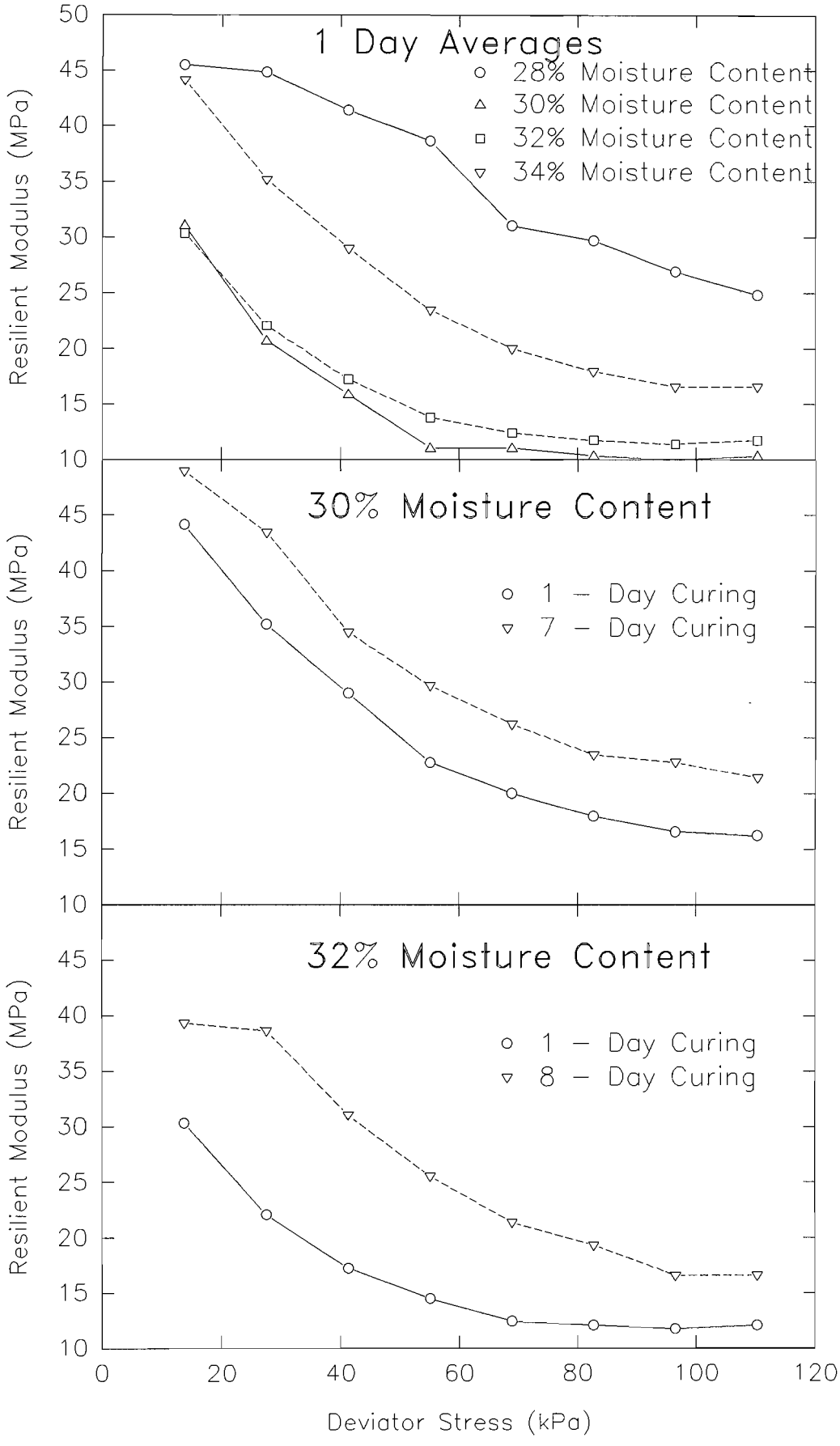

Figure 11: Clay Resilient Modulus

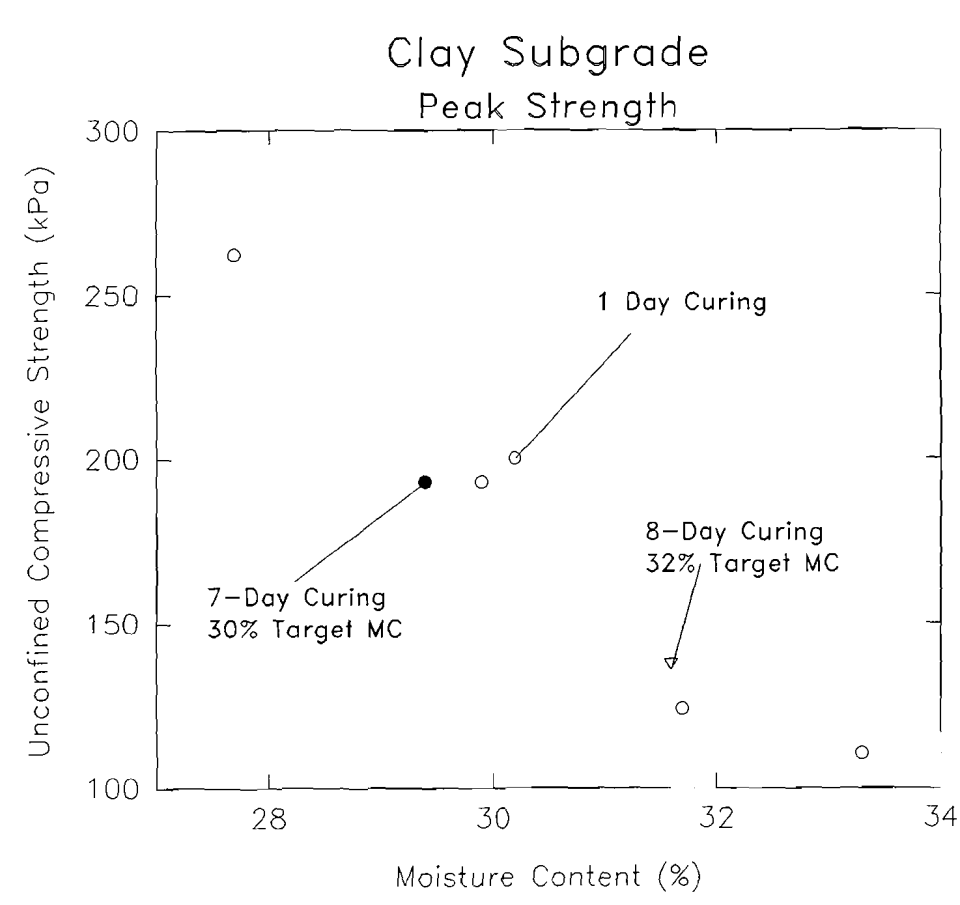

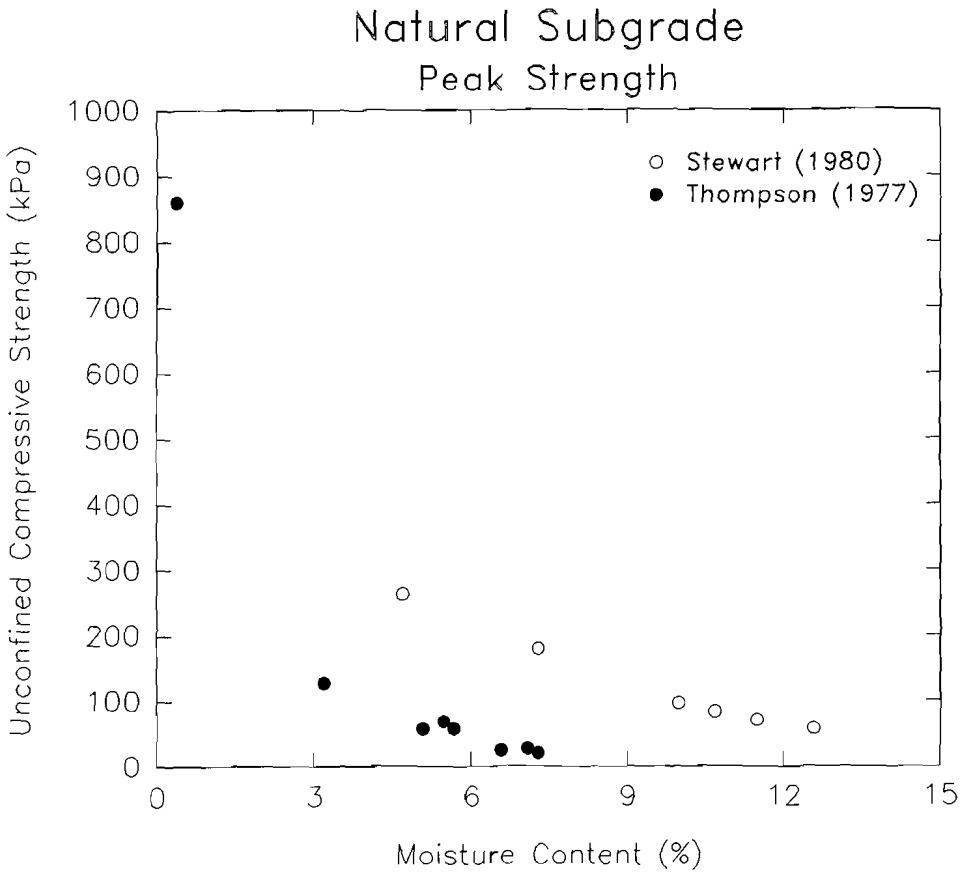

Figure 12: Unconfined Compression Strength

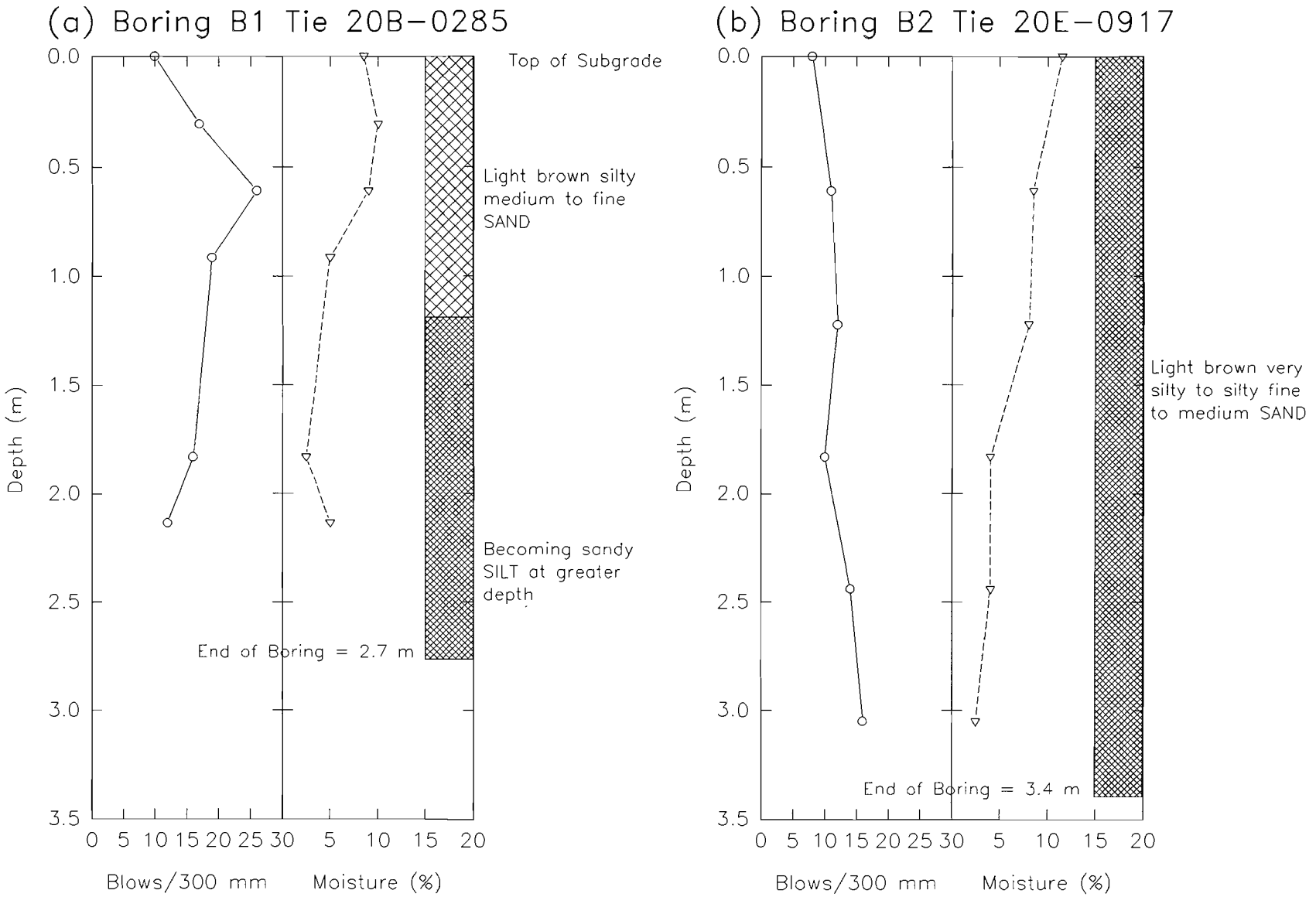

Figure 13: Boring Logs of Section 20

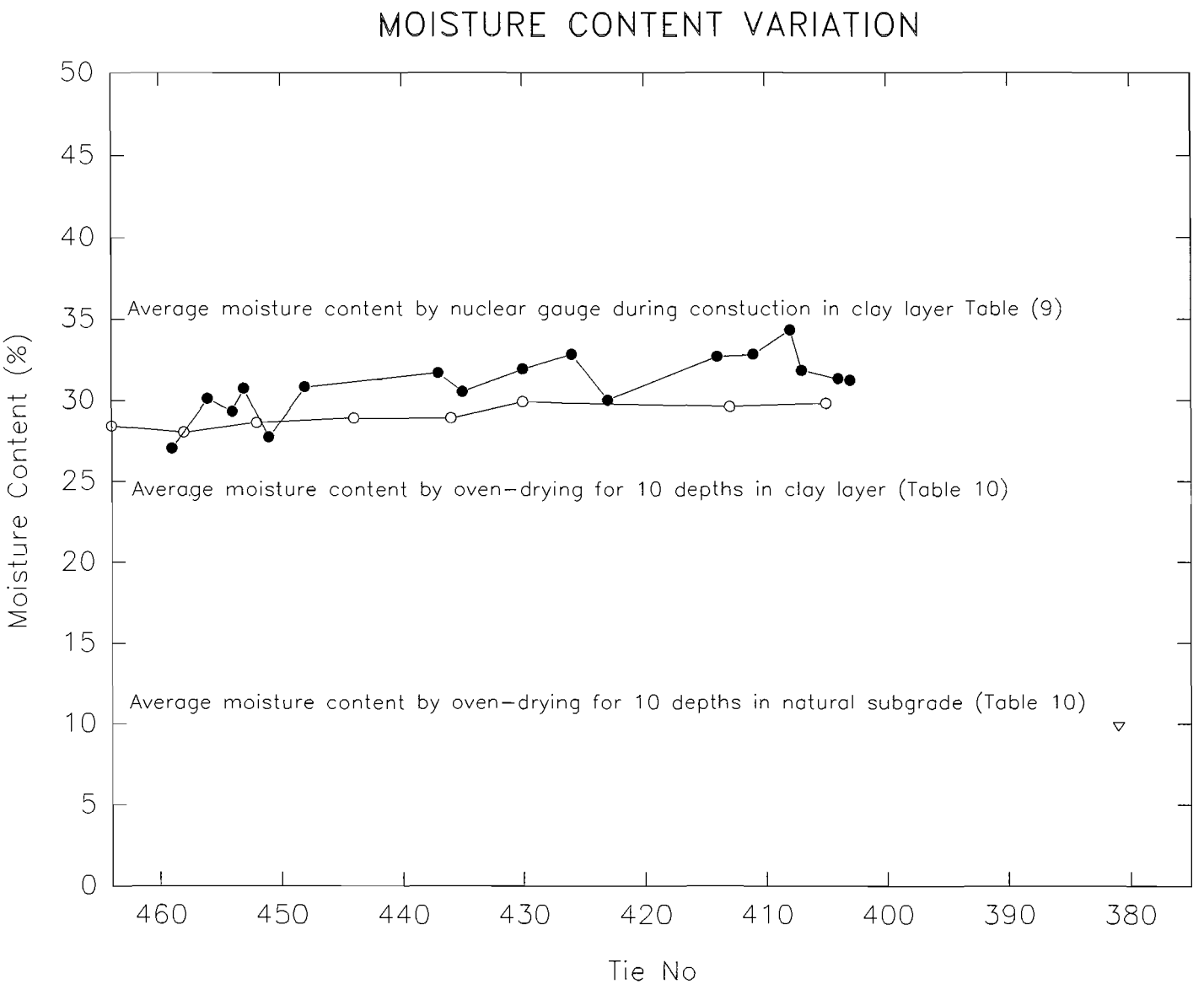

Figure 14: Moisture Distribution in Subgrade

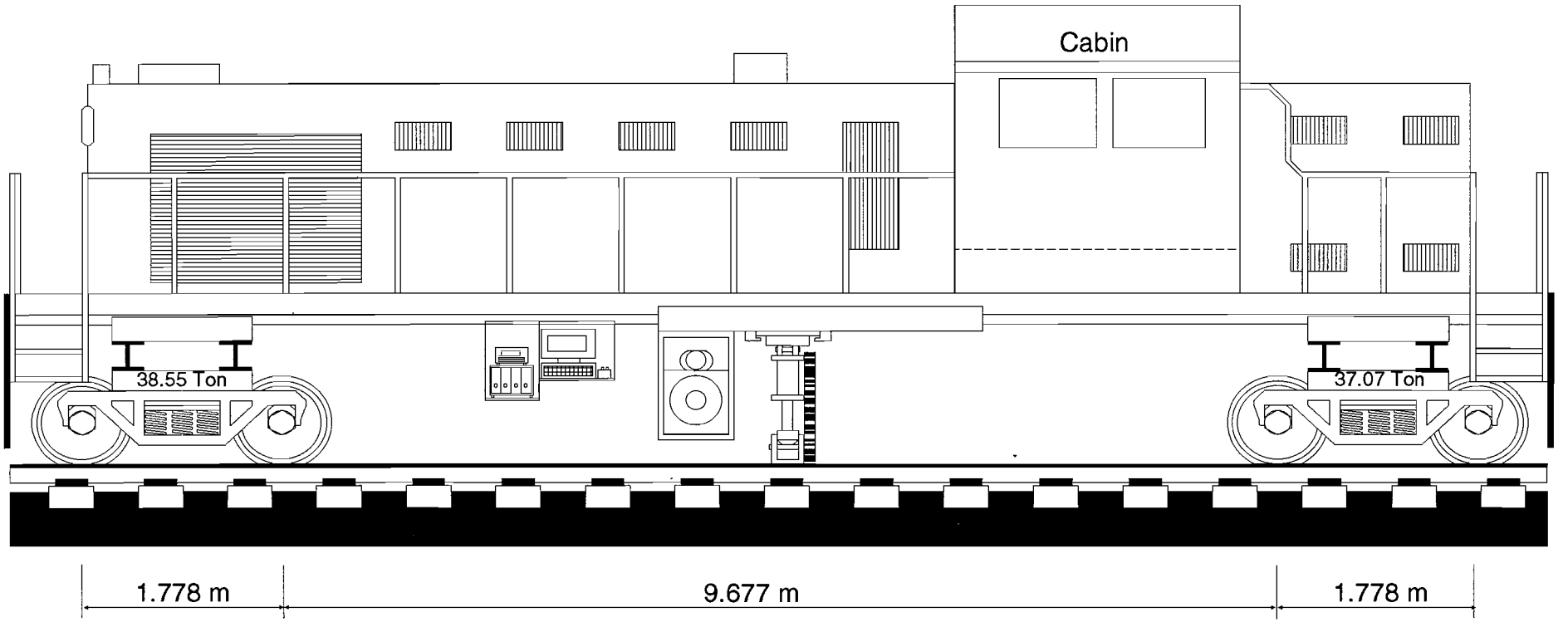

Figure 15: Track Loading Equipment

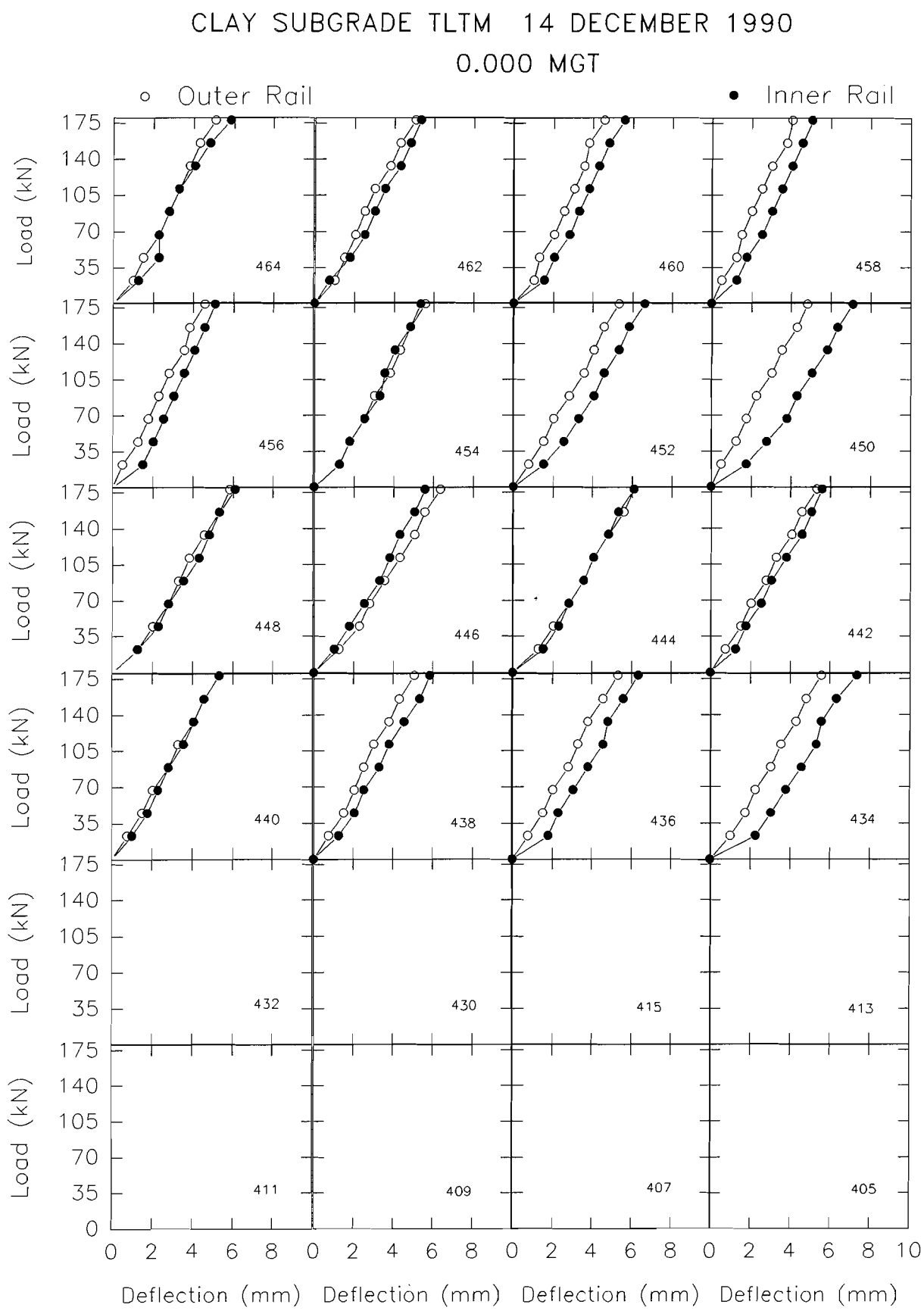

Figure 16: Clay Section Stiffness Test 14 December 1990

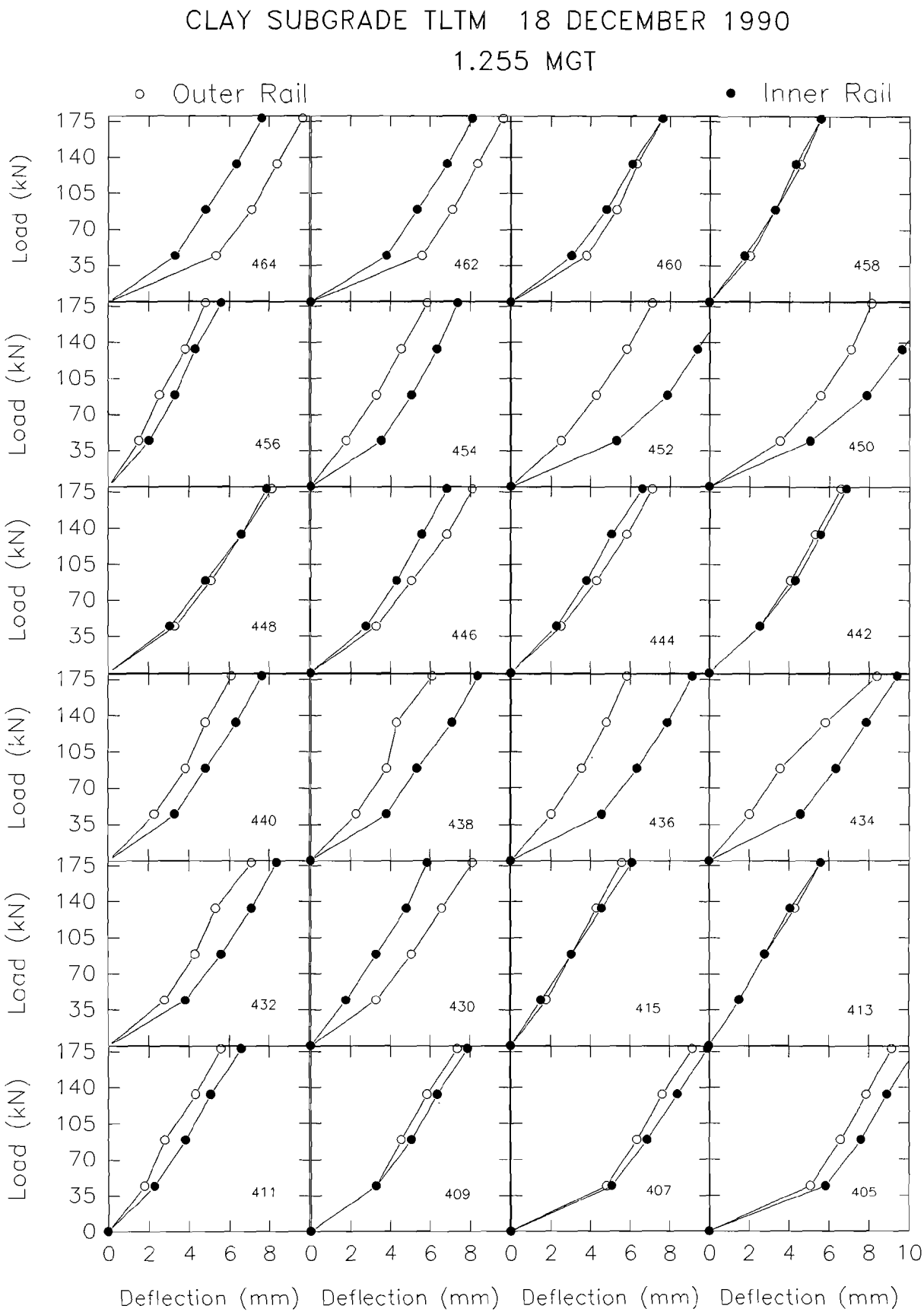

Figure 17: Clay Section Stiffness Test 18 December 1990

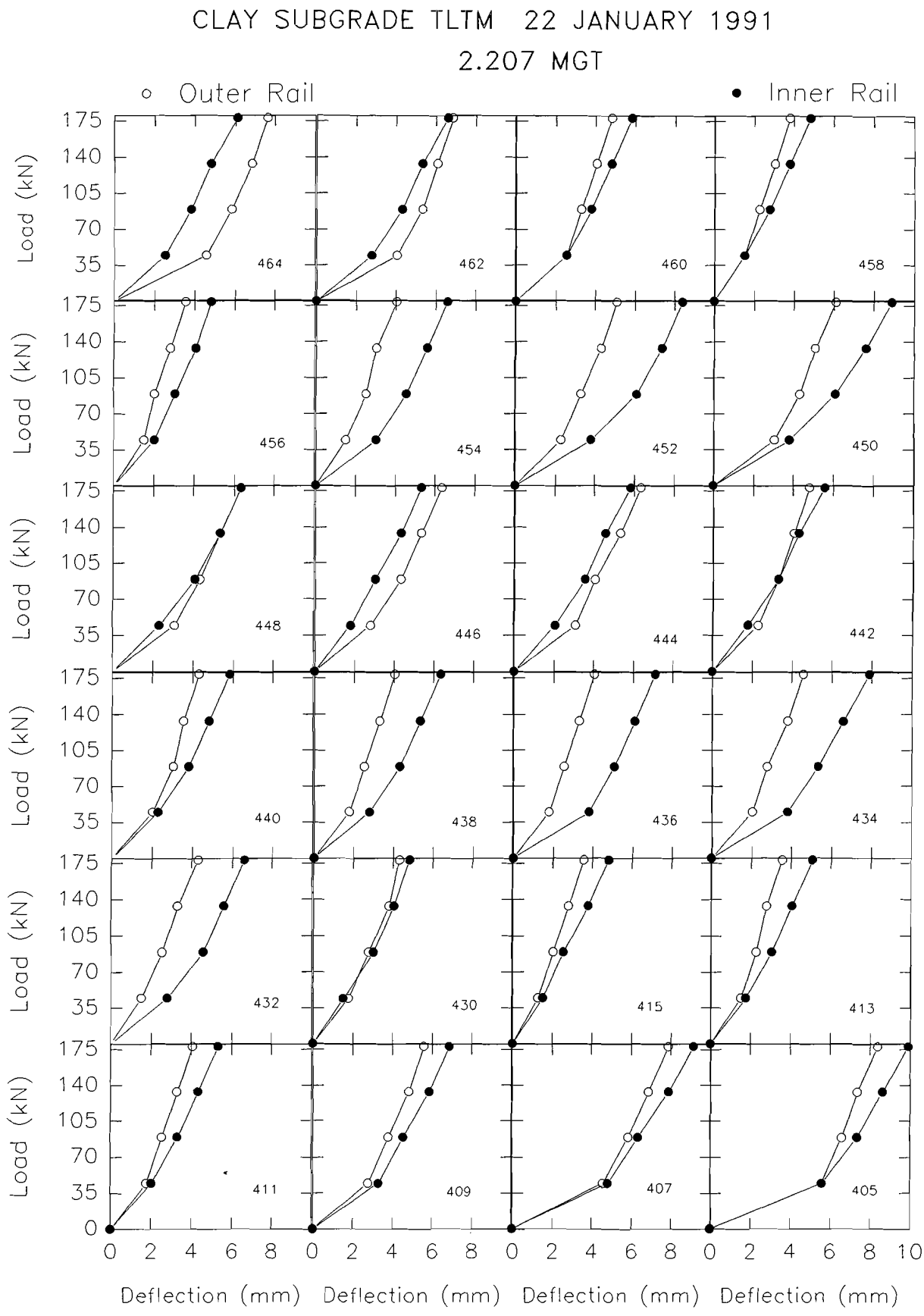

Figure 18: Clay Section Stiffness Test 22 January 1991

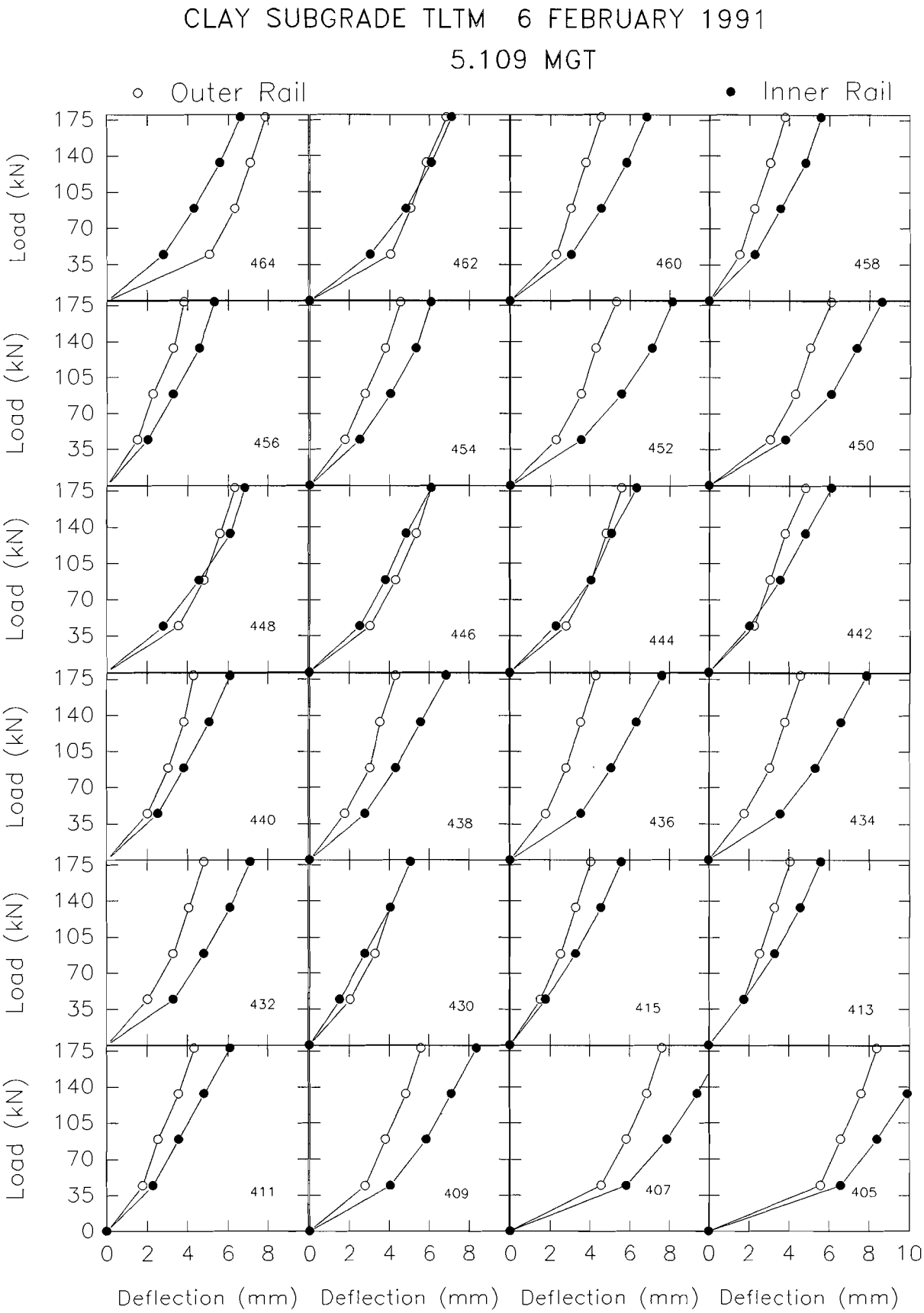

Figure 19: Clay Section Stiffness Test 6 February 1991

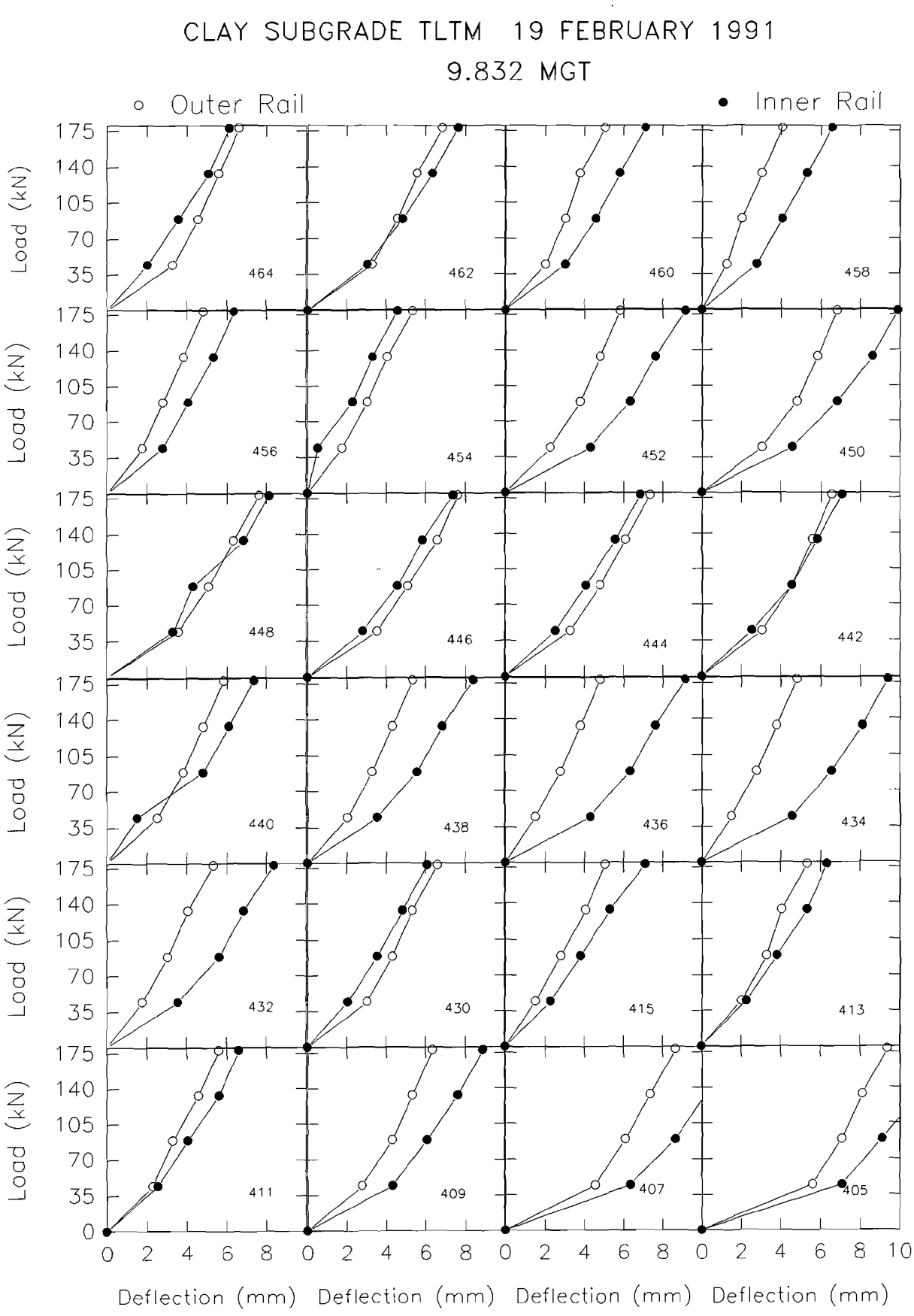

Figure 20: Clay Section Stiffness Test 19 February 1991

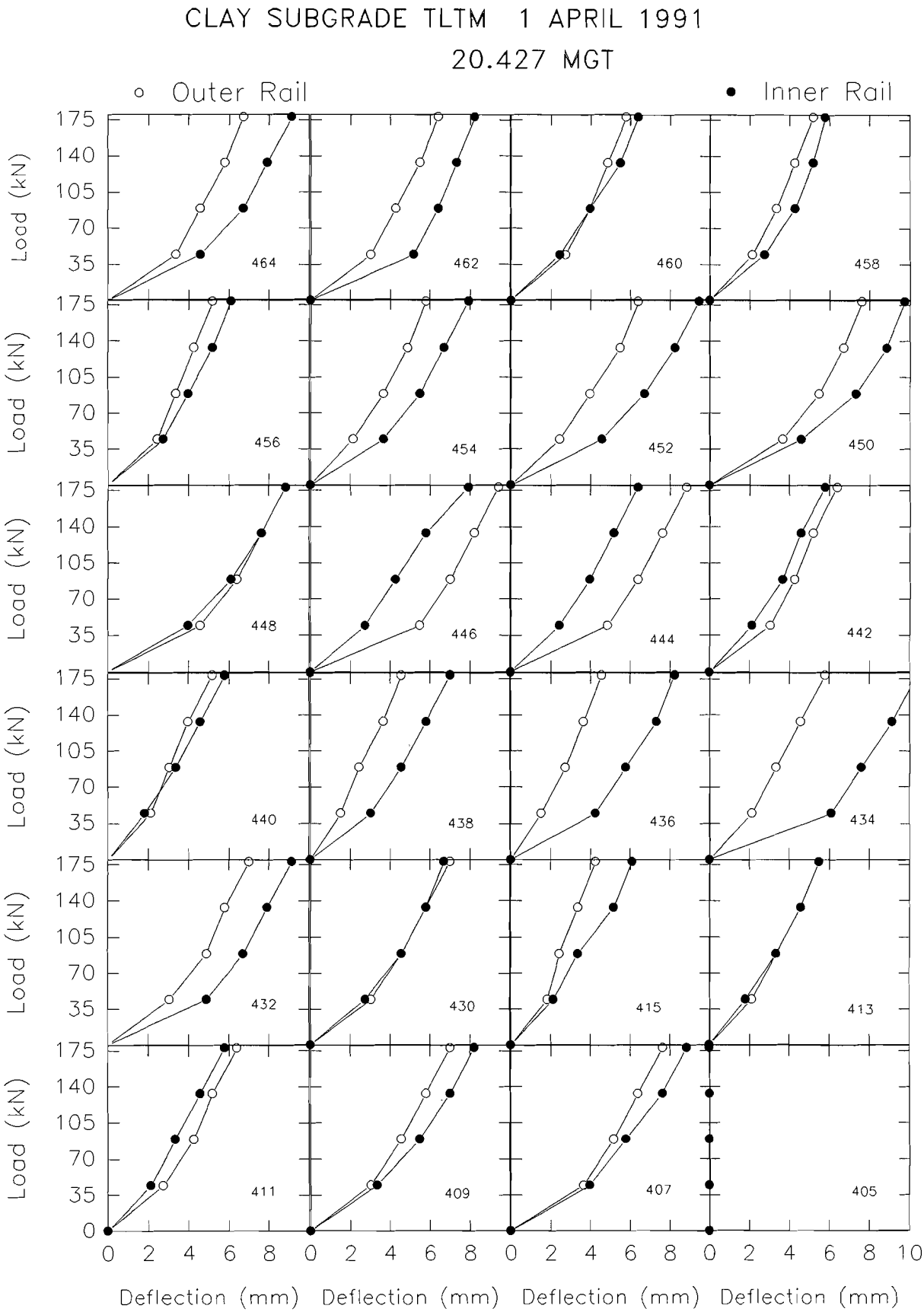

Figure 21: Clay Section Stiffness Test 1 April 1991

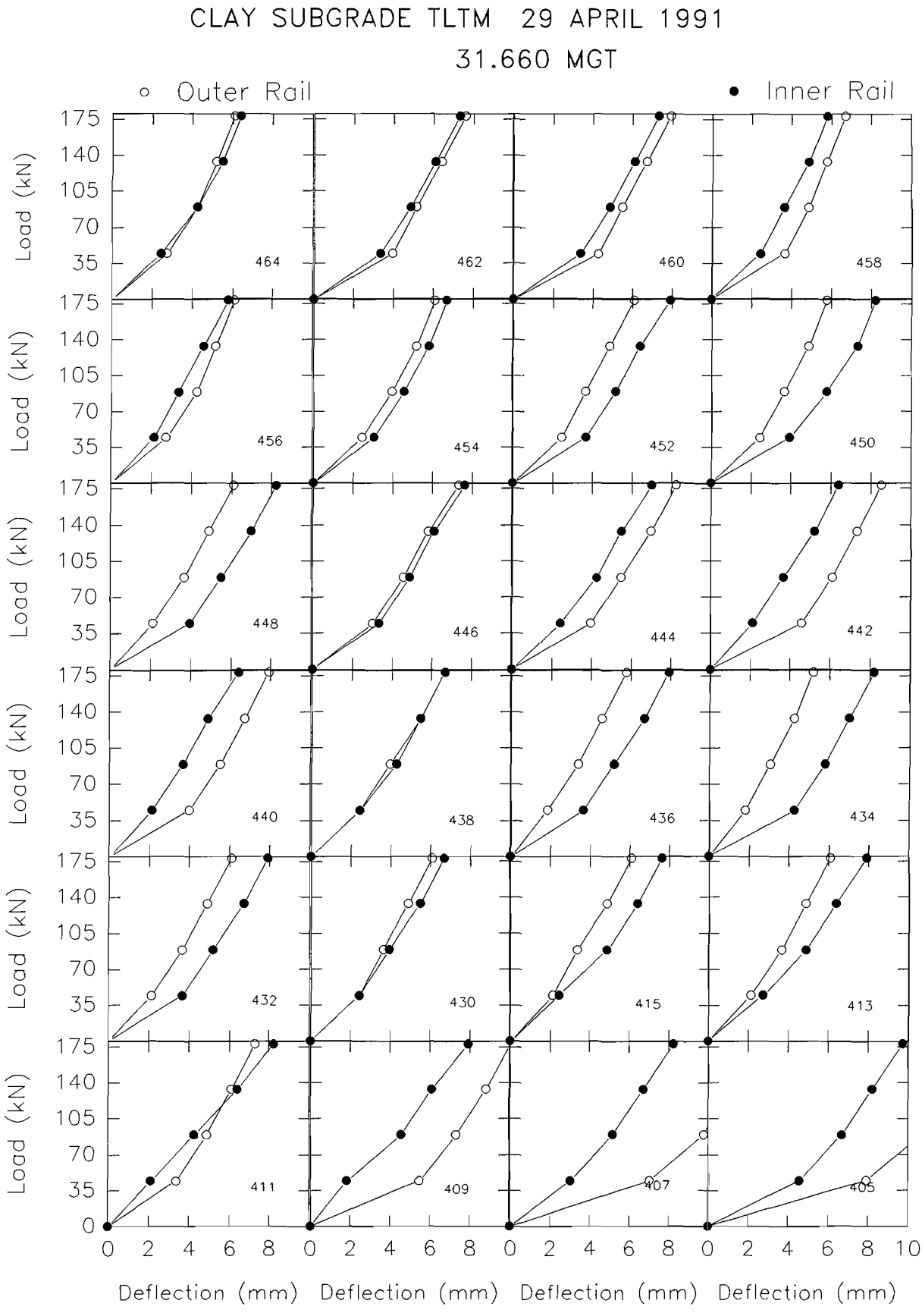

Figure 22: Clay Section Stiffness Test 29 April 1991

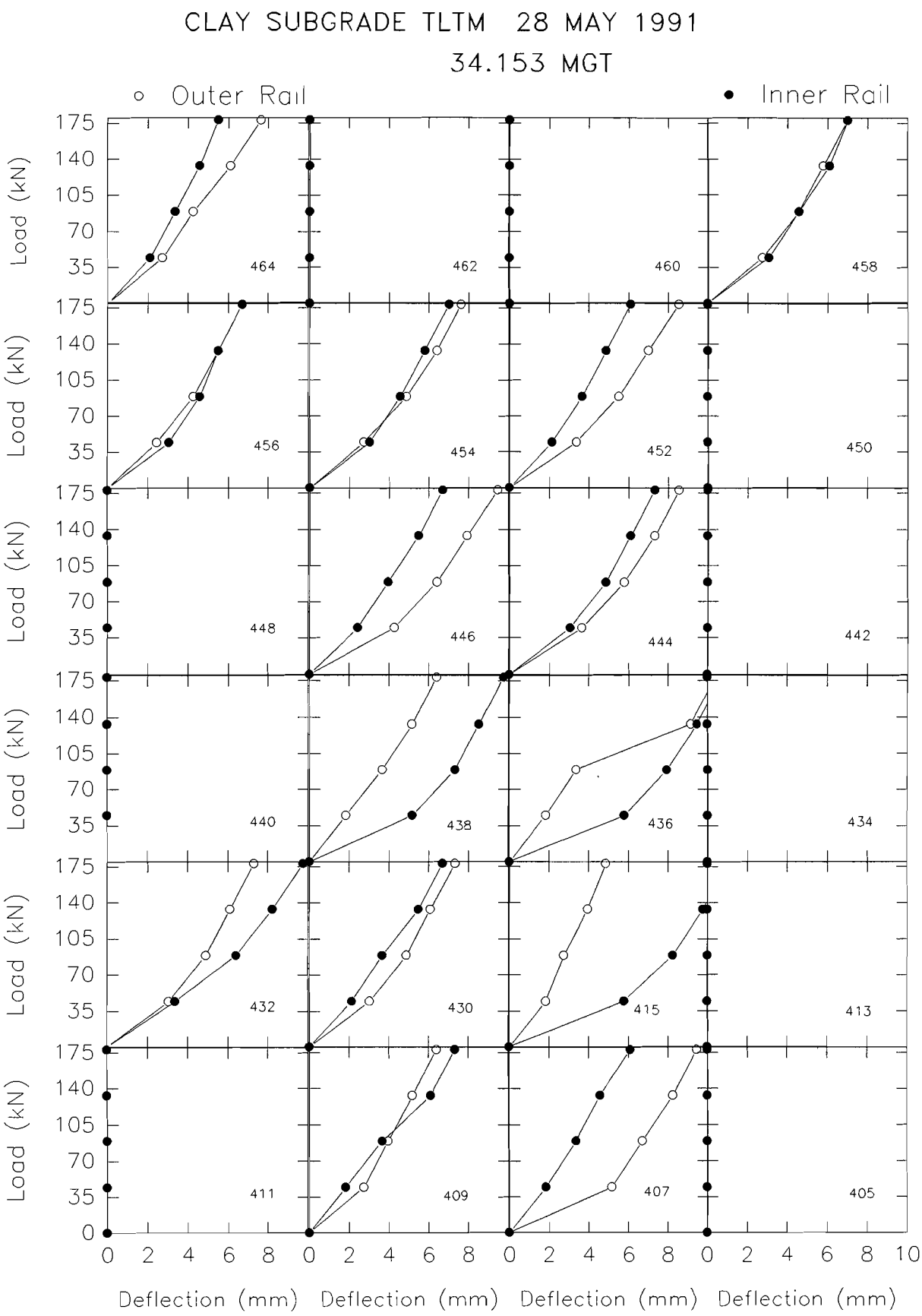

Figure 23: Clay Section Stiffness Test 28 May 1991

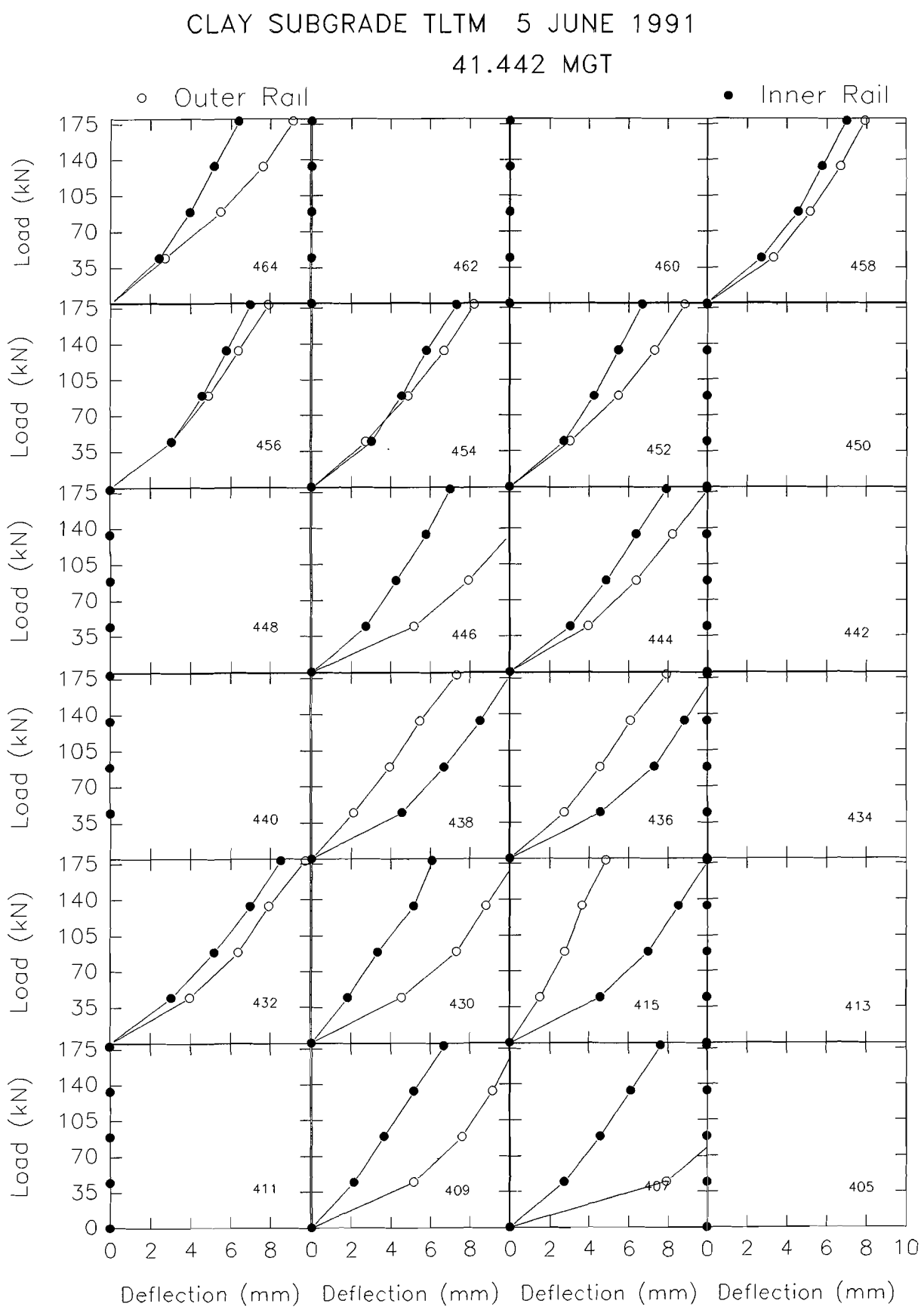

Figure 24: Clay Section Stiffness Test 5 June 1991

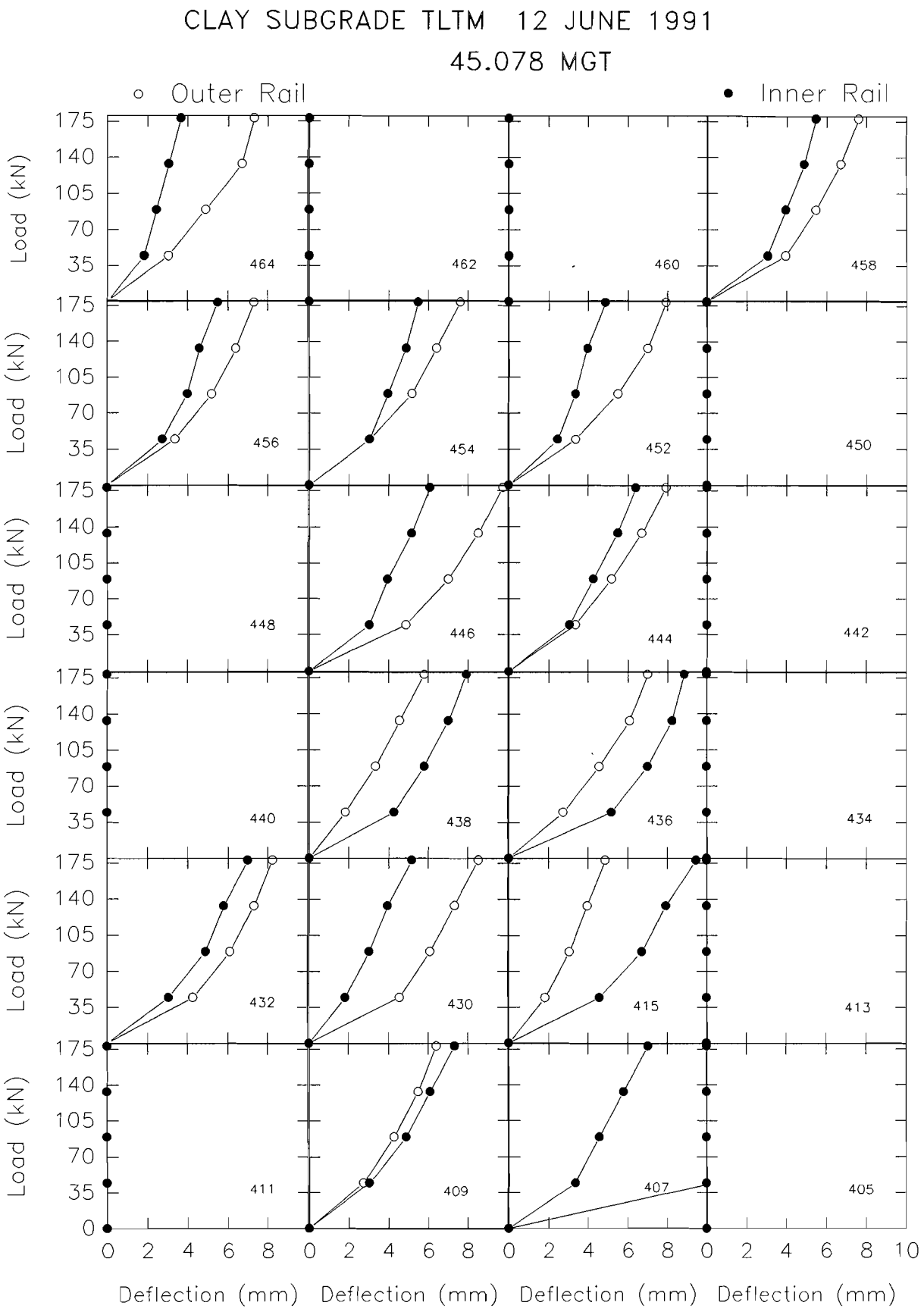

Figure 25: Clay Section Stiffness Test 12 June 1991

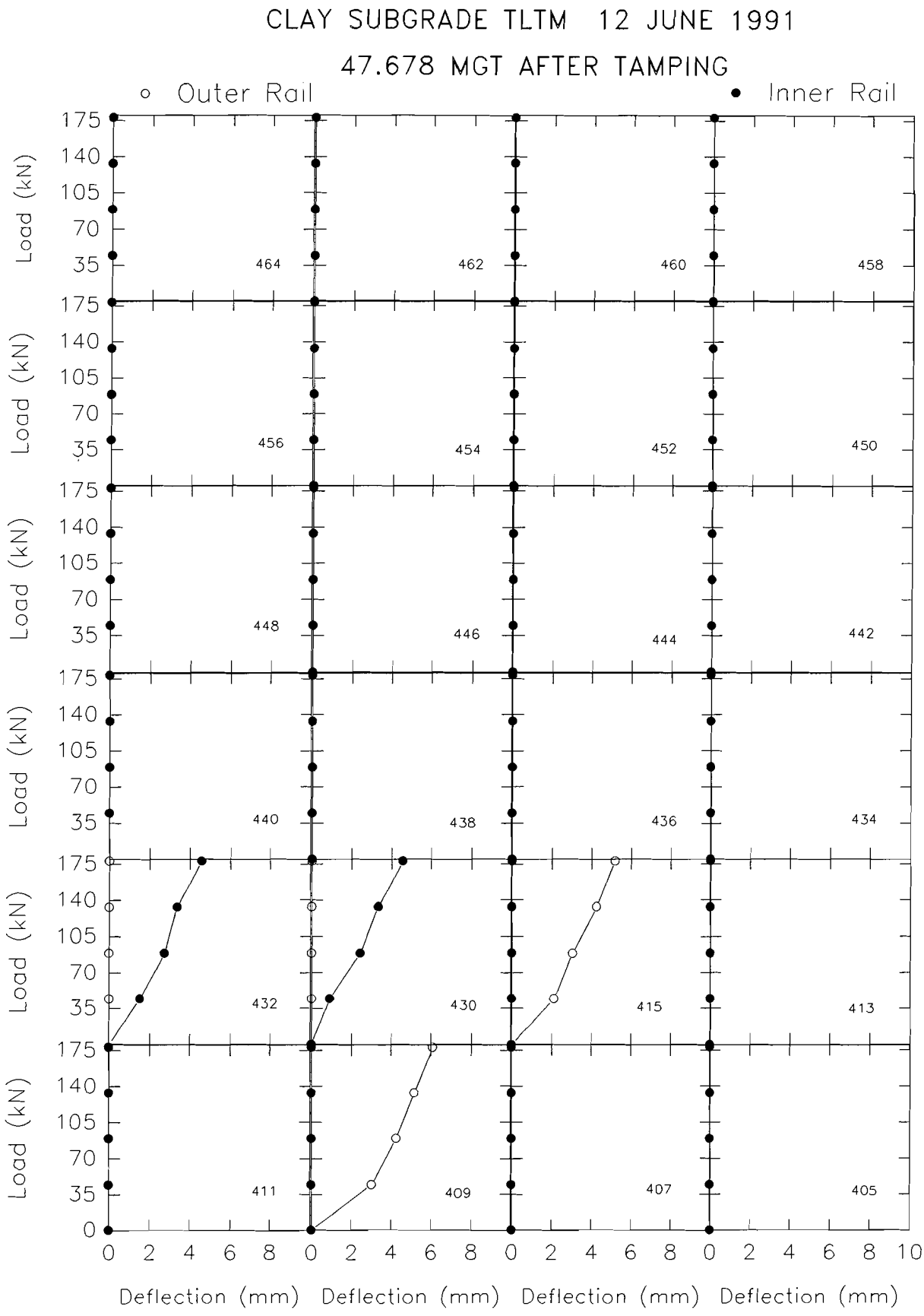

Figure 26: Clay Section Stiffness Test Post Tamping 1991

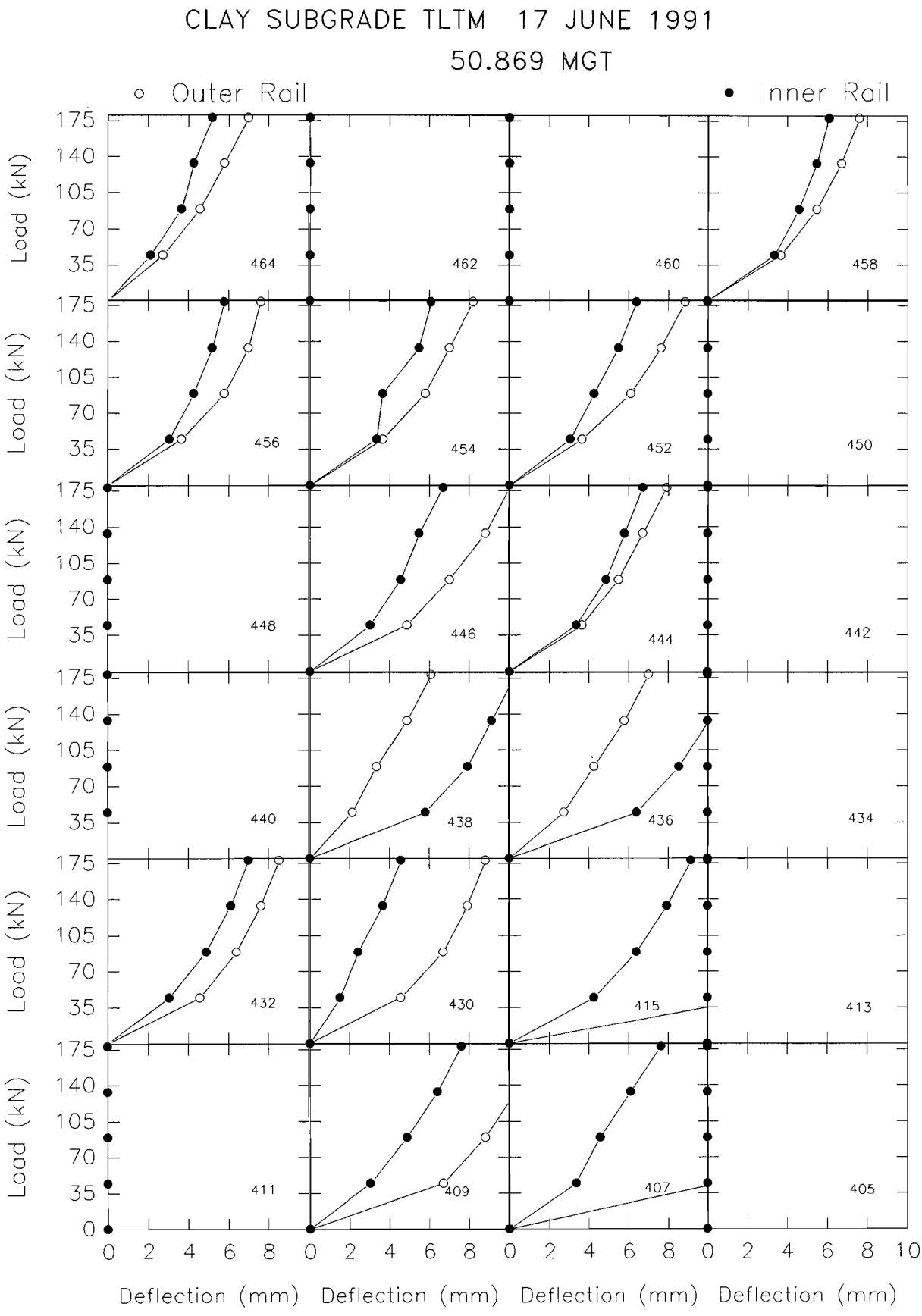

Figure 27: Clay Section Stiffness Test 17 June 1991

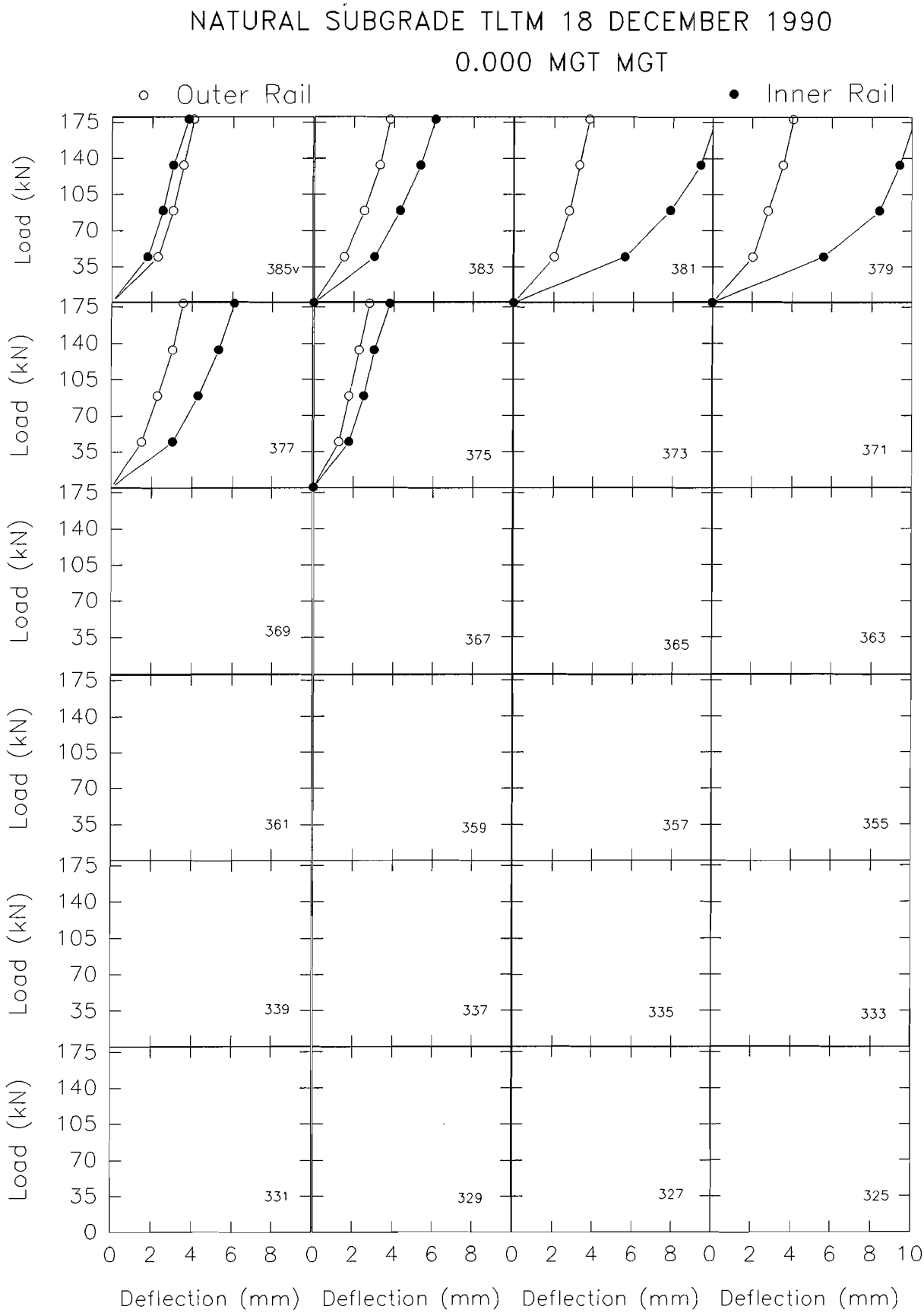

Figure 28: Natural Section Stiffness Test 18 December 1990

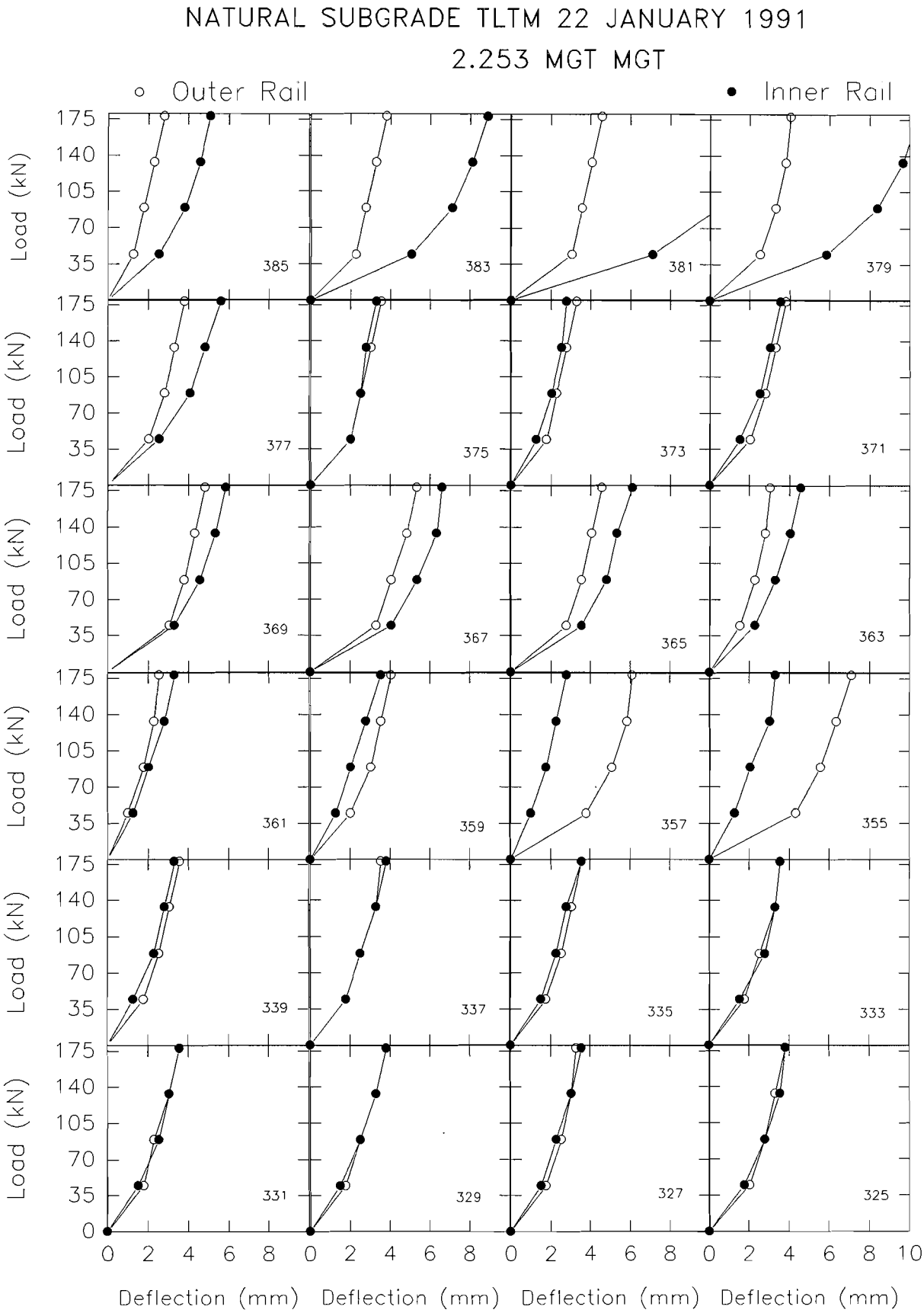

Figure 29: Natural Section Stiffness Test 22 January 1991

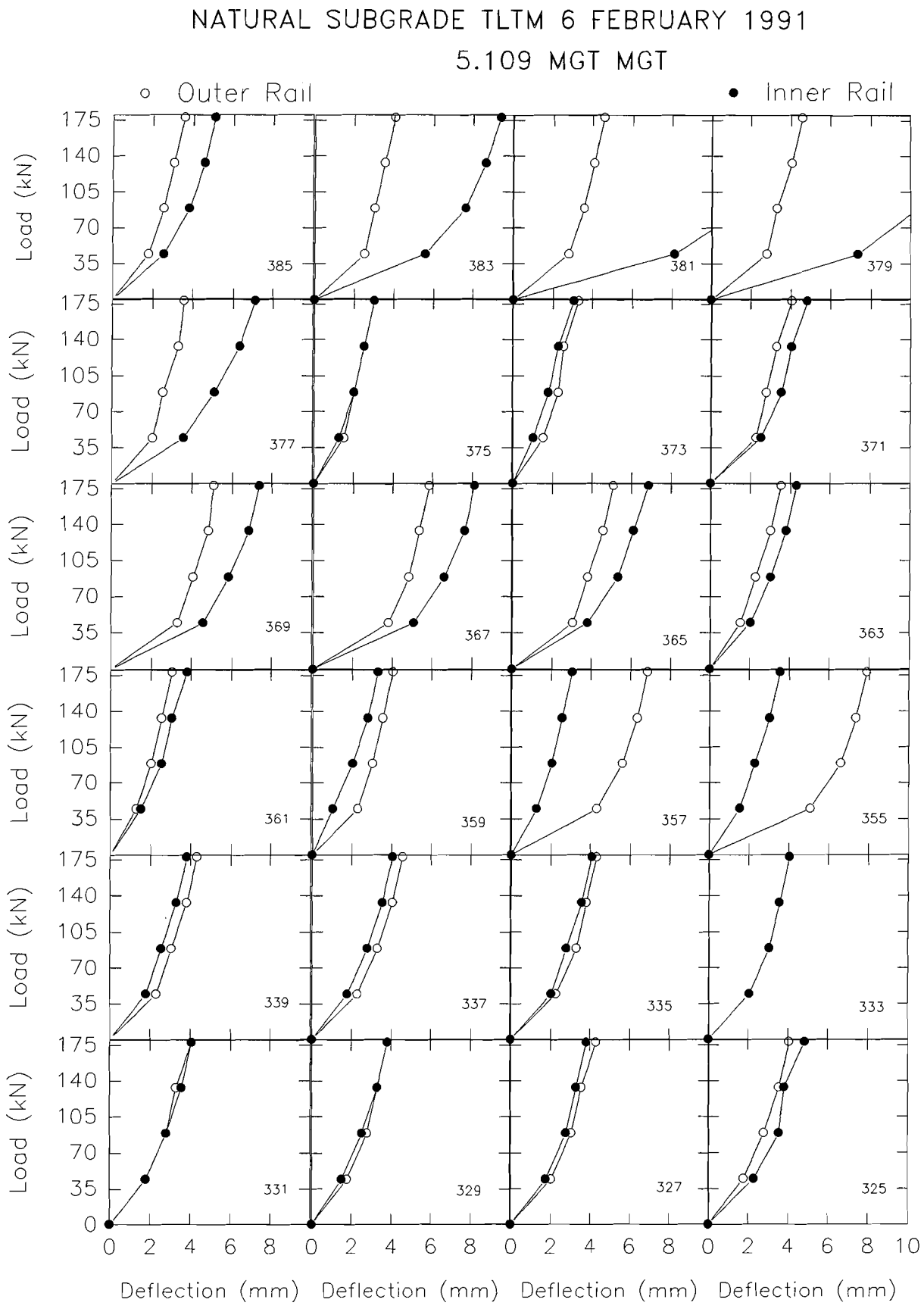

Figure 30: Natural Section Stiffness Test 6 February 1991

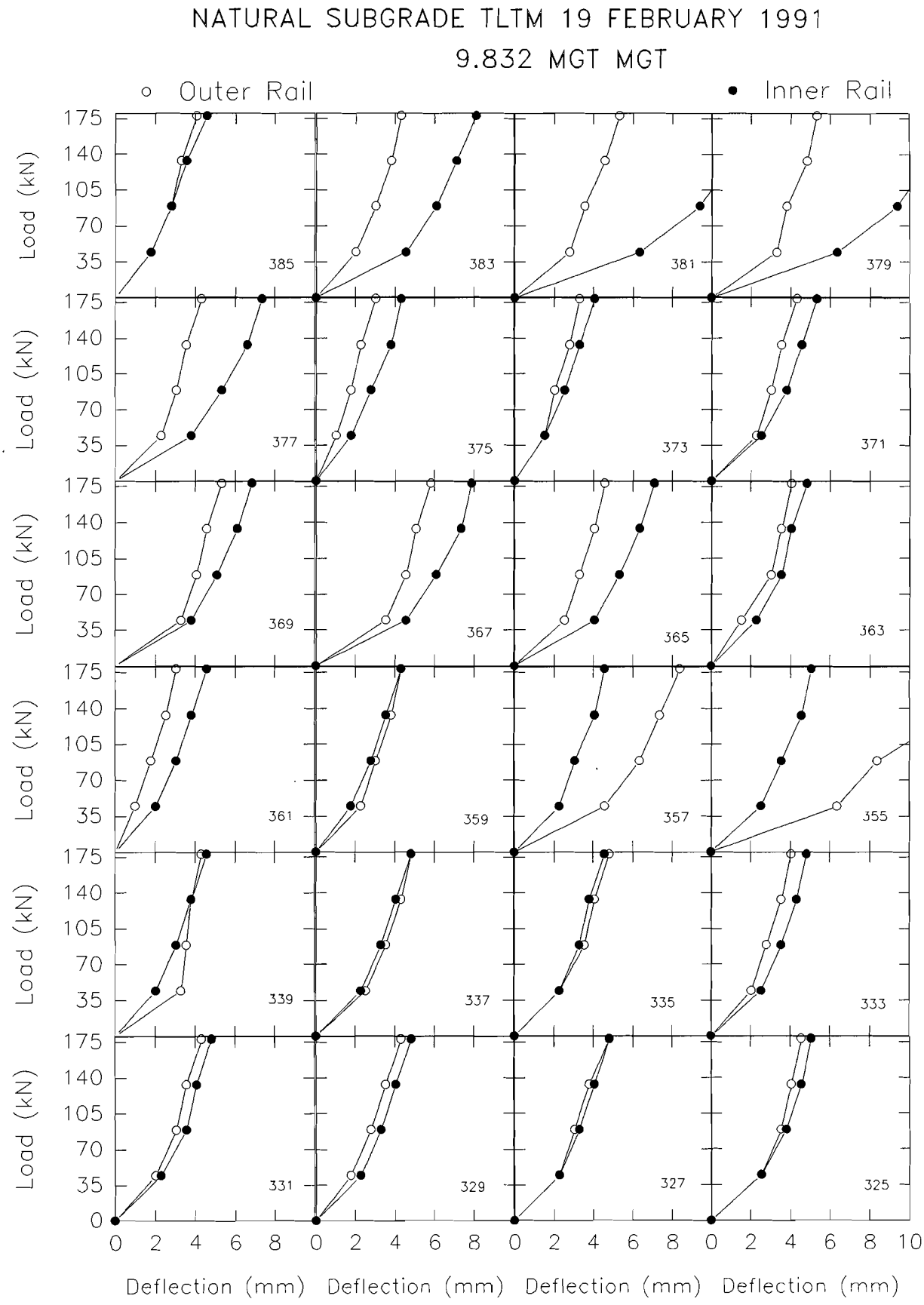

Figure 31: Natural Section Stiffness Test 19 February 1991

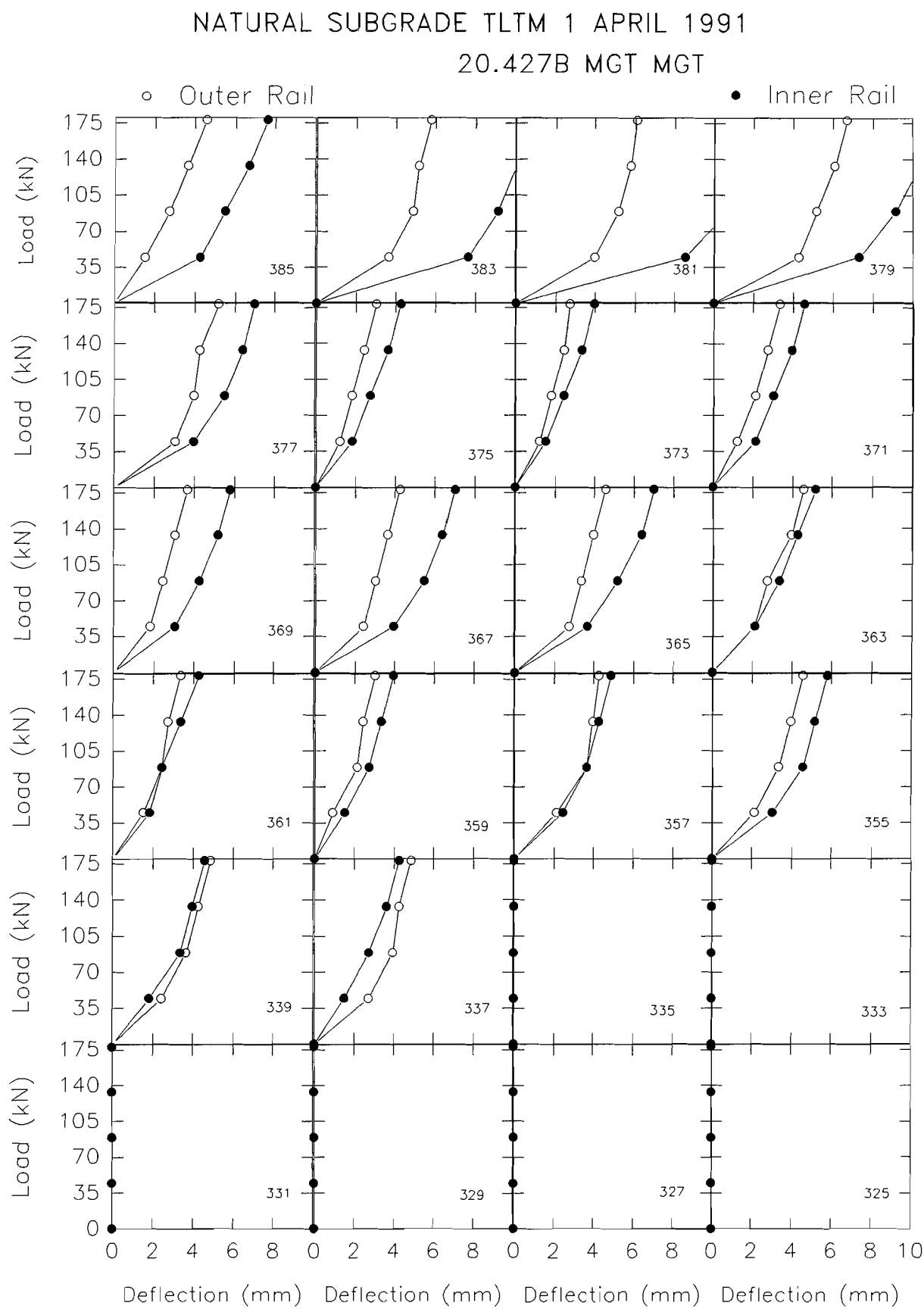

Figure 32: Natural Section Stiffness Test 1 April 1991

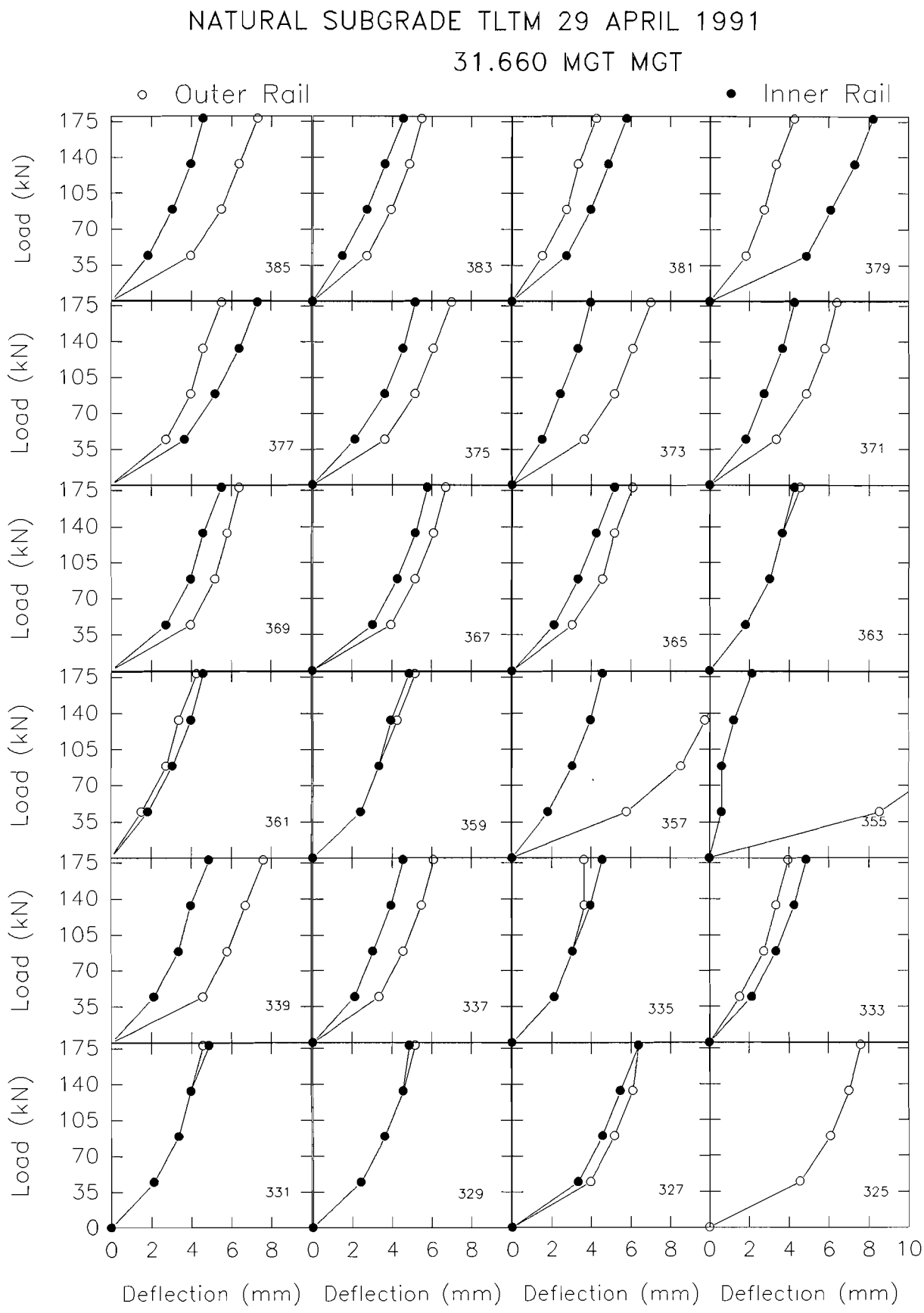

Figure 33: Natural Section Stiffness Test 29 April 1991

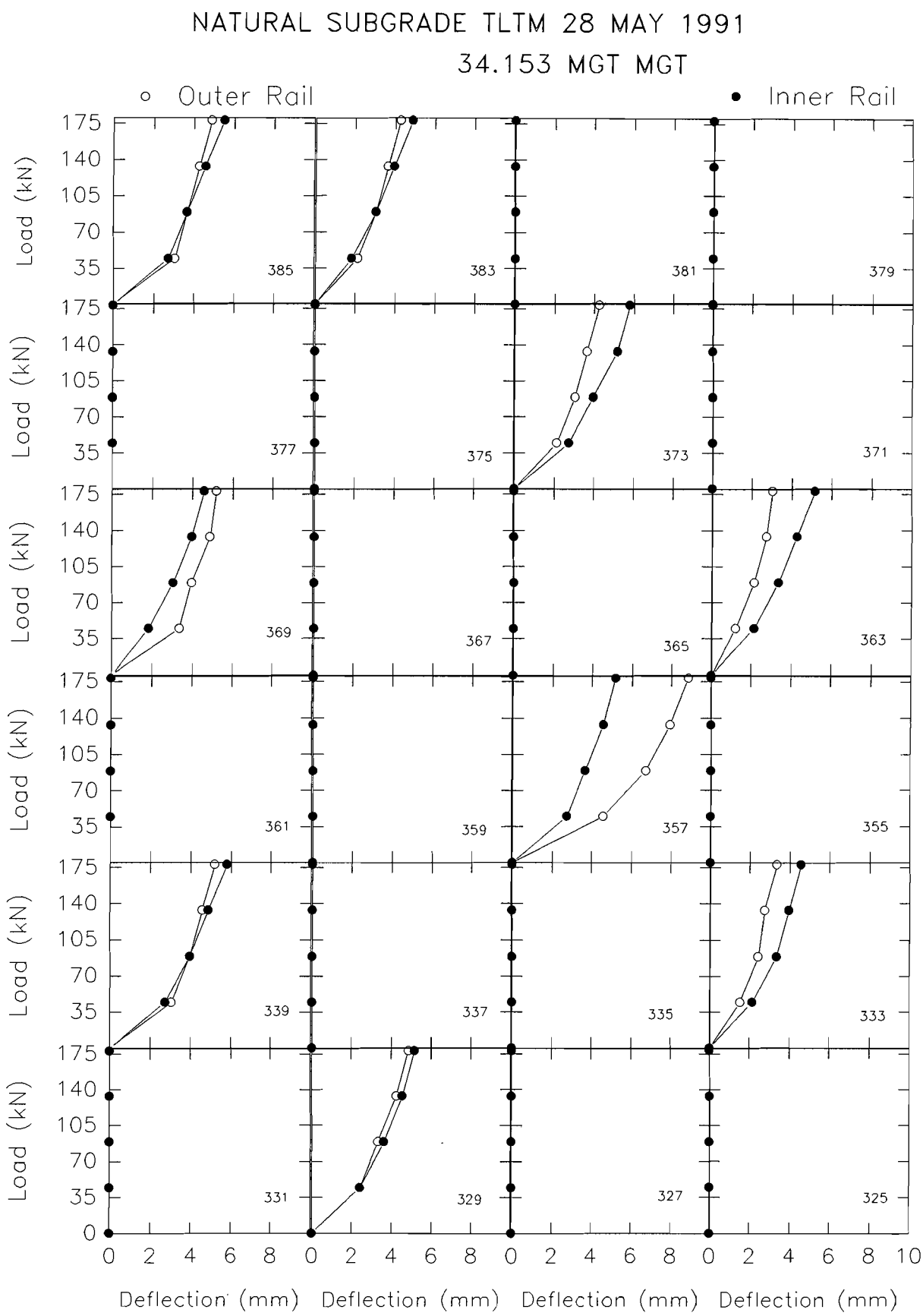

Figure 34: Natural Section Stiffness Test 28 May 1991

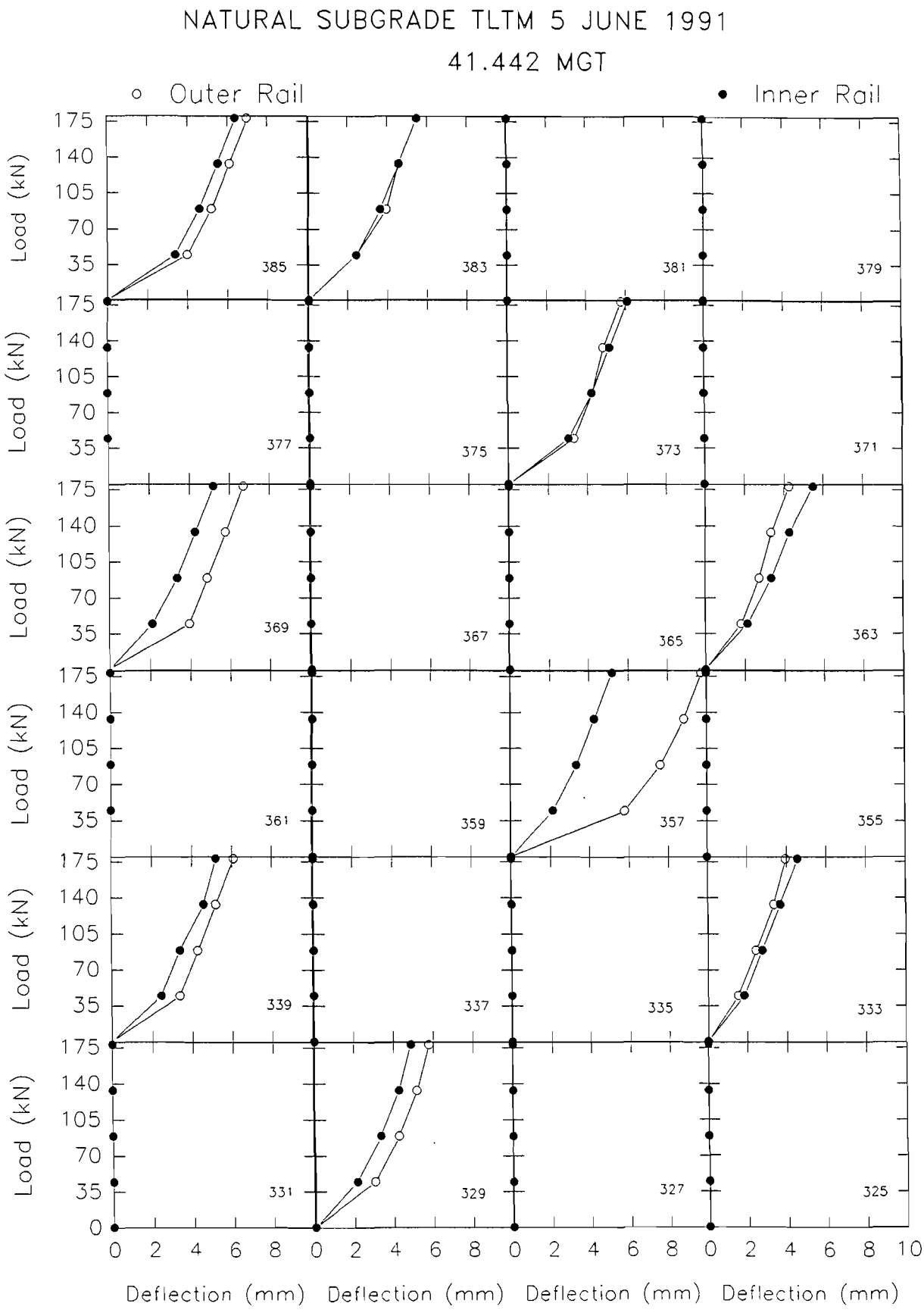

Figure 35: Natural Section Stiffness Test 5 June 1991

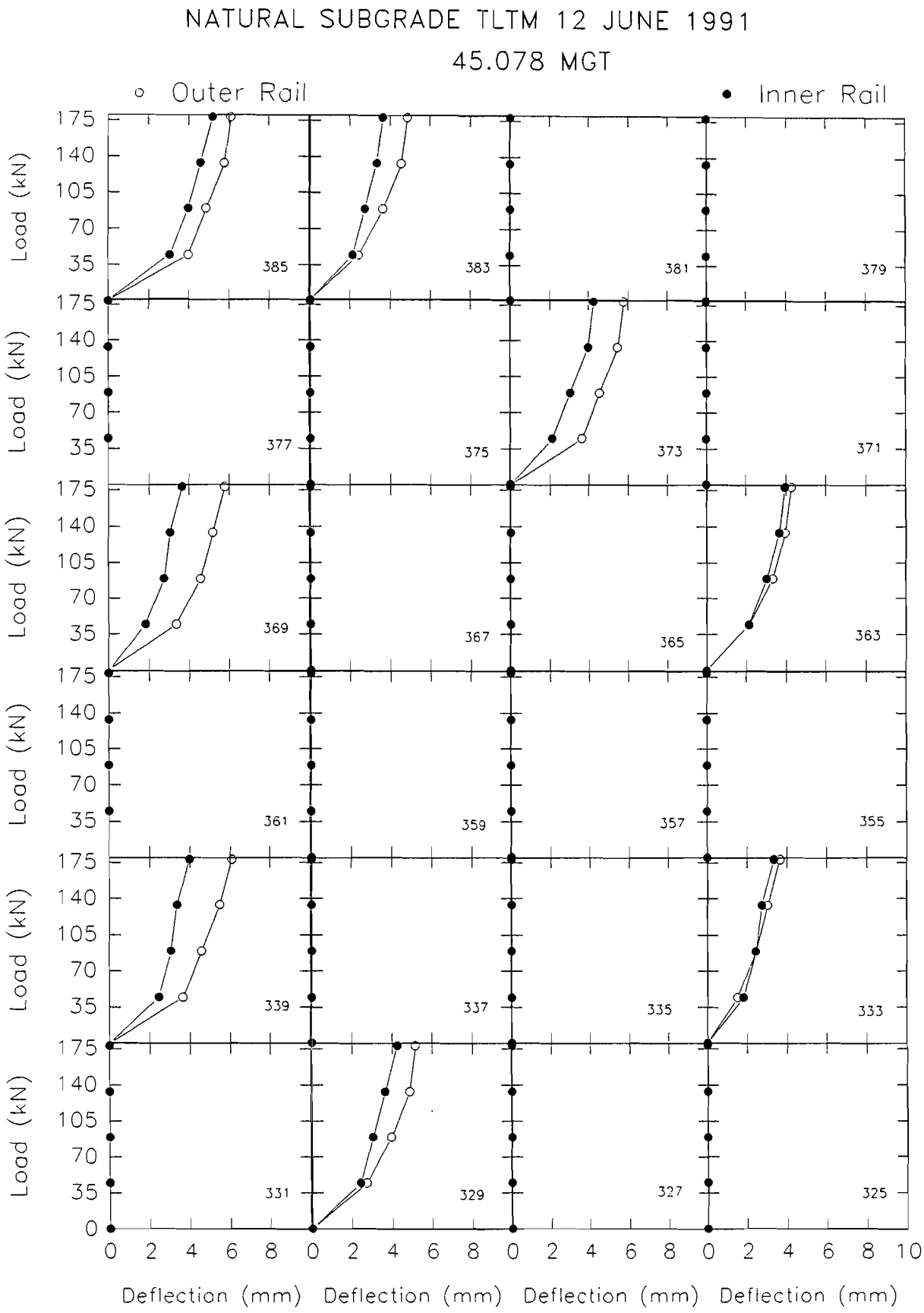

Figure 36: Natural Section Stiffness Test 12 June 1991

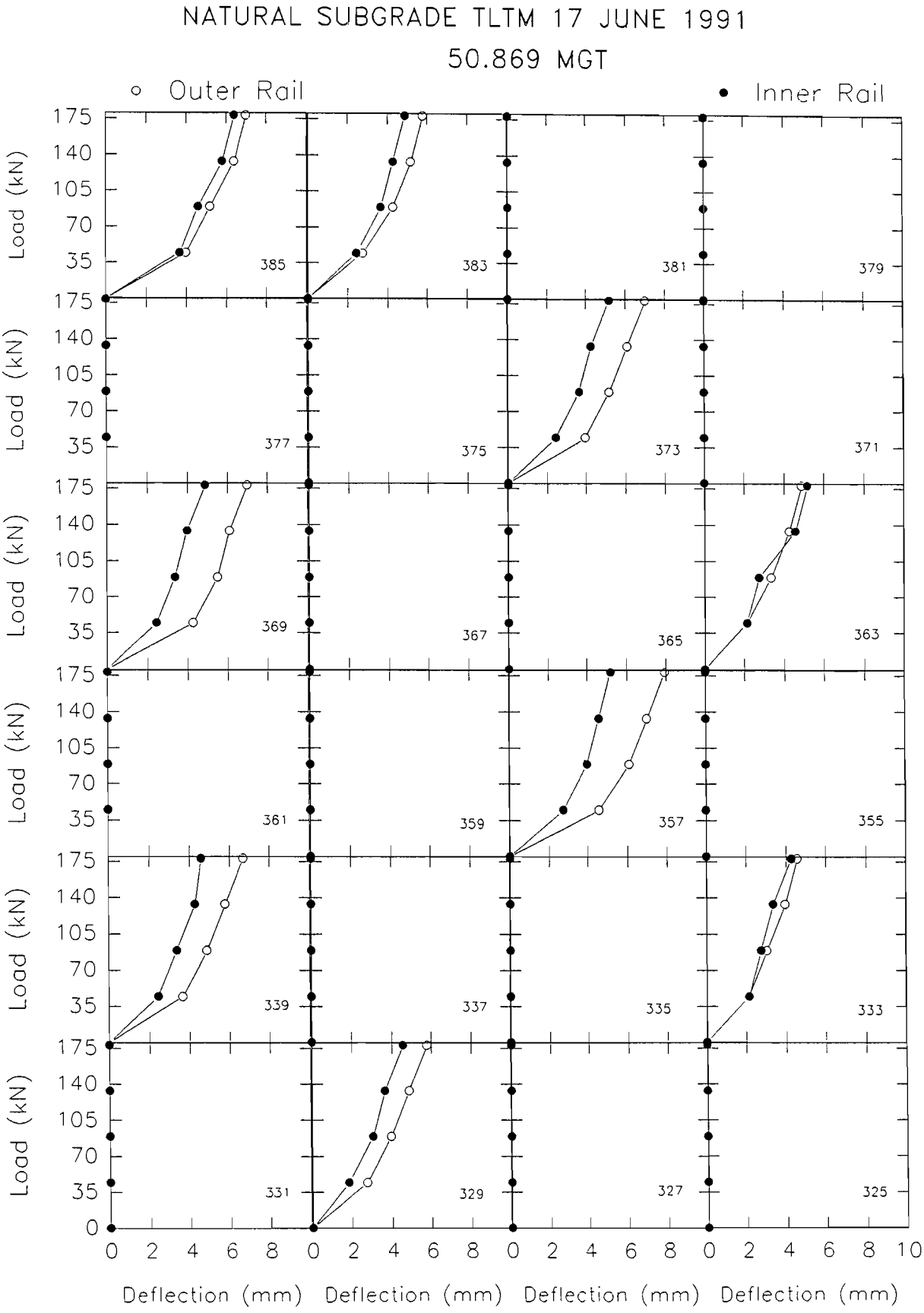

Figure 37: Natural Section Stiffness Test 17 June 1991

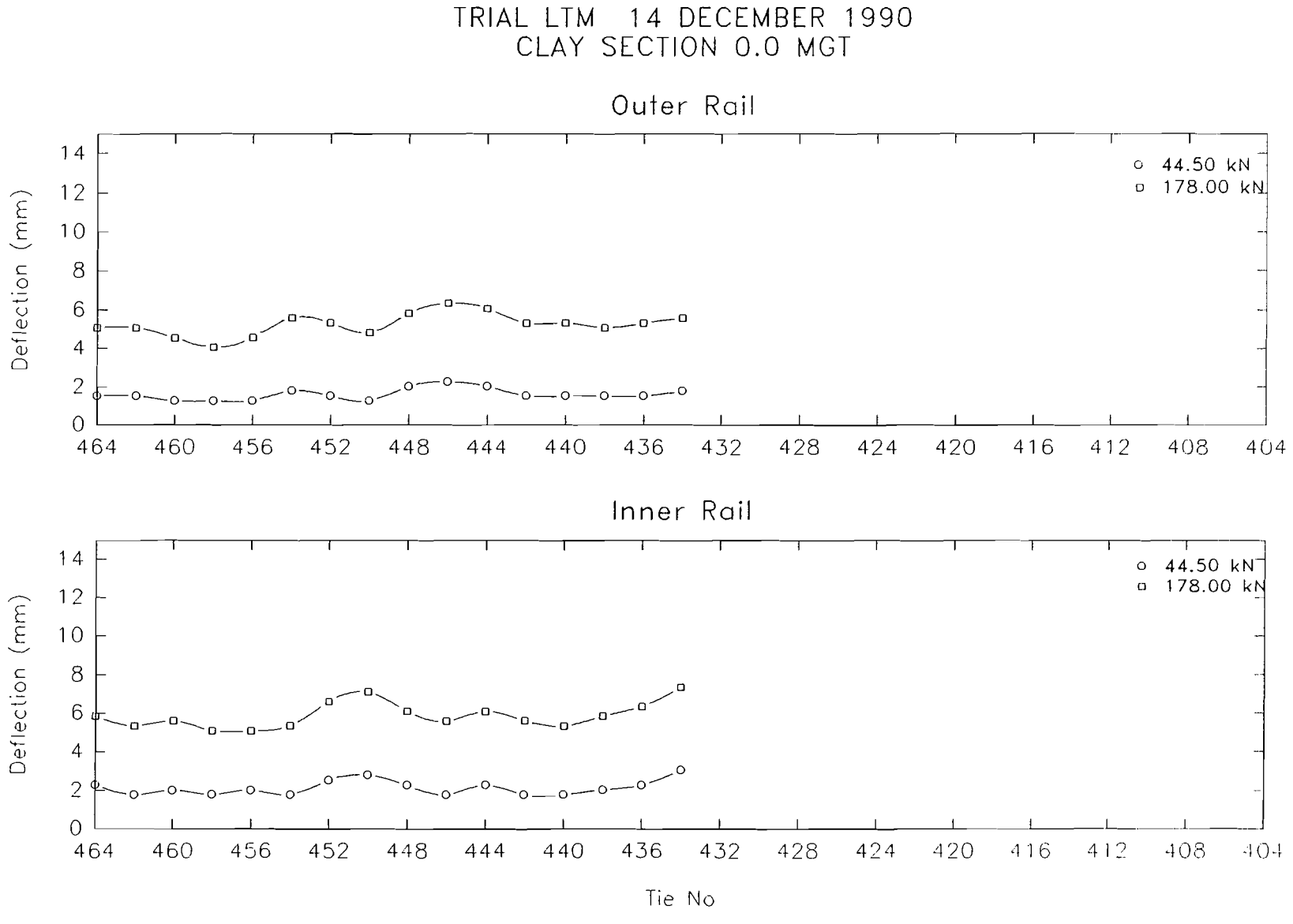

Figure 38: Running Deflection 14 December 1990

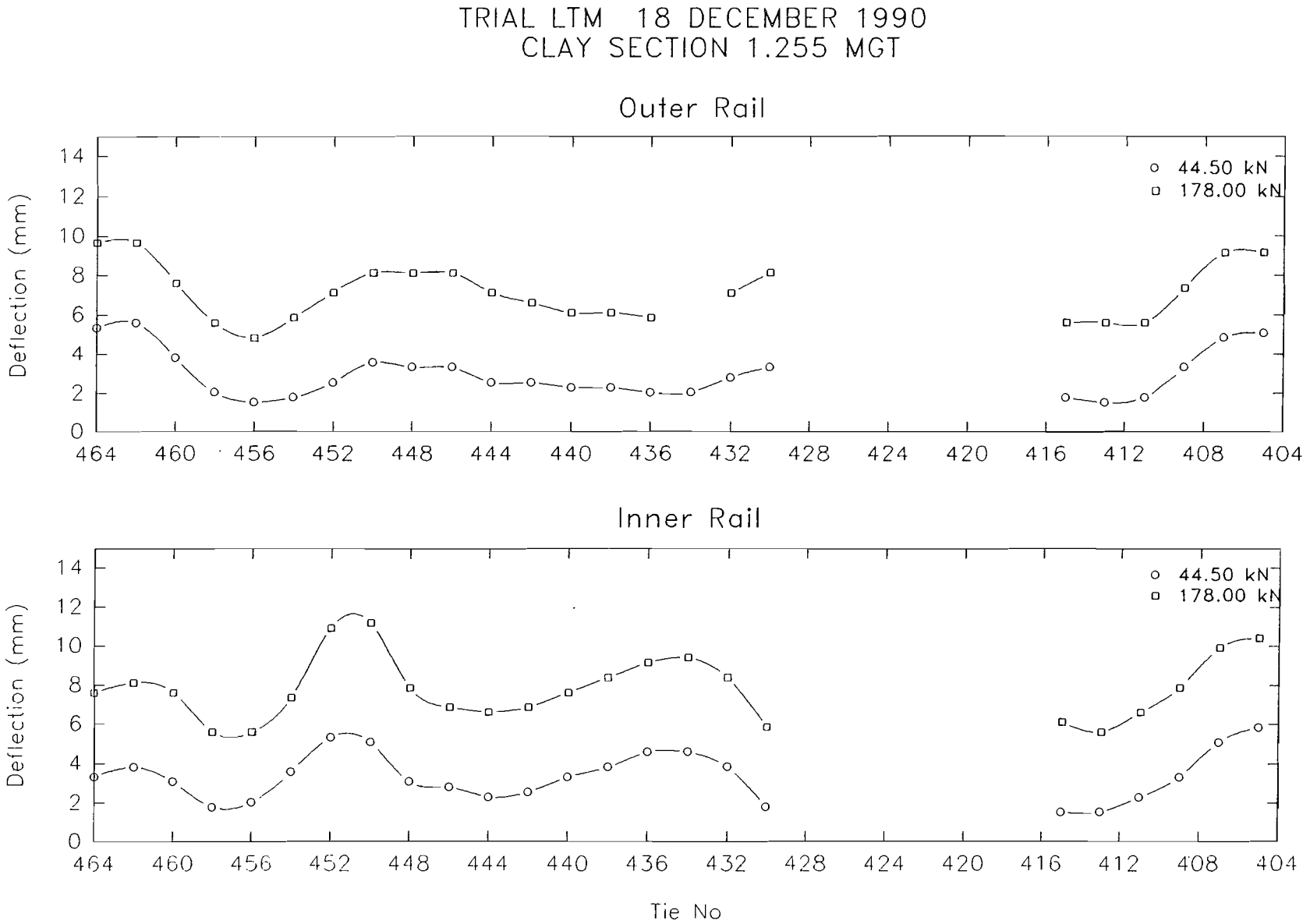

Figure 39: Running Deflection 18 December 1990

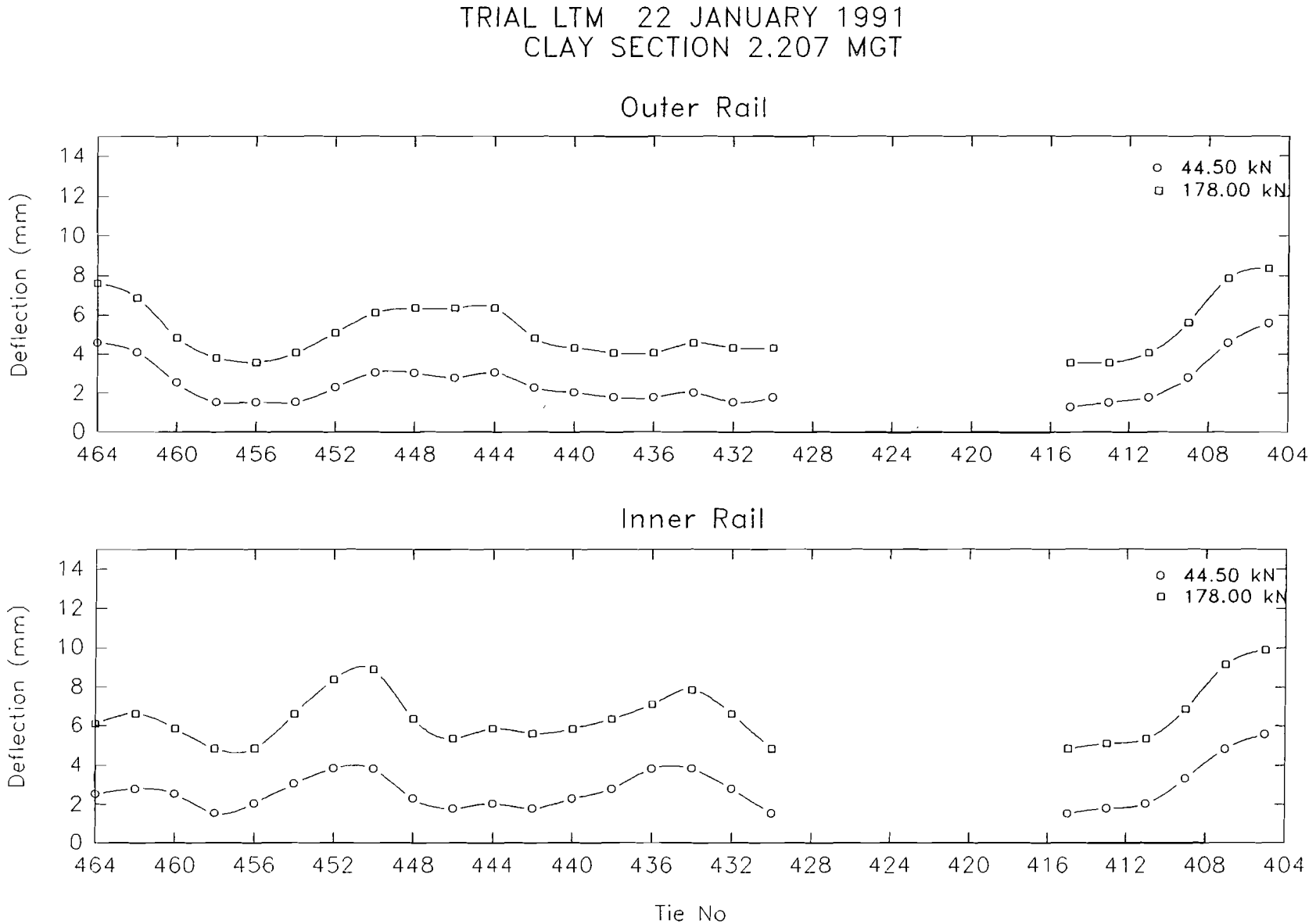

Figure 40: Running Deflection 22 January 1991

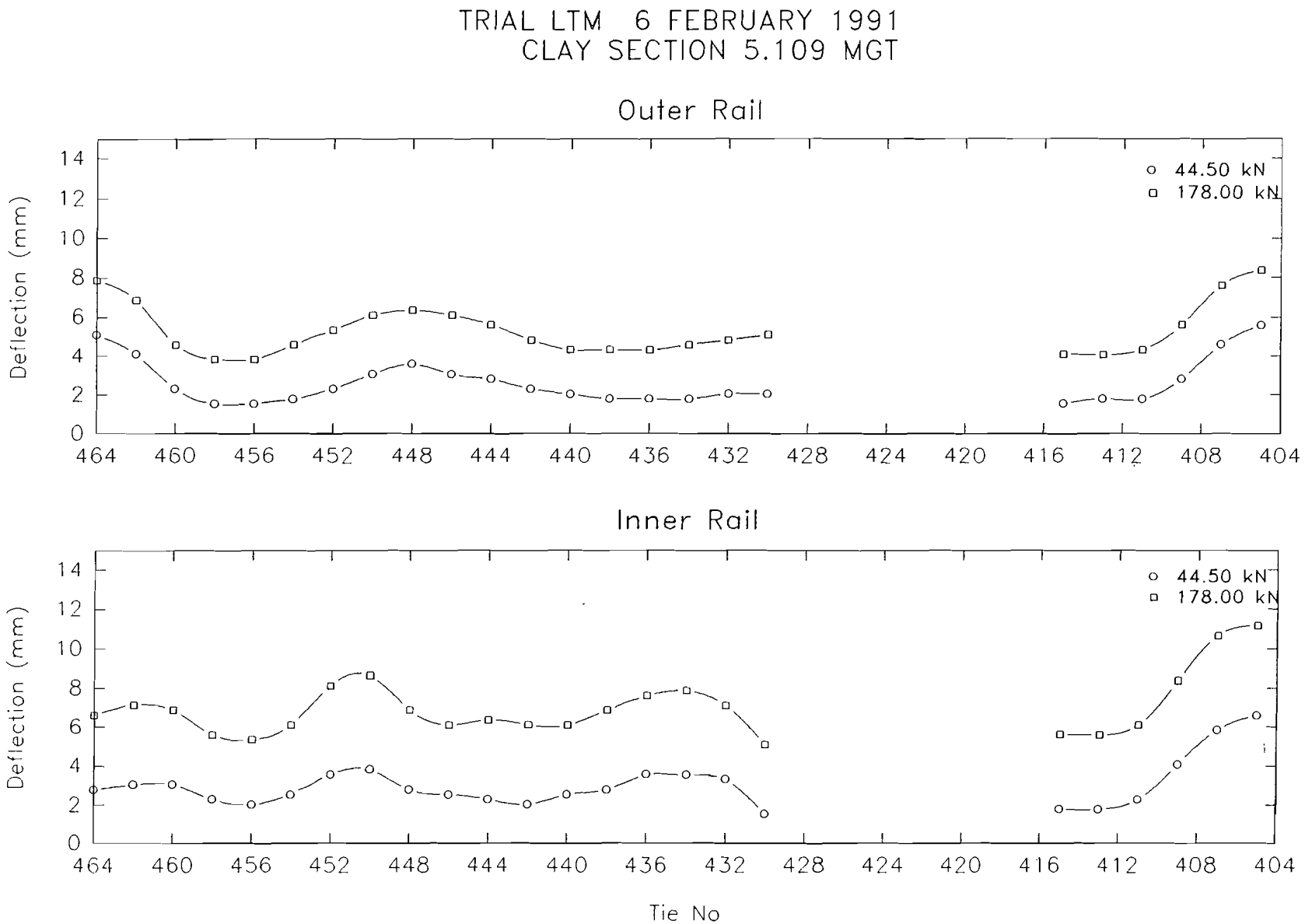

Figure 41: Running Deflection 6 February 1991

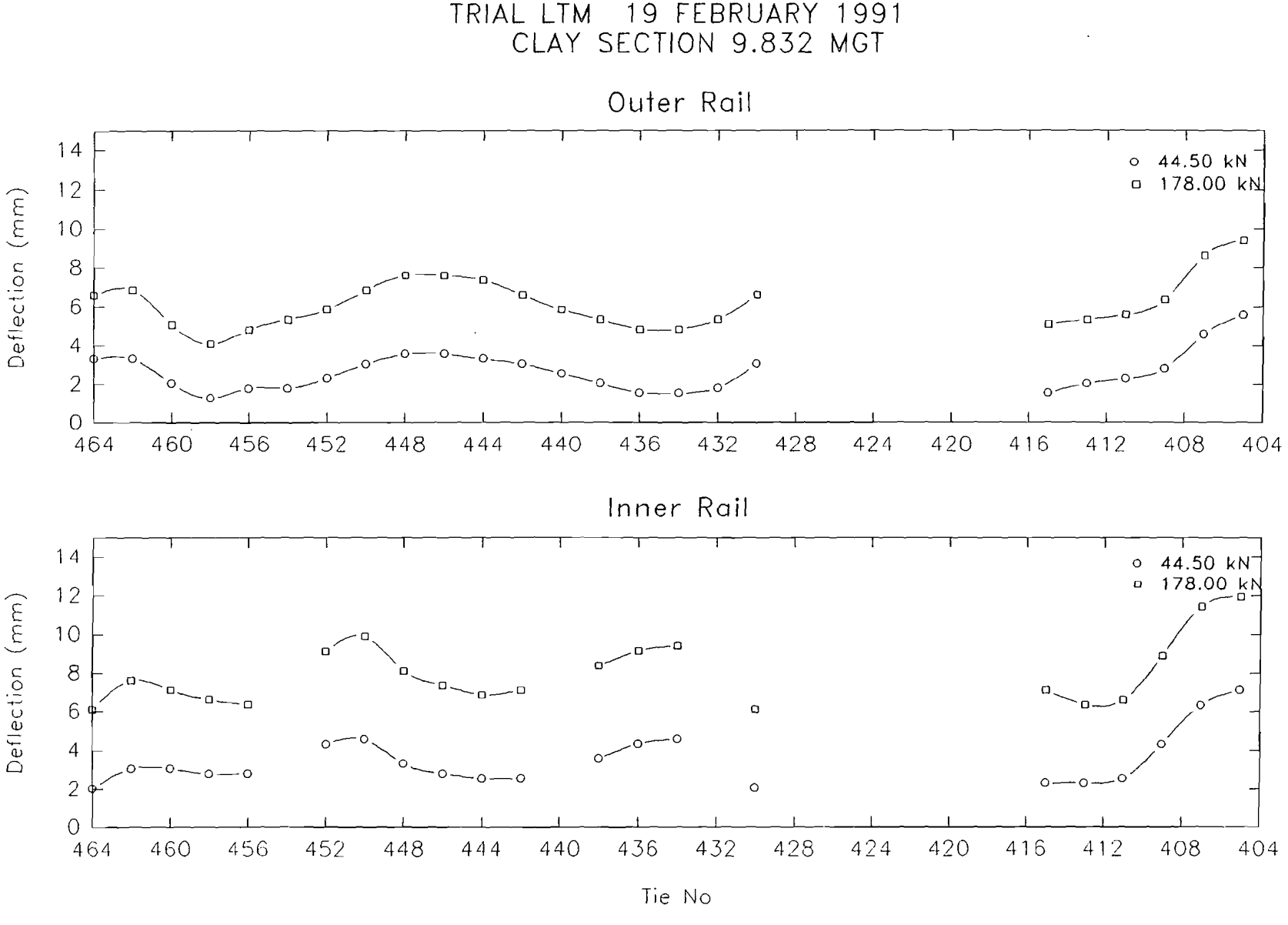

Figure 42: Running Deflection 19 February 1991

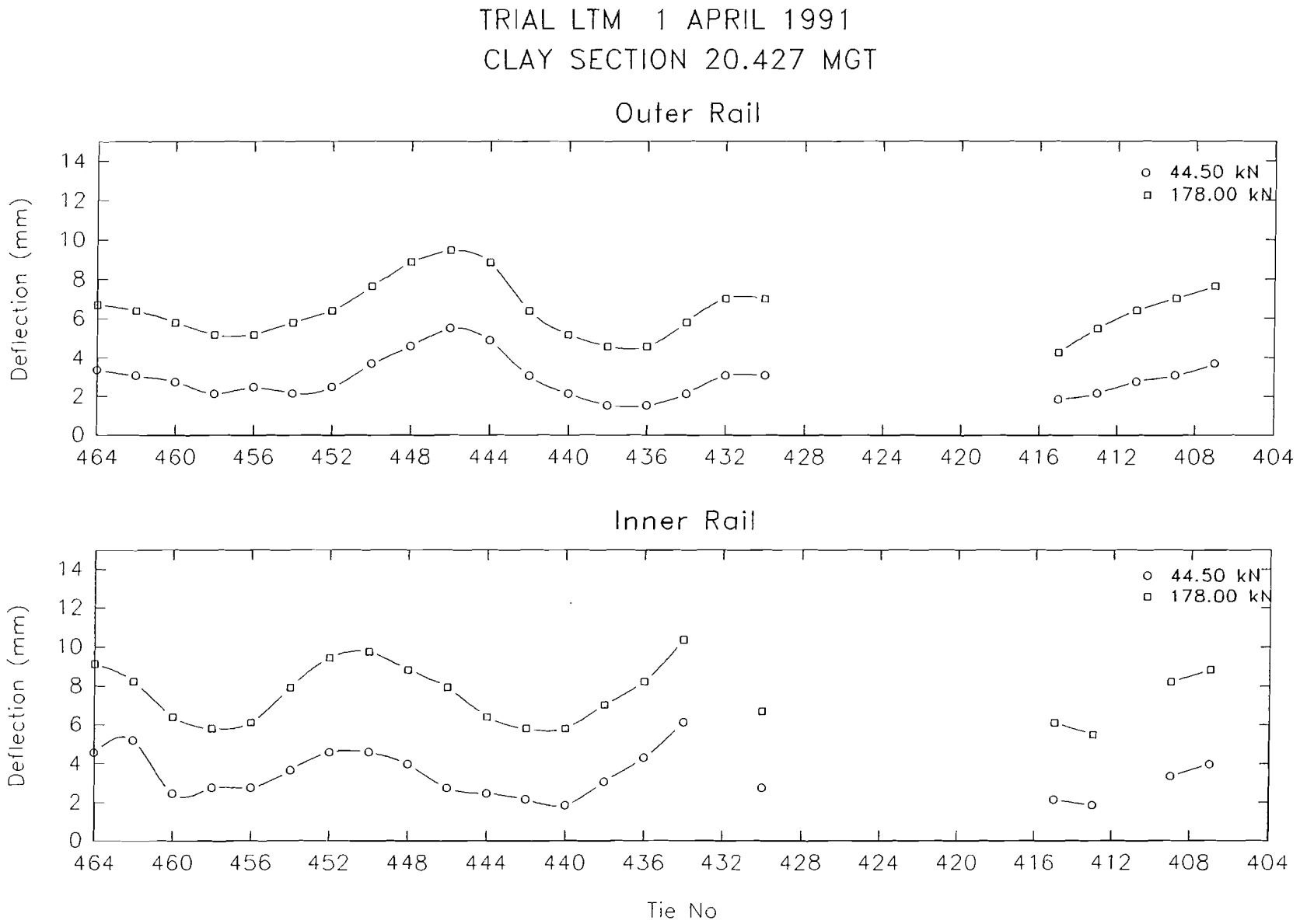

Figure 43: Running Deflection 1 April 1991

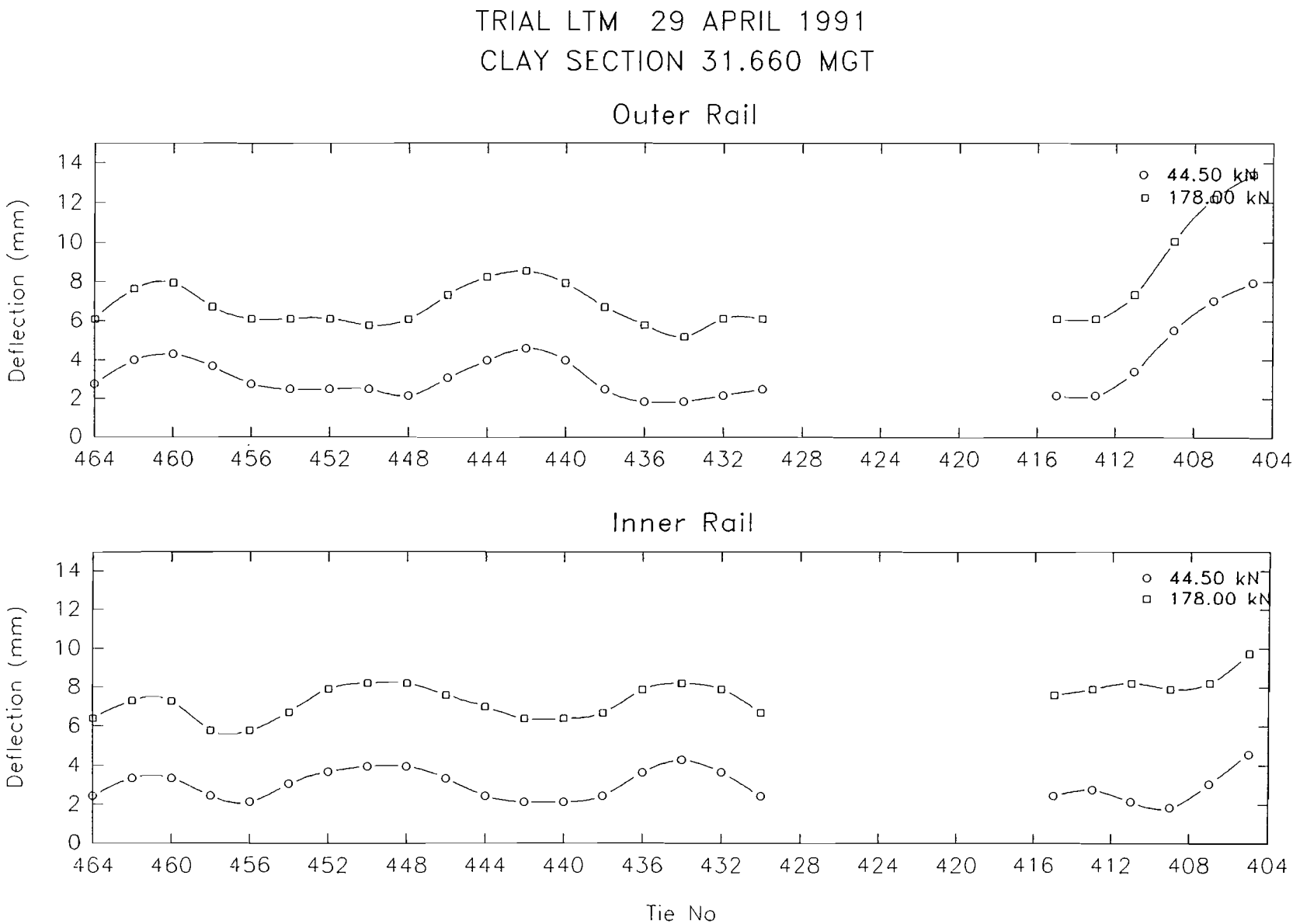

Figure 44: Running Deflection 29 April 1991

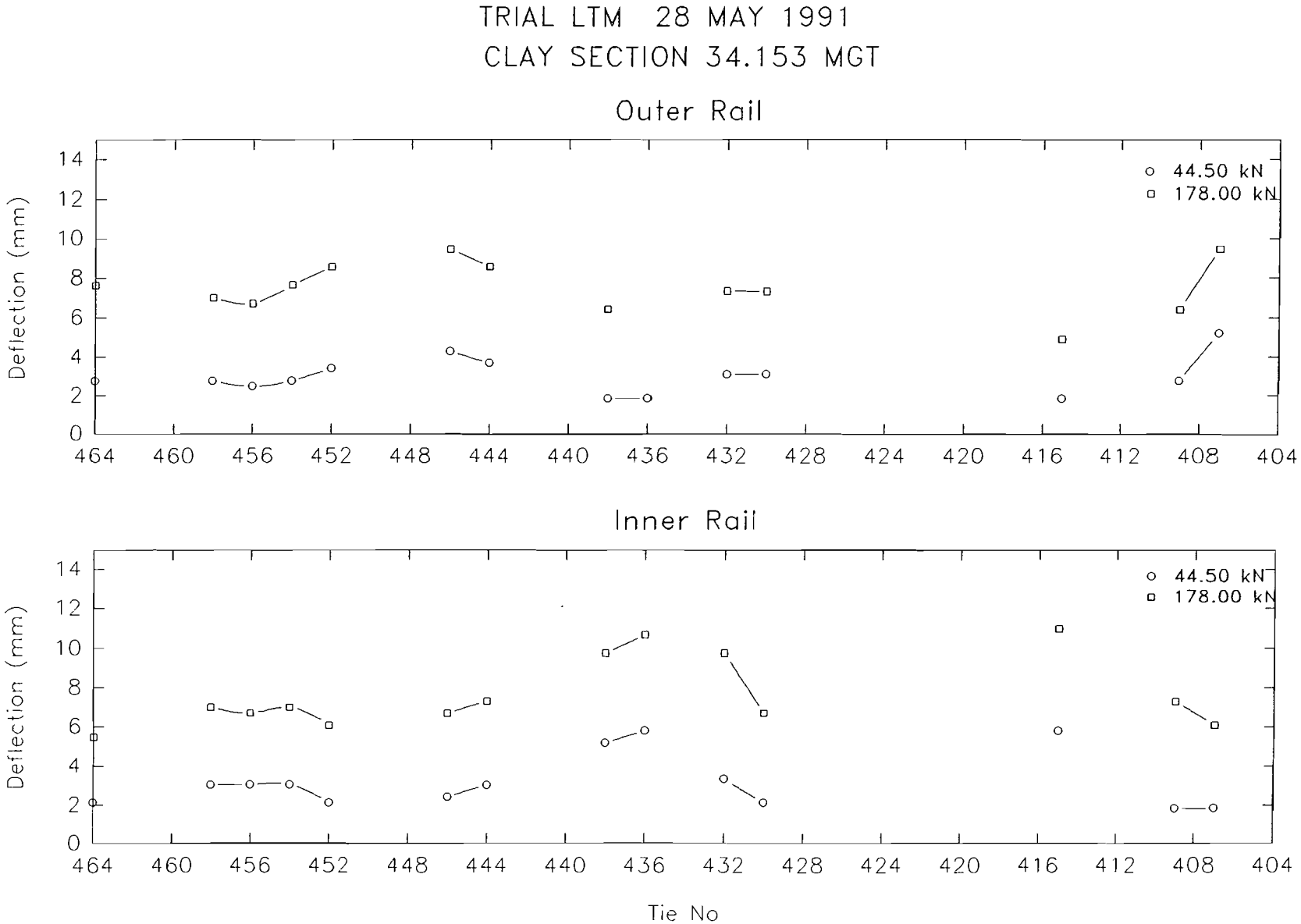

Figure 45: Running Deflection 28 May 1991

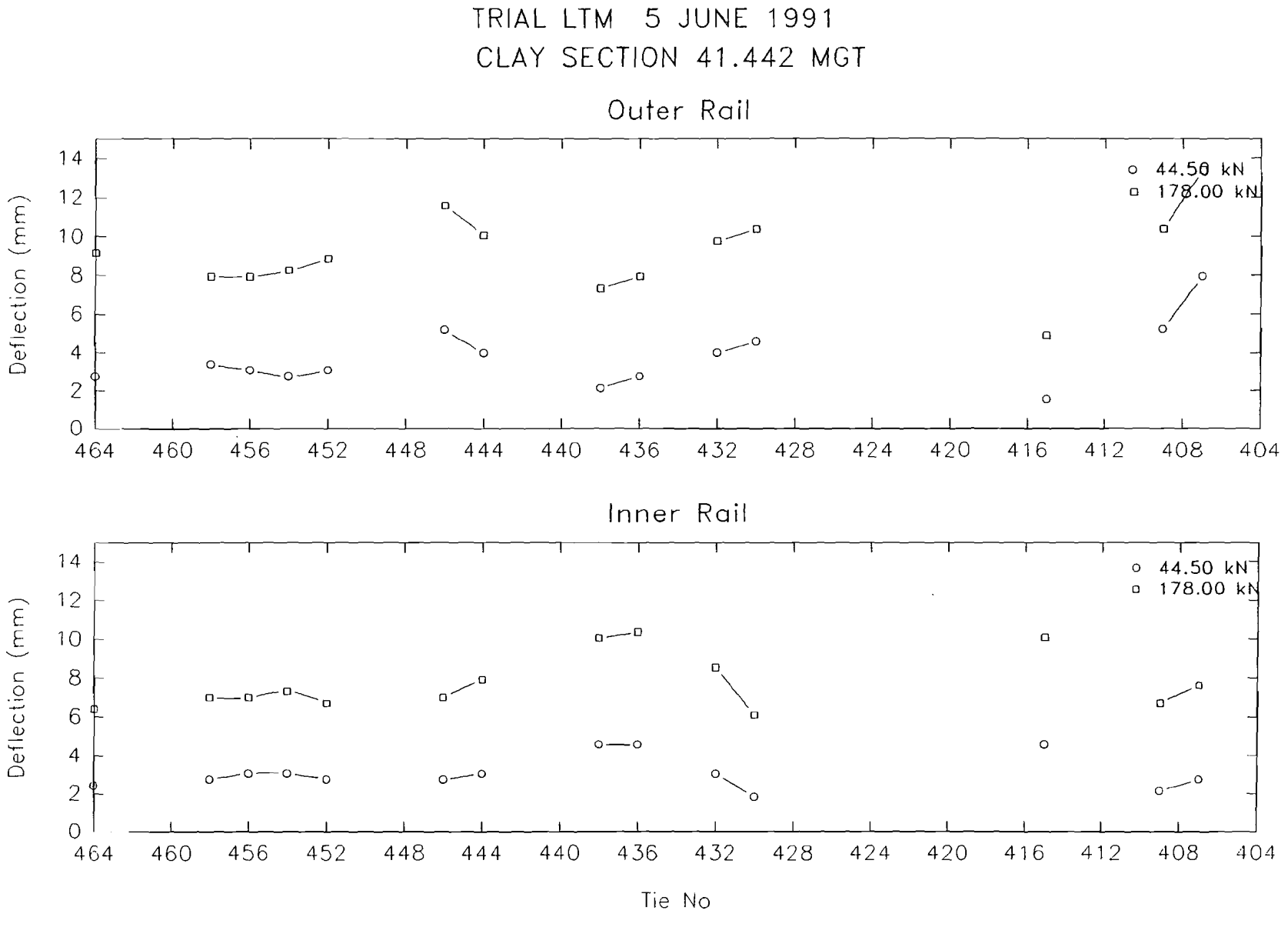

Figure 46: Running Deflection 5 June 1991

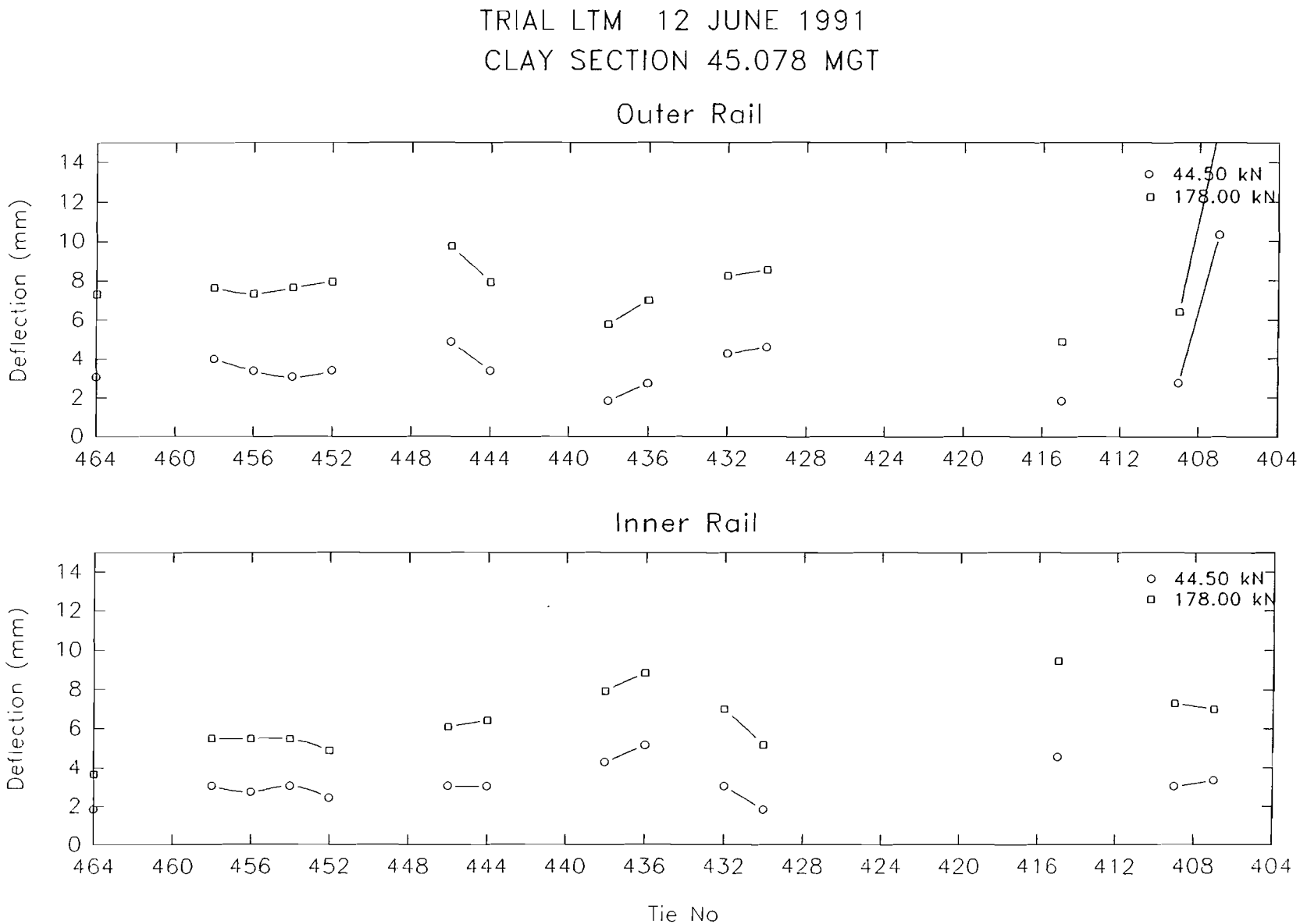

Figure 47: Running Deflection 12 June 1991

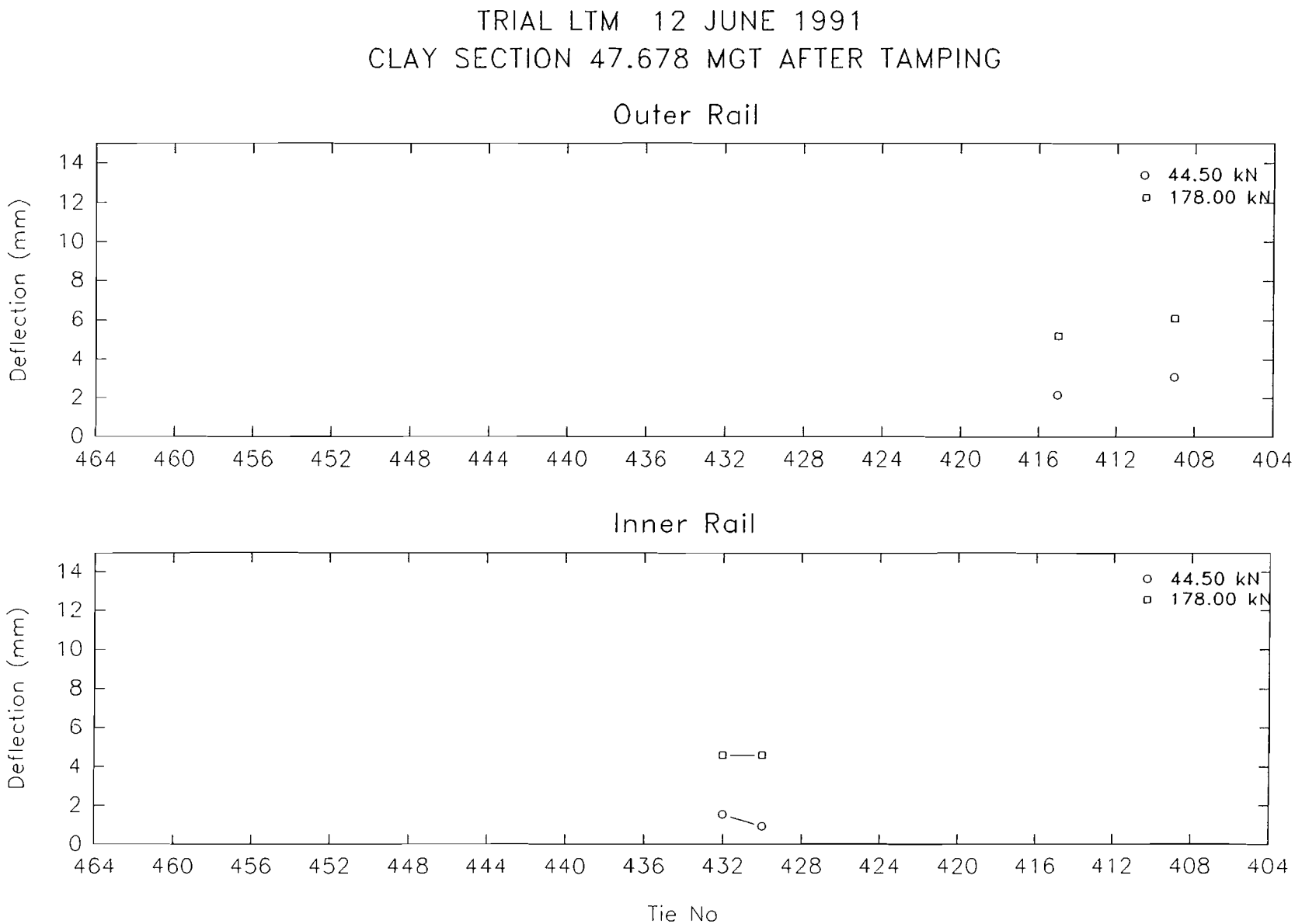

Figure 48: Running Deflection After Tamping

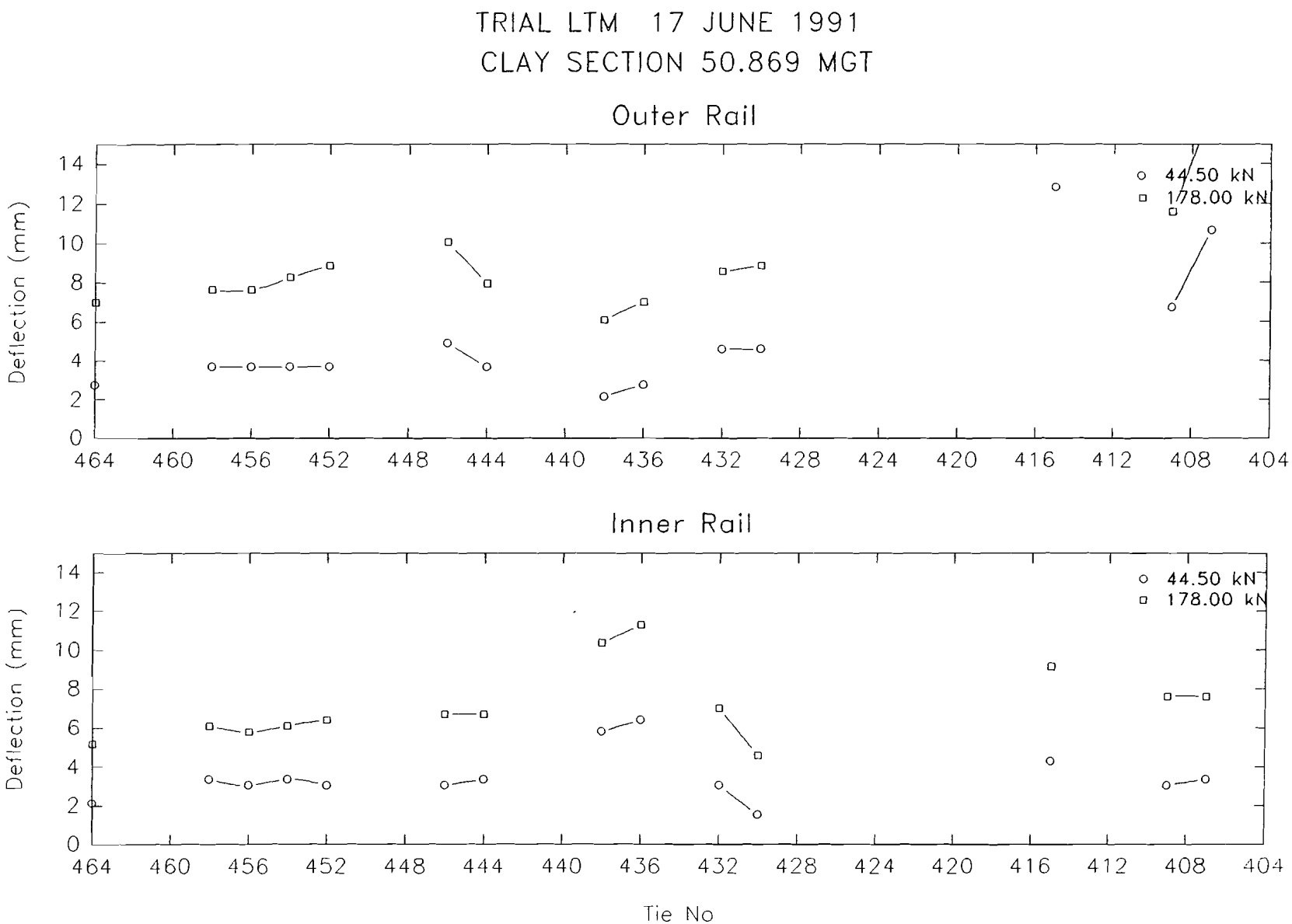

Figure 49: Running Deflection 17 June 1991

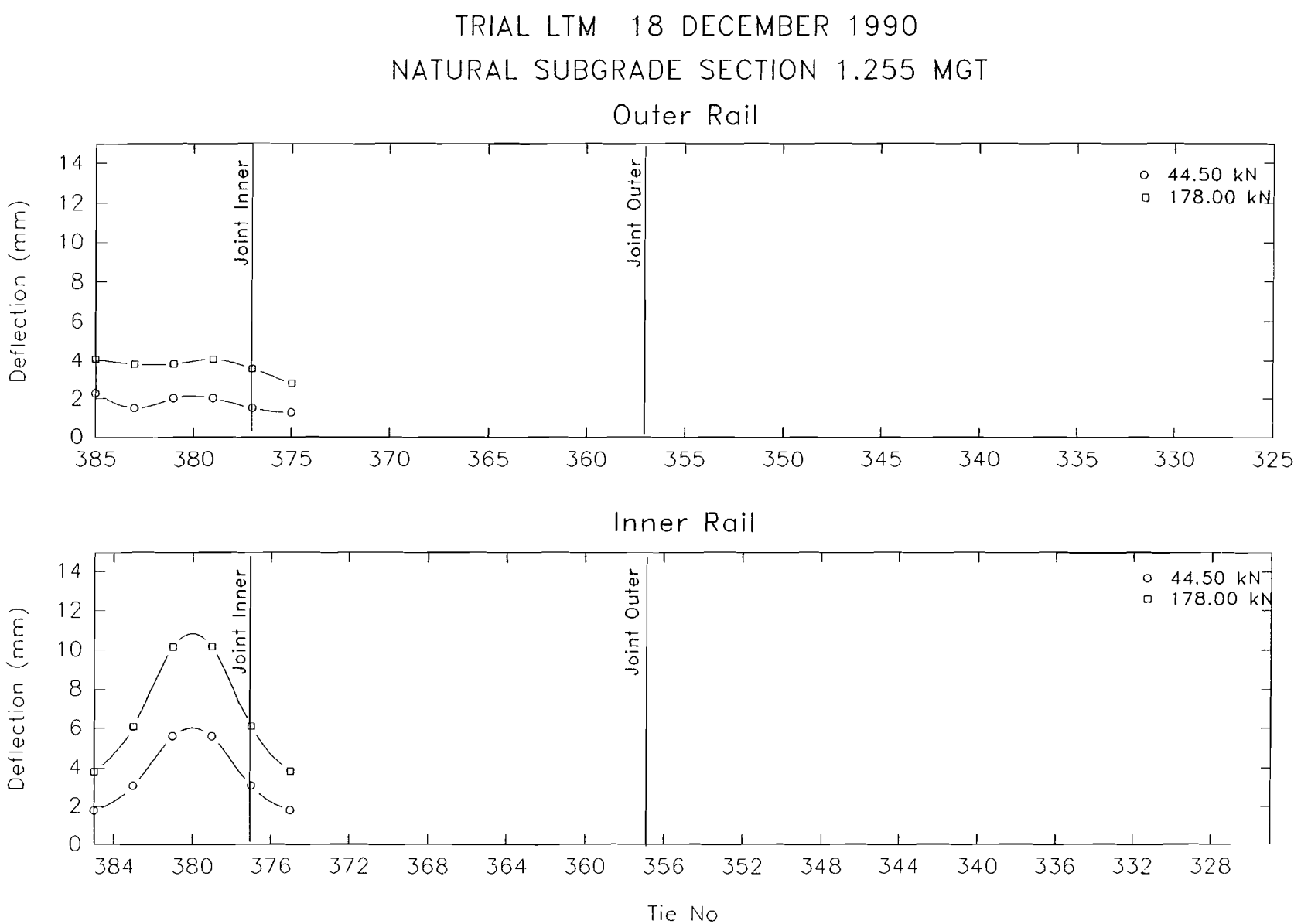

Figure 50: Running Deflection 18 December 1990

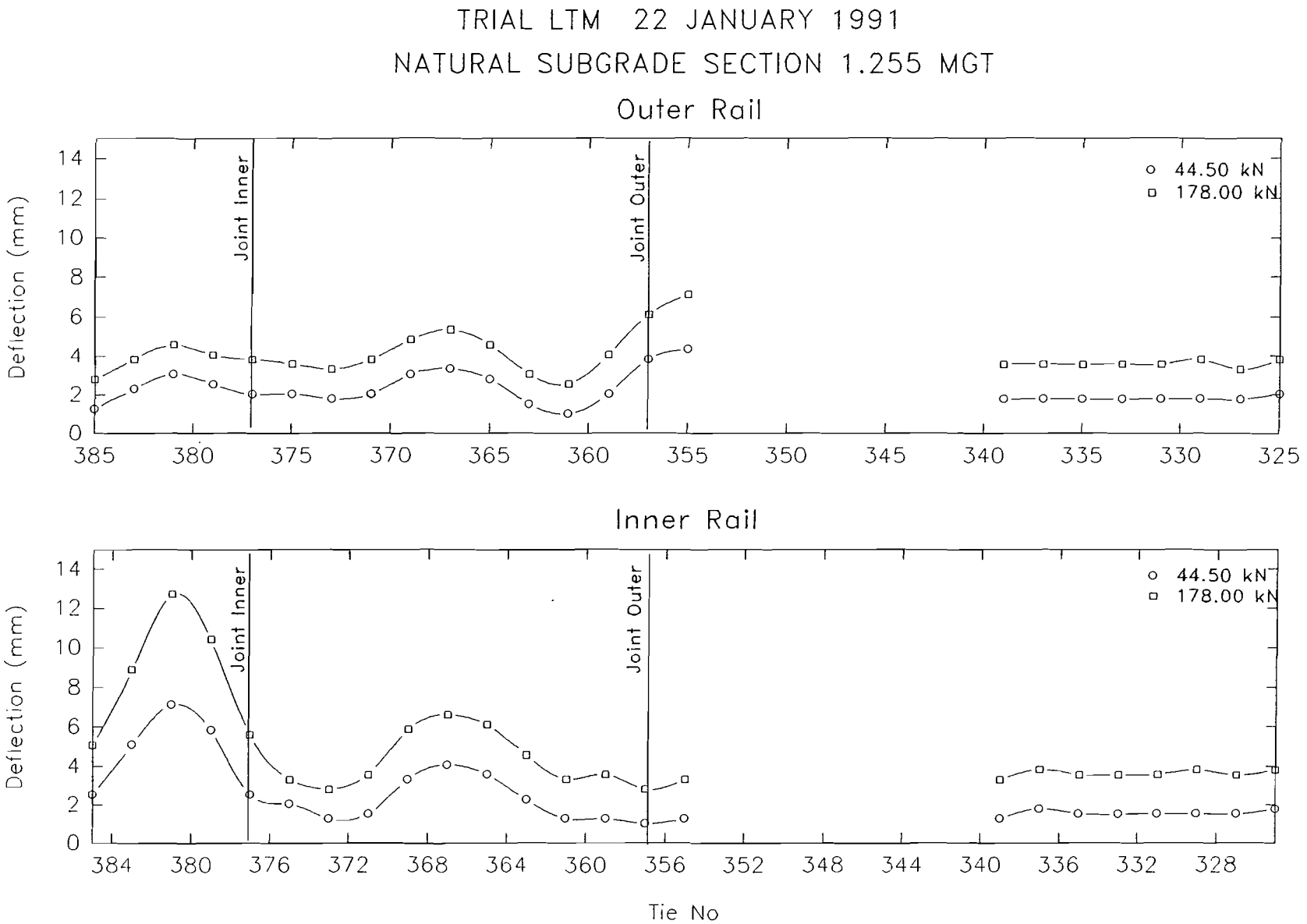

Figure 51: Running Deflection 22 January 1991

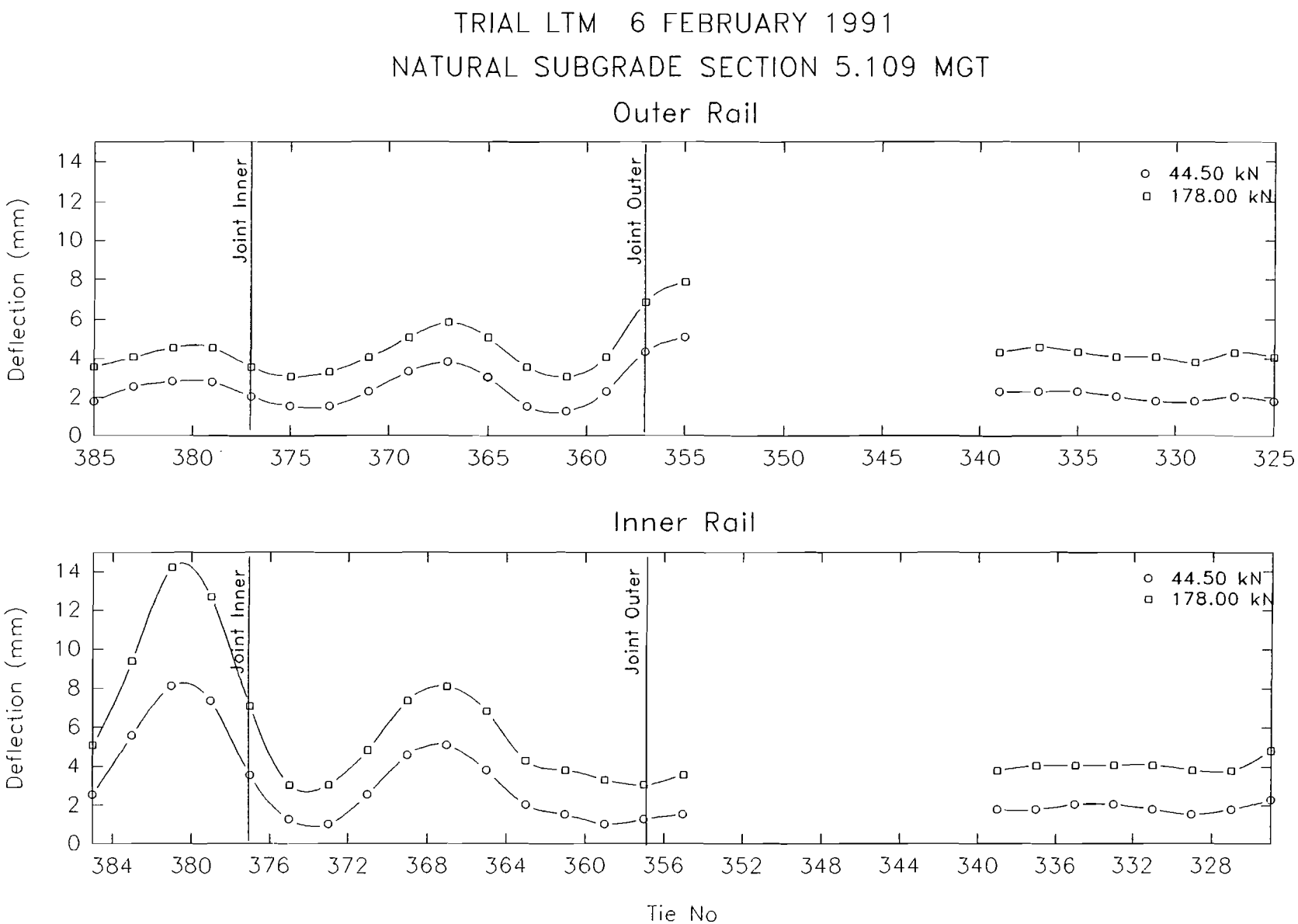

Figure 52: Running Deflection 6 February 1991

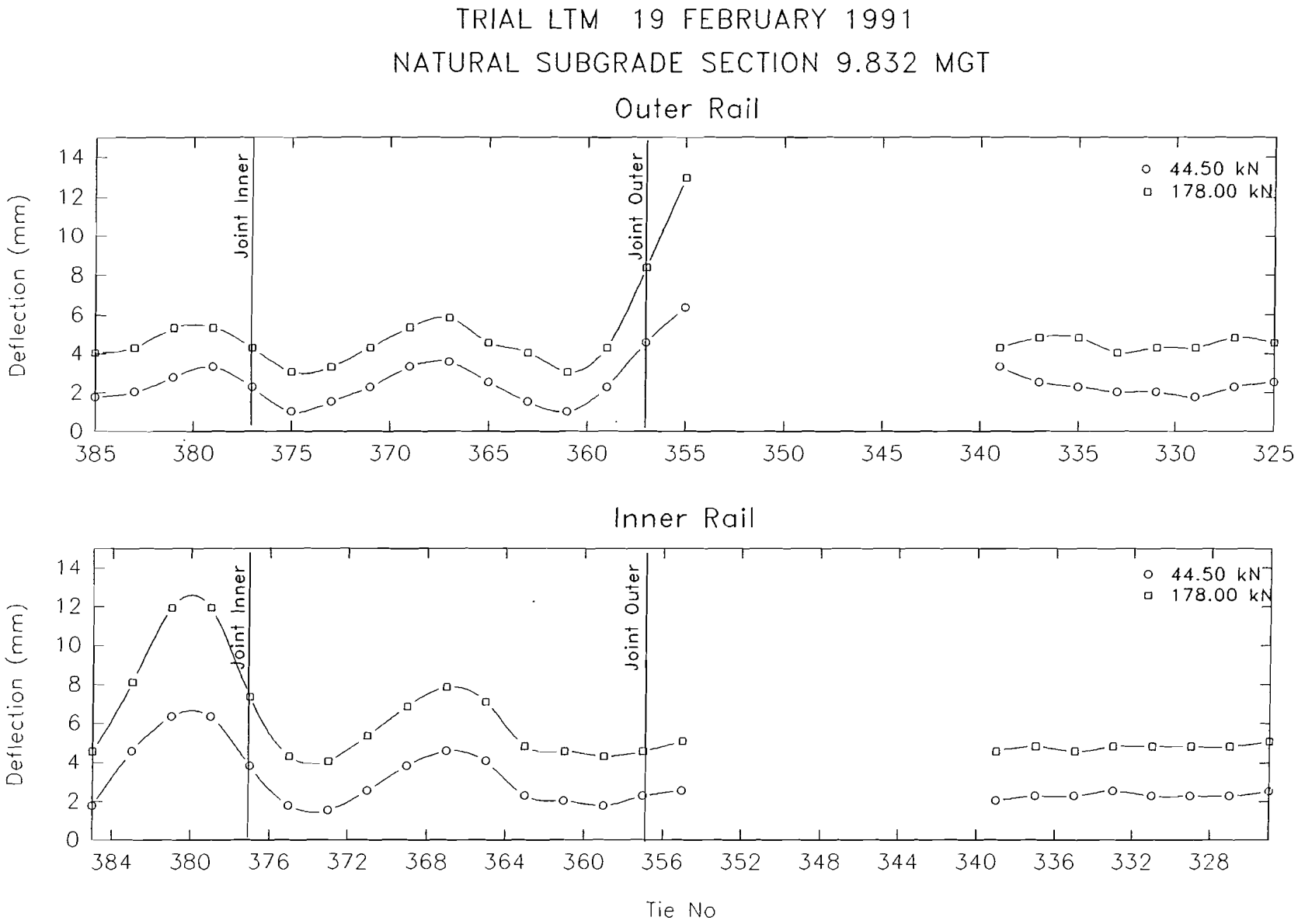

Figure 53: Running Deflection 19 February 1991

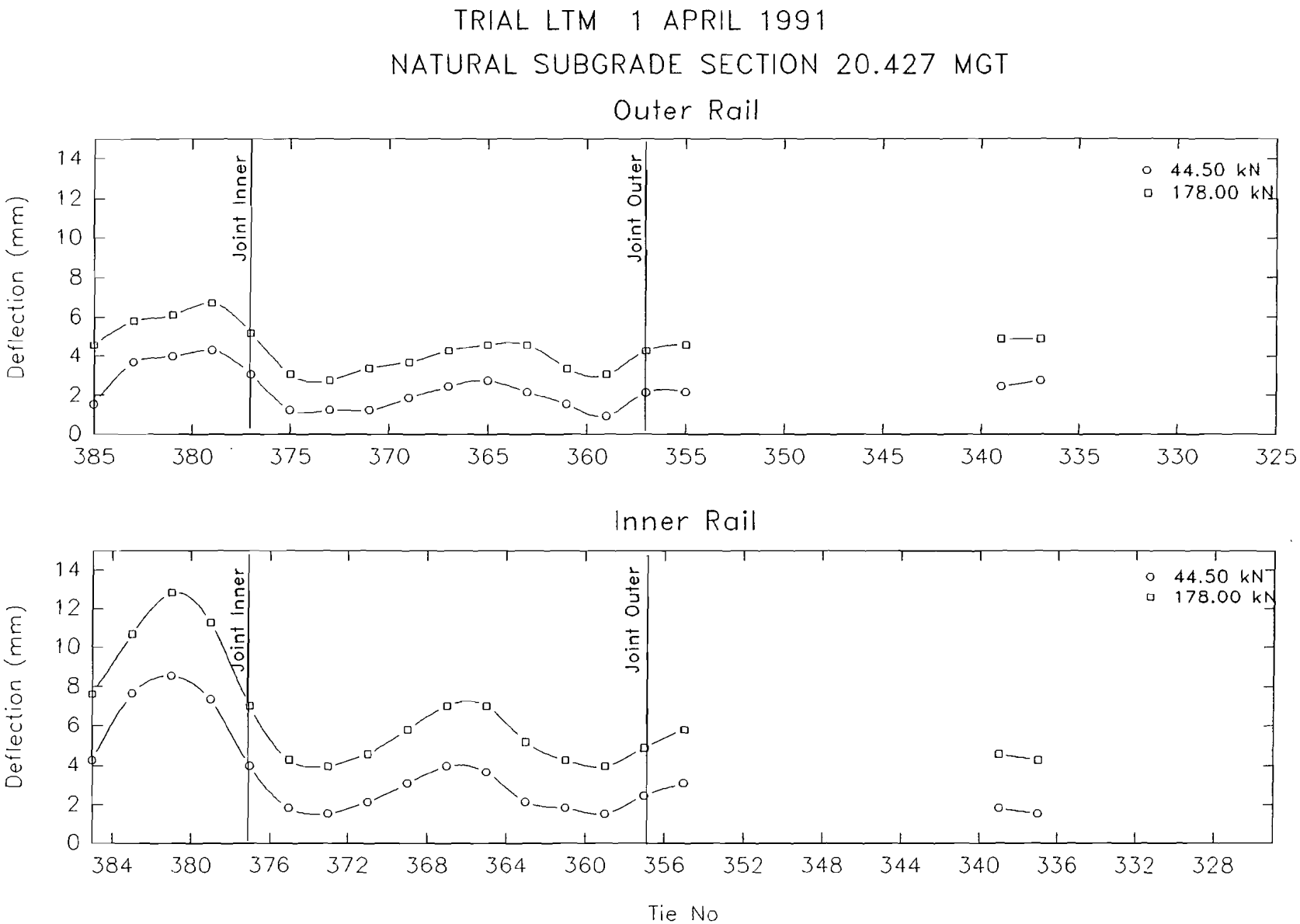

Figure 54: Running Deflection 1 April 1991

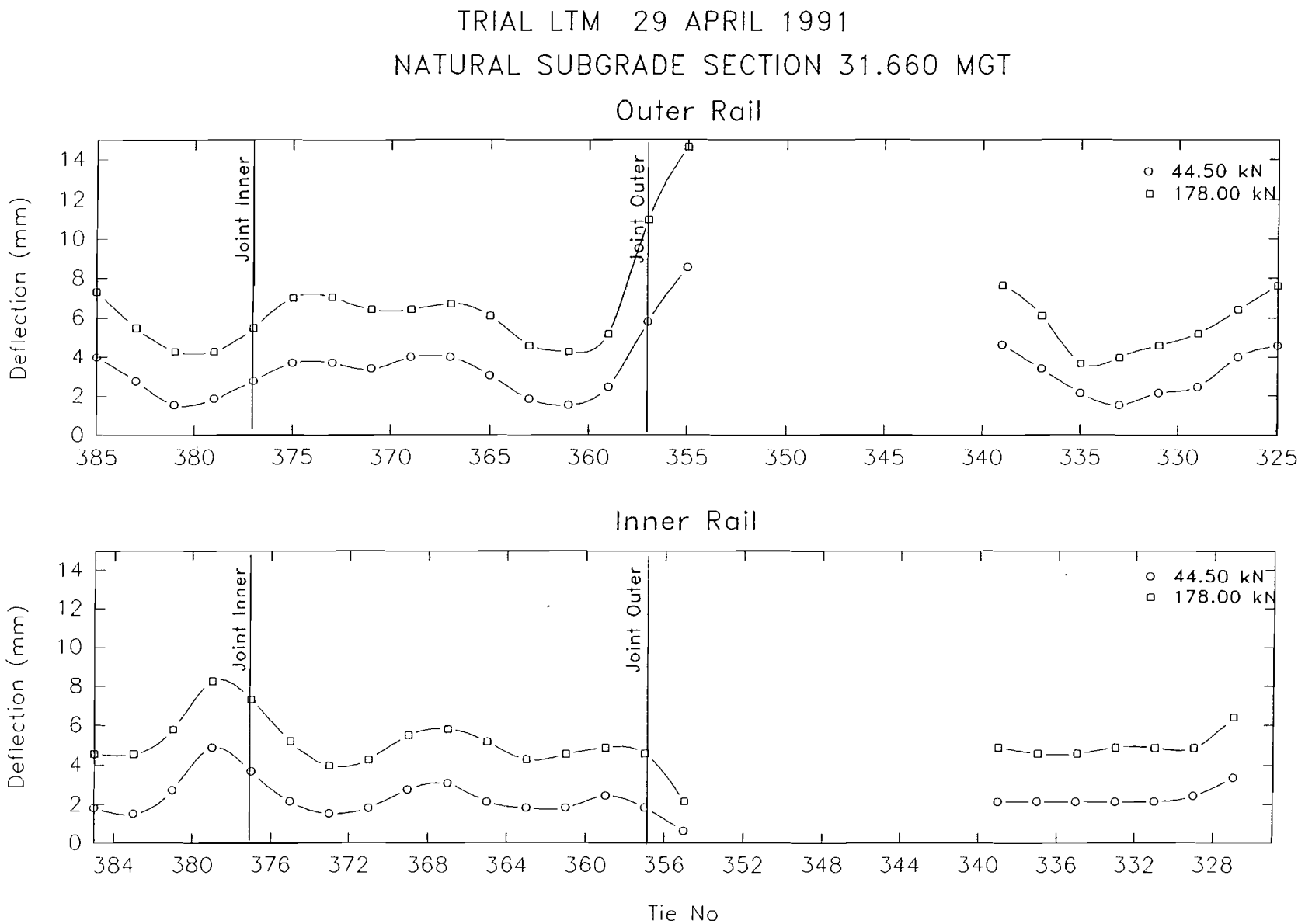

Figure 55: Running Deflection 29 April 1991

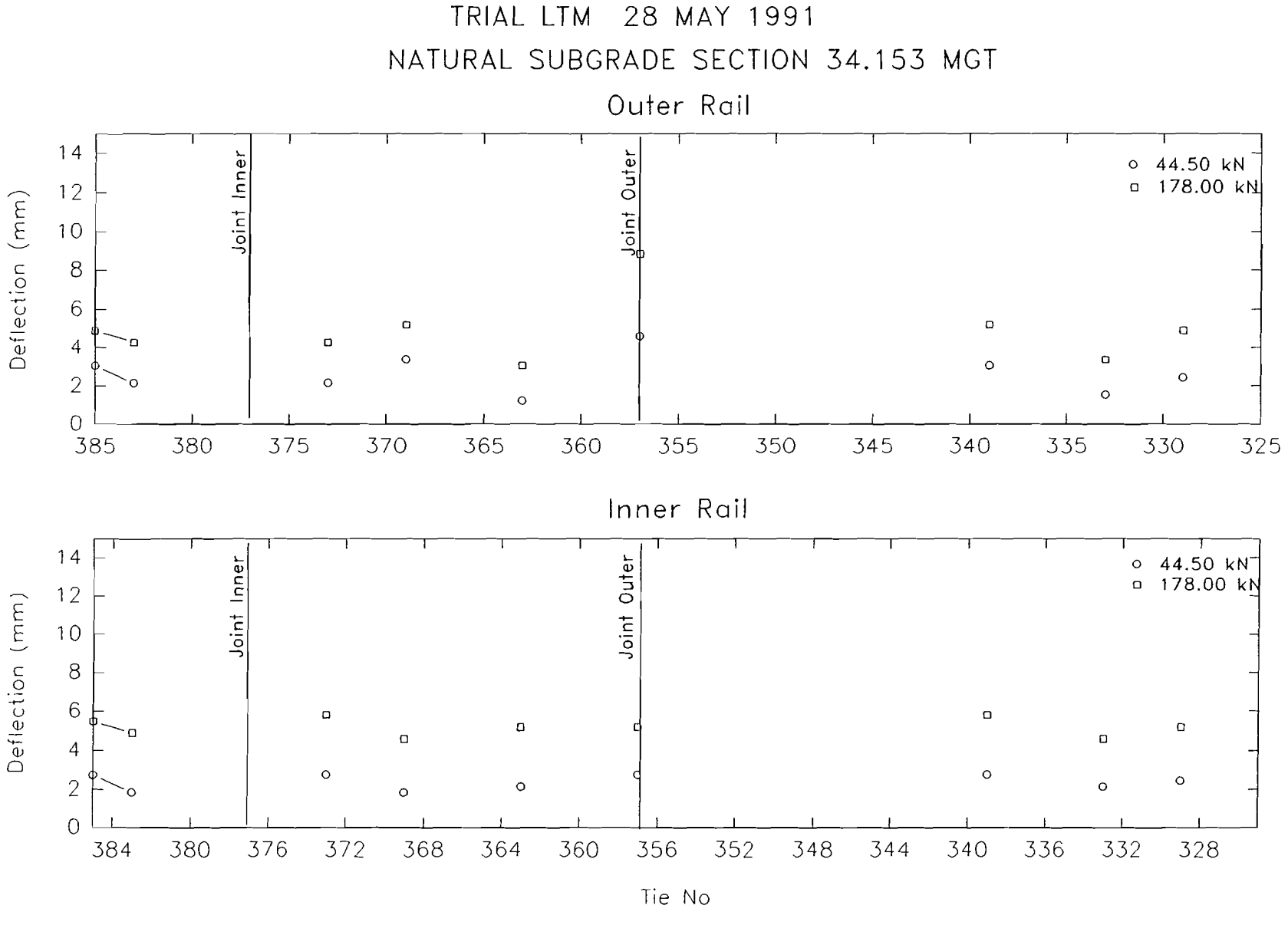

Figure 56: Running Deflection 28 May 1991

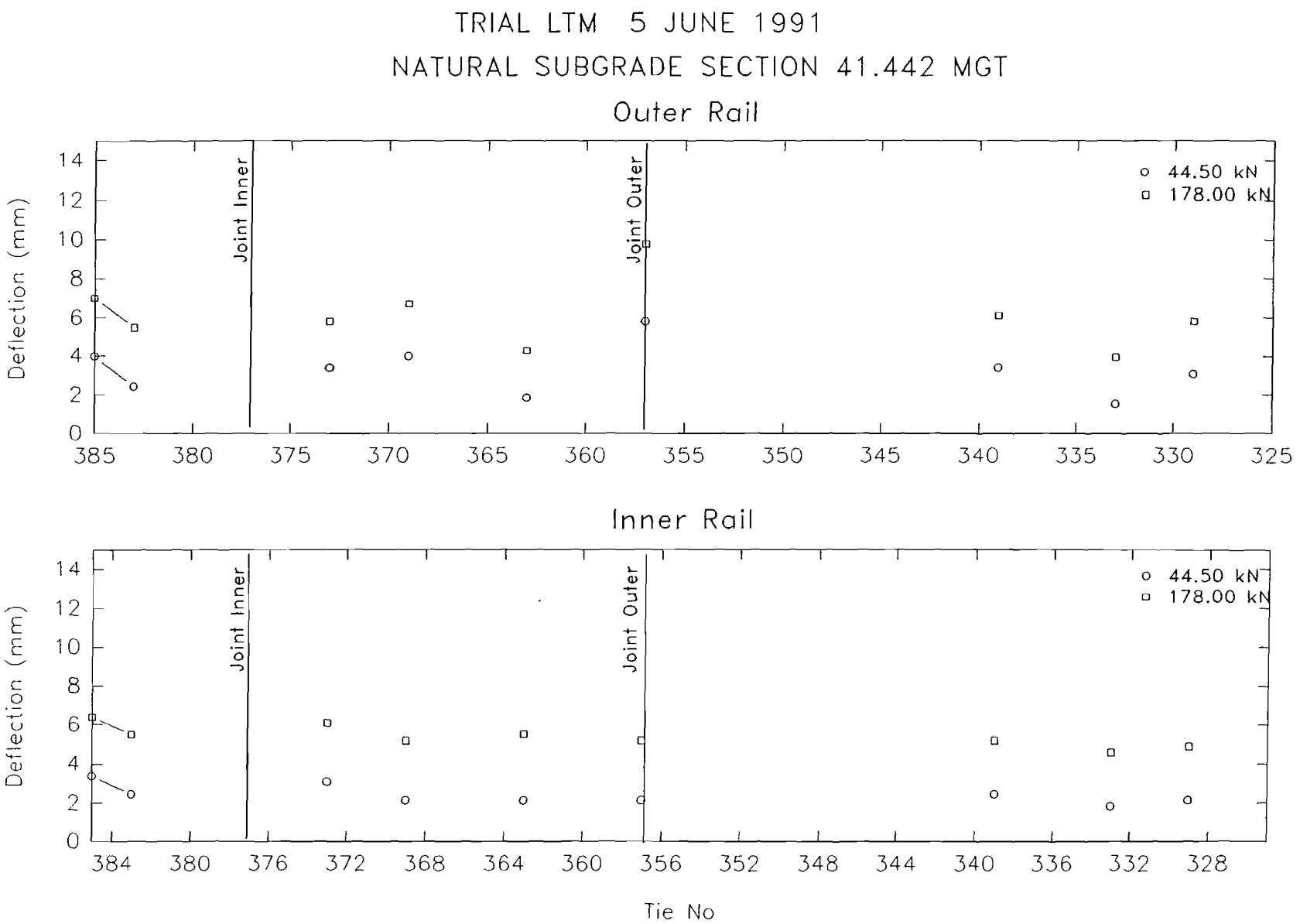

Figure 57: Running Deflection 5 June 1991

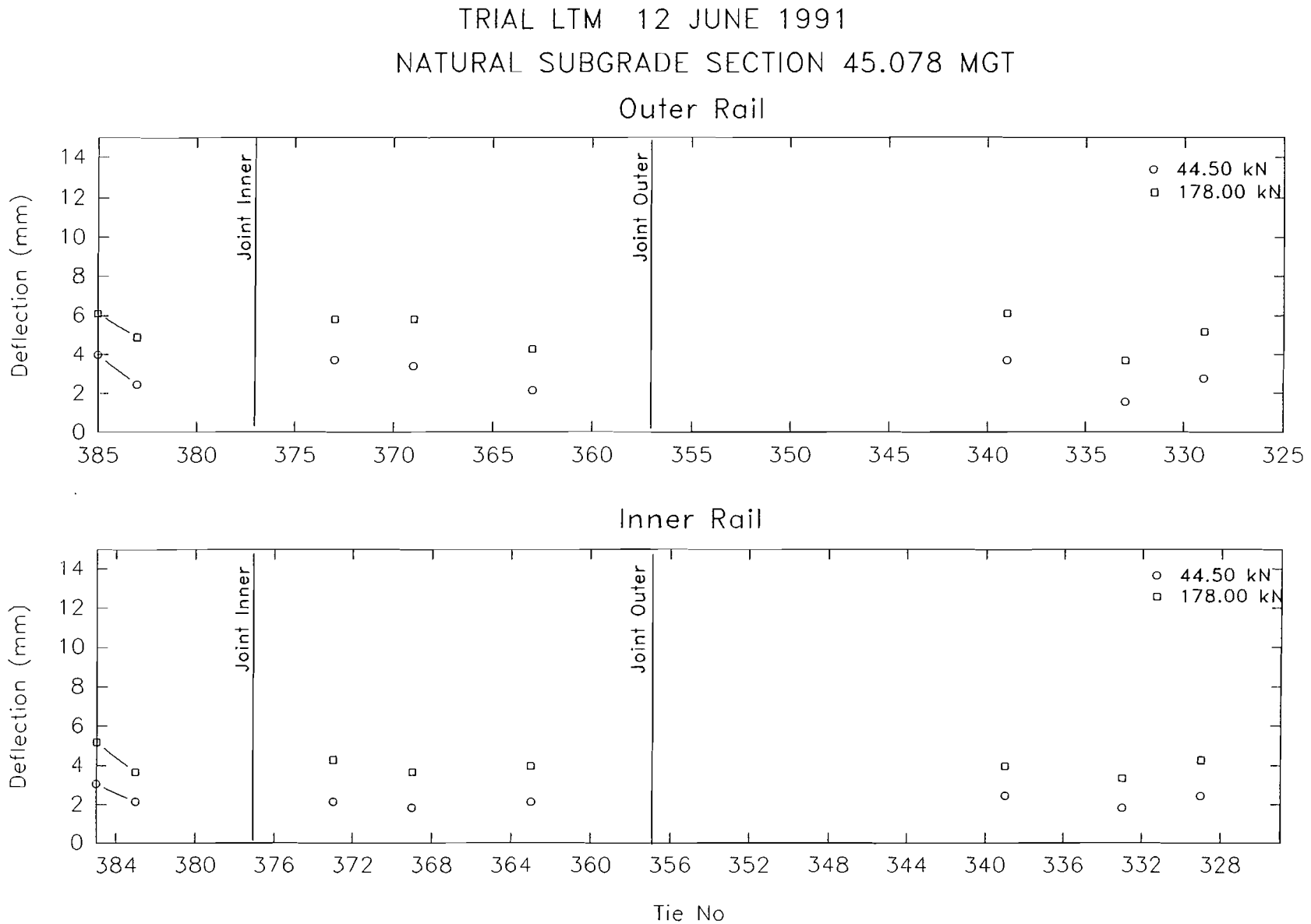

Figure 58: Running Deflection 12 June 1991

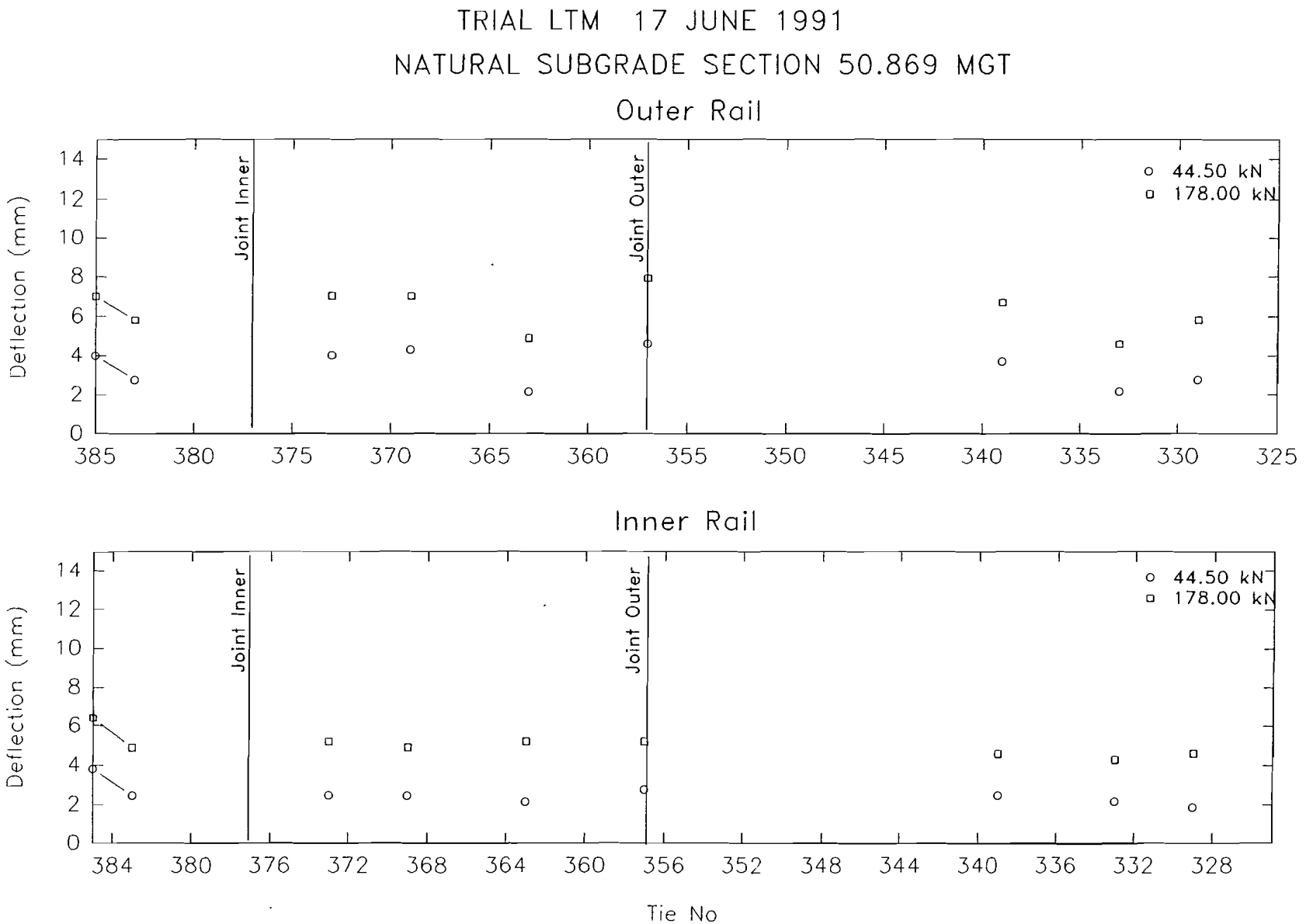

Figure 59: Running Deflection 17 June 1991

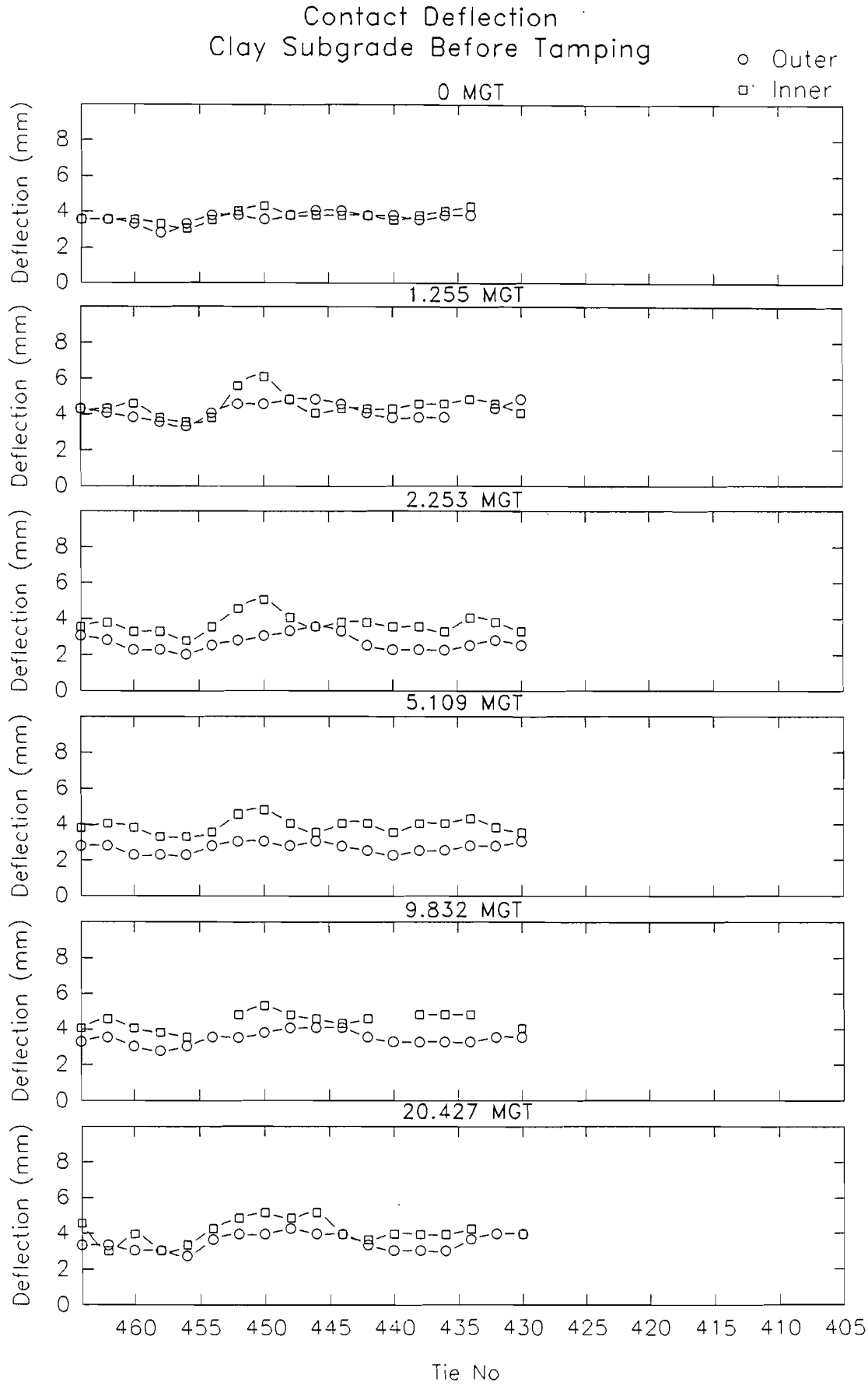

Figure 60: Clay Subgrade Contact Deflection for Period 1

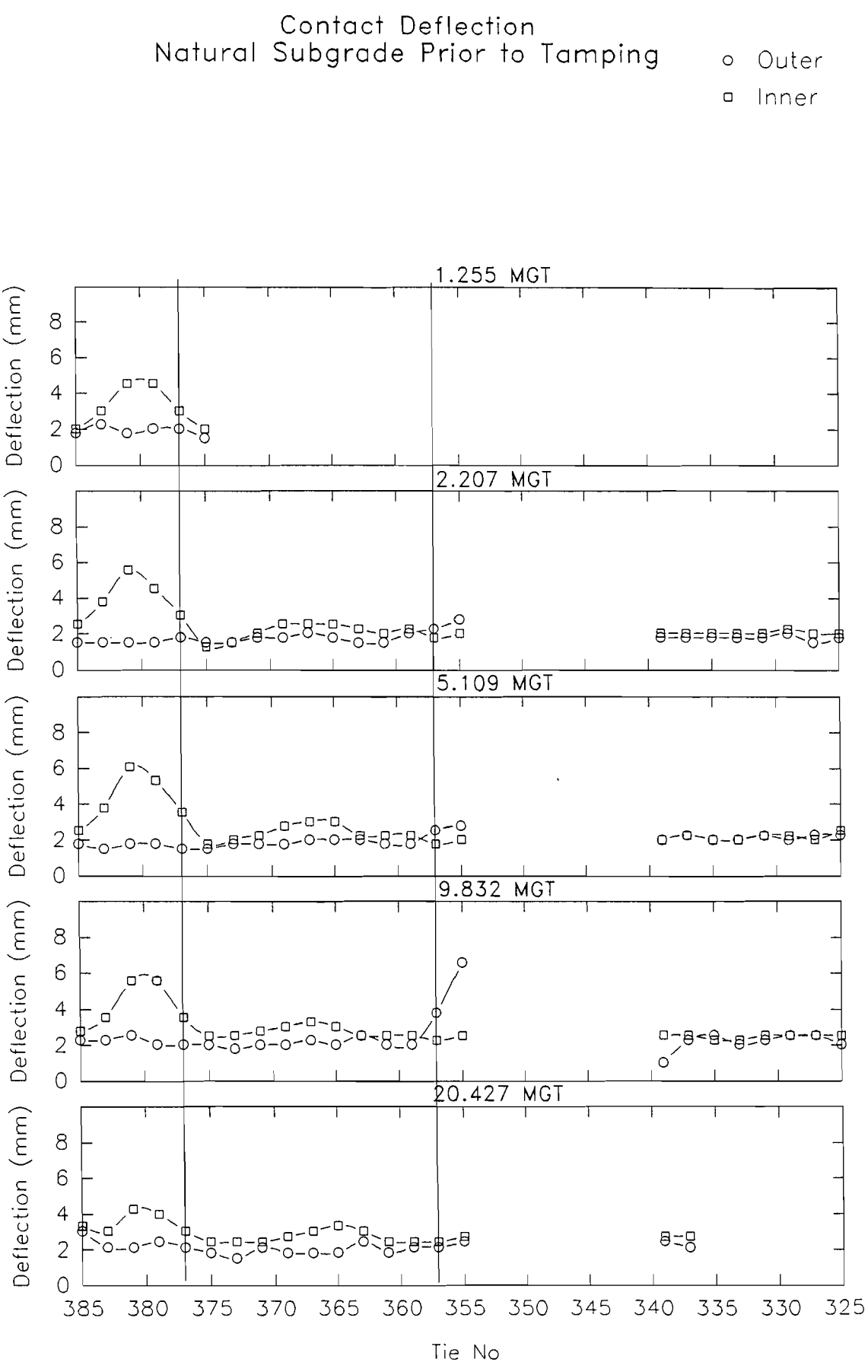

Figure 61: Natural Subgrade Contact Deflection for Period 1

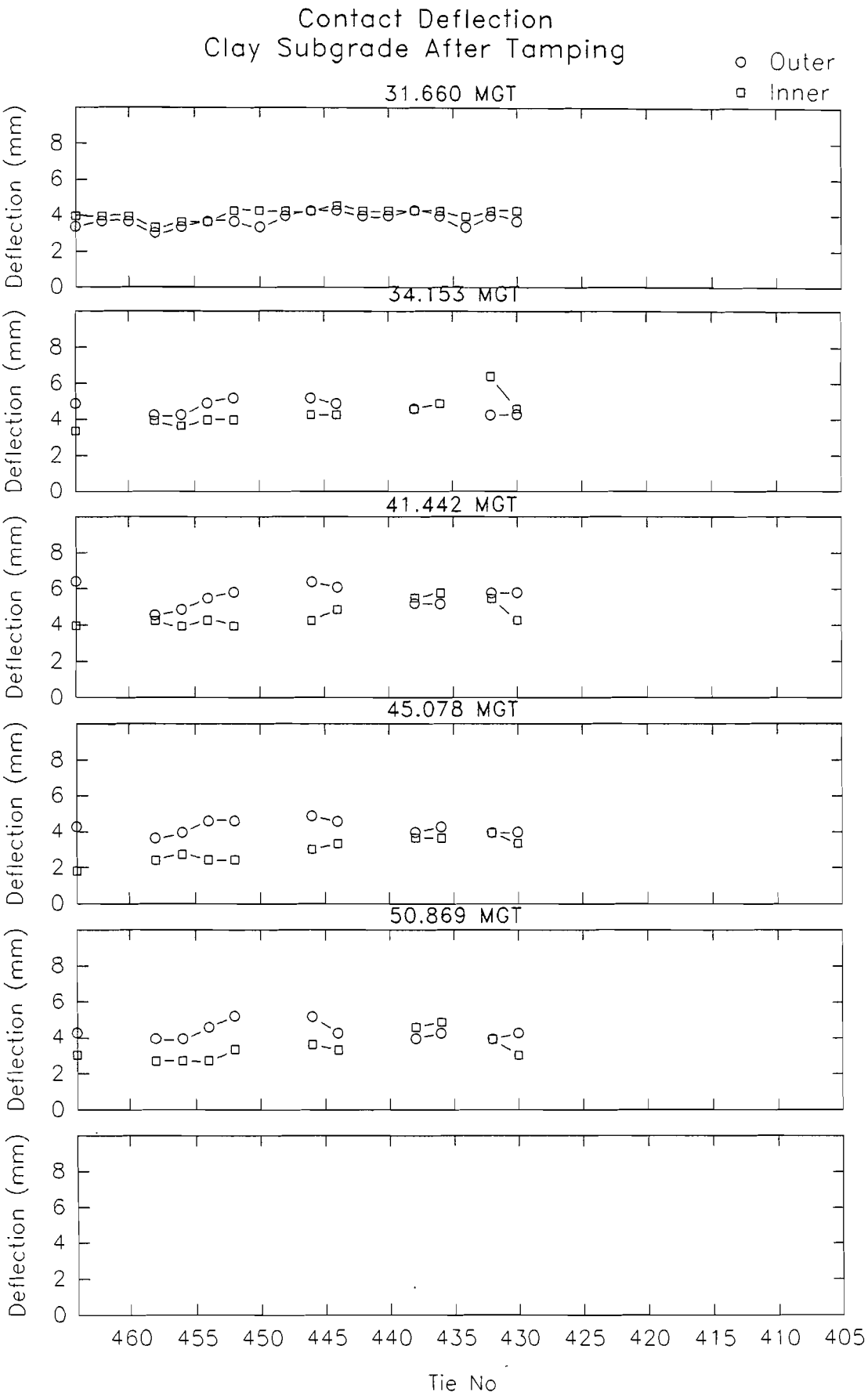

Figure 62: Clay Subgrade Contact Deflection for Period 2

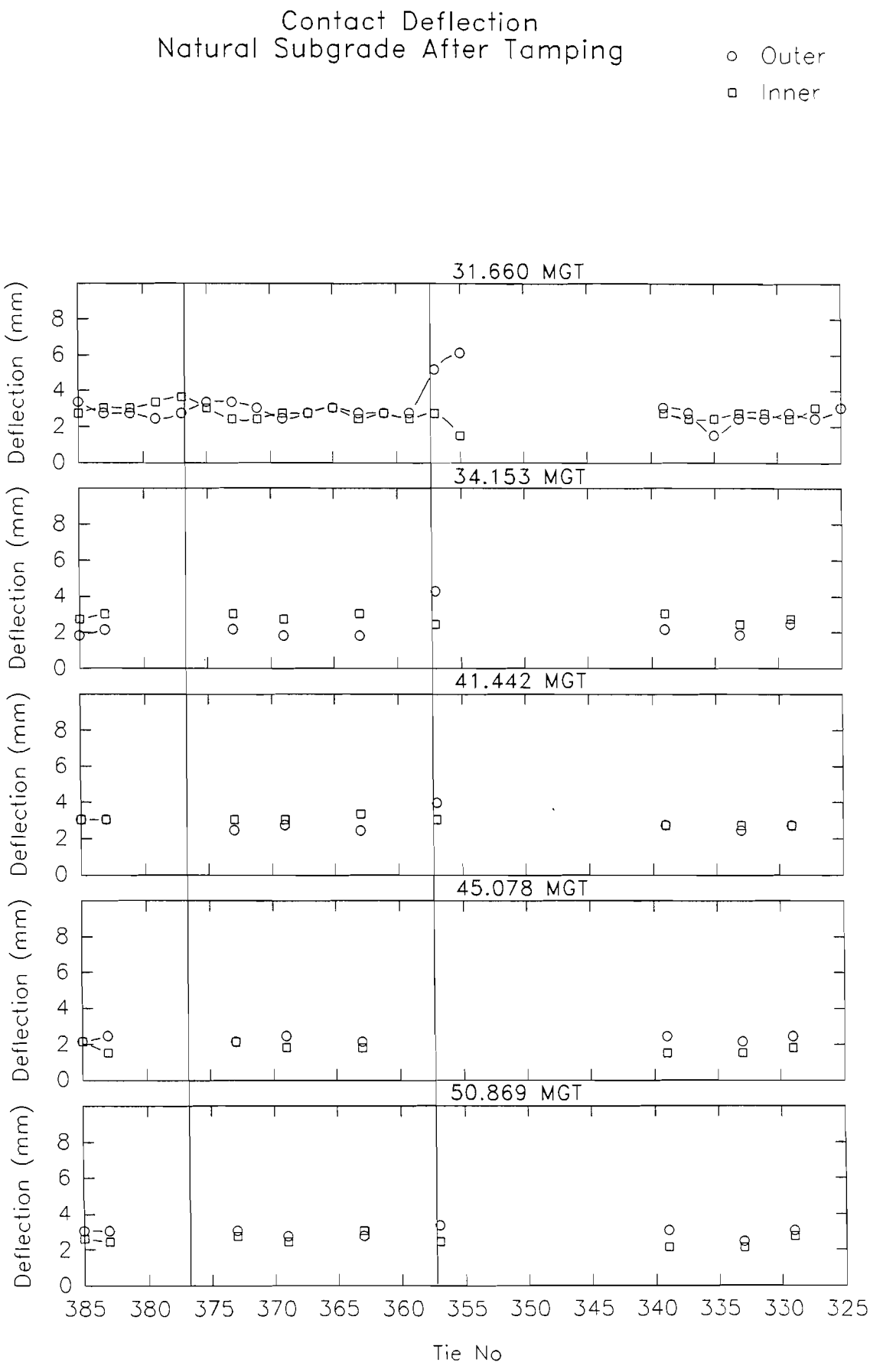

Figure 63: Natural Subgrade Contact Deflection for Period 2

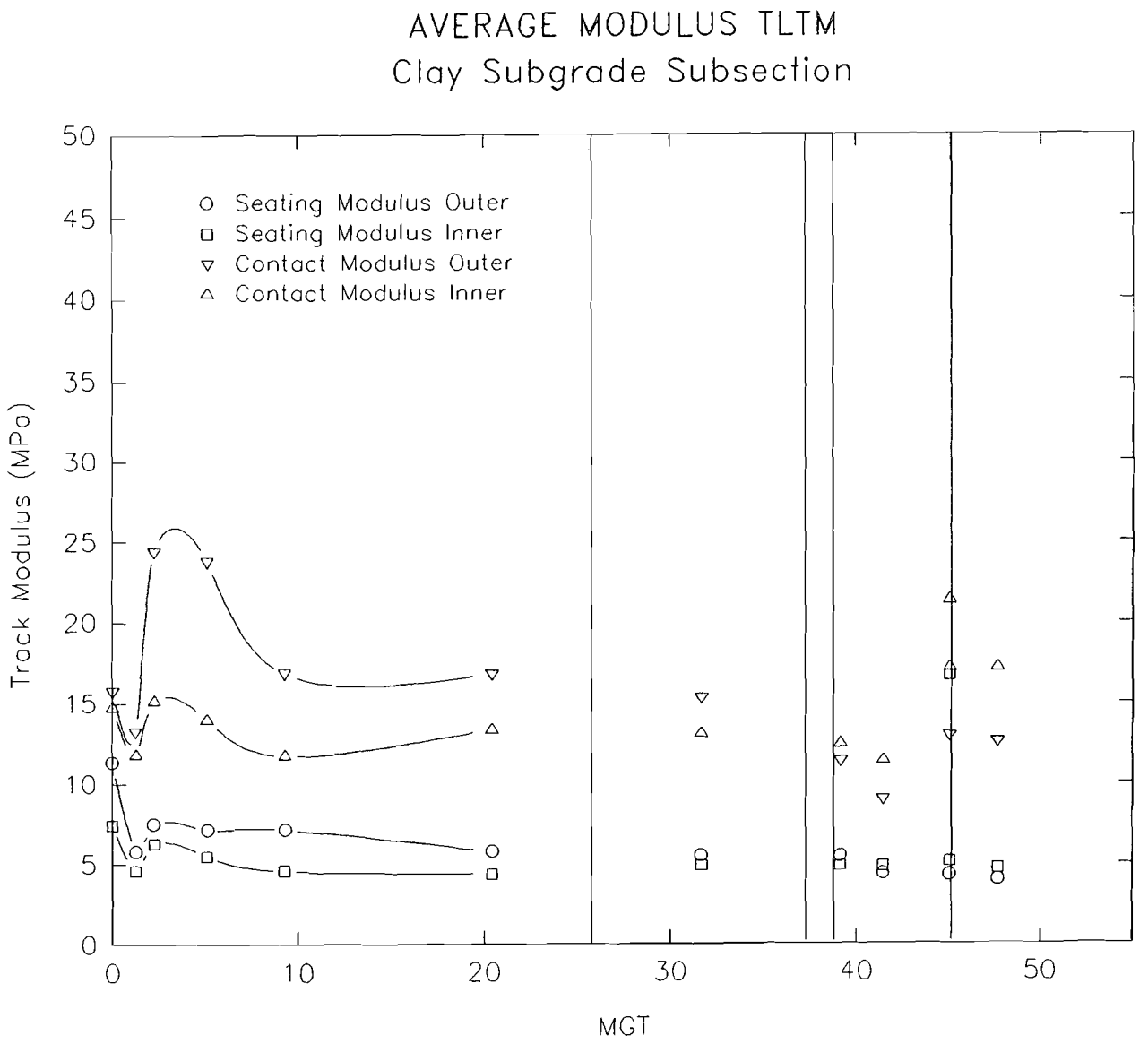

Figure 64: Clay Section Average Modulus

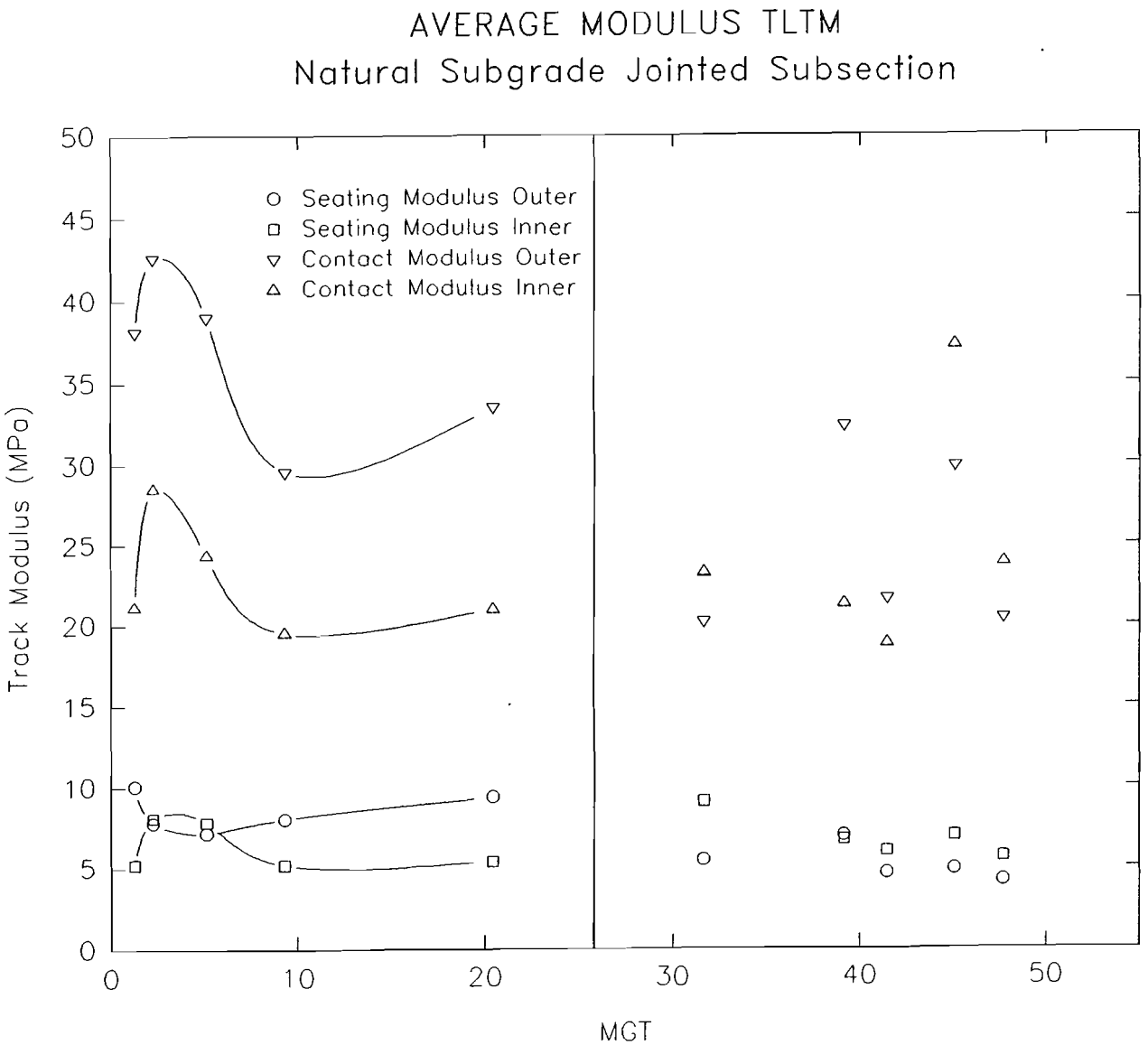

Figure 65: Average Modulus - Jointed Natural Subsection

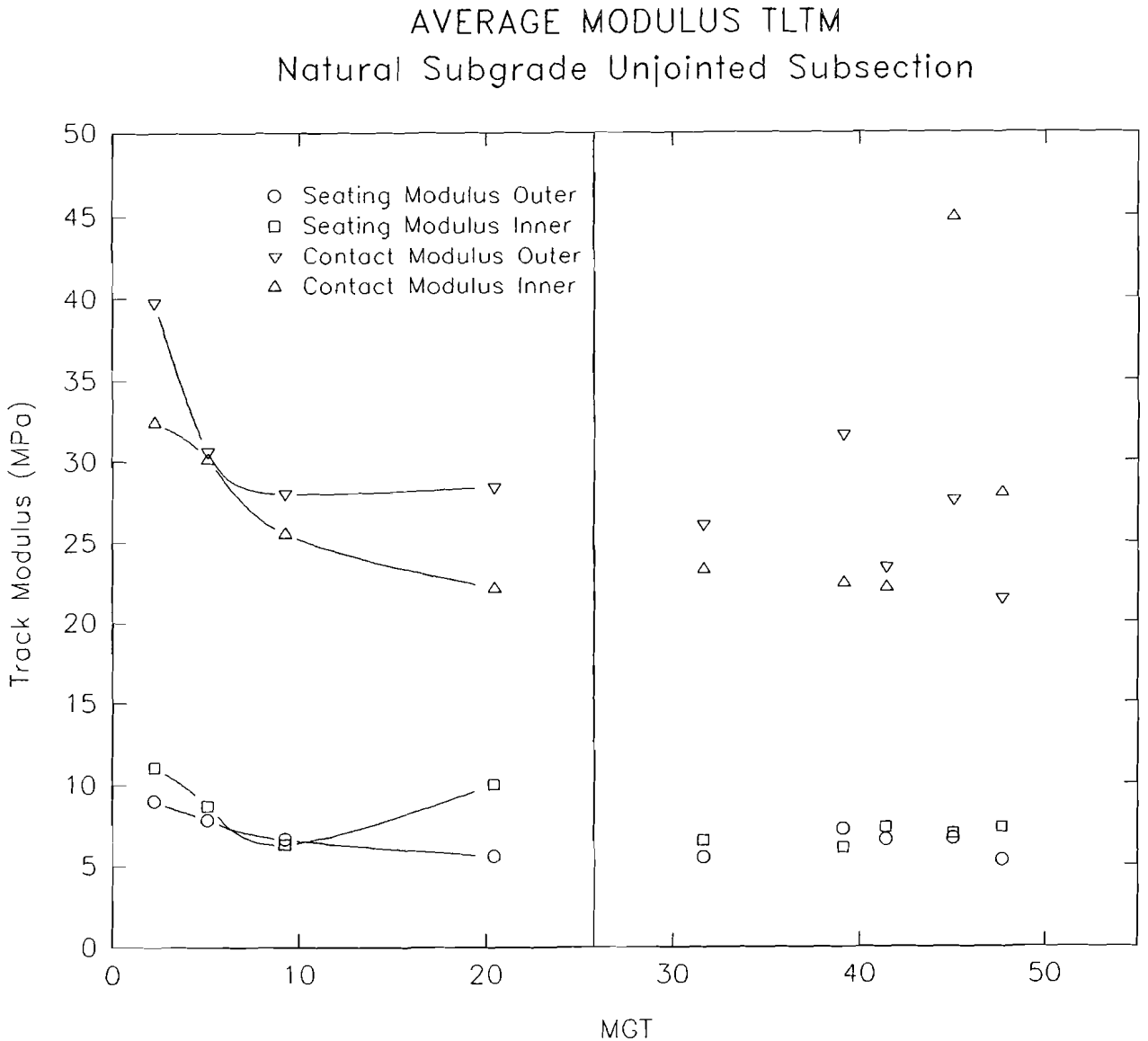

Figure 66: Average Modulus - Unjointed Natural Subsection

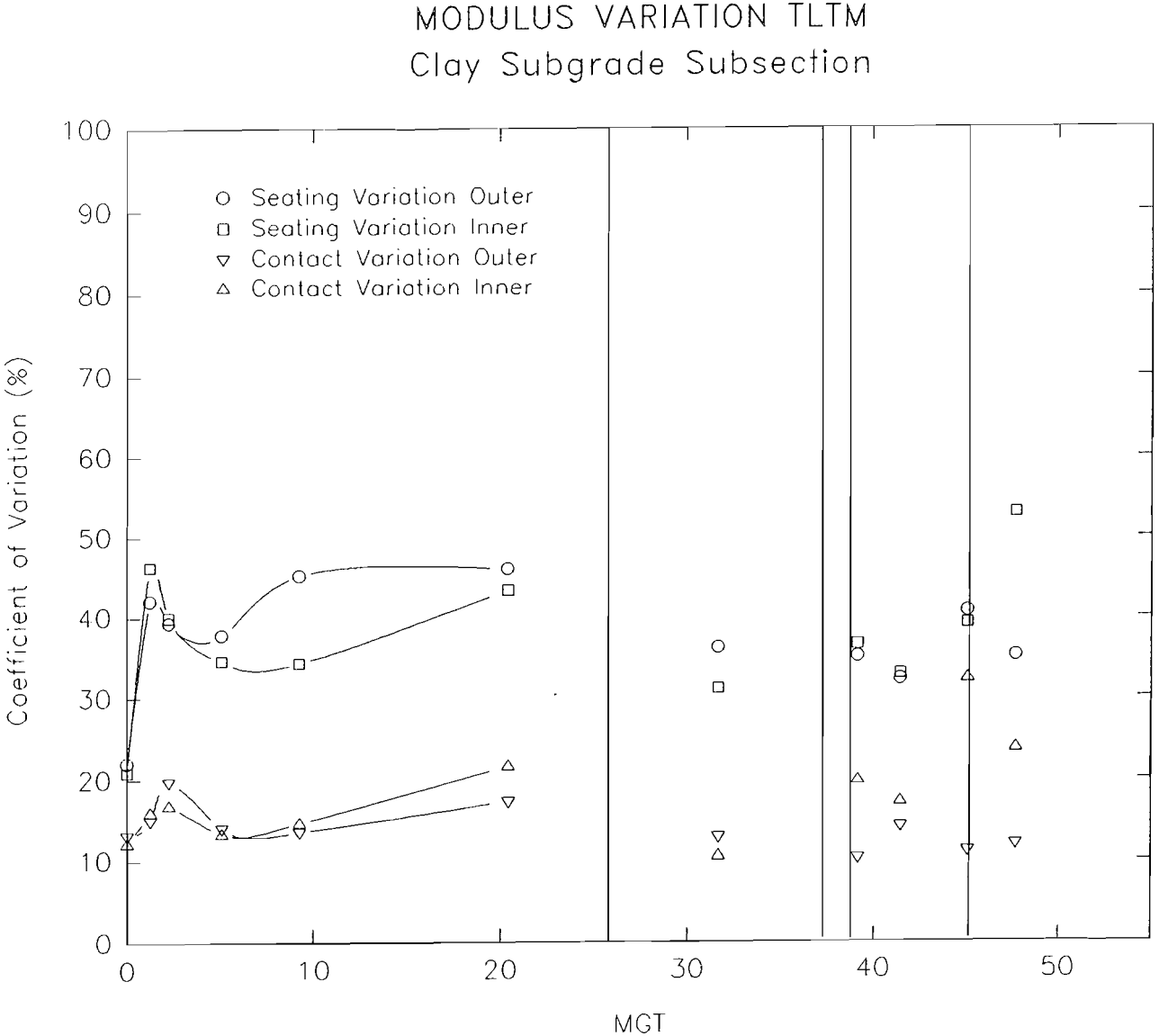

Figure 67: Variation in Modulus for Clay Subgrade

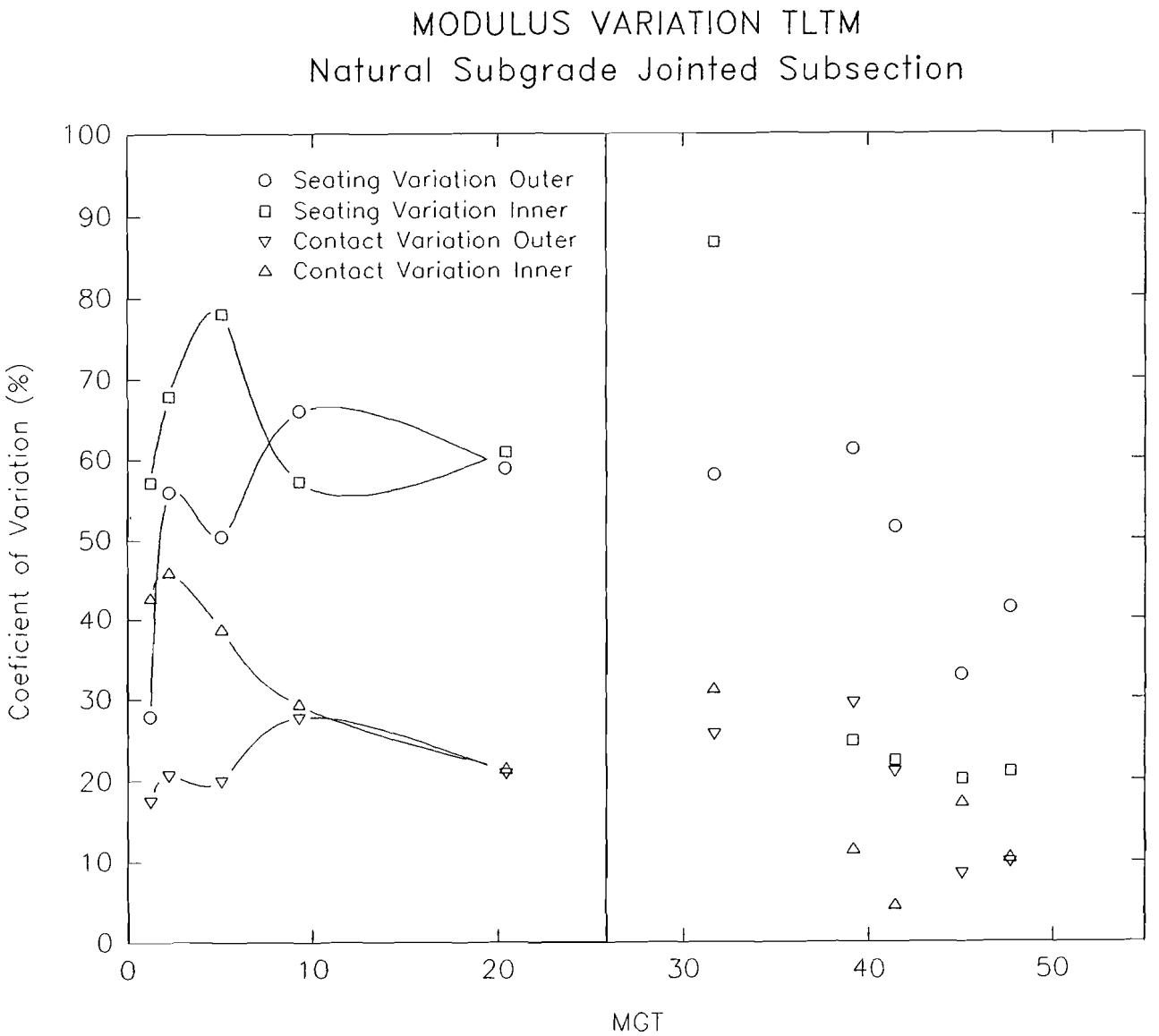

Figure 68: Modulus Variation - Jointed Natural Subsection

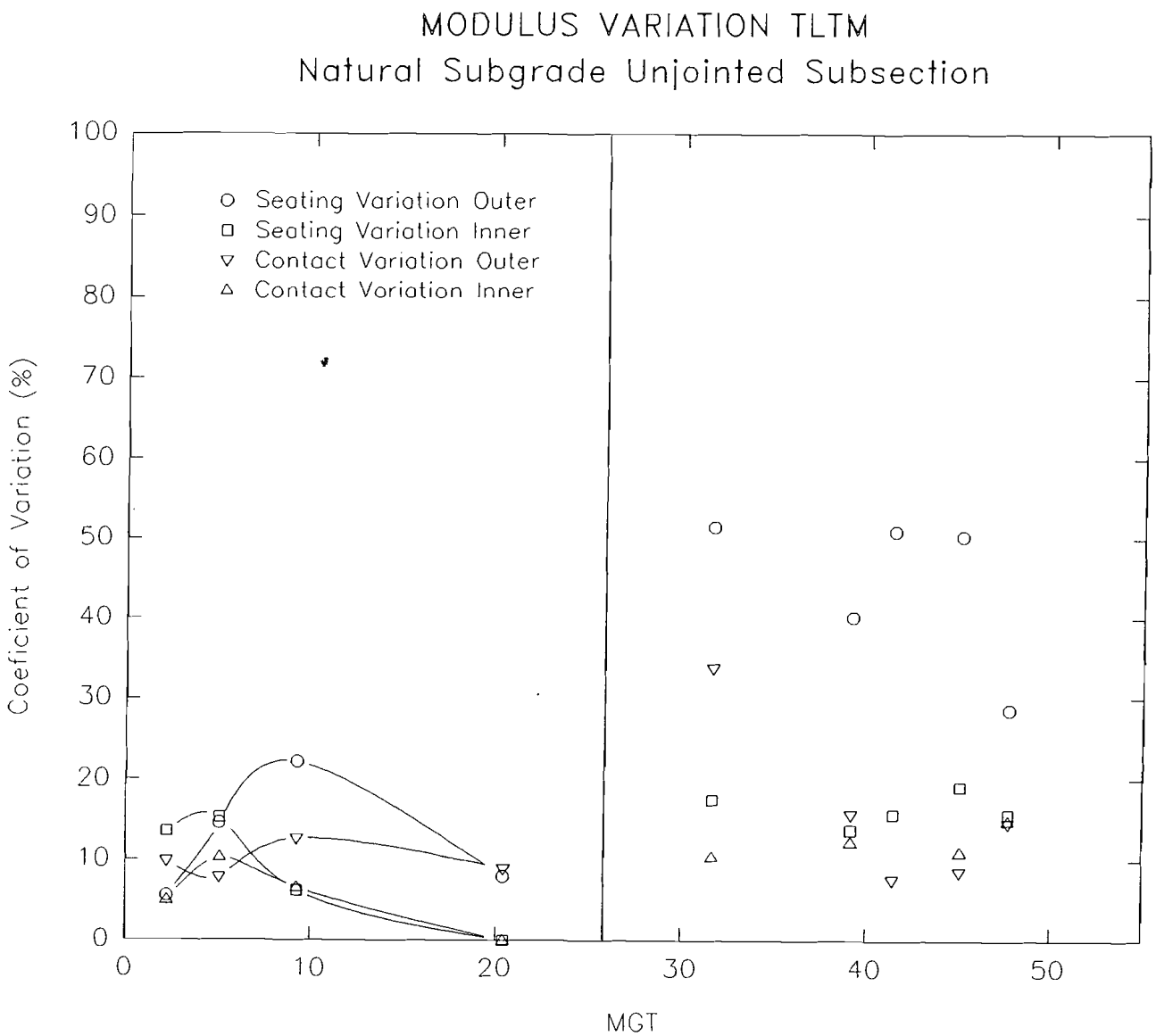

Figure 69: Modulus Variation - Unjointed Natural Subsection

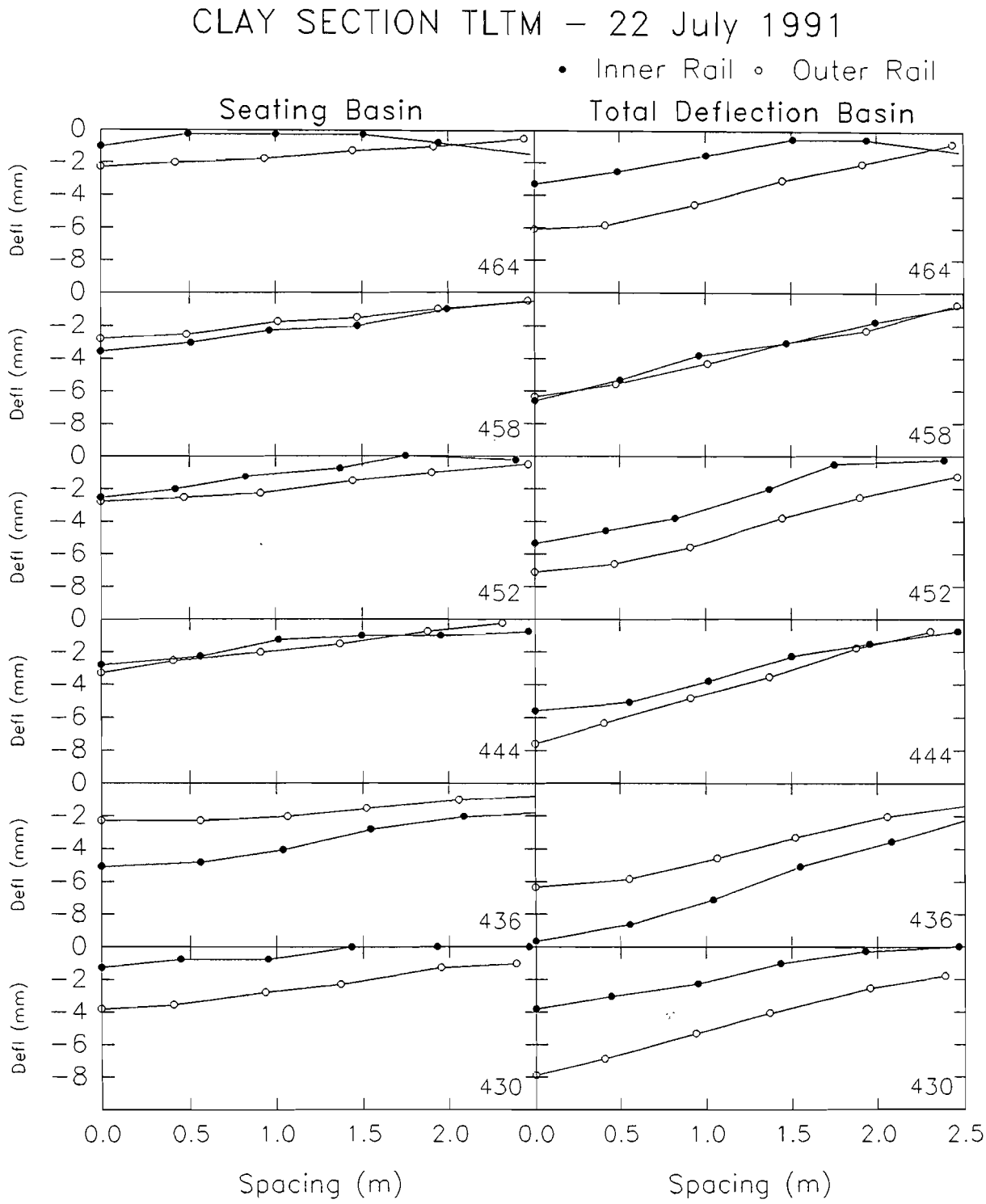

Figure 70: Clay Section Seating & Total Deflection Basins

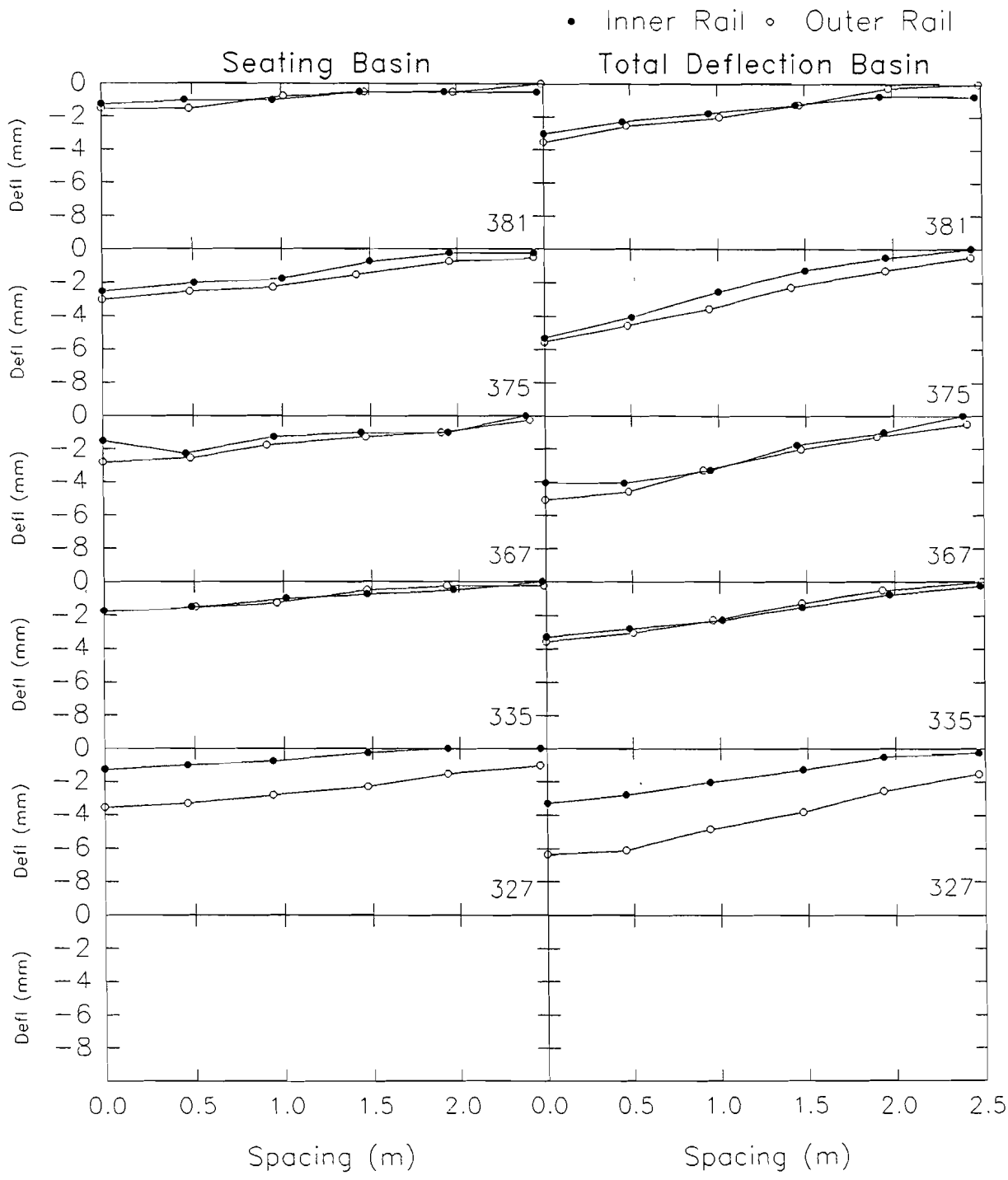

Figure 71: Natural Section Seating & Total Deflection Basins

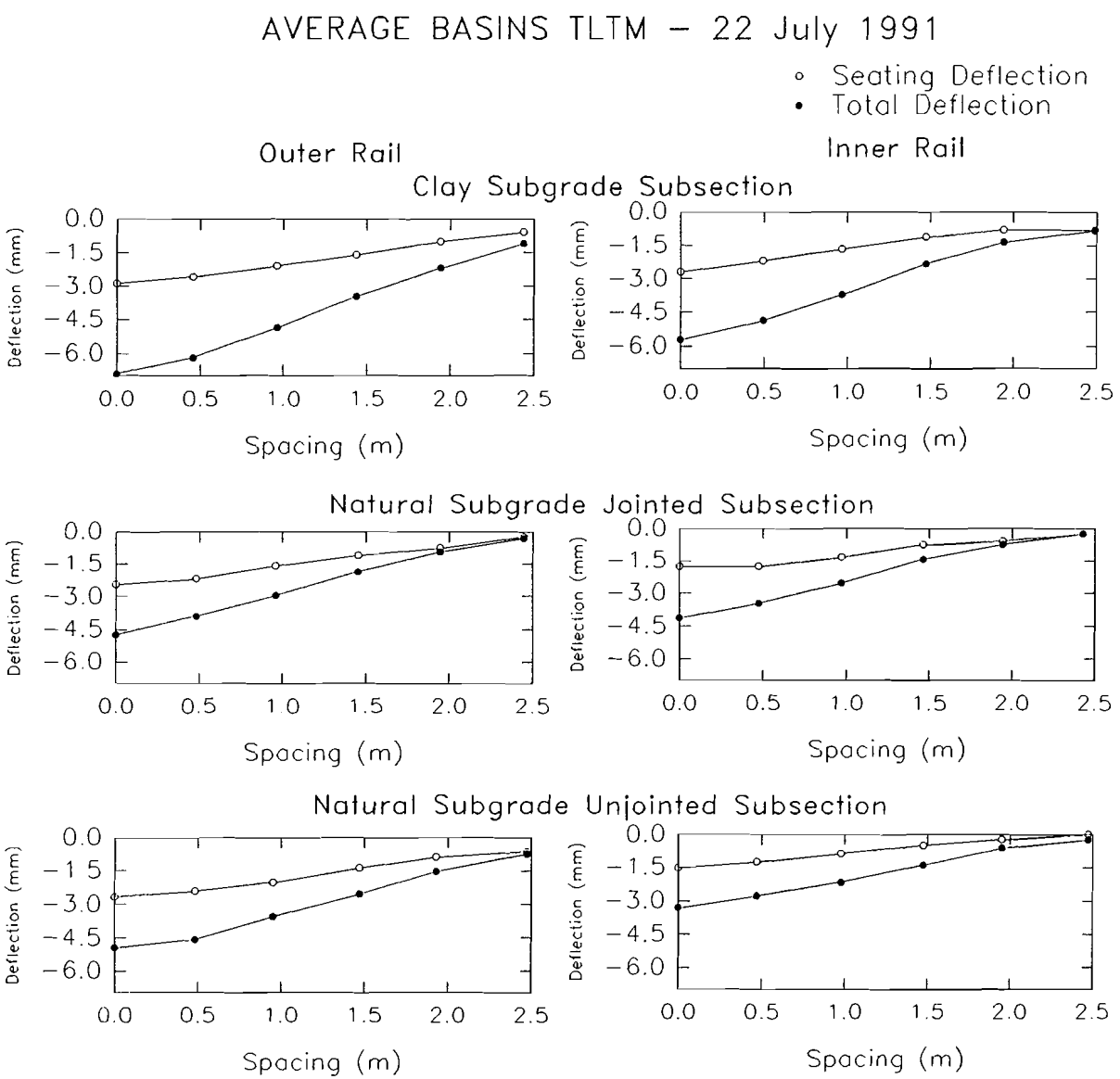

Figure 72: Average Seating and Total Deflection Basins

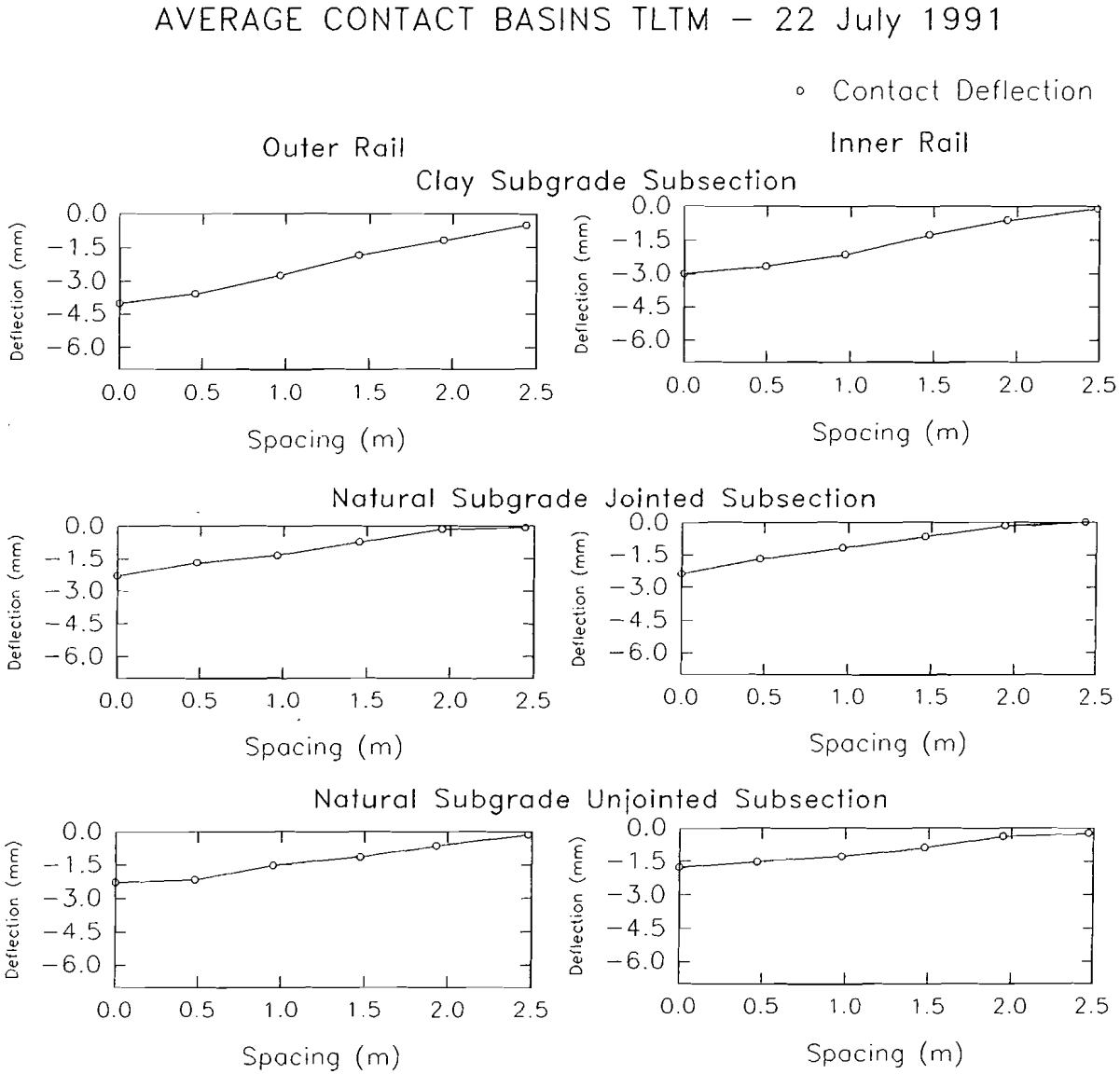

Figure 73: Average Contact Basin

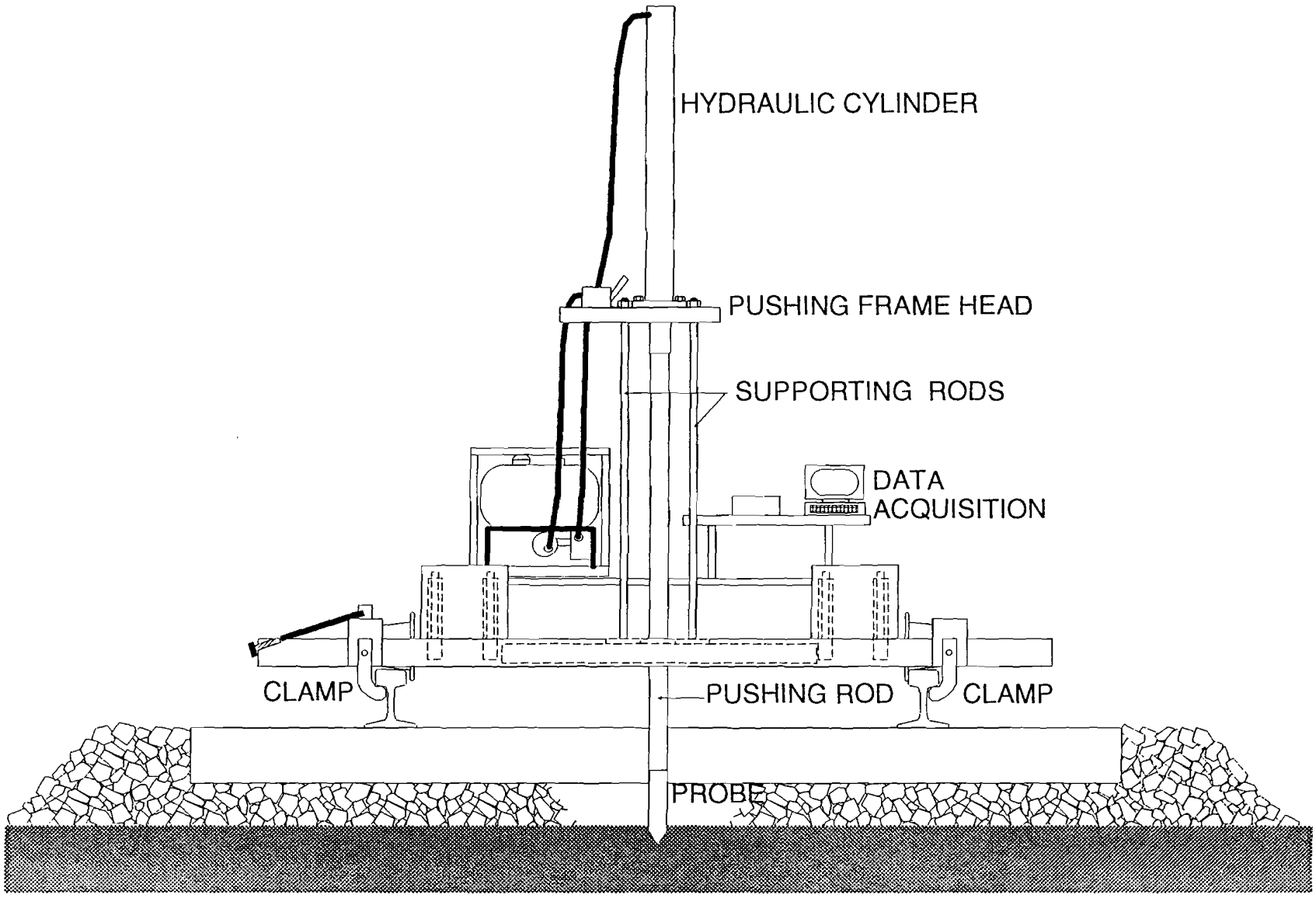

Figure 74: CPT Test Setup

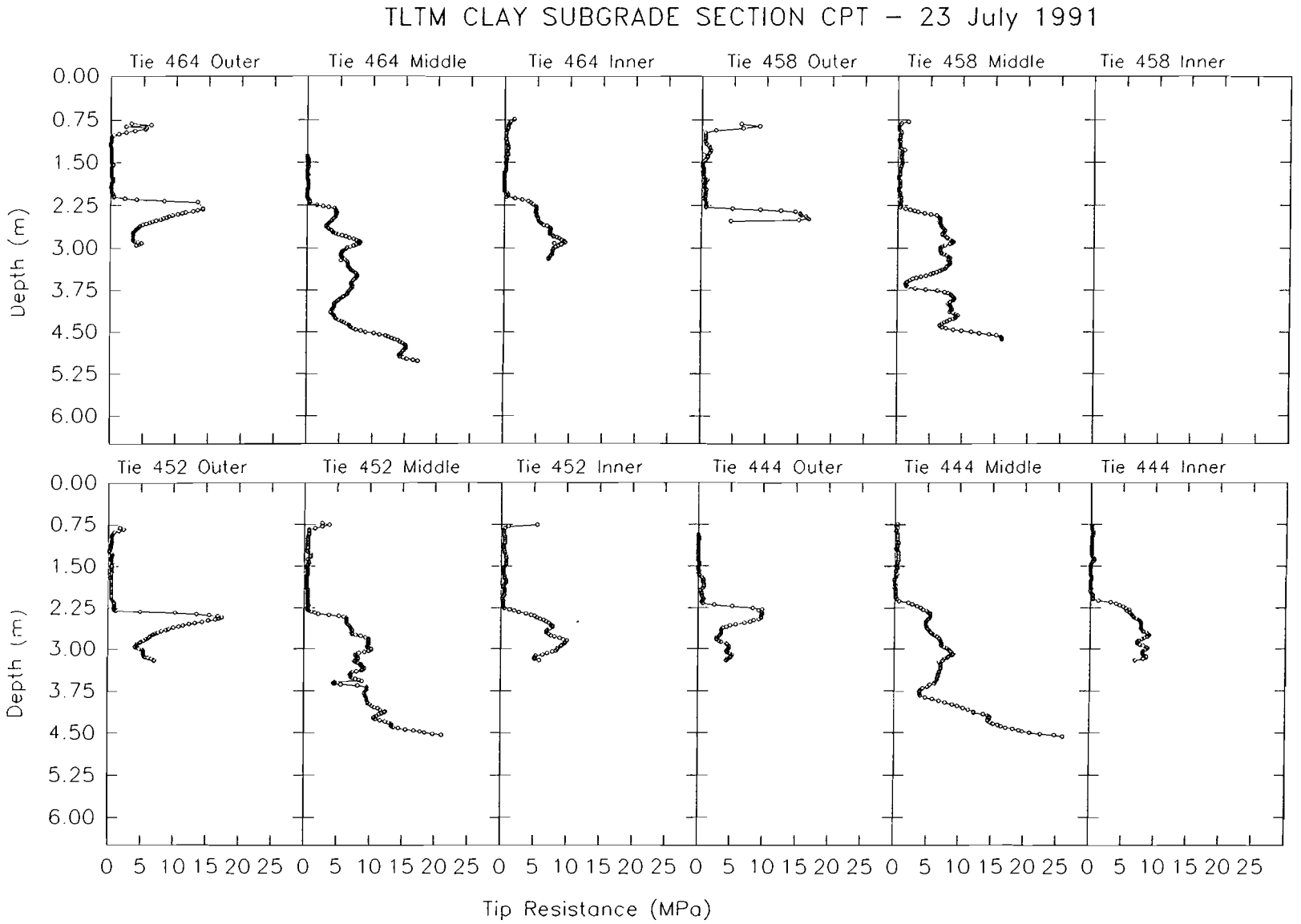

Figure 75(a): Clay CPT Profiles

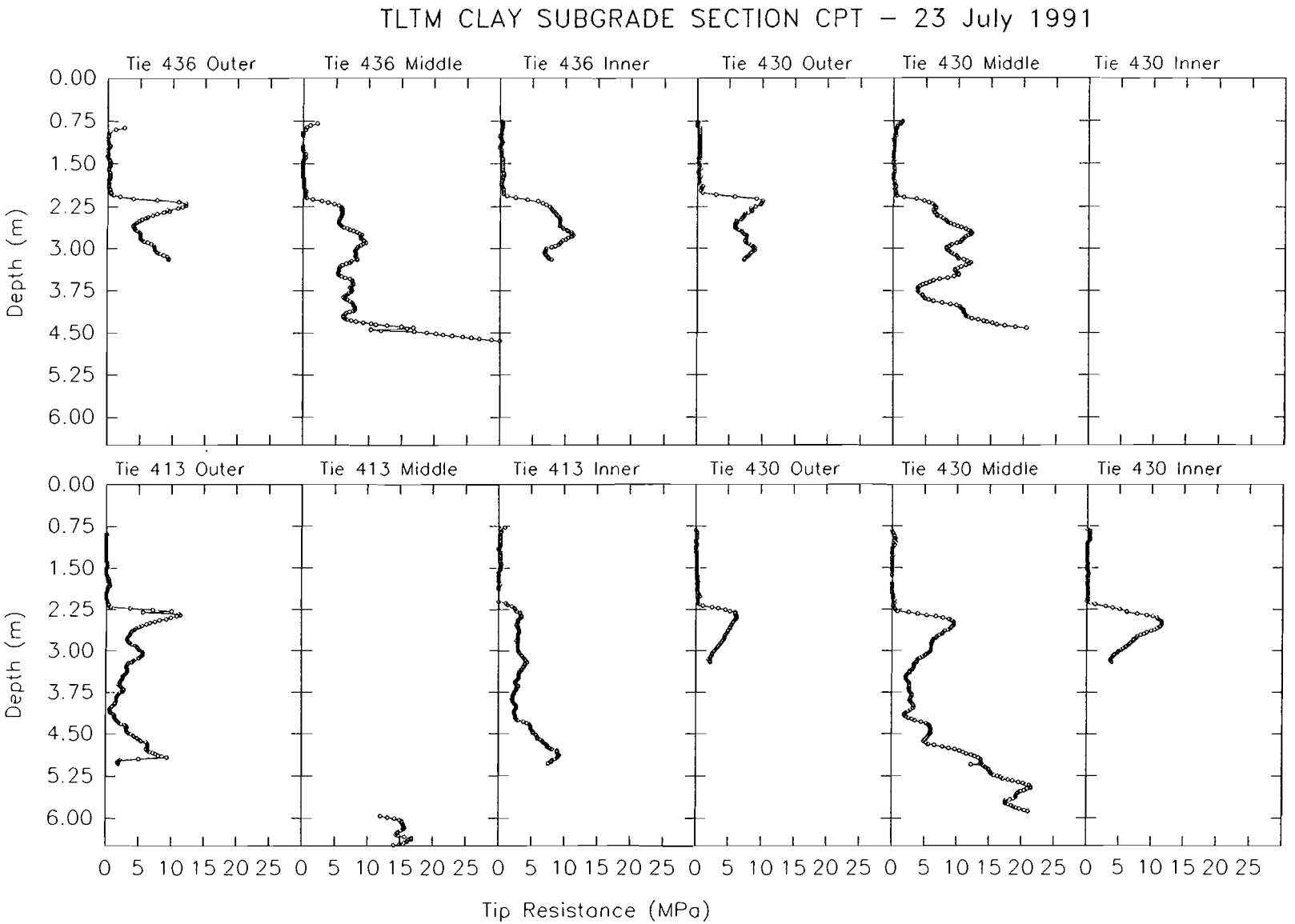

Figure 75(b): Clay CPT Profiles (Continued)

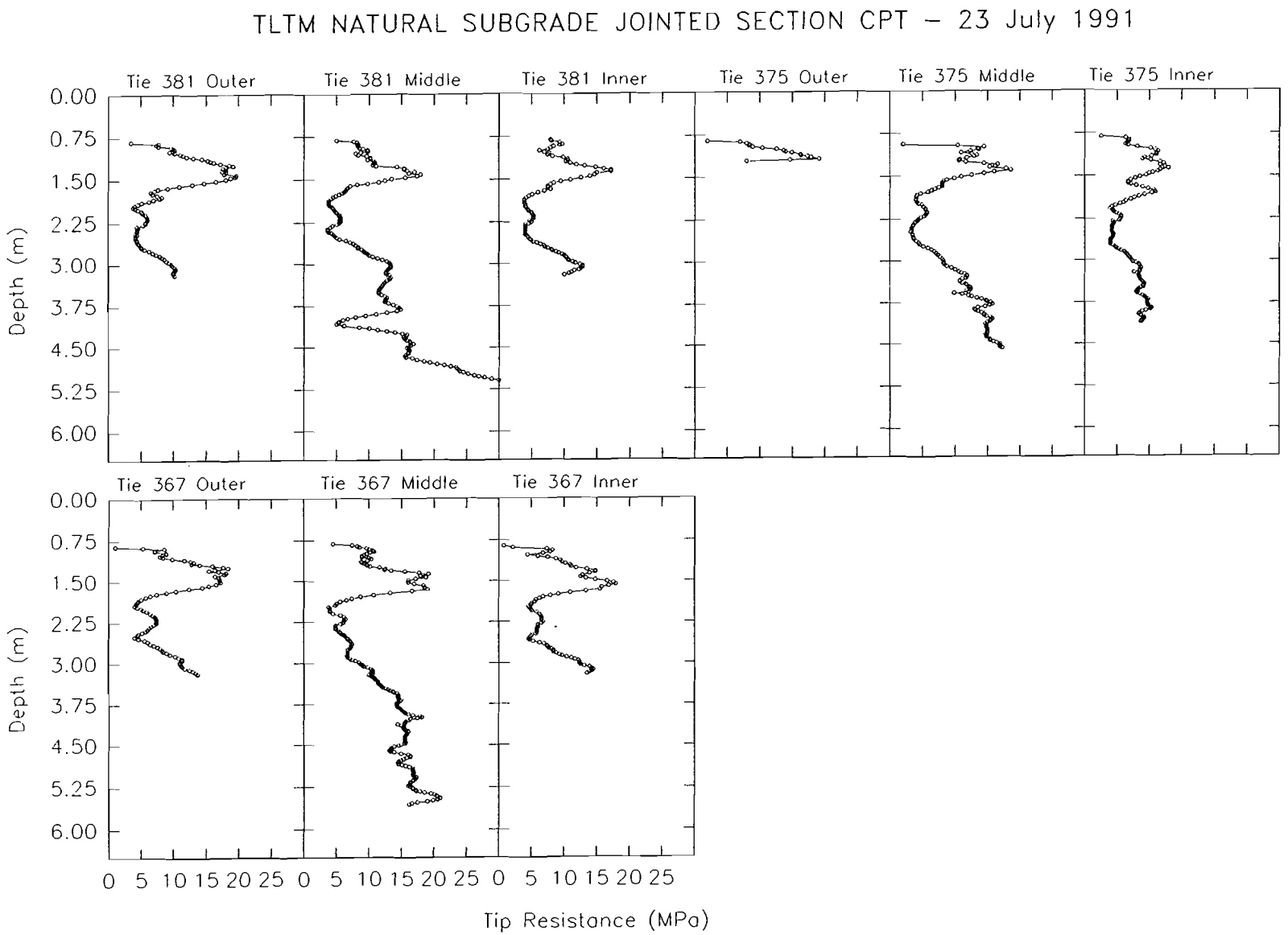

Figure 76(a): Natural Subgrade CPT Profiles

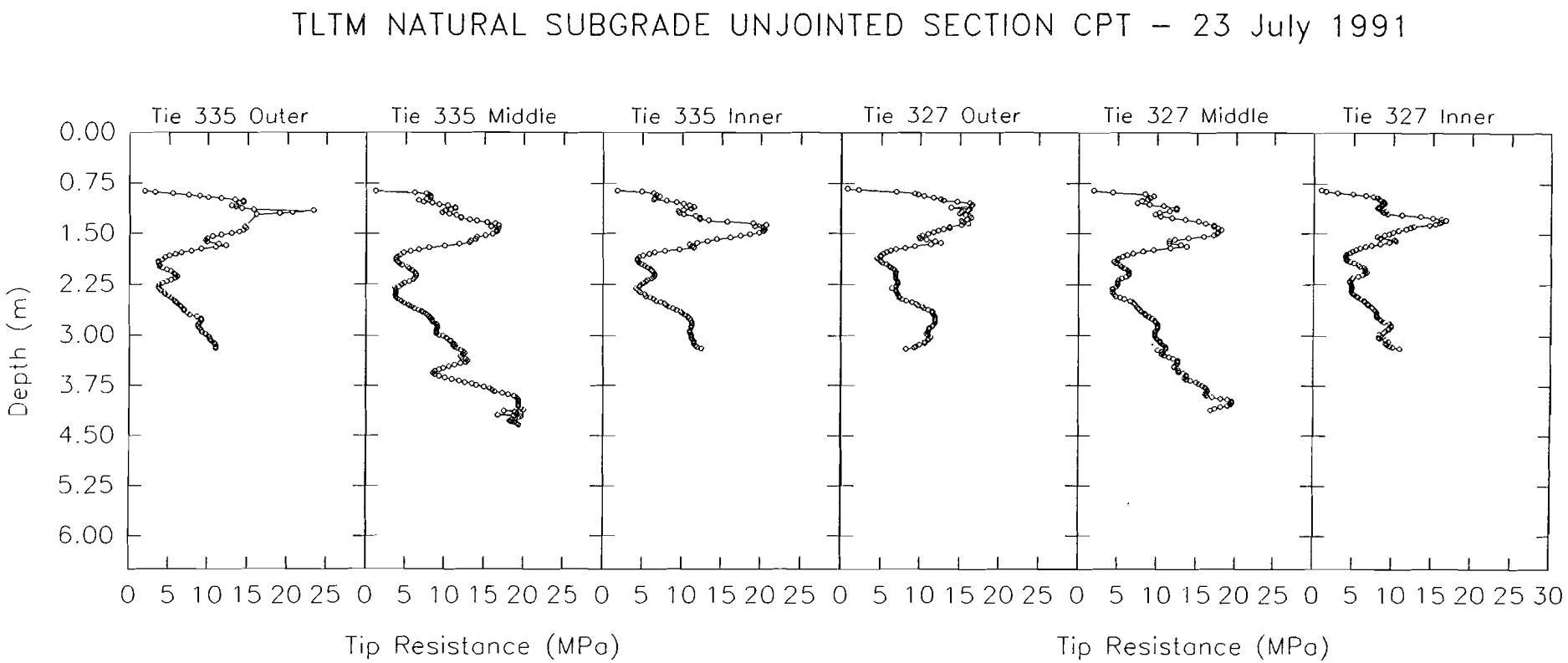

Figure 76(b): Natural Subgrade CPT Profiles (Continued)

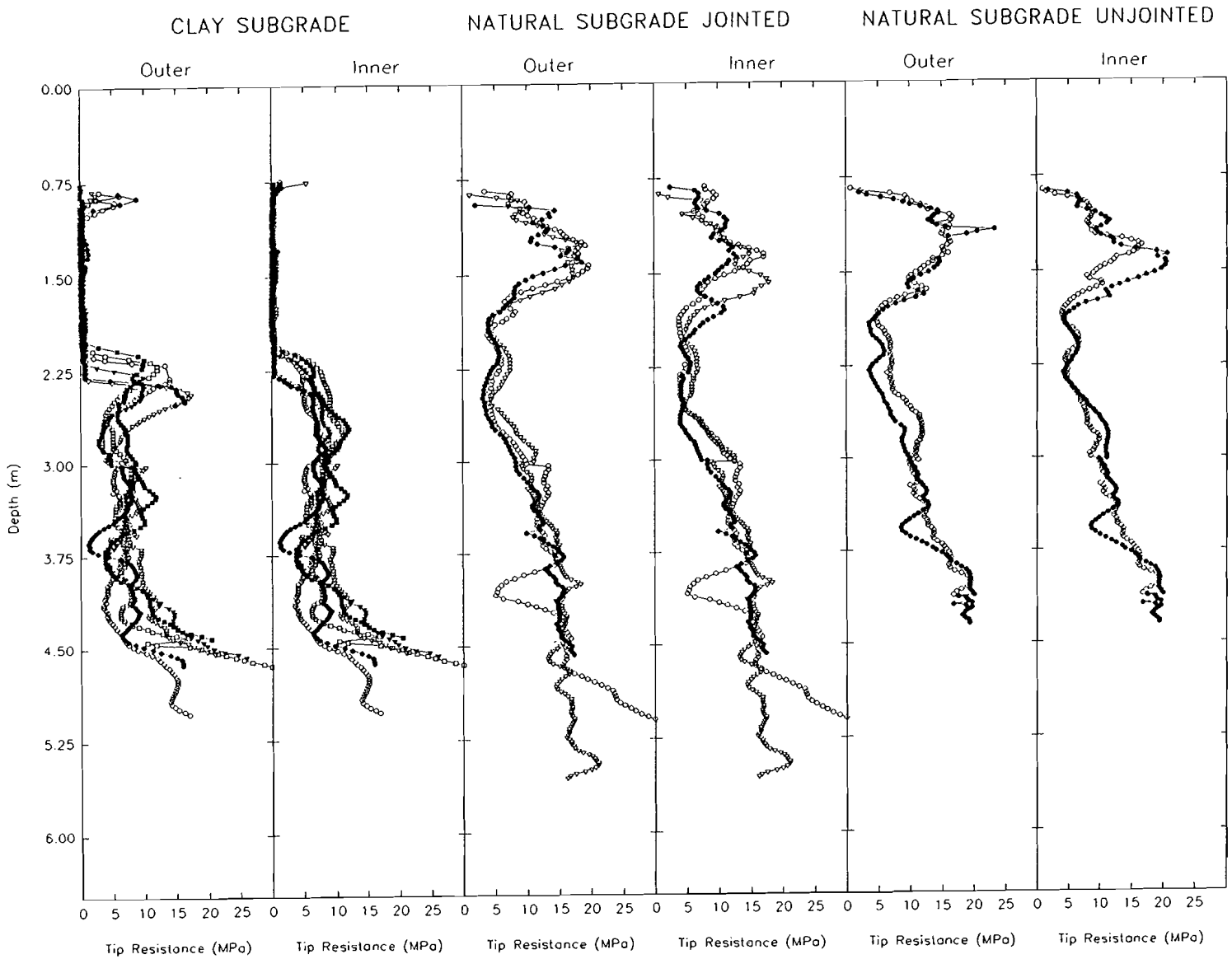

Figure 77: Average CPT Profiles

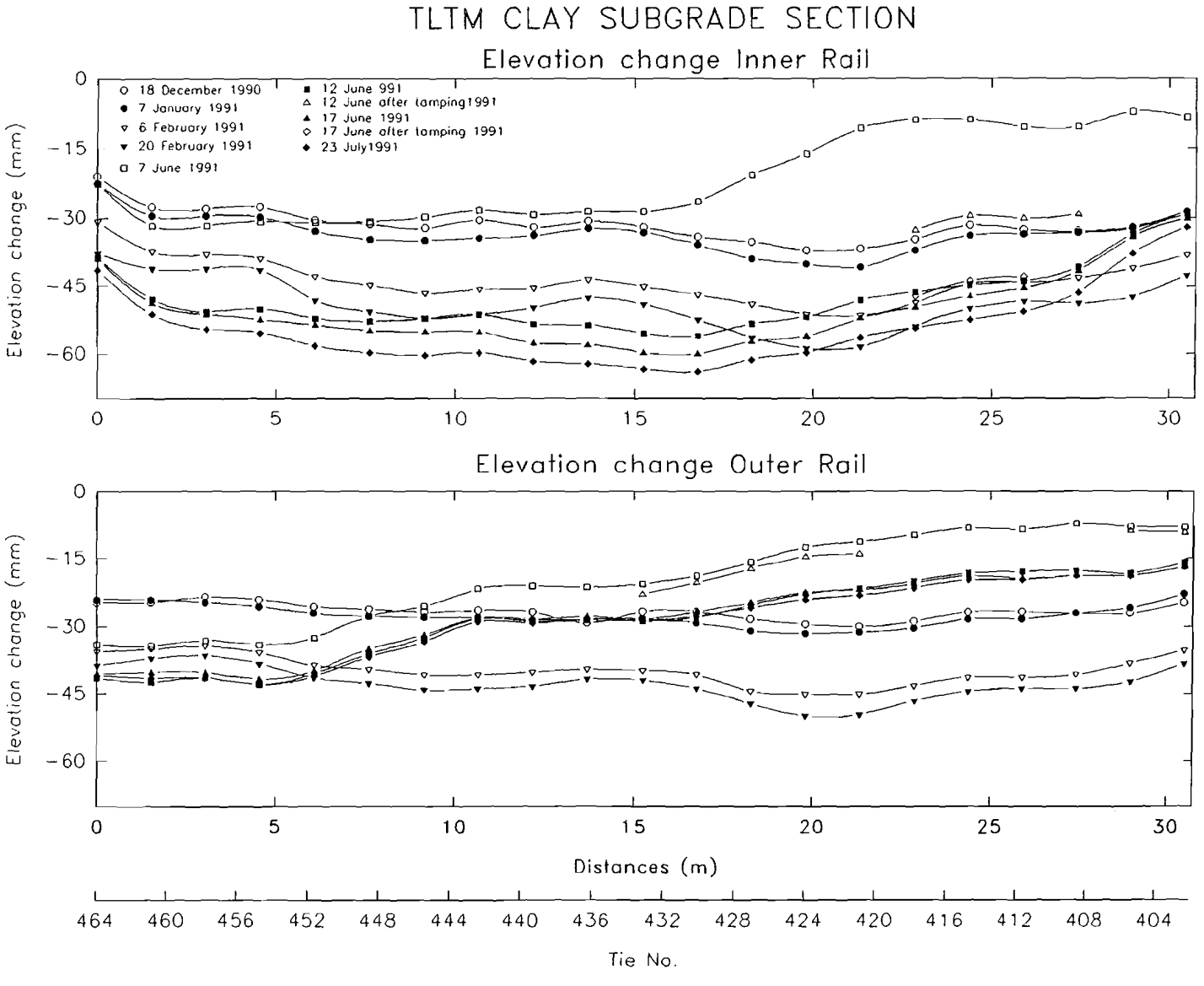

Figure 78: Clay Subgrade Elevation Change

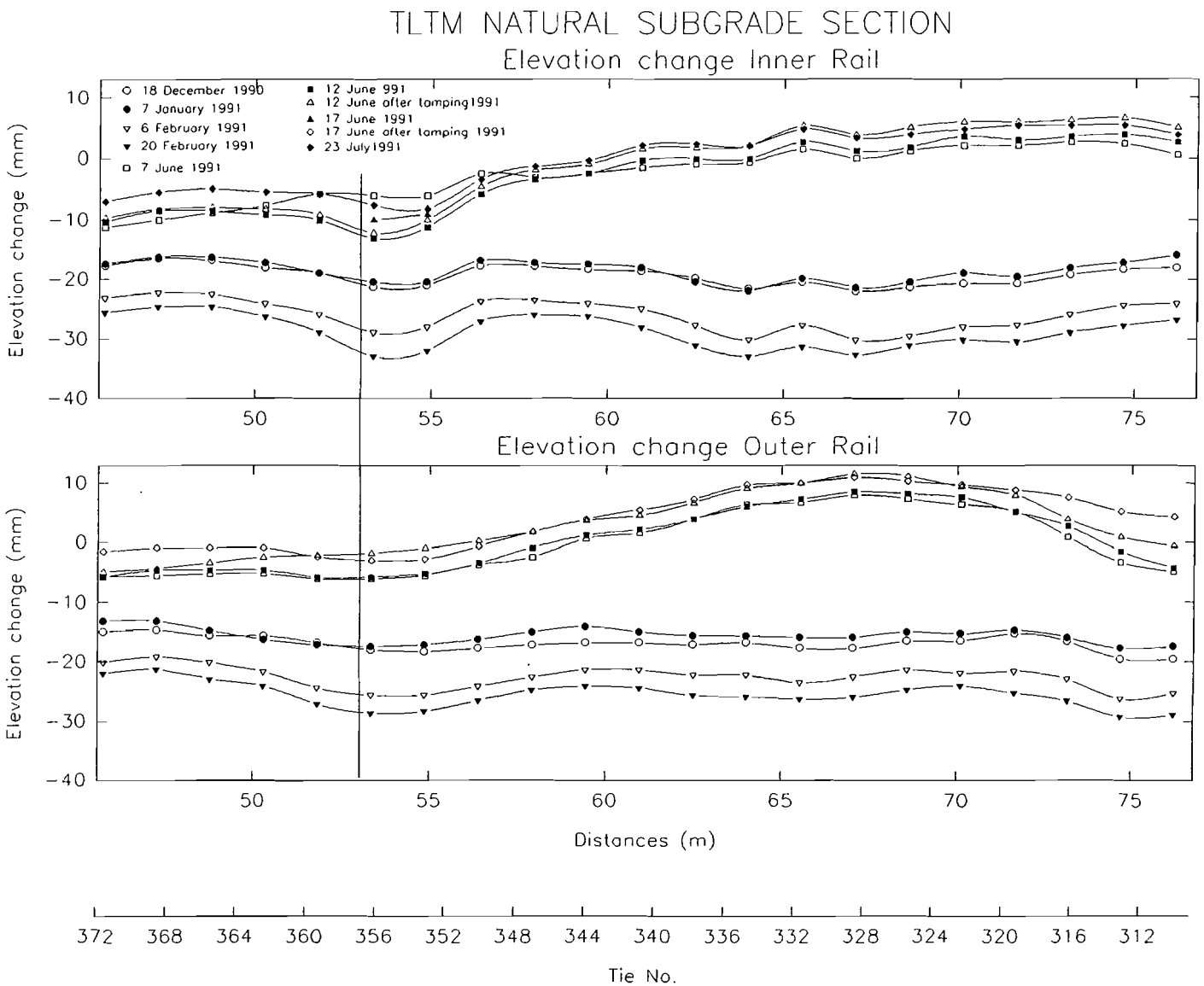

Figure 79: Natural Subgrade Elevation Change

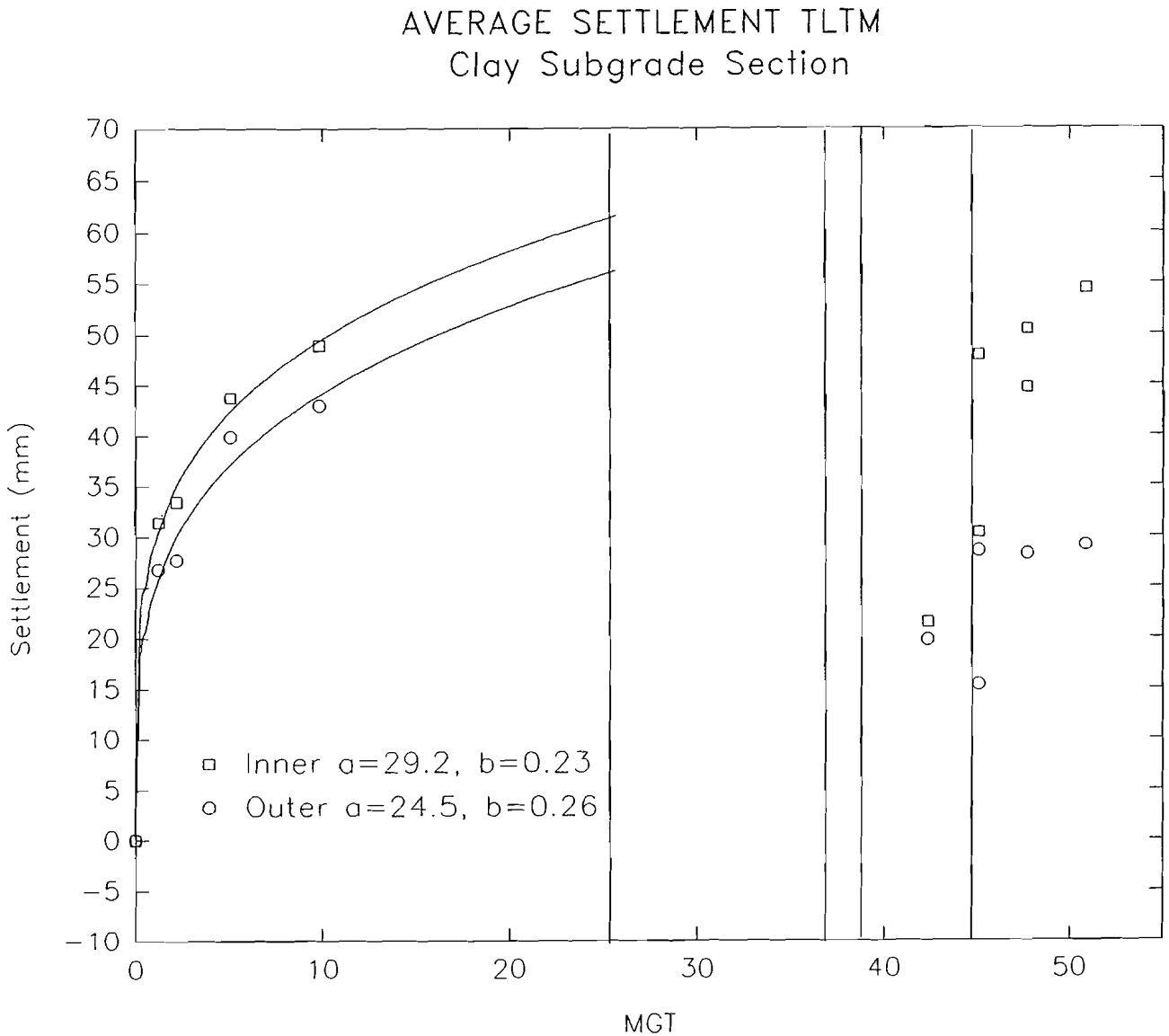

Figure 80: Clay Subgrade Settlement

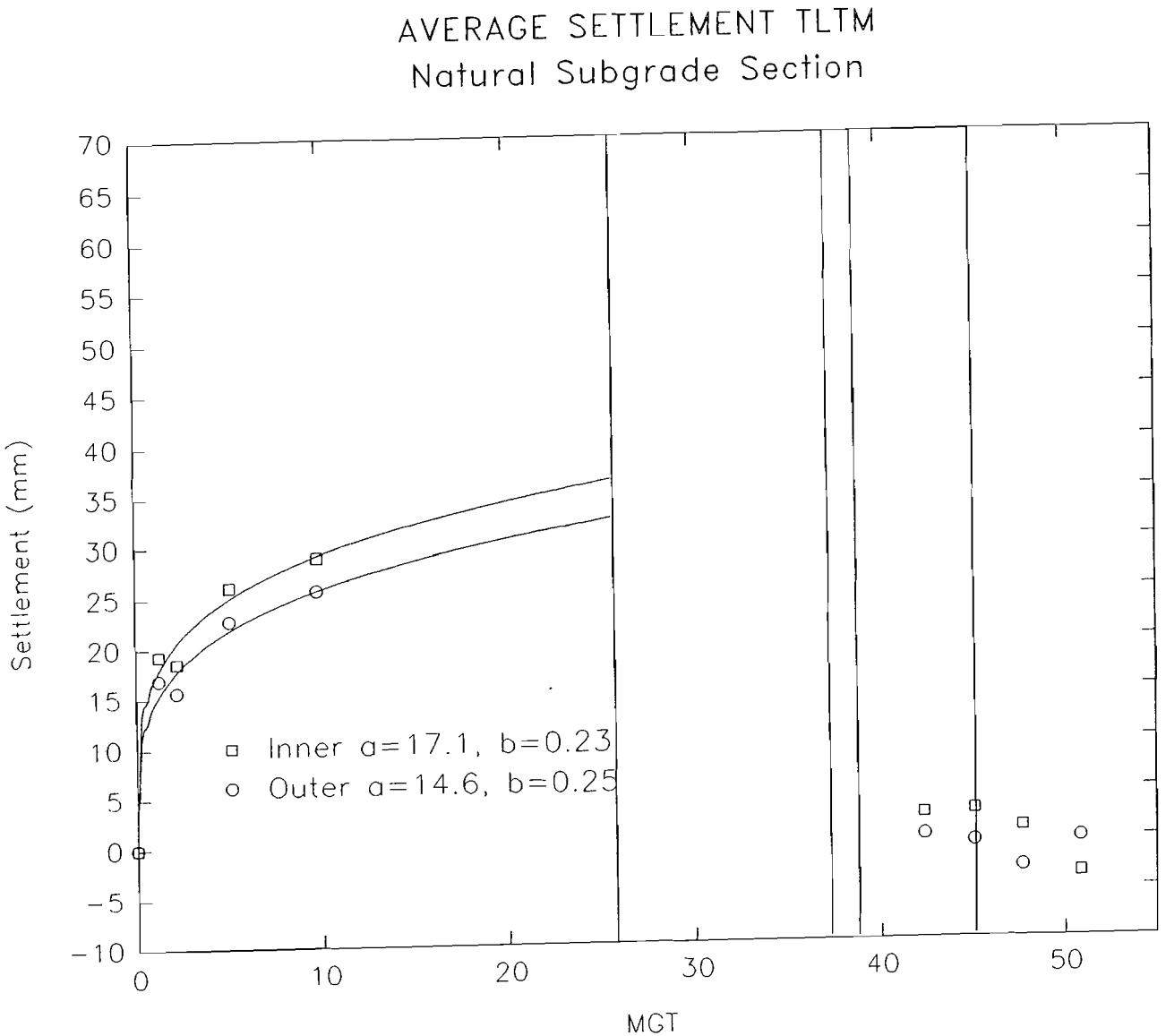

Figure 81: Natural Subgrade Settlement

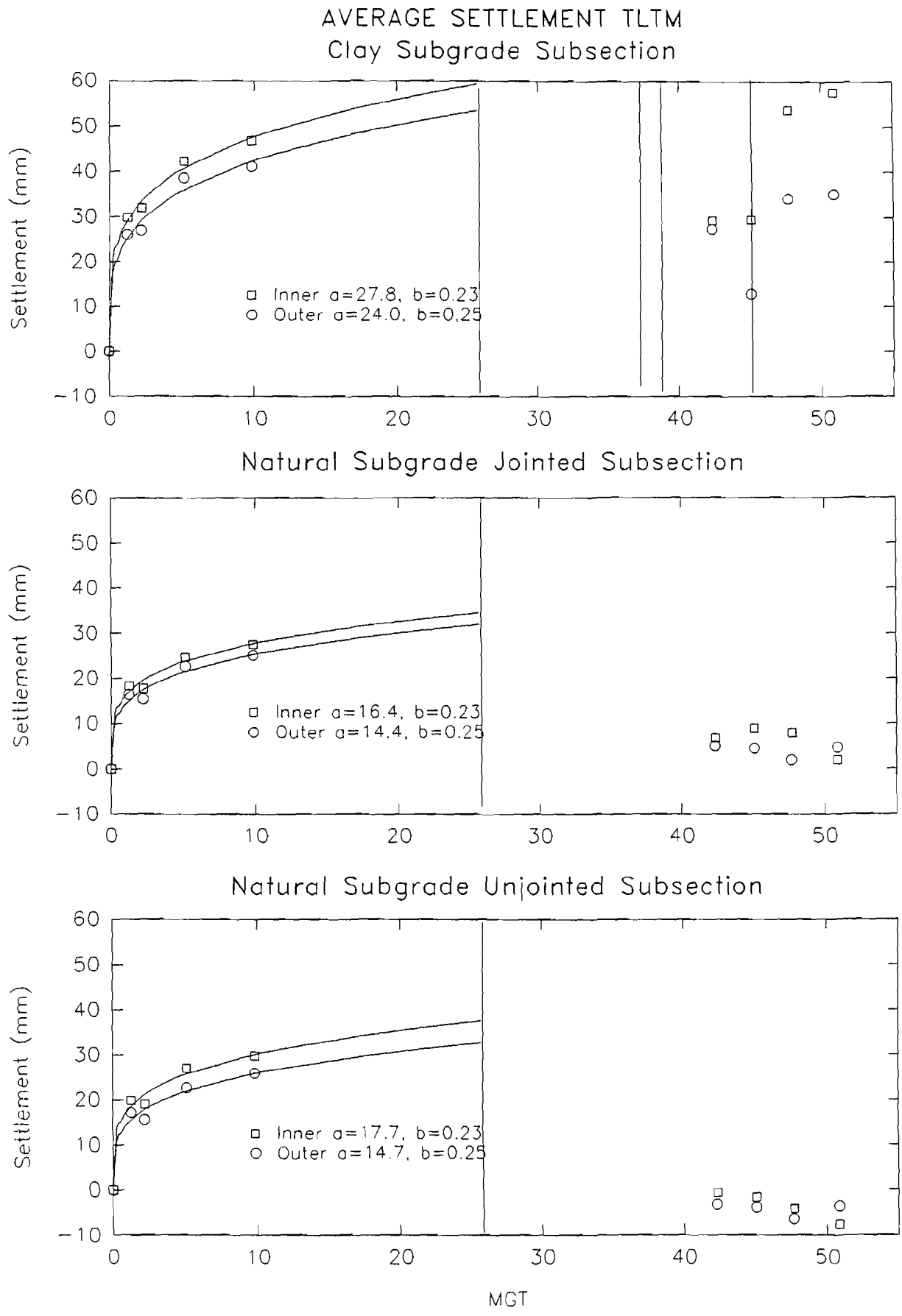

Figure 82: Settlements of Subsections

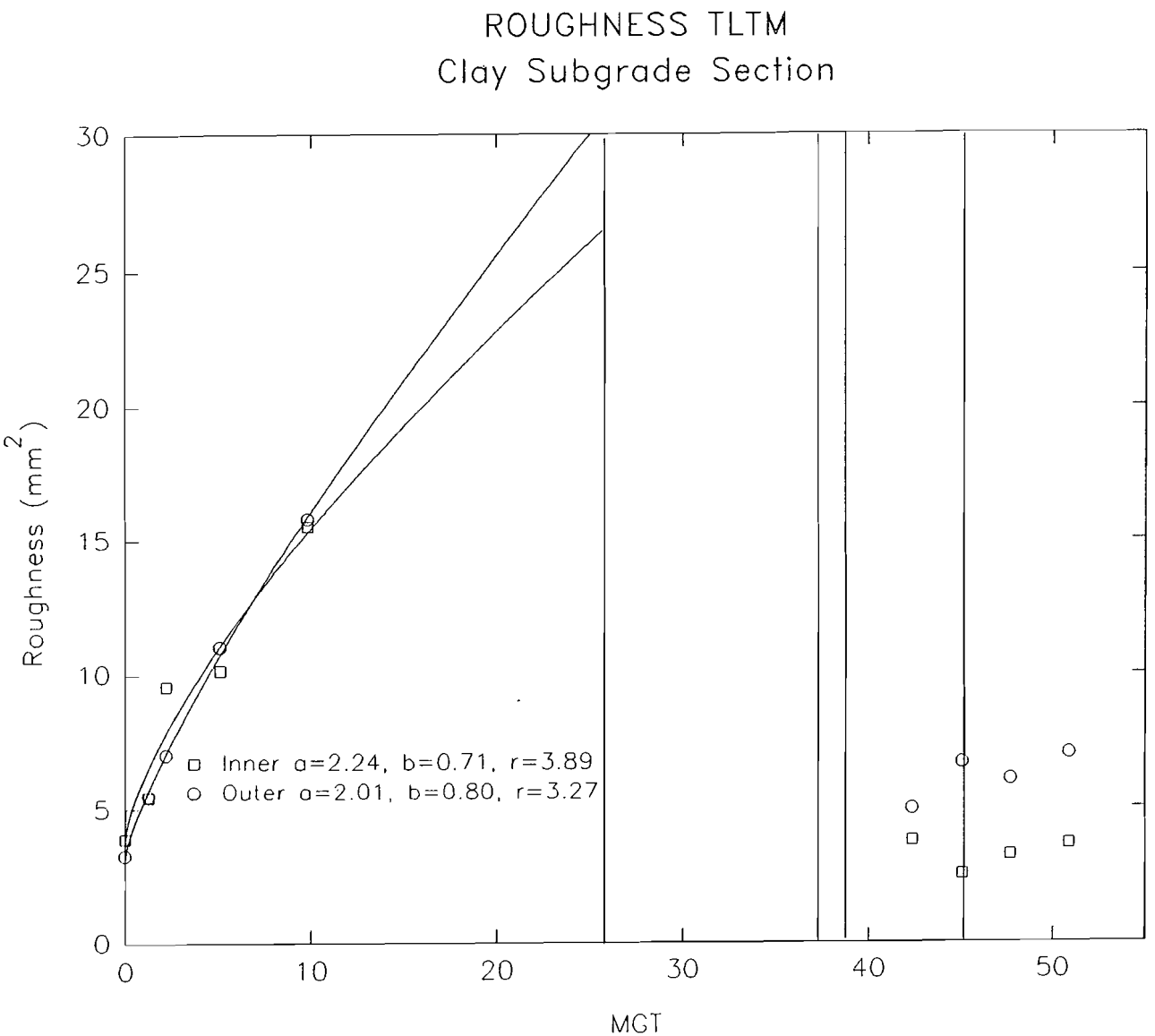

Figure 83: Clay Subgrade Roughness

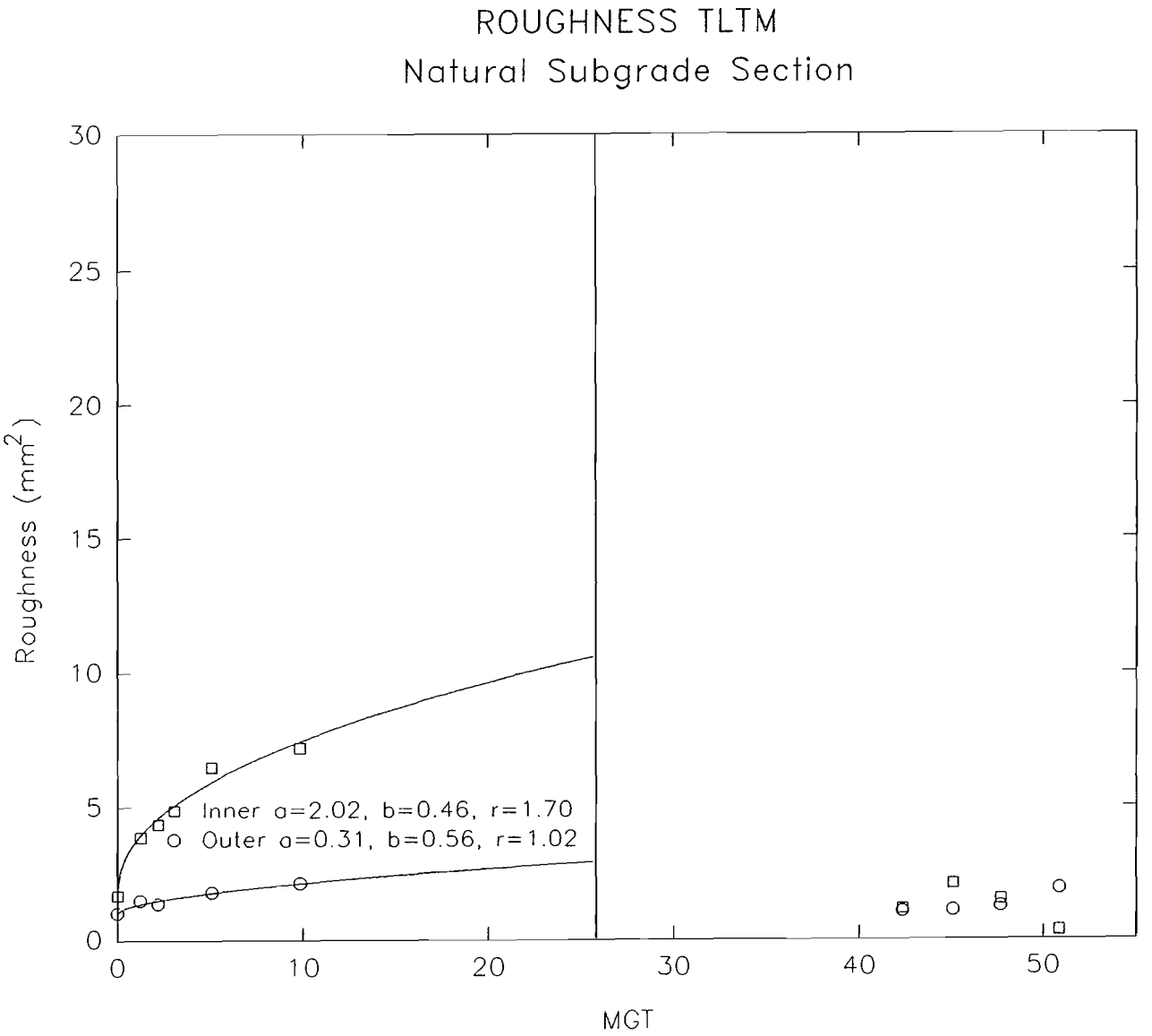

Figure 84: Natural Subgrade Roughness

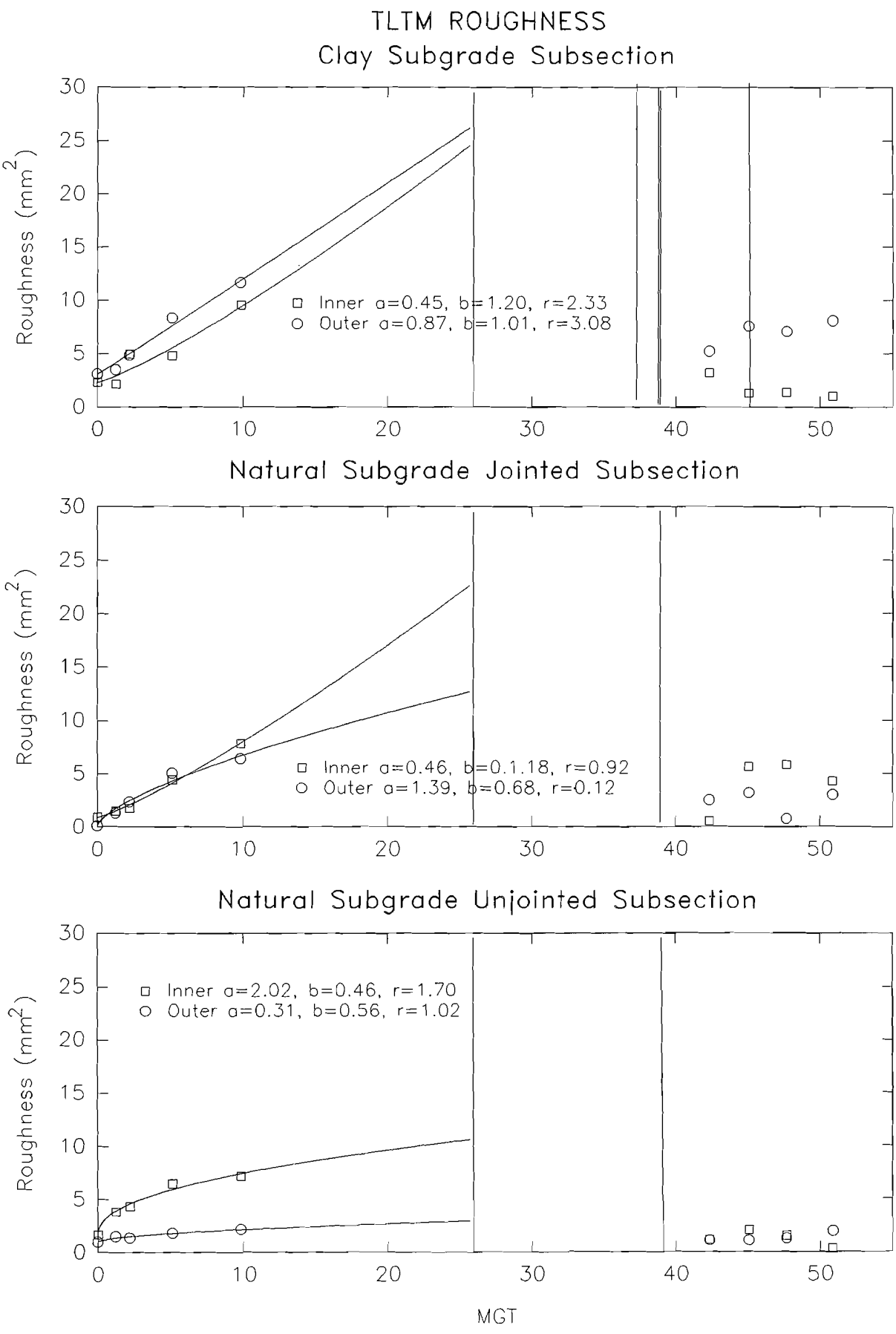

Figure 85: Roughness of Subsections

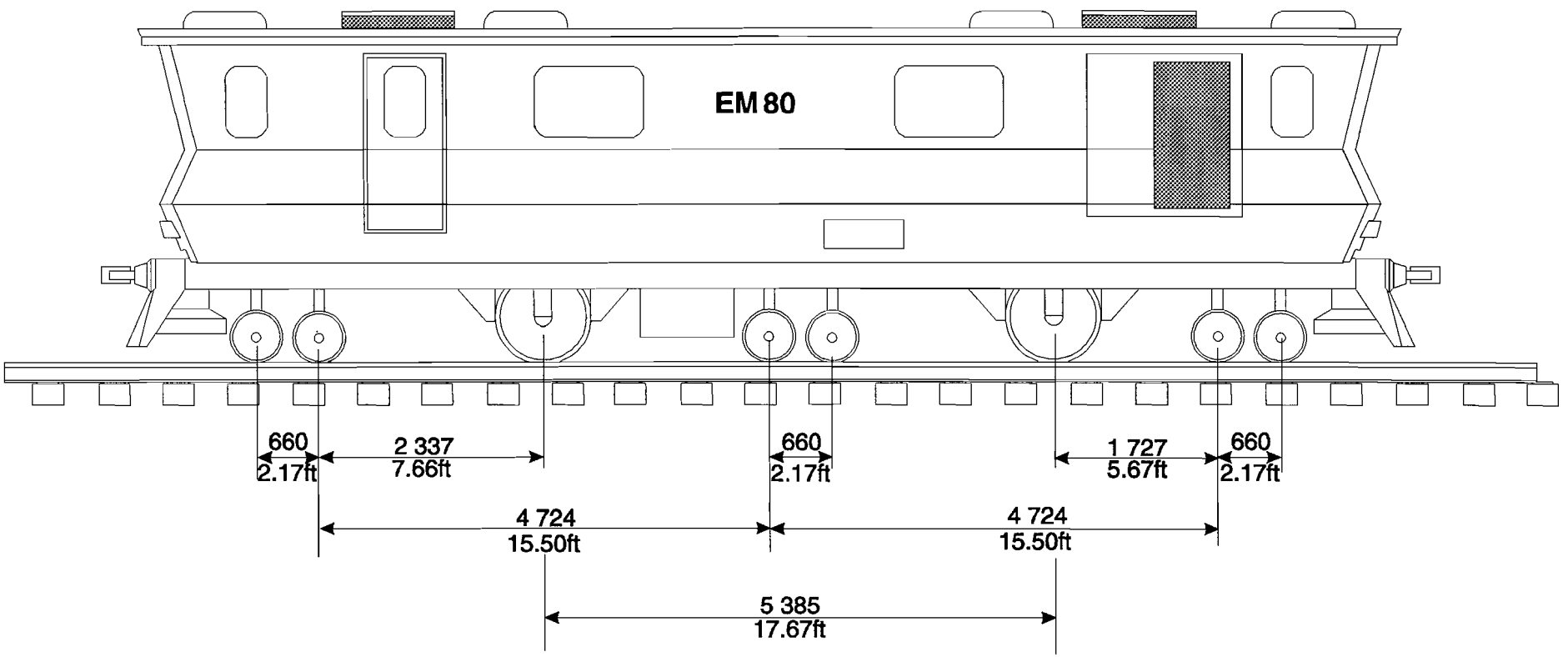

Figure 86: Geometry Car Axle Configuration

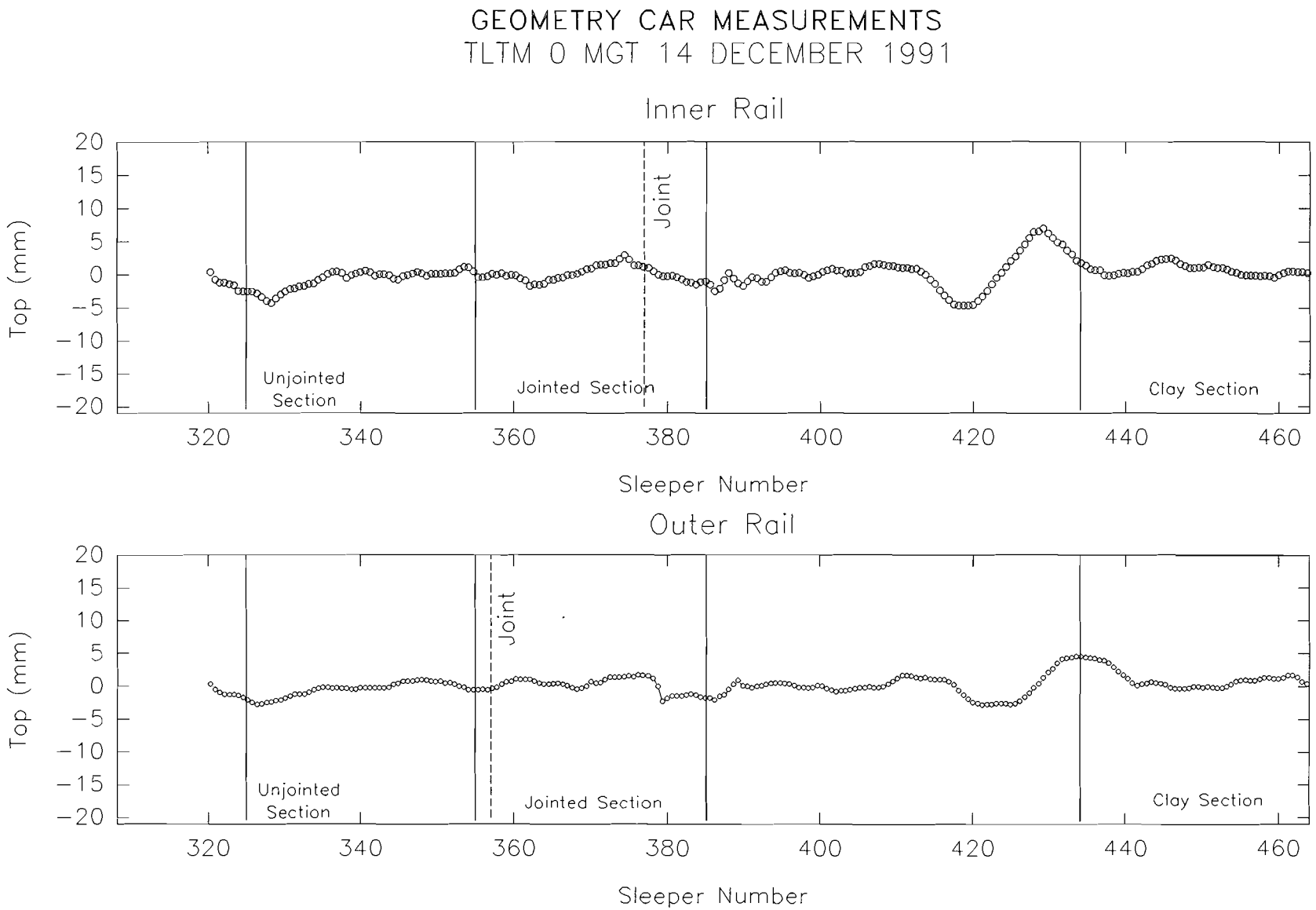

Figure 87: Top at 0 MGT

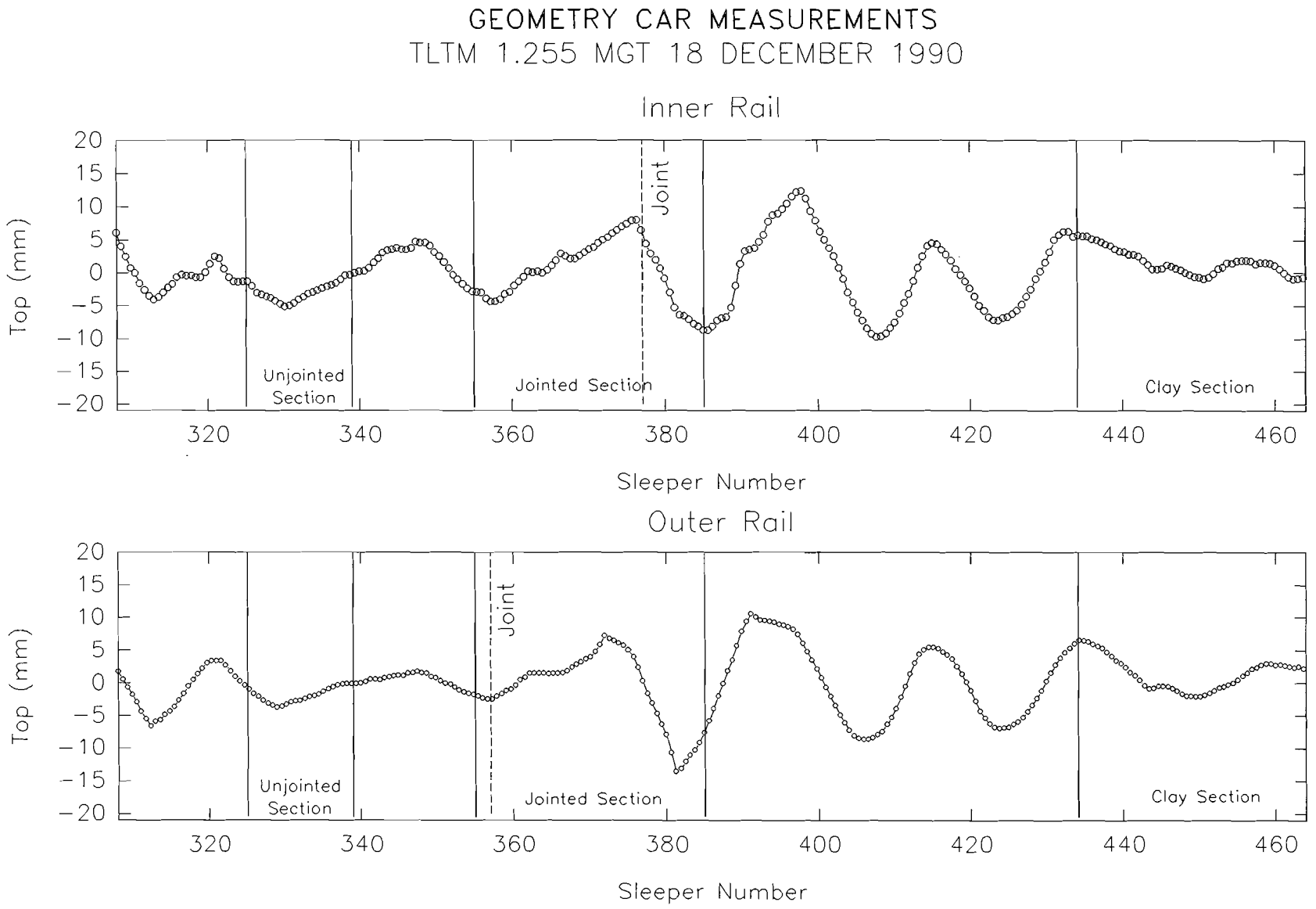

Figure 88: Top at 1.255 MGT

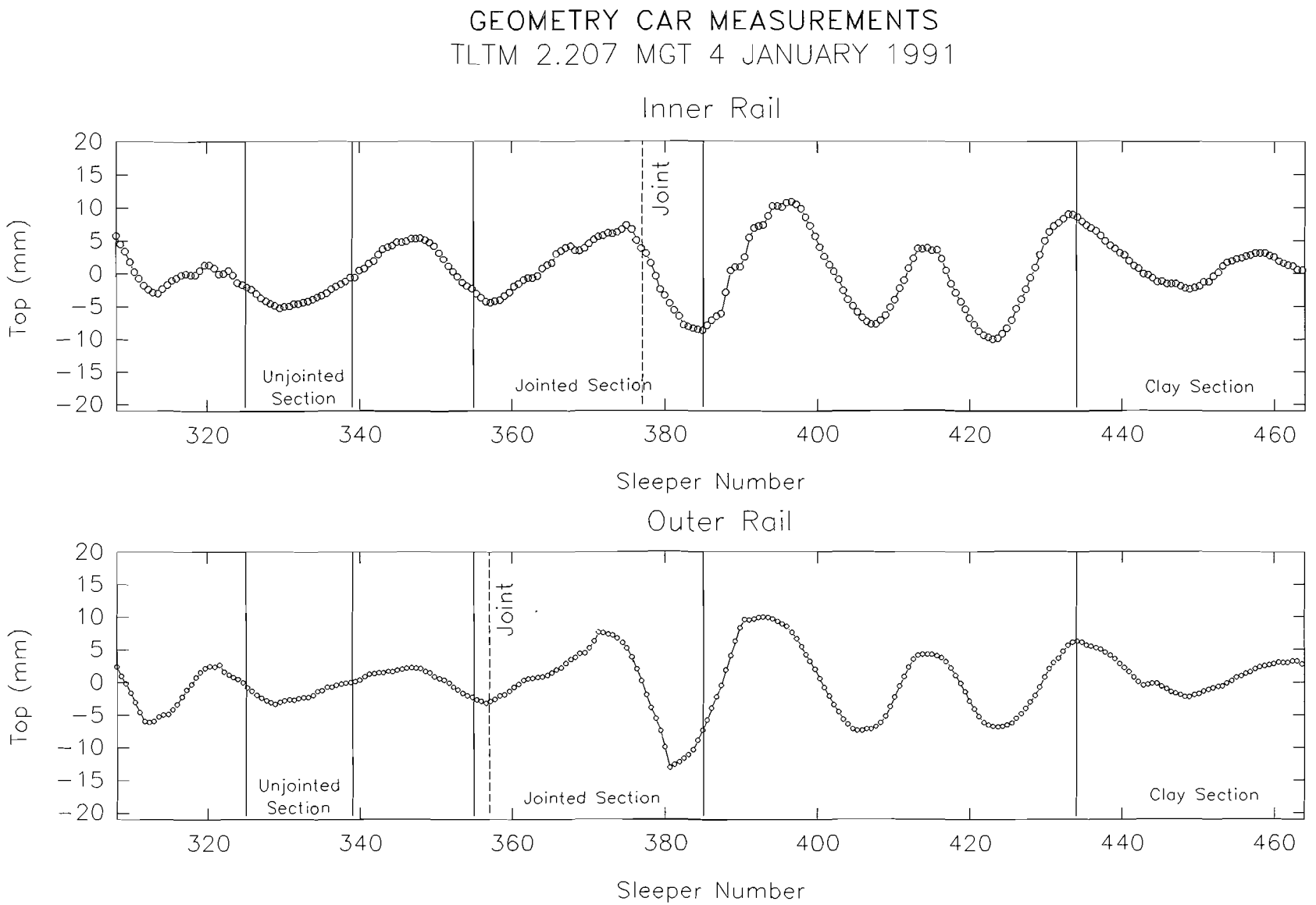

Figure 89: Top at 2.207 MGT

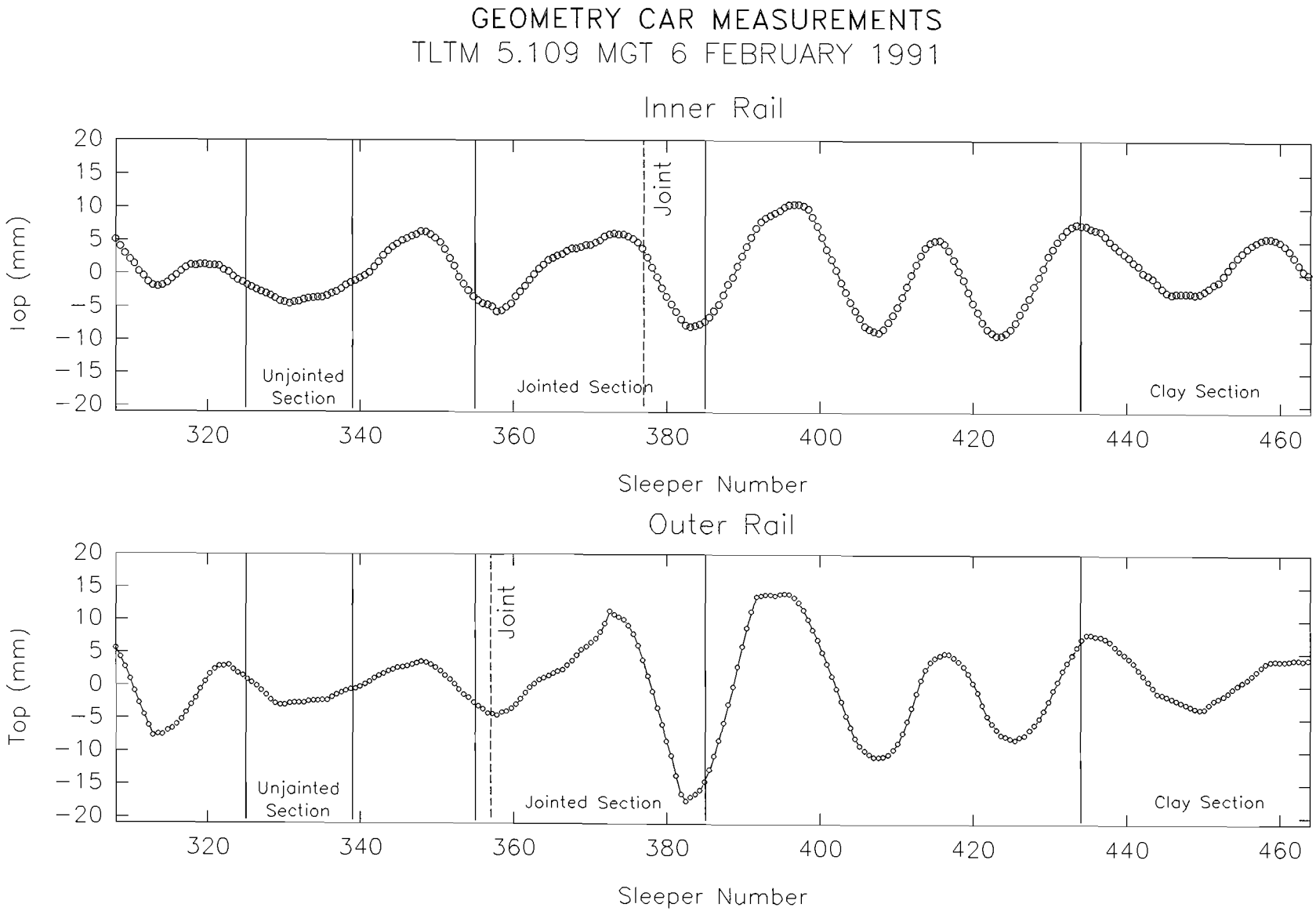

Figure 90: Top at 5.109 MGT

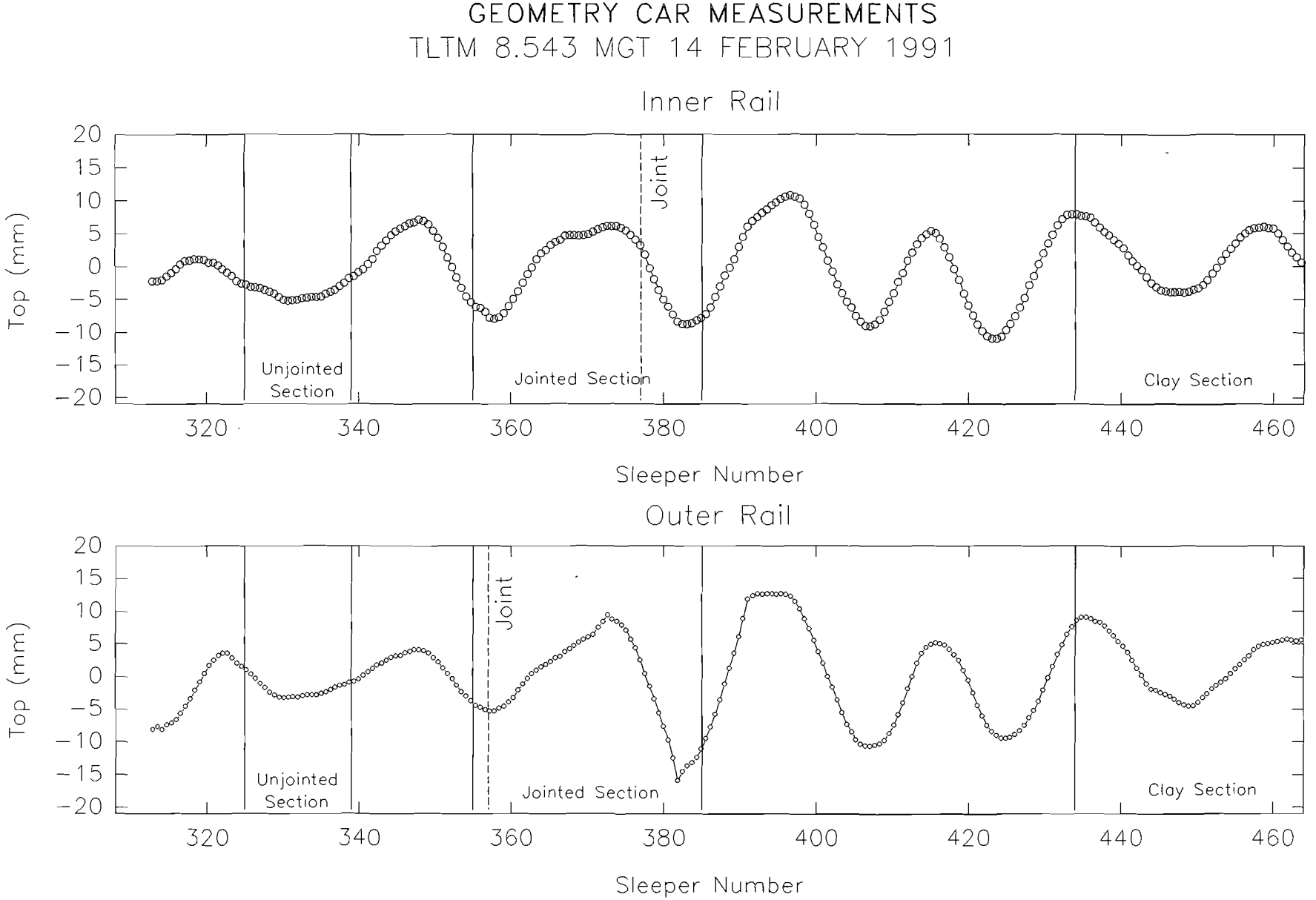

Figure 91: Top at 8.543 MGT

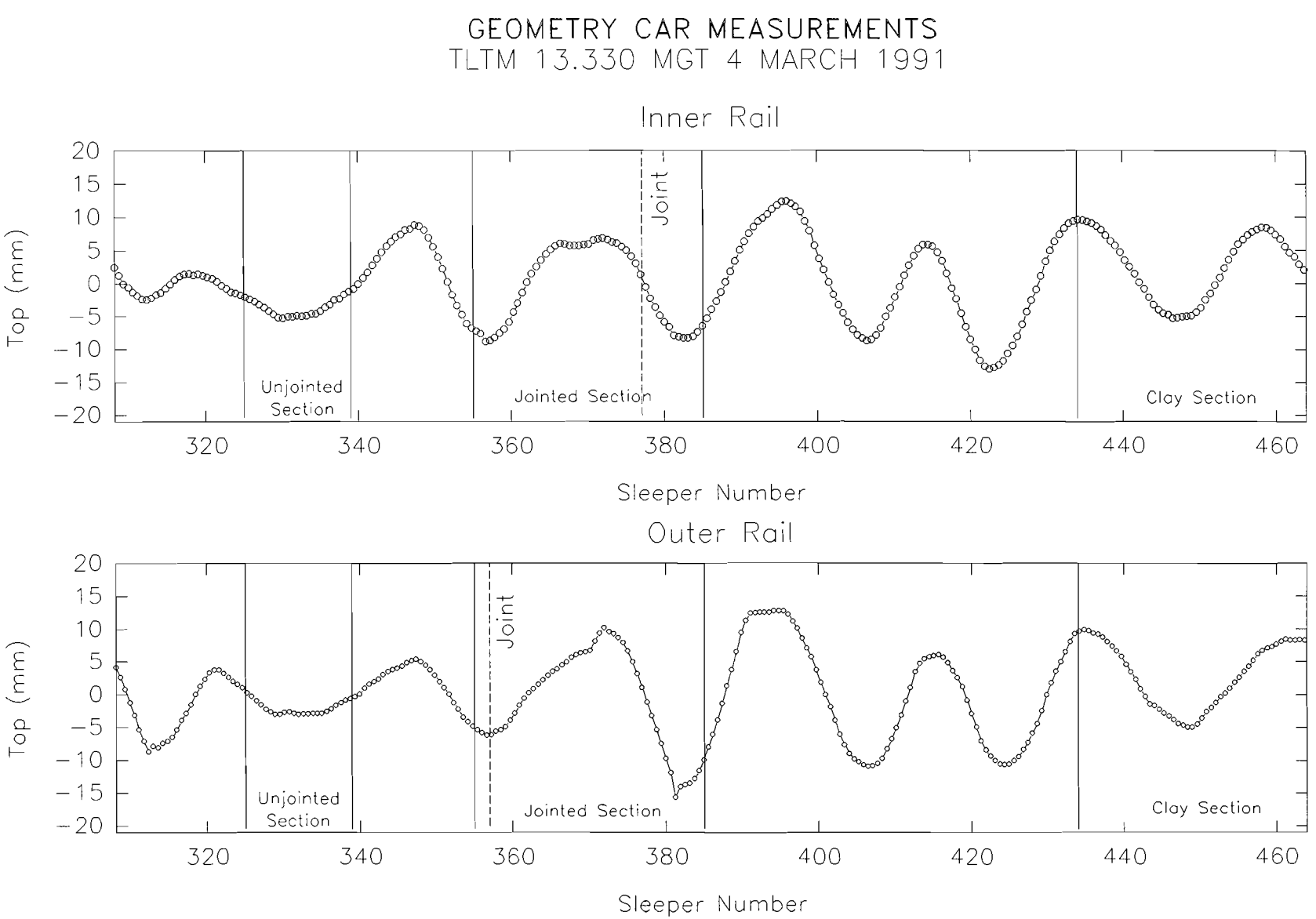

Figure 92: Top at 13.330 MGT

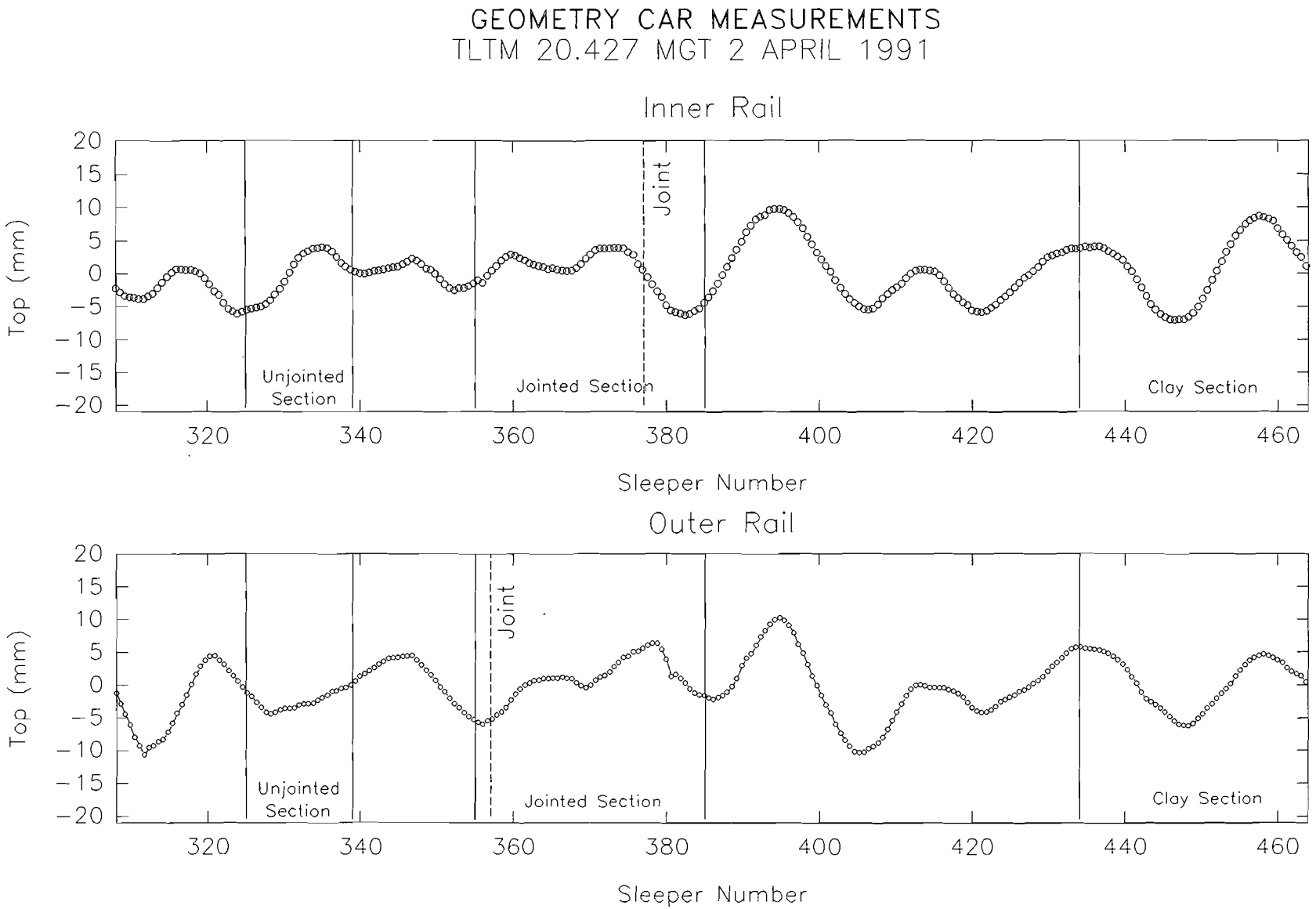

Figure 93: Top at 20.427 MGT

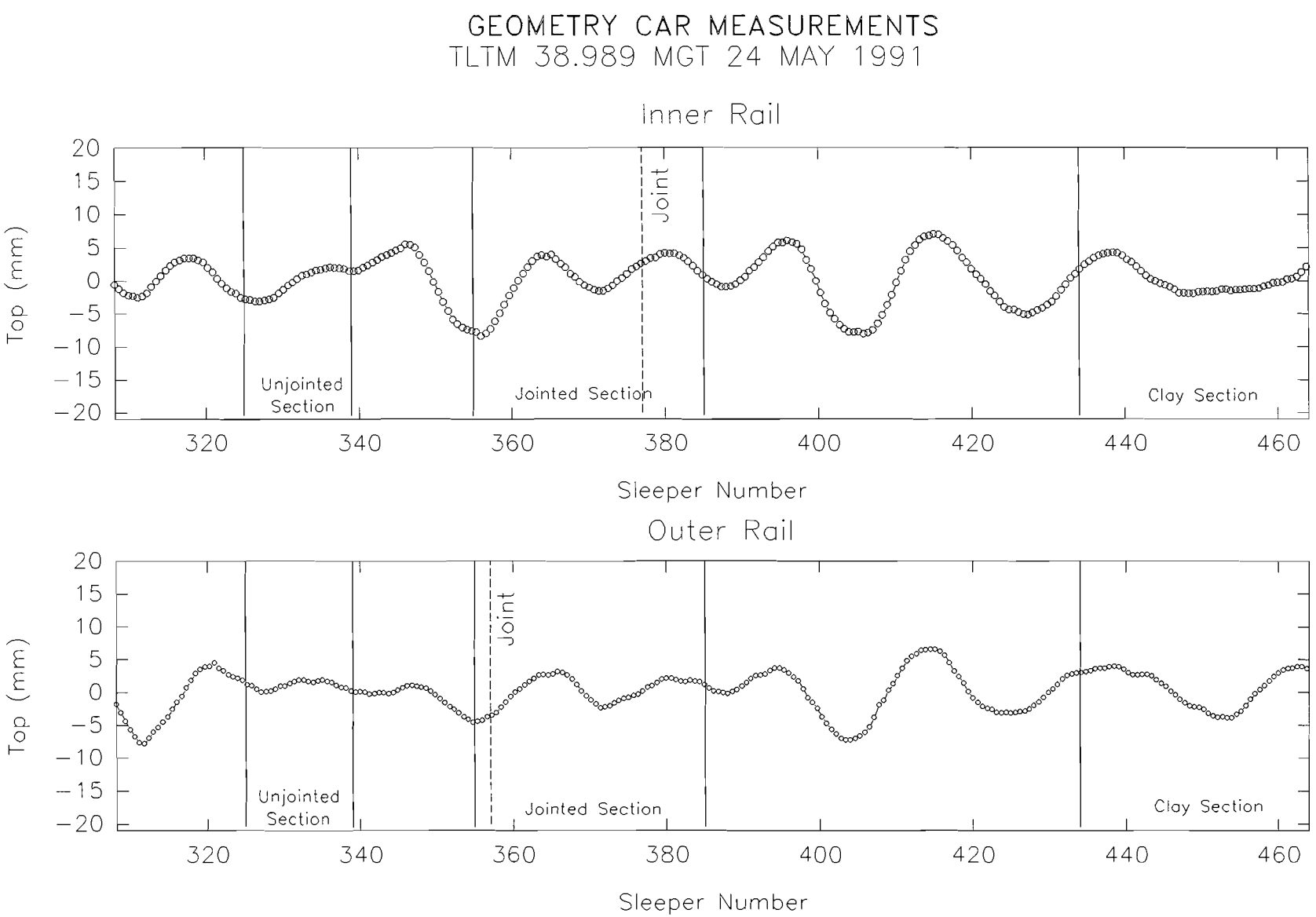

Figure 94: Top at 38.989 MGT

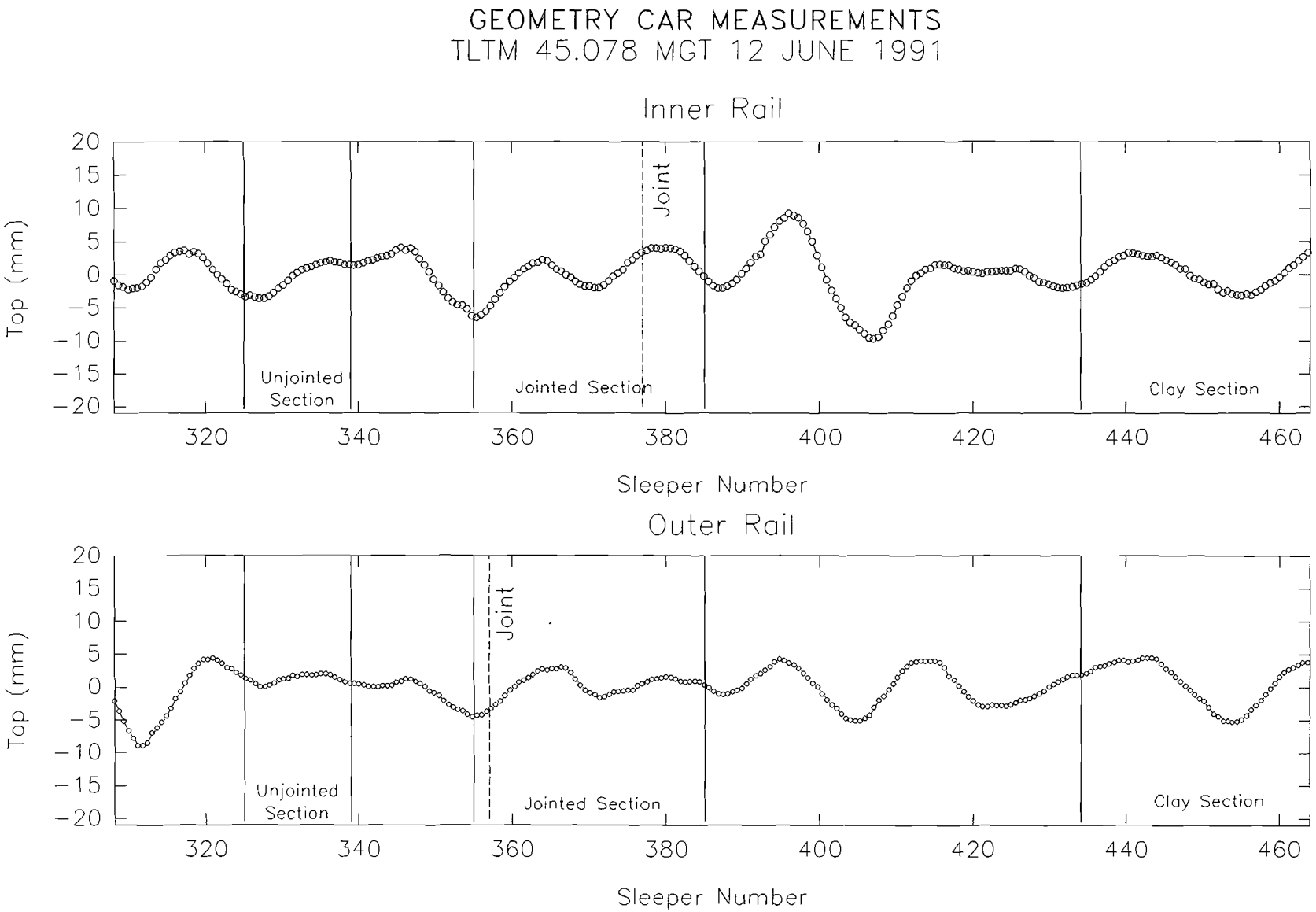

Figure 95: Top at 45.078 MGT

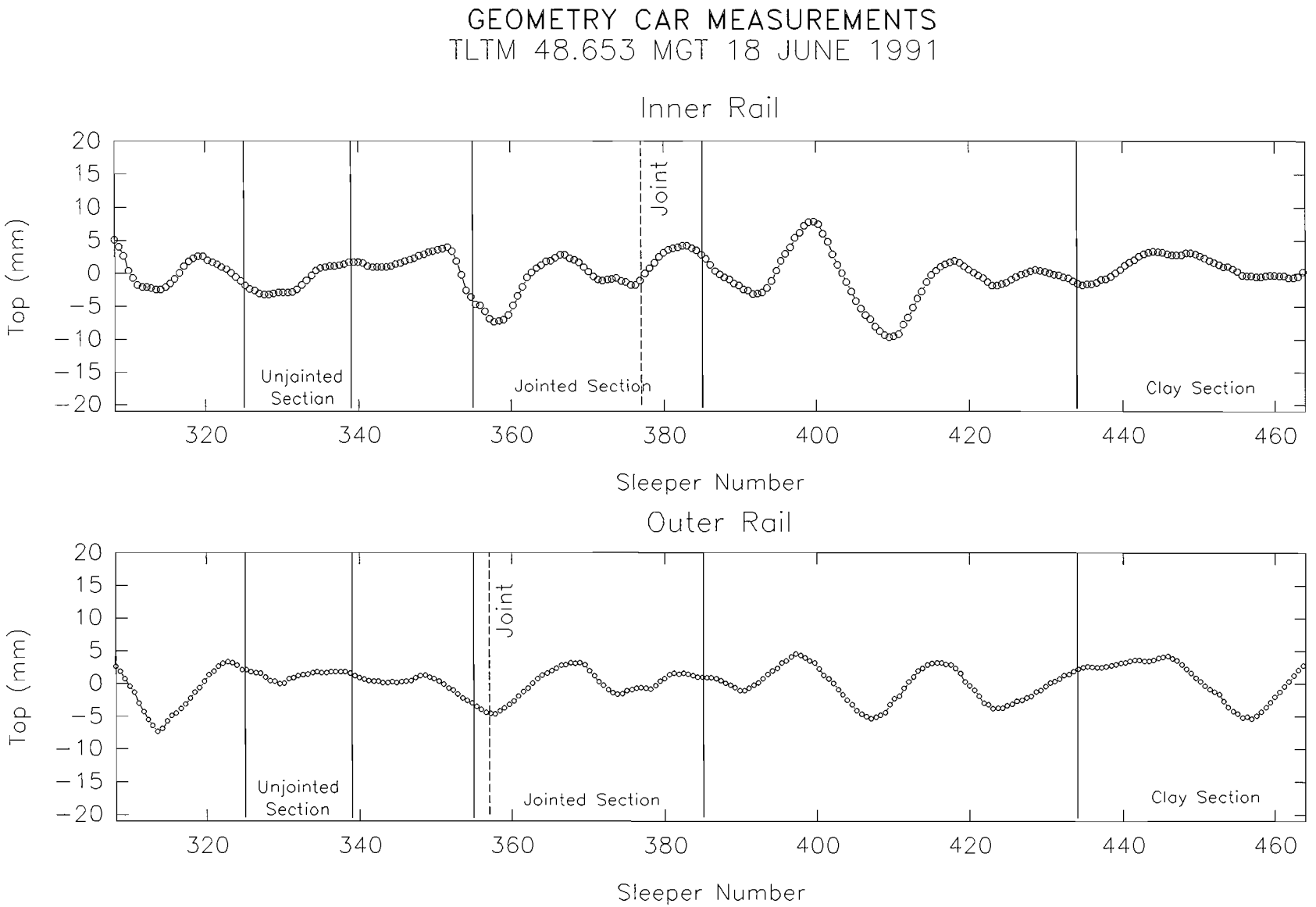

Figure 96: Top at 48.653 MGT

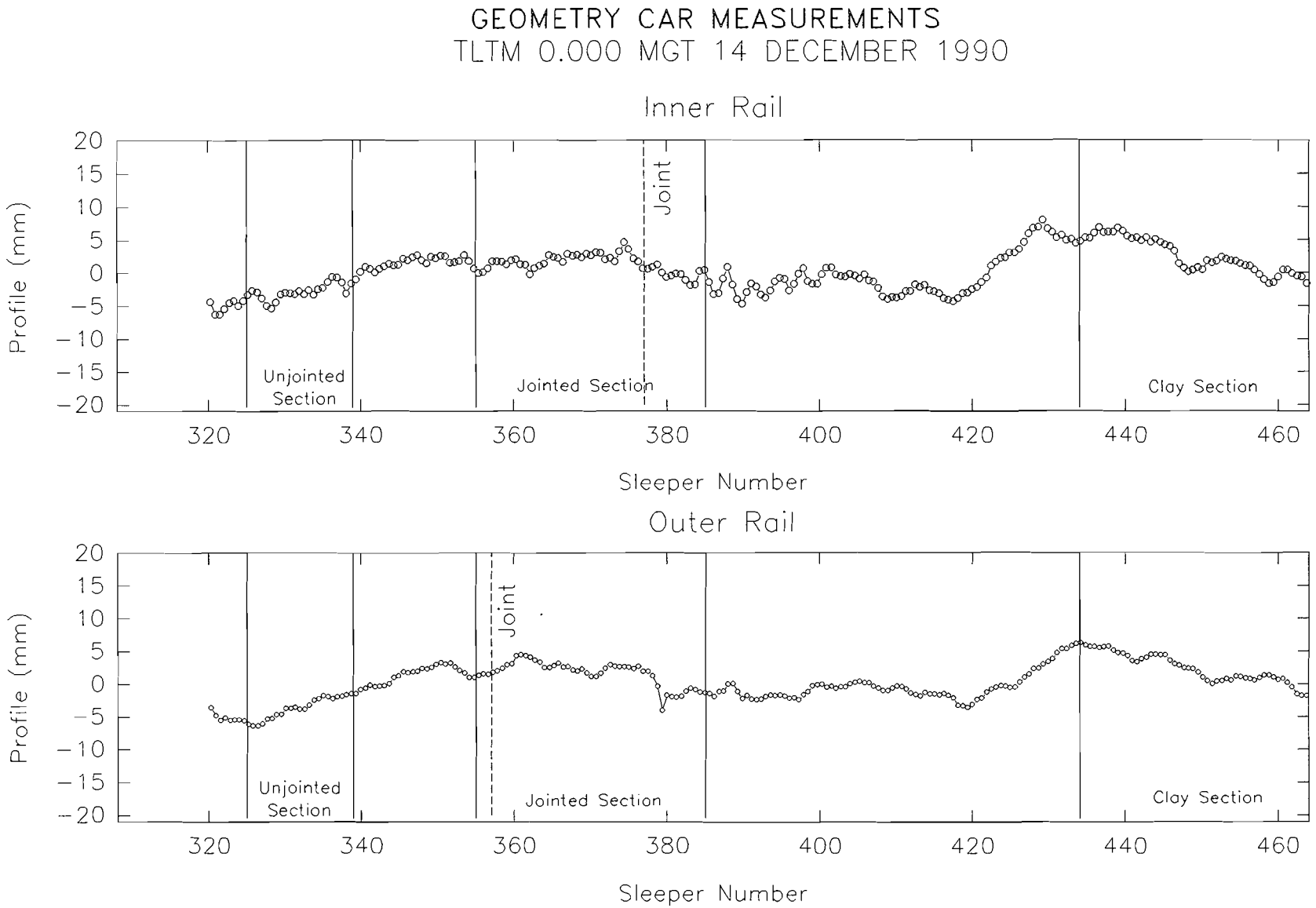

Figure 97: Profile at 0 MGT

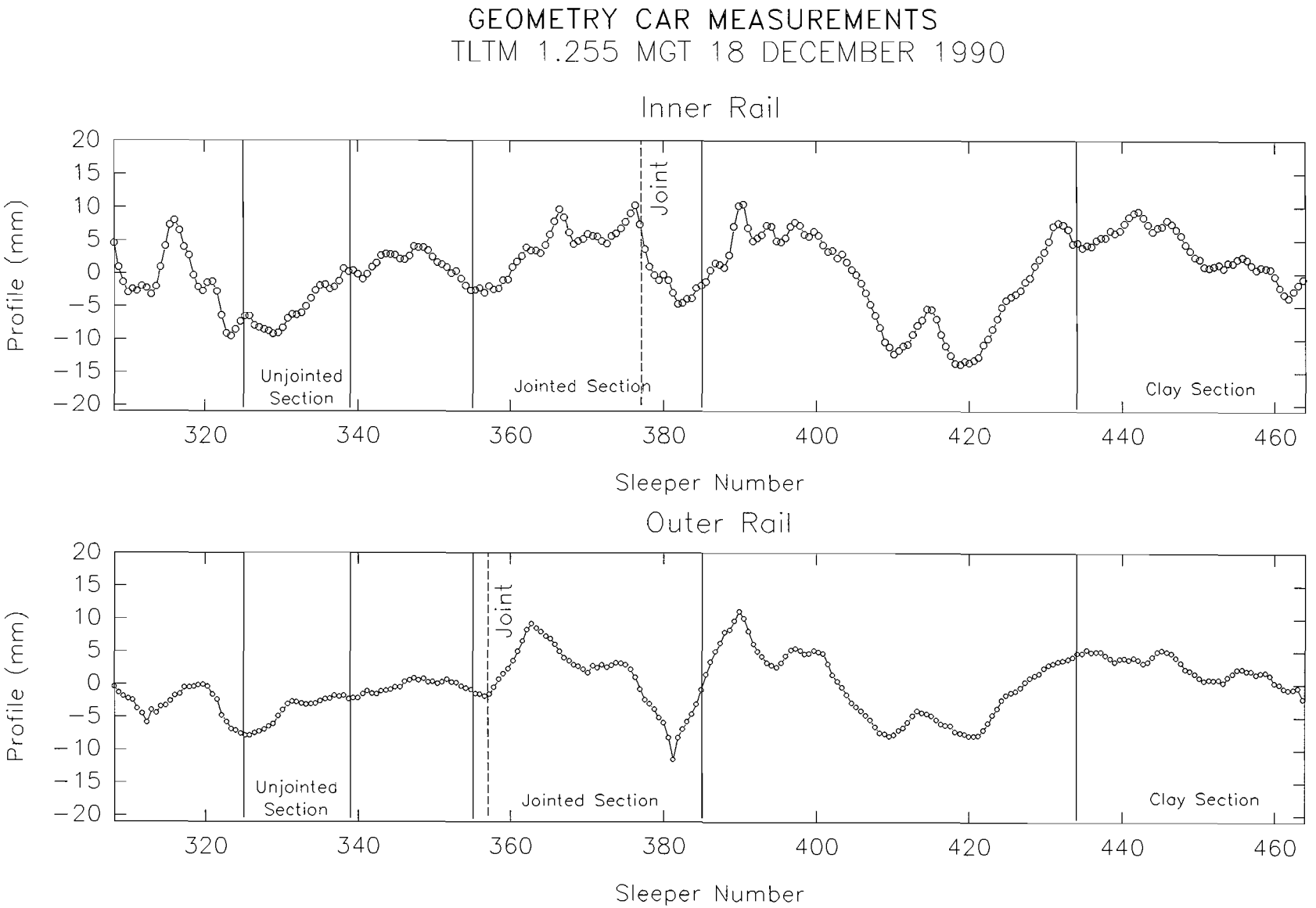

Figure 98: Profile at 1.255 MGT

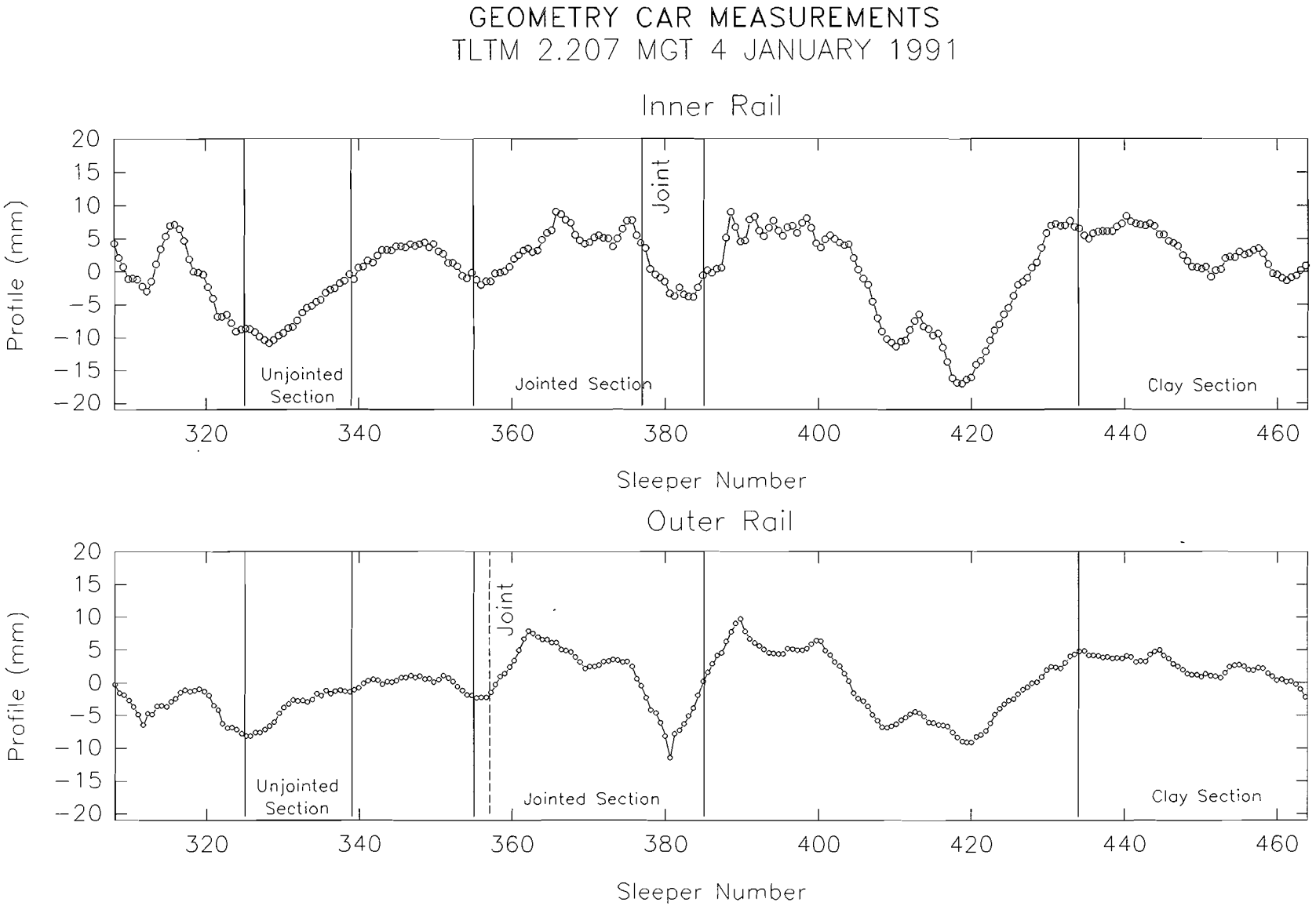

Figure 99: Profile at 2.207 MGT

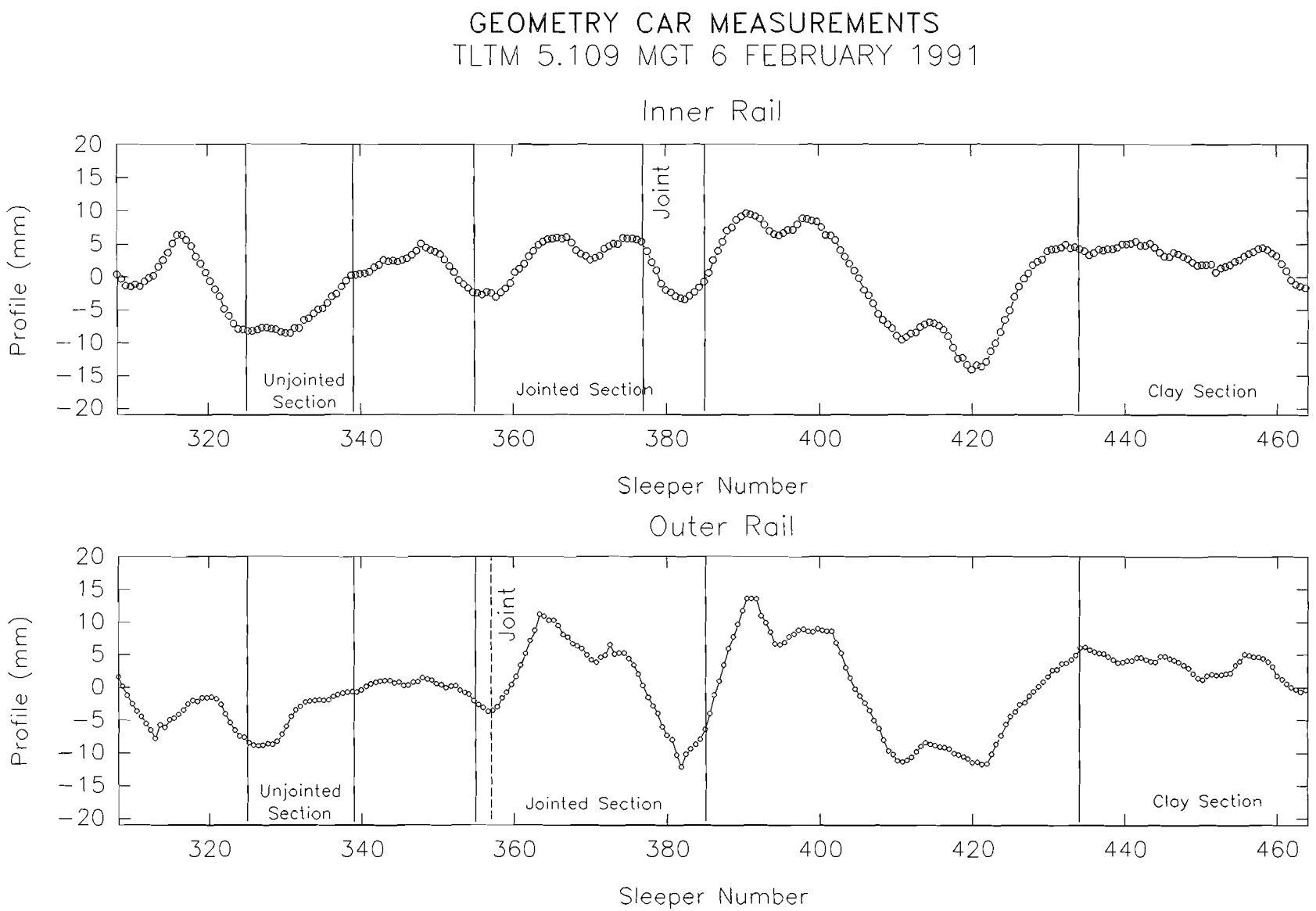

Figure 100: Profile at 5.109 MGT

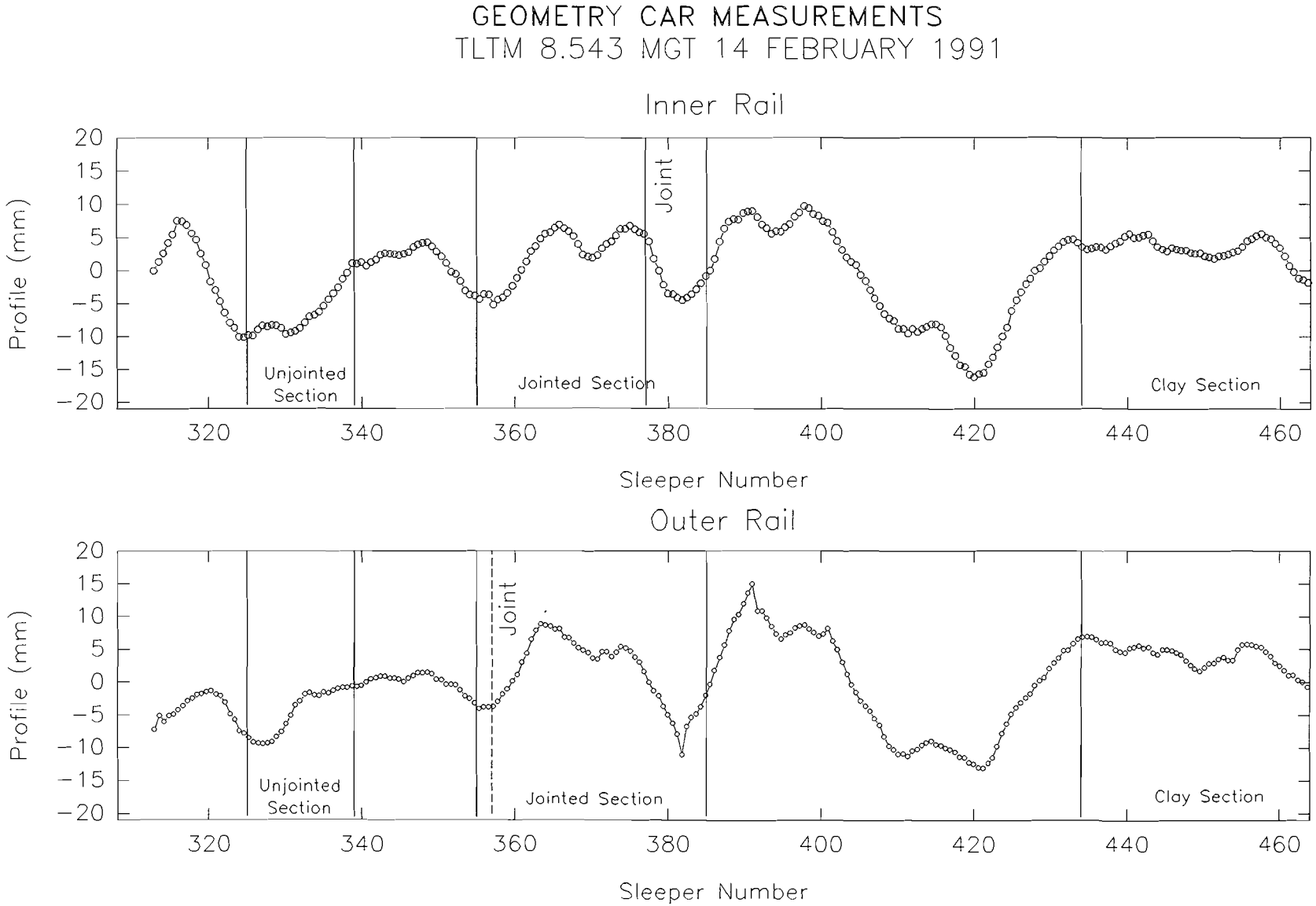

Figure 101: Profile at 8.543 MGT

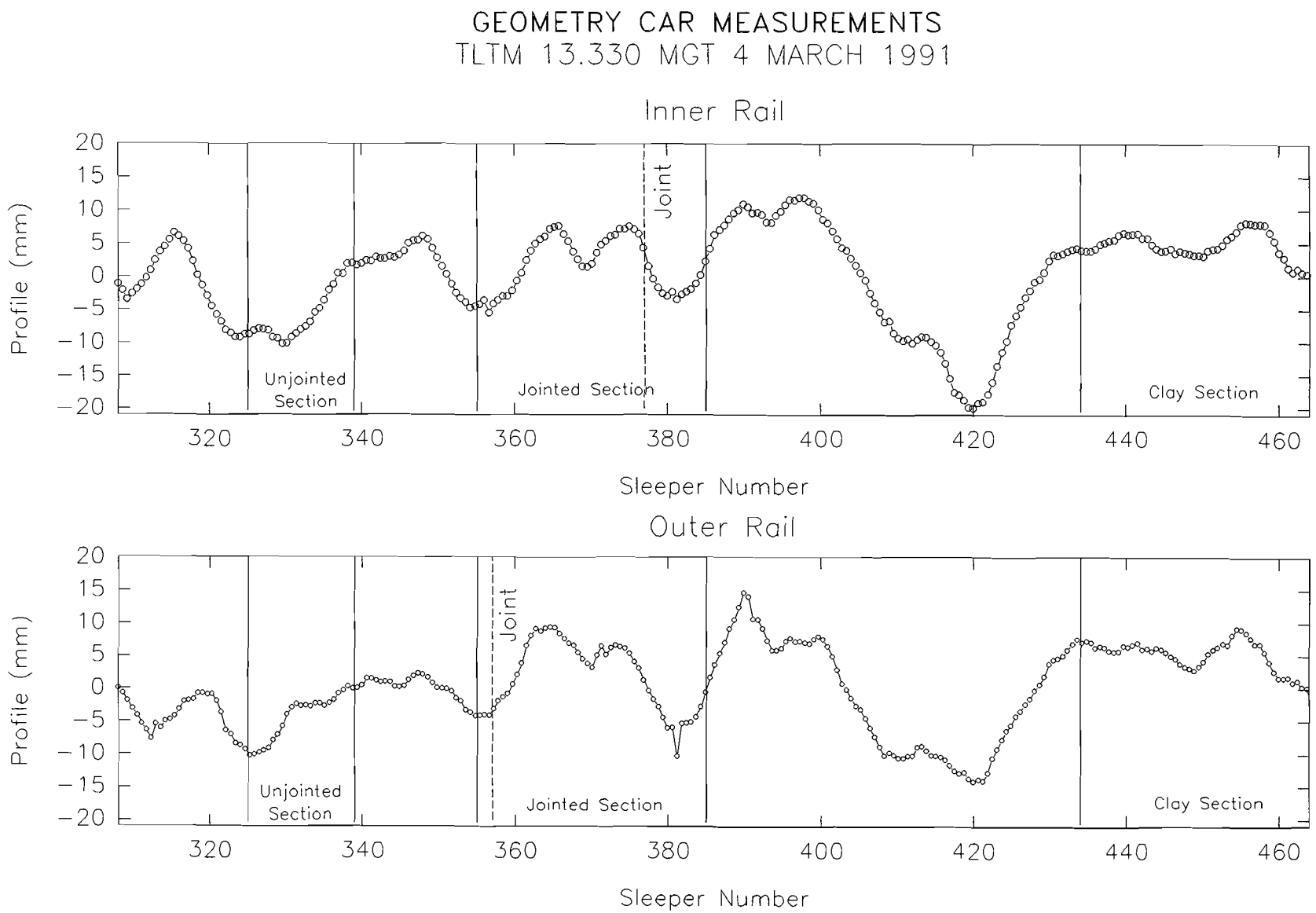

Figure 102: Profile at 13.330 MGT

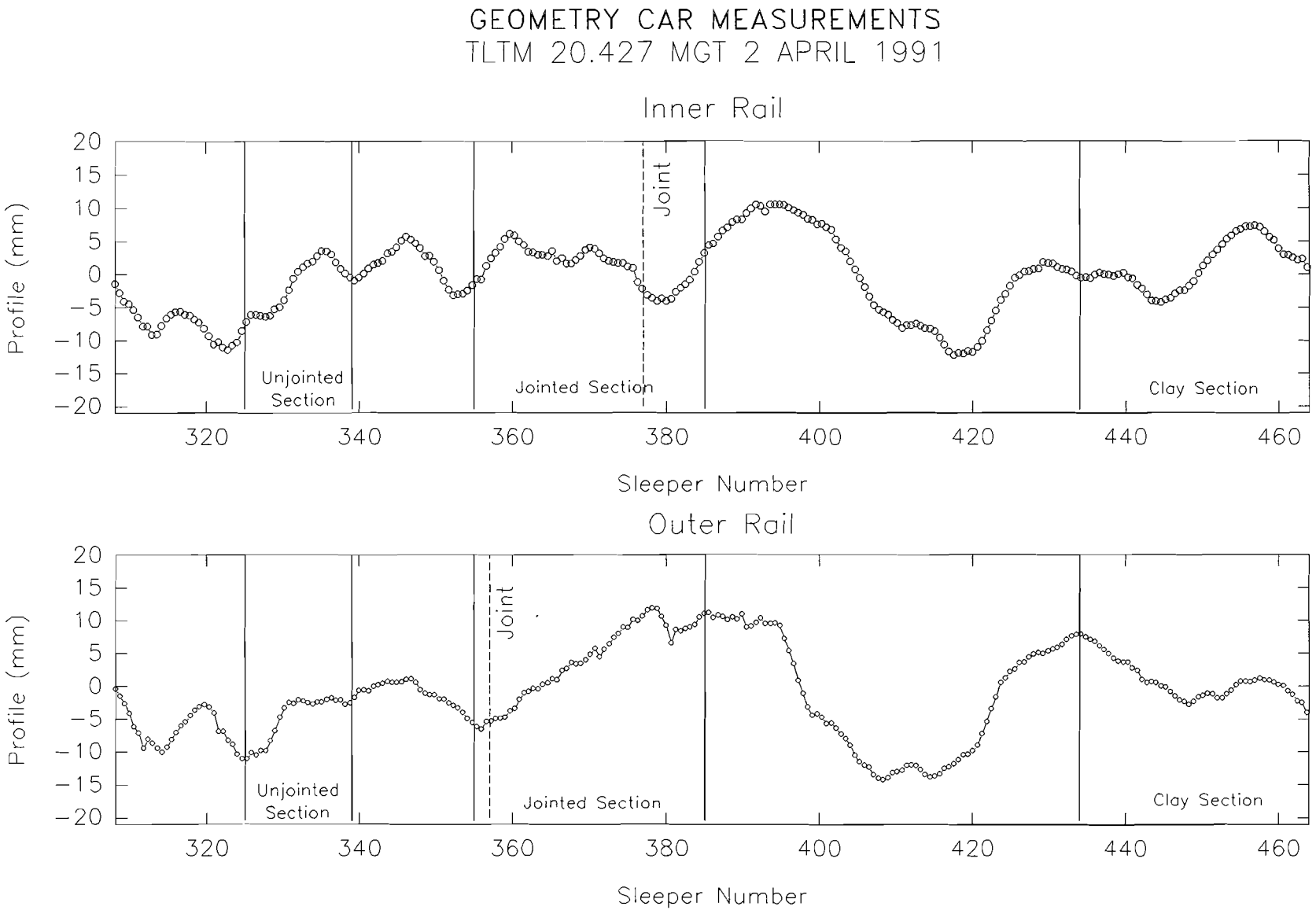

Figure 103: Profile at 20.427 MGT

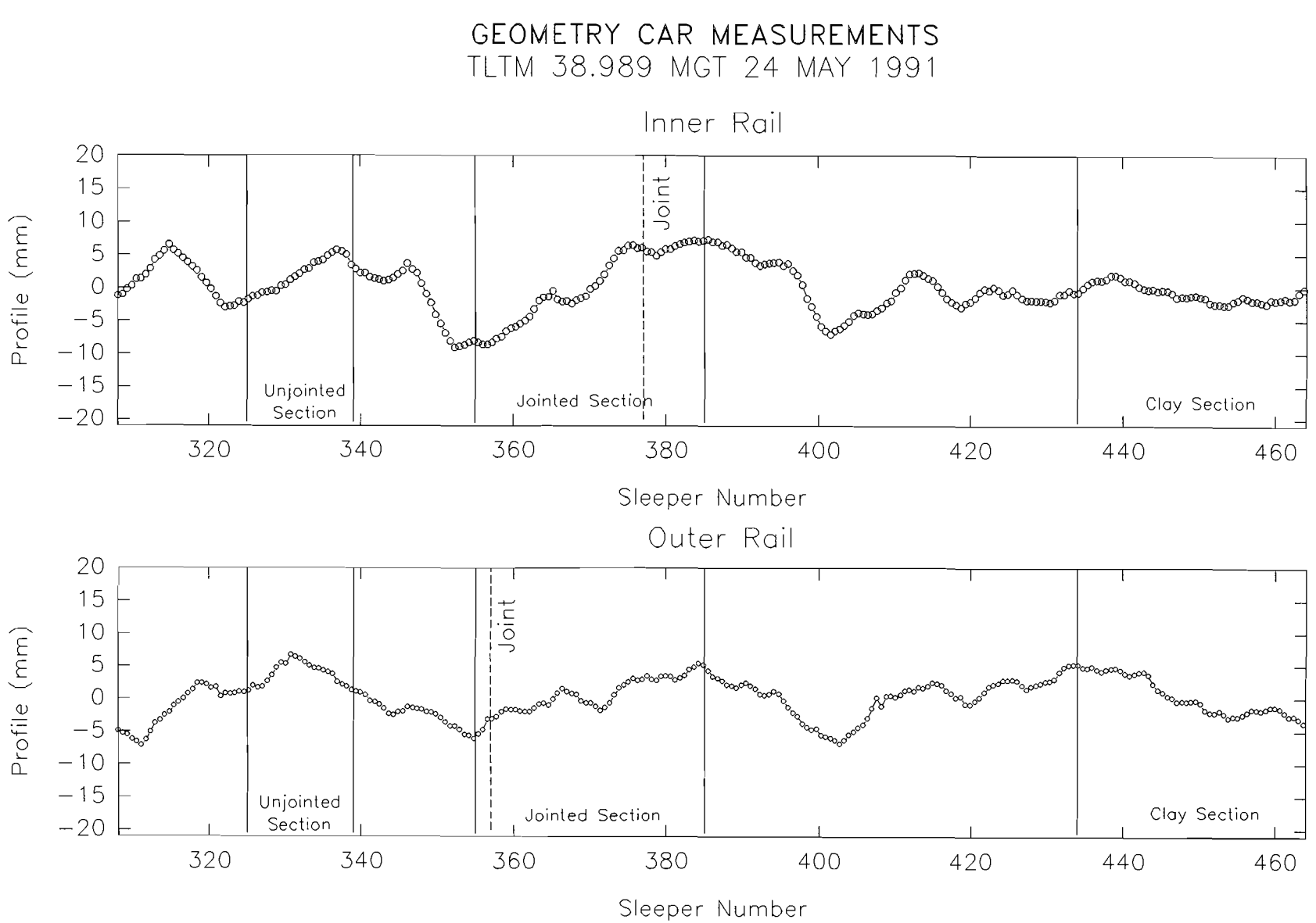

Figure 104: Profile at 38.989 MGT

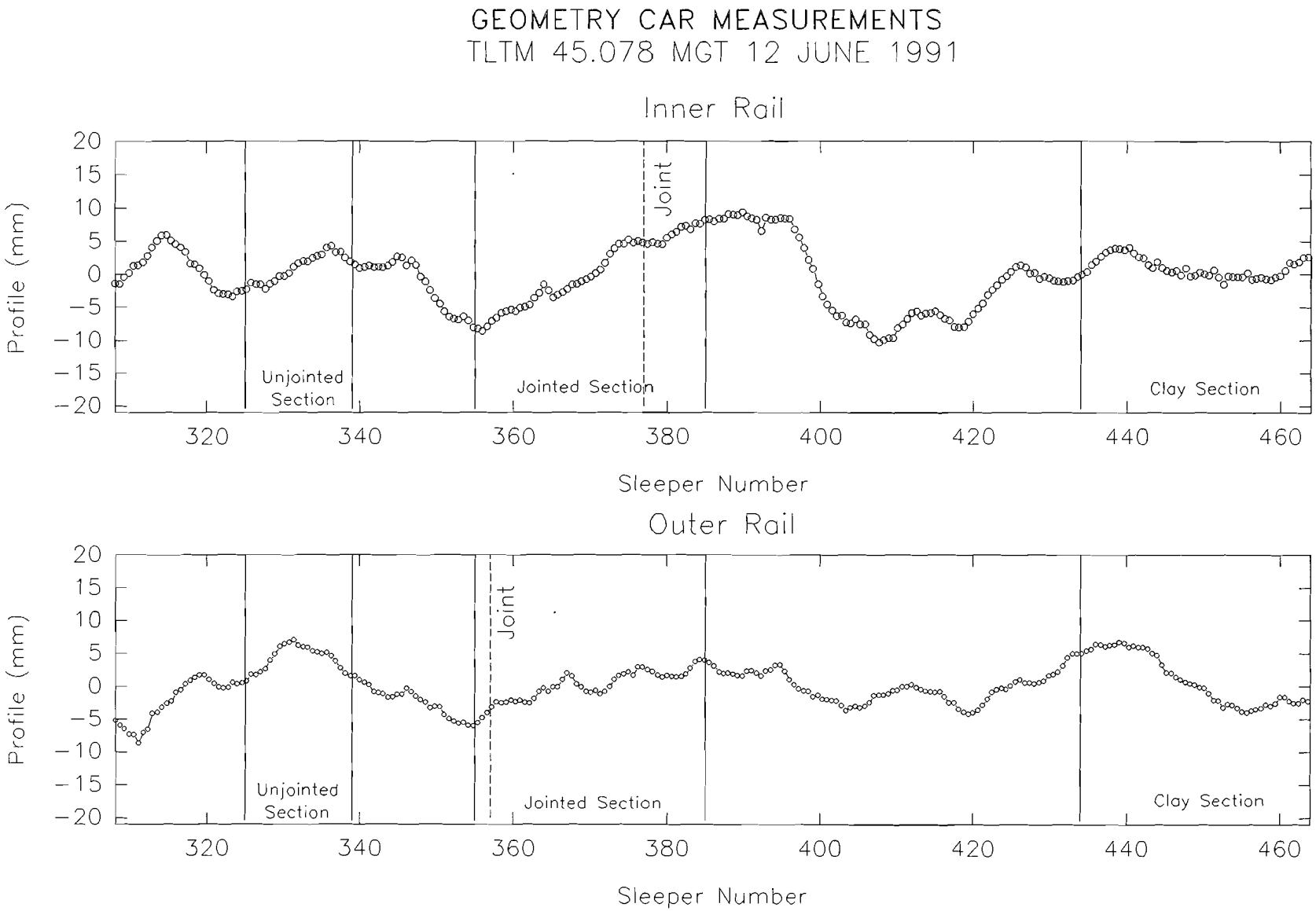

Figure 105: Profile at 45.078 MGT

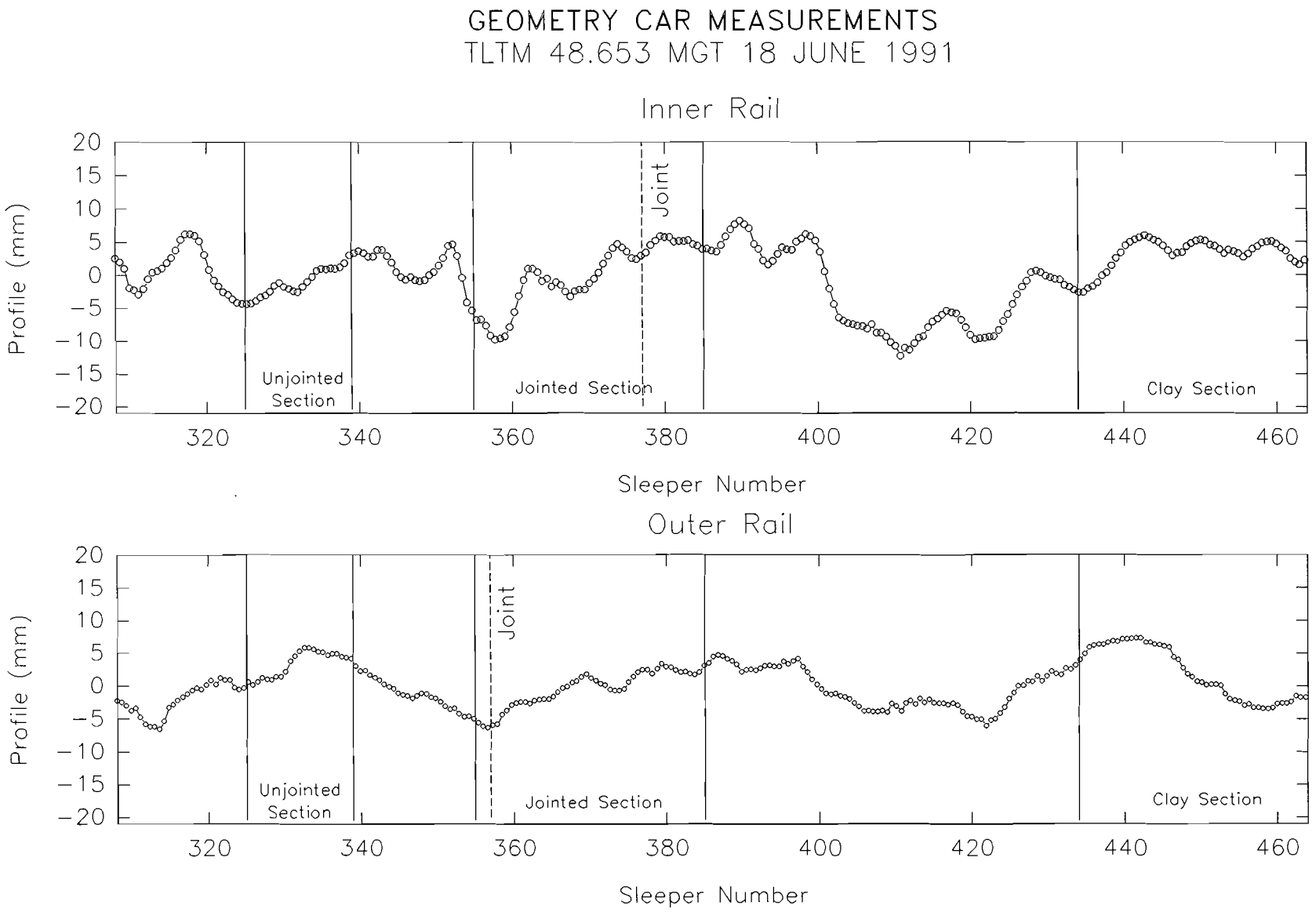

Figure 106: Profile at 48.653 MGT

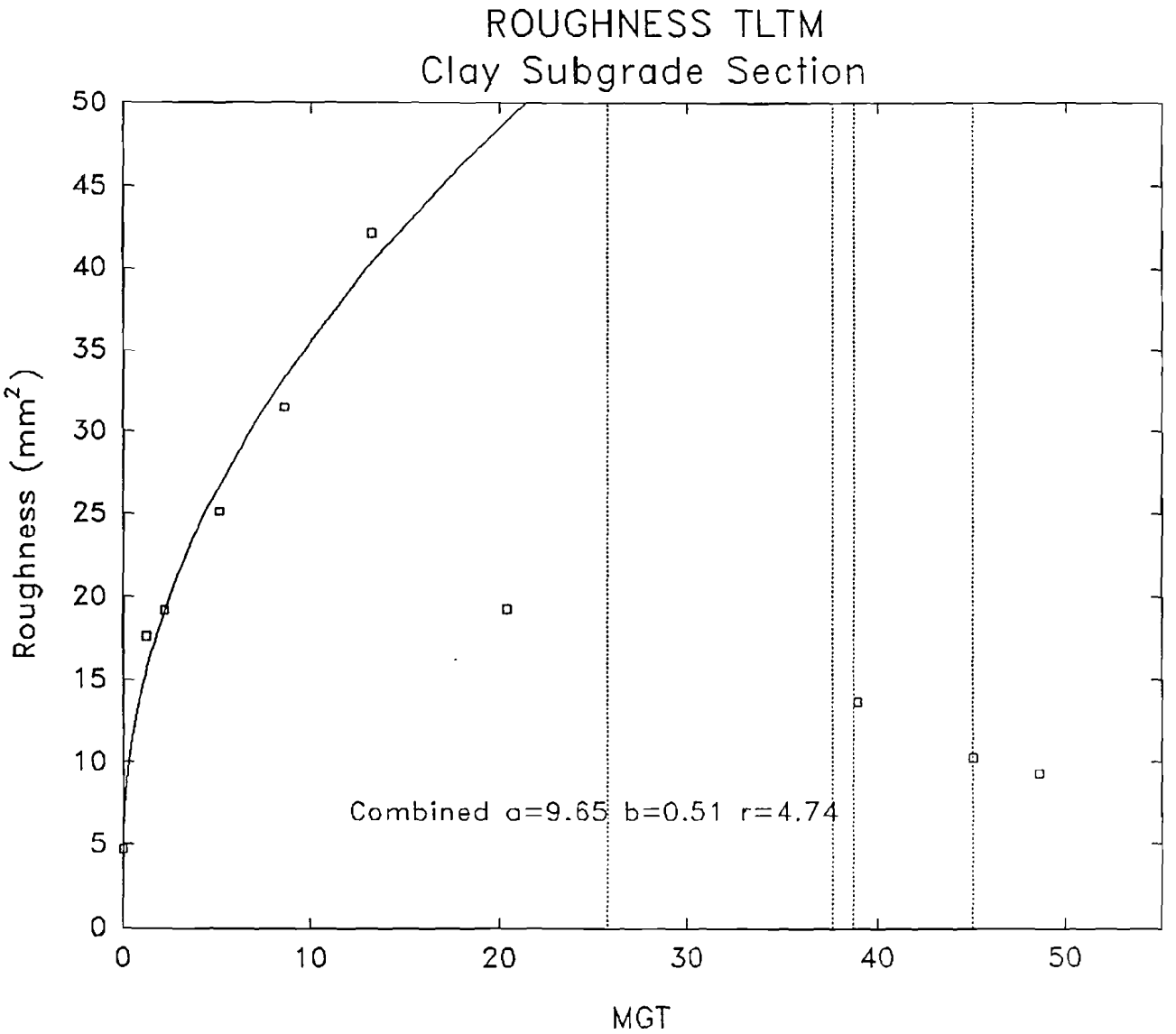

Figure 107: EM80 Roughness Clay Section

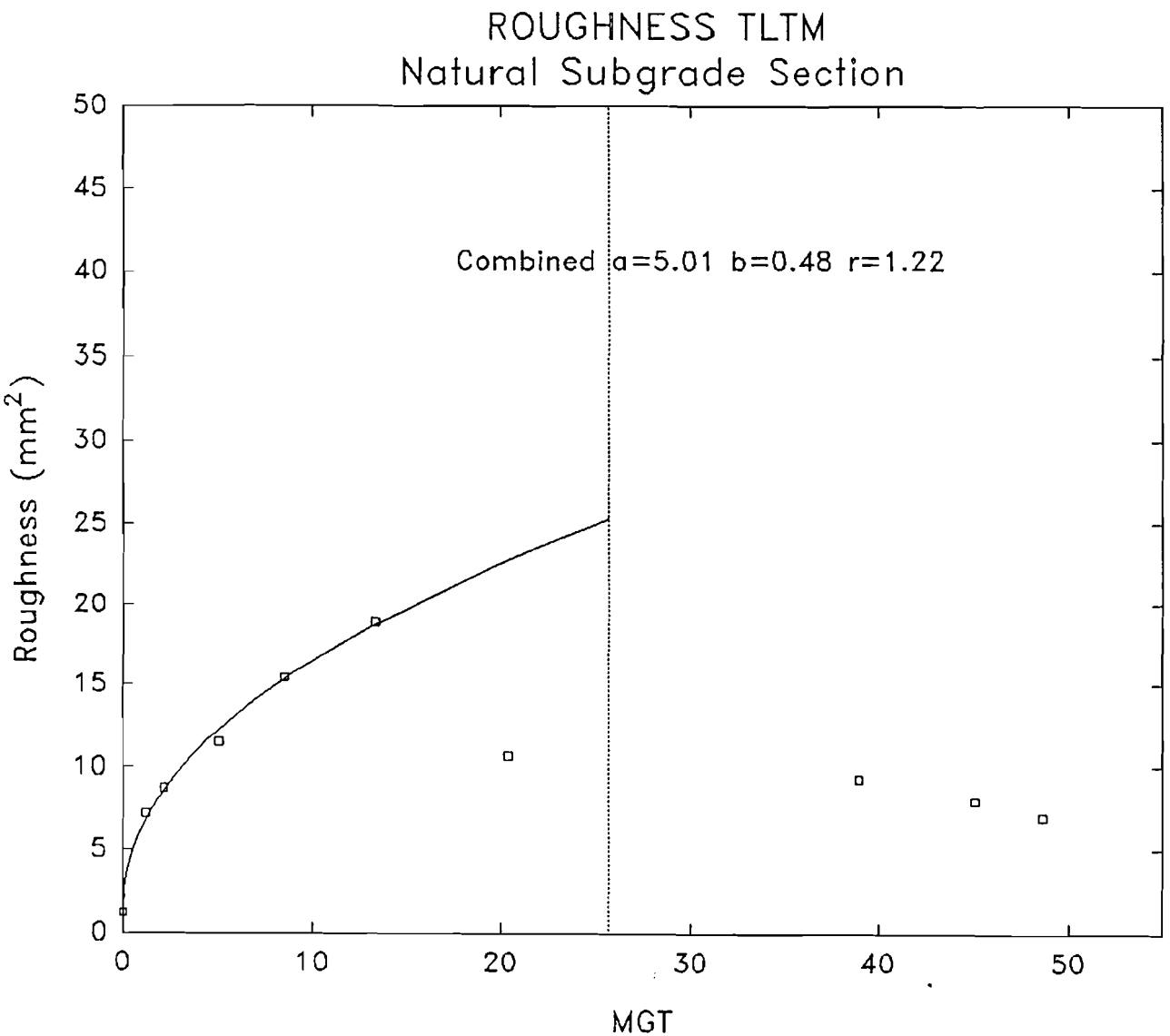

Figure 108: EM80 Top Roughness Natural Section

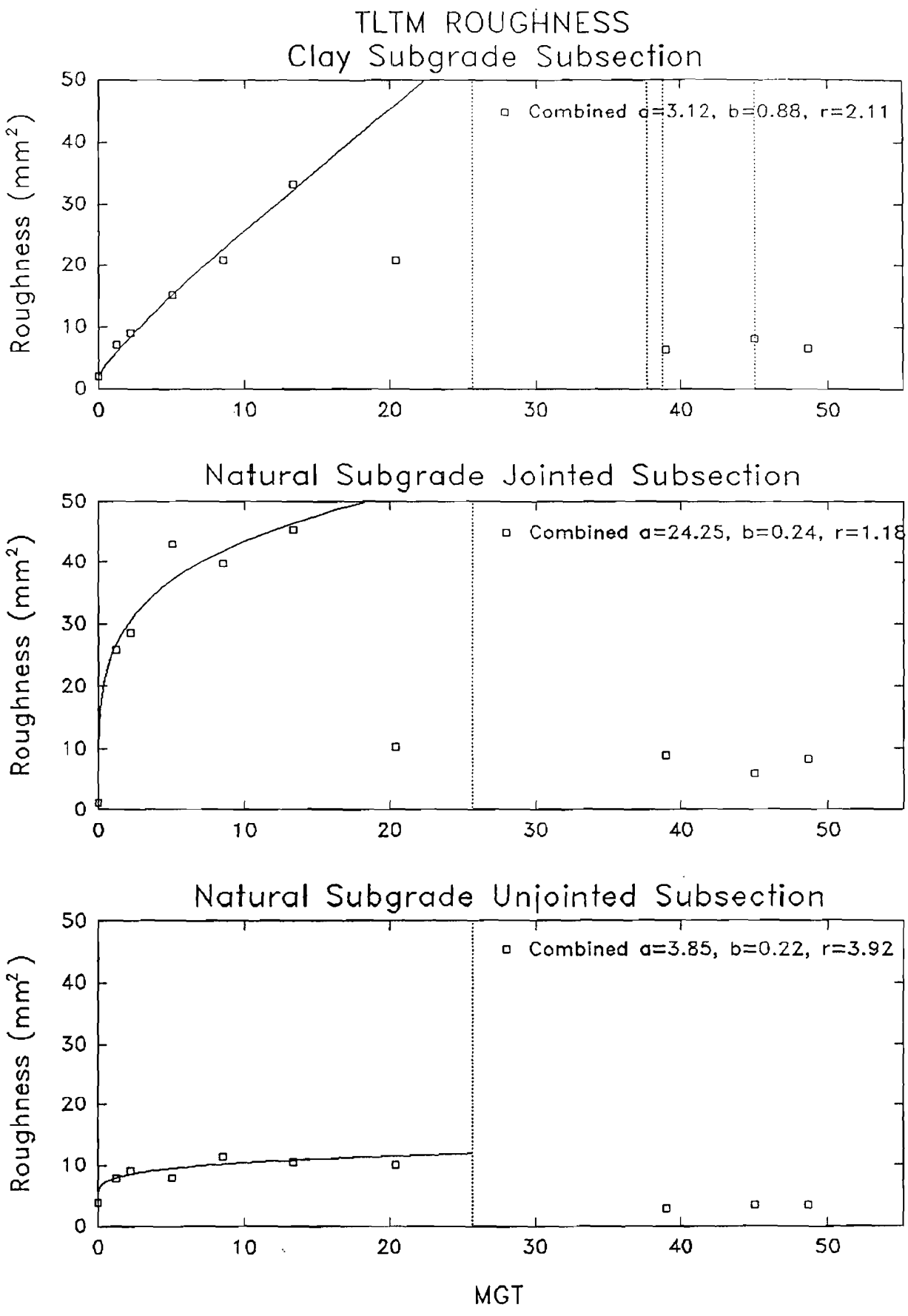

Figure 109: EM80 Top Roughness Subsections

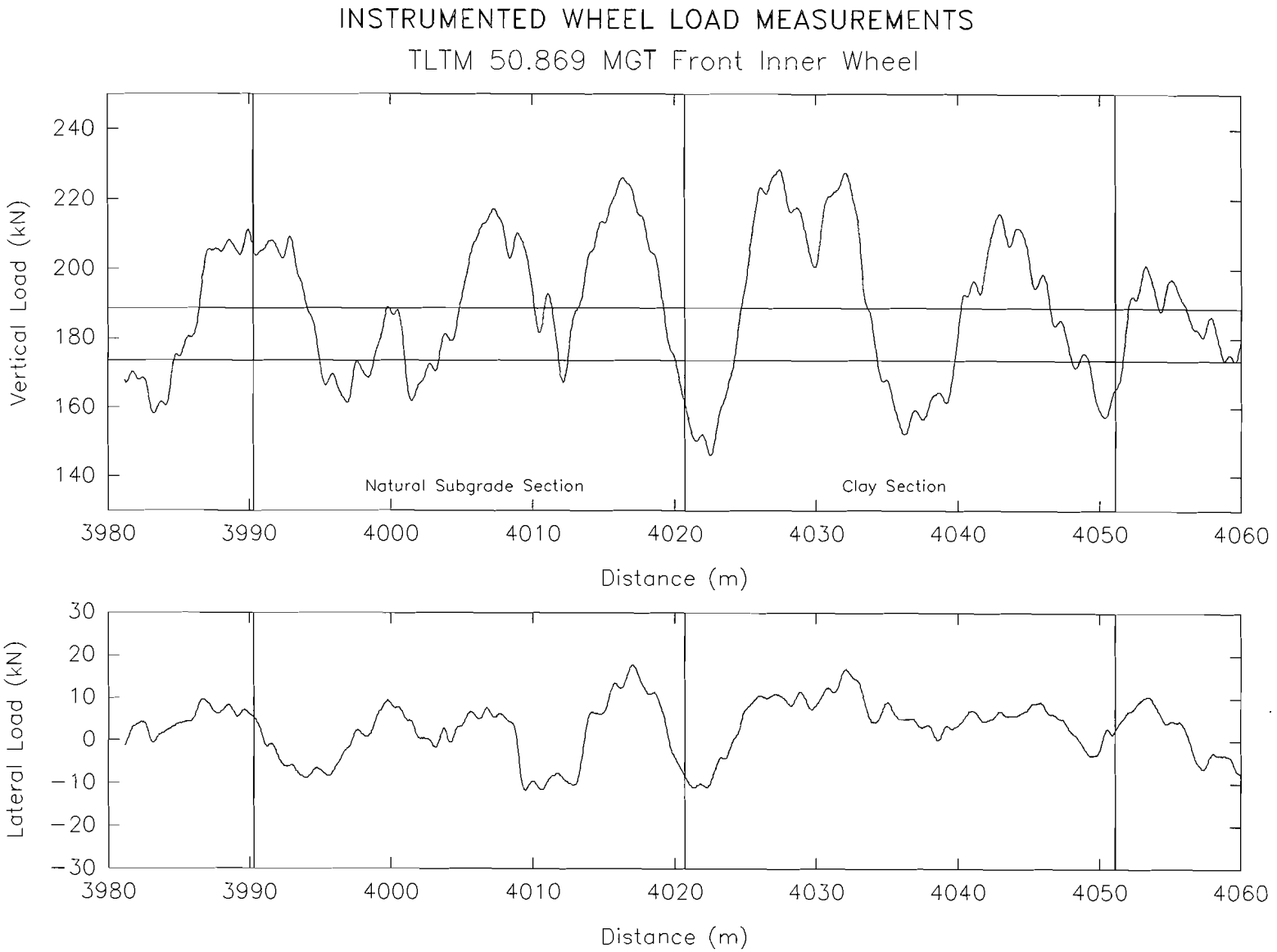

Figure 110: Wheel Load Measurements Front Inner Wheel

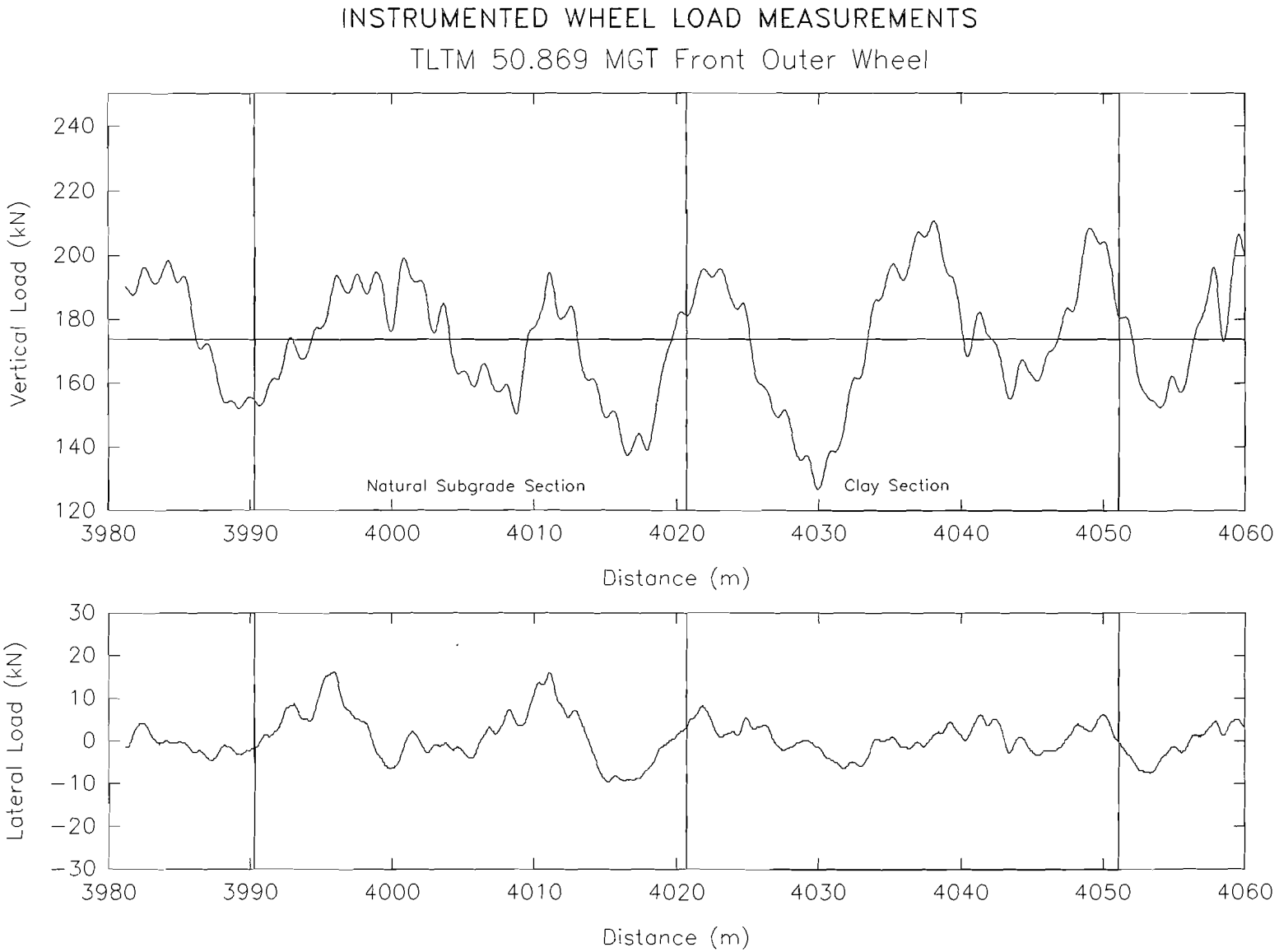

Figure 111: Wheel Load Measurements Front Outer Wheel

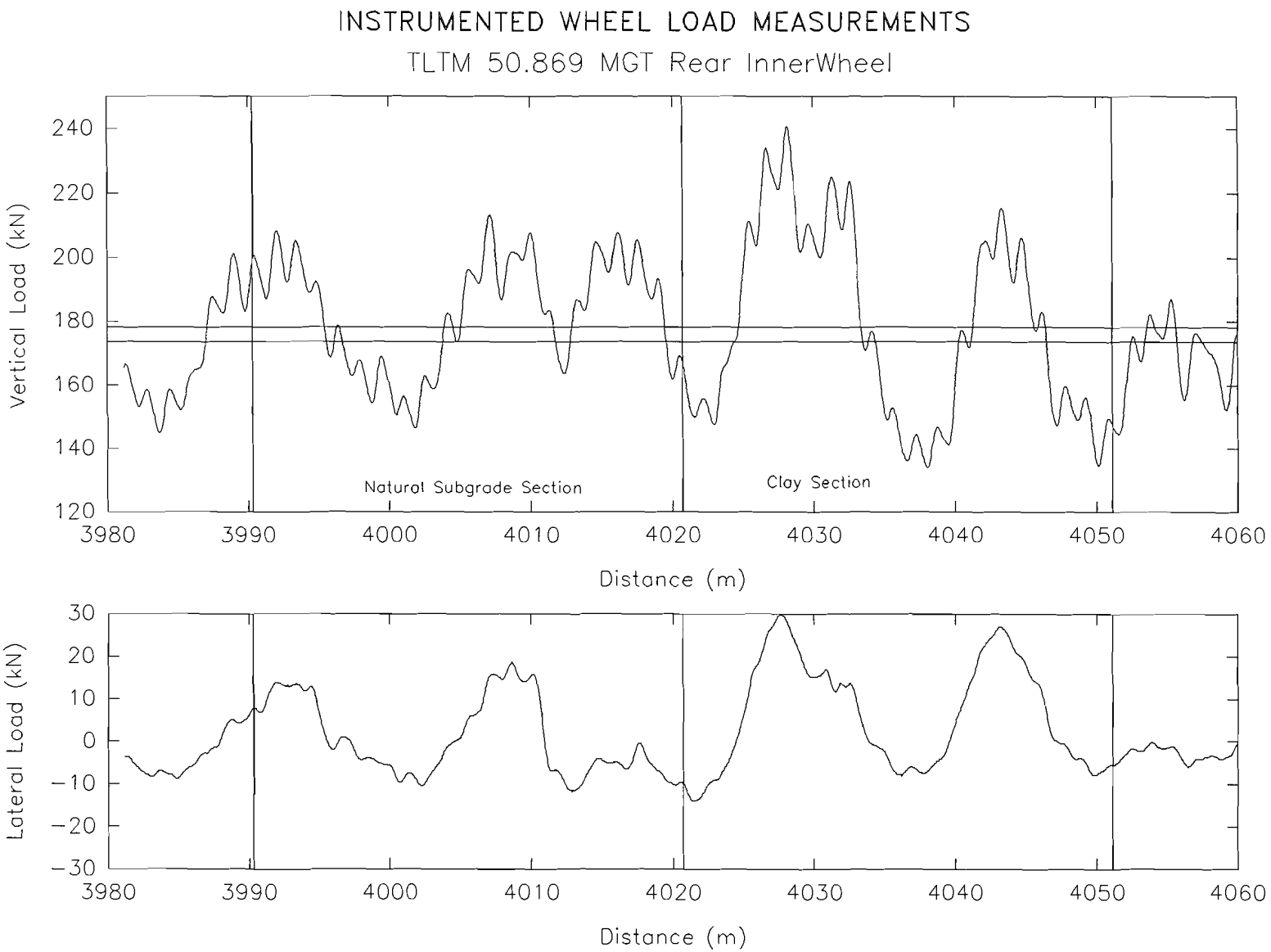

Figure 112: Wheel Load Measurements Rear Inner Wheel

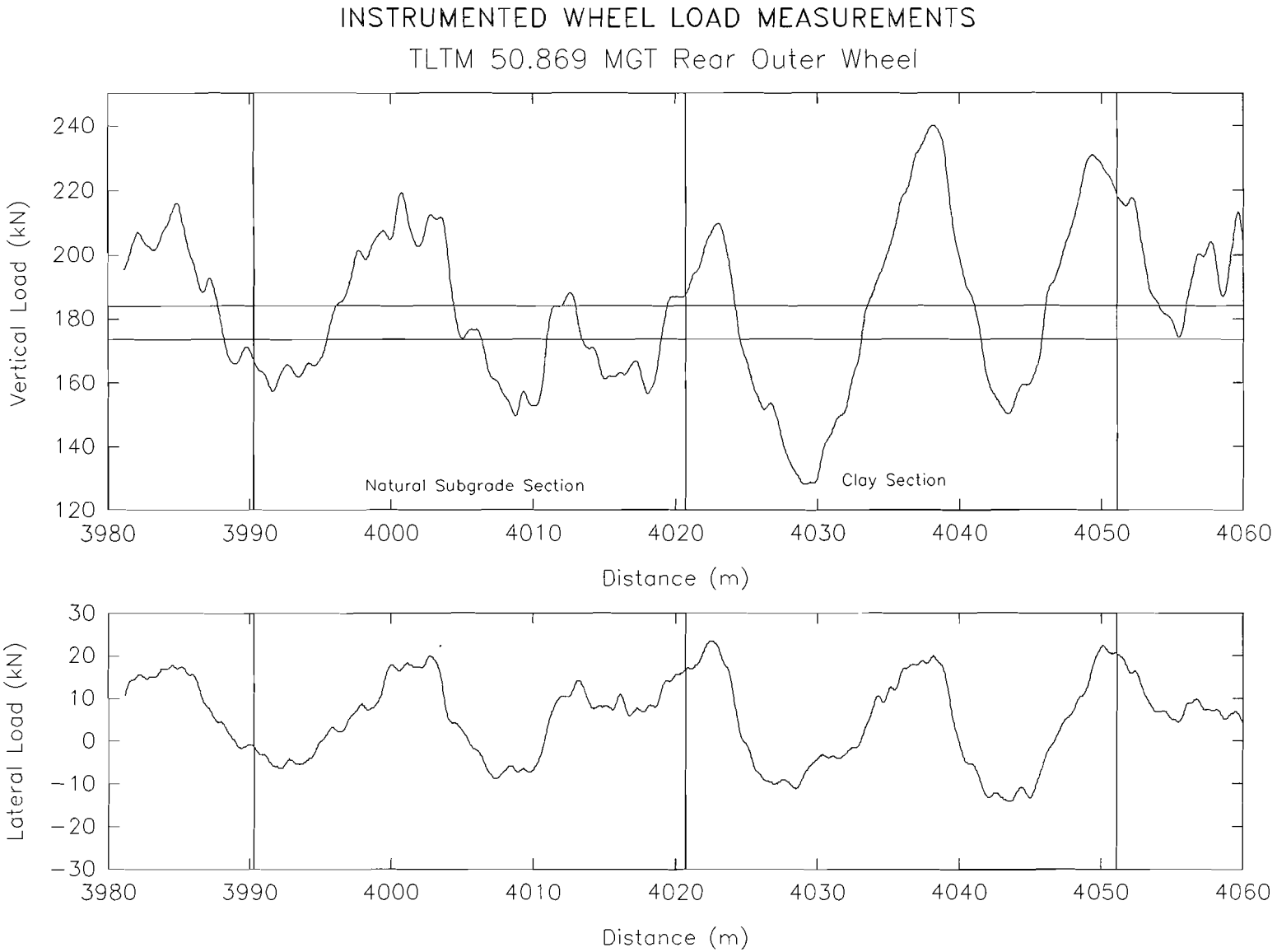

Figure 113: Wheel Load Measurements Rear Outer Wheel

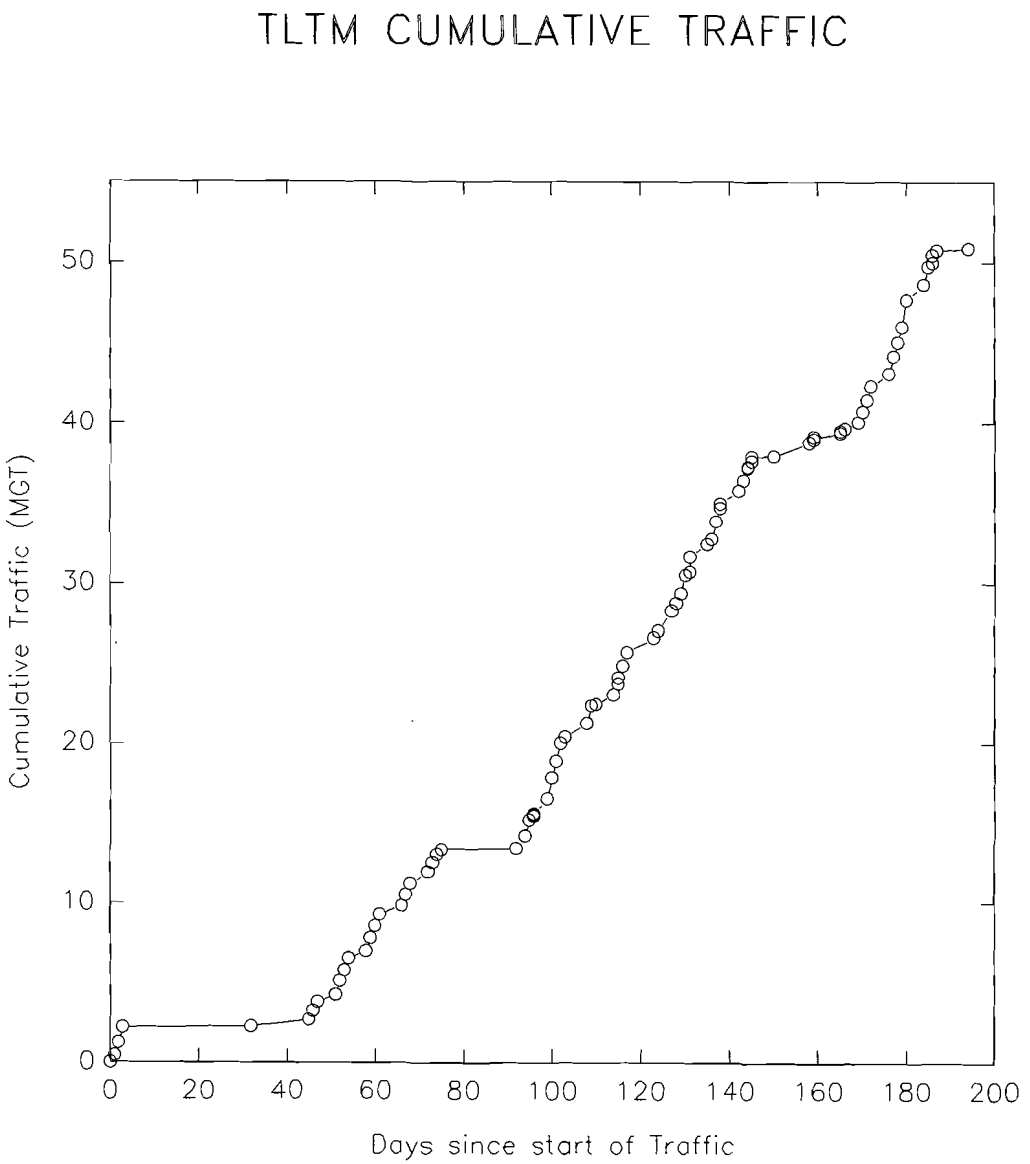

Figure 114: Cumulative Traffic

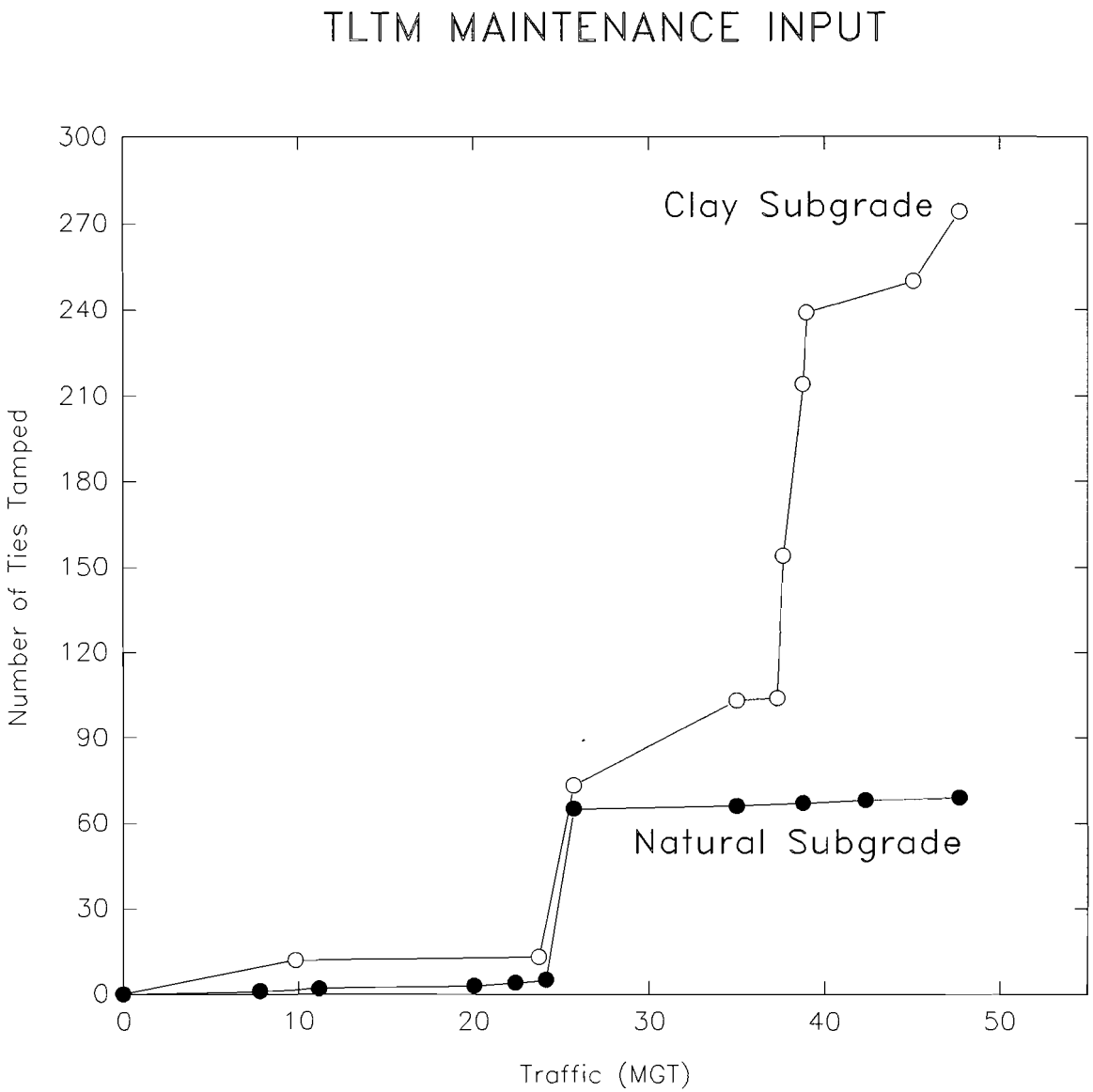

Figure 115: Maintenance Input